TRANSCRIPTIONAL REGULATION OF EFFECTOR AND MEMORY RESPONSES DURING ACUTE AND CHRONIC LYMPHOCYTIC CHORIOMENINGITIS VIRUS (LCMV) INFECTION

A Dissertation Presented

By

ELIZABETH ANNE OLESIN
Maiden Name (SCHUTTEN)

Submitted to the Faculty of the University of Massachusetts Graduate School of Biomedical Sciences, Worcester, in partial fulfillment of the requirements for the degree of

DOCTOR OF PHILOSOPHY

October 17, 2018

Program of Immunology and Microbiology

TRANSCRIPTIONAL REGULATION OF EFFECTOR AND MEMORY RESPONSES DURING ACUTE AND CHRONIC LYMPHOCYTIC CHORIOMENINGITIS VIRUS (LCMV) INFECTION

A Dissertation Presented

By

ELIZABETH ANNE OLESIN

The signatures of the Dissertation Defense Committee signifies completion and approval as to style and content of the Dissertation

Leslie J. Berg Ph. D., Thesis Advisor

Lawrence Stern Ph. D., Member of Committee

Samuel Behar Ph. D., Member of Committee

Michael Brehm Ph. D., Member of Committee

Christine Biron Ph. D., Member of Committee

The signature of the Chair of the Committee signifies that the written dissertation meets the requirements of the Dissertation Committee

Susan Swain Ph.D, Chair of Committee

Mary Ellen Lane, Ph. D.,
Dean of the Graduate School of Biomedical Sciences

Program in Immunology and Microbiology

October 17, 2018

Acknowledgements

First and foremost I would like to thank Dr. Leslie Berg for allowing me to complete my thesis work in her lab and for being a wonderful mentor. She has provided me with helpful insight into my project, while also allowing me room to grow as a scientist. Without her help this work would not be possible, and I am deeply grateful for all of her mentorship throughout the years. Thank you so much for giving me this amazing opportunity, and for mentoring me these past several years.

I would next like to thank the members of my Thesis Research Advisory Committee, Dr. Susan Swain, Dr. Raymond Welsh, Dr. Samuel Behar, and Dr. Lucio Castilla for all of their help and guidance throughout the years. I would also like to thank specifically Ray and Lucio for all of the one-on-one meetings we had discussing the intricacies of LCMV infection models and Runx proteins. Your guidance has been invaluable throughout the years, and I am grateful for all of your help. I would additionally like to thank Dr. Michael Brehm and Dr. Lawrence Stern for serving on my Dissertation Examination Committee.

Next I would like to thank past and present members of the Berg lab. A huge thanks needs to go to Regina Whitehead and Sharlene Hubbard. Regina has always been a lab mom to me. She keeps the ship afloat, and has always been there to support (and scold) me when I needed it, whether it be personal or

professional. She is always ready to dive into any issue headfirst that may arise, and I am eternally grateful for all of her support throughout the years. Thank you so much for everything these past 6 years. Sharlene is hands-down one of the most important people in lab. Without her work, we would have no mice! I would like to thank Sharlene for caring for and maintaining our mouse colony for all these years. She has always been extremely kind and willing to help (even when I needed 80 mice bled the following day…). Thank you so much for all of your help and for putting up with all of my ridiculous requests!

I would also like to thank the previous lab members Hyun Mu Shin and Ribhu Nayar who were my mentors when I rotated and first joined the Berg lab. Hyun Mu was very kind and supportive, helping me learn molecular techniques I had little to no previous experience with. He was always quick to praise my good work, and just as quick to show me my mistakes. Thank you for your guidance. I would also like to thank Ribhu Nayar for all of her mentorship. She really took me under her wing when I rotated and first joined, and together we made a very strong team. Ribhu is a very strong-willed and extremely intelligent person, and I feel so lucky to have been able to work with someone who is so capable, so knowledgable, and so interested in helping me learn and grow. She taught me everything there is to know about flow cytometry, plaque assays, and so much more. Ribhu really is a one in a million kind of person, and I am so grateful to have had such a wonderful mentor, and to have such an amazing friend. Thank

you so much for everything Ribhu!

Next I would like to thank Jim Conley and Hyoung-Soo Cho. All three of us joined the lab the same year (Jim and I were 30 minutes apart), so it gave us a camaraderie of sorts. We all struggled through our qualifying exams at the same time, sat through seminar lunches together giving the obligatory nod and laugh when people asked about graduation as we got older, and went to trivia together (which Jim and Hyoung-Soo just totally blew me out of the water during). It's been a lot of fun these past years, and I'm grateful I got to spend every one of them with you guys. I would like to give a special thanks to Jim, who is always ready to go to lunch at 1 o' clock, and ready to talk about any problems, lab or personal, I may be going through.

Next I would like to thank Mike Gallagher, Yves Falanga, and Nilima Kolli for their friendship and guidance these past couple years. While Mike and Yves sat on the opposite side of the lab, Nilima was right across from me. Thank you Nilima for all of guidance in biochemical assays. You knowledge of Biochemistry completely blows my mind, and I am so grateful to have had you right there whenever I had a question about the intricacies of western blotting or ChIP. I would also like to thank Nilima for all those long chats we would have in the afternoon, introducing me to the UMass hiking club, and for letting me watch her fish when she went on vacation. I would also like to thank my rotation students:

Yu Jung Lu, Kristin Abramo, and Priya Saikumar-Lakshmi for their help during their rotations.

Next I would like to thank all of the people in the department who helped make this research possible. I would like to thank Keith Daniels for all of his help and guidance with LCMV infections/flow cytometry issues/living in Millbury, as well as use of his peptides and monomers. I would also like to thank Carey Zammitti for her help with plaque assays, and for the millions of VERO splits I took from her whenever I needed to do a plaque assay. Thank you guys for all of your help these past years. I would also like to thank Priya Devarajan and Cate Castonguay for their help with the Runx2 Influenze infections and Priya for her helpful guidance and discussions these past couple years. Thank you guys so much for all of your help!

Finally I would like to thank my friends and family, who have been supporting me from the sidelines these past couple years. I would like to thank my mom, Jan, and sisters, Jenny and Cathy, who have been more than understanding about the hectic schedule of a graduate student, and the timeline of obtaining a Ph.D. I would not be here in the first place without the support of my mom, who always pushed me to follow my dreams. Thank you so guys so much for supporting me, and always reminding me to believe in myself. No bird soars too high if he soars with his own wings.

I would also like to thank my husband Alex, who has been my rock these past seven years. I am not sure I could have done this without you. You have always been there to help when I needed it, and during crunch times you have helped made sure the house remained in some form of working order. You have kept me mentally stimulated with stories of how fiber optic cables are made and how they work, and in turn have helped me learn how to explain what I do to a chemical engineer. Your unending support and belief in me has helped me get to where I am today. Thank you so much for everything. I am so lucky to have such a wonderful person in my life.

I also need to thank my graduate student friends, Carrie Kovalak, Brian Duke, and Jim Conley. We have comiserated together for so many hours, and have told each other potholes we fell into so that the others could avoid them. Thank you guys for being the best comrades a girl could ask for!

Abstract

Transcriptional regulation of $CD8^+$ T cell differentiation during acute and chronic viral infections is an intricate web made up of many of transcription factors. While several transcription factors have been elucidated in this process, there are still many more that remain elusive. In this work, we look into the role of two transcription factors, IRF4 and Runx2, and their role in $CD8^+$ T cell terminal effector cells and memory precursor cells during acute LCMV-Armstrong infection. We found that IRF4 expression was regulated by TCR signal strength during infection, and that IRF4 expression levels directly correlated with the magnitude of the effector cell response. IRF4 was also shown to regulate T-bet and Eomes, two transcription factors critical for $CD8^+$ T cell differentiation into effector and memory cells. From these results, we were interested in the potential role of IRF4 during chronic LCMV-clone 13 infection, where ratios of T-bet and Eomes are critical for viral clearance. We found that haplodeficiency of IRF4 in the T cell compartment lead to an increase in the ratio of Eomes to T-bet in T cells, which in turn affected the proportion of $Eomes^{hi}$ versus T-bet^{hi} cells and resulted in a loss in ability to clear viral infection. *Irf4*$^{+/-}$ *Eomes*$^{+/-}$ compound heterozygous mice were generated to test if decreasing Eomes expression would rescue the *Irf4*$^{+/-}$ phenotype. *Irf4*$^{+/-}$ *Eomes*$^{+/-}$ mice were phenotypically similar to WT mice in terms of Eomes to T-bet ratios, and were able to clear viral infection, demonstrating a critical role of IRF4 in regulating T-bet and Eomes during chronic viral infection. Next we looked into the role of Runx2 during acute LCMV-

Armstrong infection and found that Runx2-deficient pathogen-specific $CD8^+$ T cells had a defect in the total number of memory precursor cells compared to WT controls. We further showed that Runx2 was inversely correlated with TCR signal strength, and that Runx2 expression was repressed by IRF4. From these work, we have introduced two more transcription factors that are critical for $CD8^+$ T cells differentiation during acute and chronic viral infection. Given the sheer number of transcription factors known to regulate these processes, having a full understanding of the transcriptional network will allow us to find the best targets for therapeutic intervention for treatments ranging from vaccine development and autoimmunity to cancer immunotherapy and treatment of chronic viral infections.

Table of Contents

List of Figures

List of Symbols, Abbreviations, or Nomenclature

7-AAD	7-Aminoactinomycin D
Ab	Antibody
Ag	Antigen
AP1	Activator Protein 1
APC	Antigen Presenting Cell
APC	Allophycocyanin (Materials and Methods ONLY)
BATF	B-Cell Activating Transcription Factor
Bcl2	B-Cell Lymphoma 2
Bcl6	B-Cell Lymphoma 6
BCR	B Cell Receptor
Blimp-1	B-Lymphocyte Induced Maturation Protein 1
BSP	Bone Sialoprotein
Ca^{2+}	Calcium
CCD	Cleidocranial Dysostosis
CCR5	C-C Chemokine Receptor 5
CDK	Cyclin-Dependent Kinases
CRAC	Calcium-Release-Activated Ca^{2+} Channels
CTLA-4	Cytotoxic T Lymphocyte Associated Protein 4
CXCR3	C-X-C Motif Chemokine Receptor 3

CXCR4	C-X-C Motif Chemokine Receptor 4
D	Day
DAG	Diacylglycerol
DC	Dendritic Cell
Dlx5	Distal-Less Homeobox 5
DN	Double Negative Cells
DNA	Deoxyribonucleic Acid
DP	Double Positive Cells
EAE	Experimental Autoimmune Encephalomyelitis
ELISA	Enzyme-Linked Immunosorbent Assay
Eomes	Eomesodermin
ERK	Extracellular Signal-Regulated Kinase
Fc	Fragment Crystallizable
FGF2	Fibroblast Growth Factor 2
FITC	Fluorescein Isothiocyanate
FoxO1	Forkhead Box Protein O1
FoxP3	Forkhead Box P3
GAS	IFNγ-Activated Sequence
GP	Glycoprotein
hr	Hour
IBS	Irritable Bowel Syndrome
ICOS	Inducible T-Cell Costimulator

Id2	Inhibitor of DNA Binding 2
Id3	Inhibitor of DNA Binding 3
IFN	Interferon
IGF-1	Insulin-Like Growth Factor 1
IgG	Immunoglobulin G
IgM	Immunoglobulin M
IκBα	Nuclear Factor of κ Light Polypeptide Gene Enhancer in B Cells Inhibitor α
IL	Interleukin
iNKT	Invariant Natural Killer T Cell
i.p.	Intraperitoneal
IP_3	Inositol Triphosphate
IRF4	Interferon Regulatory Factor 4
ISP	Immature Single Positive
ISRE	IFN-Stimulated Response Elements
ITK	IL-2 Inducible T Cell Kinase
i.v.	Intravenous
K_D	Dissociation Constant
KLH	Keynote Limpet Hemocyanin
LAG-3	Lymphocyte Activation Gene 3
LCMV	Lymphocytic Choriomeningitis Virus
LPS	Lipopolysaccharide

MAPK	Mitogen-Activated Protein Kinase
MFI	Mean Fluorescence Intensity
MHC	Major Histocompatibility Complex
MPC	Memory Precursor Cell
mRNA	Messenger Ribonucleic Acid
mTOR	Mammalian Target of Rapamycin
NFAT	Nuclear Factor of Activated T Cells
NFκB	Nuclear Factor of κ Light Polypeptide Gene Enhancer in B Cells
NMTS	Nuclear Matrix Targeting Sequence
NP	Nucleoprotein
Oct-1	Octamer Binding Transcription Factor 1
OD	Optical Density
OSE2	Osteoblast-Specific Element 2
OVA	Ovalbumin
PAMP	Pathogen-Associated Molecular Pattern
PD-1	Programmed Cell Death Protein 1
PE	Phycoerythrin
PE-Cy7	Phycoerythrin-Cyanin 7
PerCP-Cy5.5	Peridinin Chlorophyll Protein Complex-Cyanin 5.5
PFU	Plaque Forming Units
p.i.	Post Infection
PI3K	Phosphatidylinositol-4,5-Bisphosphate 3-Kinase

PIP_2	Phosphatidylinositol-4,5-Bisphosphate
PKB	Protein Kinase B
PKC	Protein Kinase C
PRR	Pathogen Recognition Receptor
RBC	Red Blood Cell
RNA	Ribonucleic Acid
RPMI	Roswell Park Memorial Institute
rRNA	Ribosomal Ribonucleic Acid
Runx2	Runt-Related Transcription Factor 2
Runx3	Runt-Related Transcription Factor 3
SEM	Standard Error of the Mean
Smad1	Mothers Against Decapentaplegic Homolog 1
Smad5	Mothers Against Decapentaplegic Homolog 5
SOS	Son of Sevenless
Sox4	SRY-Related HMG-Box 4
SP	Single Positive
ssRNA	Single Stranded Ribonucleic Acid
STAT3	Signal Transducer and Activator of Transcription 3
STAT5	Signal Transducer and Activator of Transcription 5
T-bet	T-box Transcription Factor TBX21
TCF1	T-Cell Factor 1
TCR	T Cell Receptor

TEC	Terminal Effector Cell
T_{FH}	Follicular B Helper T Cell
TGFβ	Transforming Growth Factor β
T_H2	Helper T Cell Type 2
T_H9	Helper T Cell Type 9
T_H17	Helper T Cell Type 17
TLR	Toll-Like Receptor
TNFα	Tumor Necrosis Factor α
T_{REG}	Regulatory T Cell
UBF	Upstream Binding Factor
UMMS	University of Massachusetts Medical School
VDJ	Variable, Diversity, Joining Gene Segments
WT	Wild-Type

List of Publications

Sasaki, K., A. Bean, S. Shah, E. Schutten, P. G. Huseby, B. Peters, Z. T. Shen, V. Vanguri, D. Liggitt, and E. S. Huseby. 2014. Relapsing-Remitting Central Nervous System Autoimmunity Mediated by GFAP-Specific CD8 T Cells. *The Journal of Immunology* 192: 3029–3042.

Nayar, R., E. Schutten, B. Bautista, K. Daniels, A. L. Prince, M. Enos, M. A. Brehm, S. L. Swain, R. M. Welsh, and L. J. Berg. 2014. Graded Levels of IRF4 Regulate $CD8^+$ T Cell Differentiation and Expansion, but Not Attrition, in Response to Acute Virus Infection. *The Journal of Immunology* 192: 5881–5893.

Nayar, R., E. Schutten, S. Jangalwe, P. A. Durost, L. L. Kenney, J. M. Conley, K. Daniels, M. A. Brehm, R. M. Welsh, and L. J. Berg. 2015. IRF4 Regulates the Ratio of T-bet to Eomesodermin in $CD8^+$ T Cells Responding to Persistent LCMV Infection. *PLoS ONE* 10: e0144826.

Marshall, N. B., A. M. Vong, P. Devarajan, M. D. Brauner, Y. Kuang, R. Nayar, E. A. Schutten, C. H. Castonguay, L. J. Berg, S. L. Nutt, and S. L. Swain. 2017. NKG2C/E Marks the Unique Cytotoxic CD4 T Cell Subset, ThCTL, Generated by Influenza Infection. *The Journal of Immunology* 198: 1142–1155.

Olesin, E., Nayar, R., Saikumar-Lakshmi, P., Berg, L.J. 2018. The transcription factor Runx2 is required for long-term persistence of antiviral $CD8^+$ memory T cells. *Immunohorizons* 2:7 251-261

CHAPTER I: Introduction

The immune system is one of the eleven major organ systems of the human body. It's primary function is to protect the host from foreign pathogens. The human body has skin and mucosal surfaces that act as a natural barrier to prevent foreign bodies from entering the host. However, if one of these barriers becomes compromised, or if a foreign pathogen is able to get through the barrier, the immune system is able to eliminate foreign pathogens from the host by recognition and destruction of the foreign body.

The first branch of the immune system to respond to the presence of foreign antigen is the innate immune system. This branch is called "innate" because these immune cells are able to identify foreign pathogens using germline products based on components that are often shared between many pathogens. An example of this would be an innate immune cell being able to recognize the flagellin of an invading *Salmonella typhi* bacterium, a shared trait that can be found on many different types of bacteria. Innate immune cells are able to identify these foreign bodies through pathogen recognition receptors (PRRs) that identify pathogen-associated molecular patterns (PAMPs). Innate immune cells are able to respond rapidly to infection, with their primary goal being to limit the spreading of infection via phagocytosis of foreign bodies, activation of complement, recruiting immune cells to the infection site through the production of cytokines, and activation of the adaptive immune system by antigen presentation.

The second branch of the immune system is the adaptive immune system. The adaptive immune response is activated when an infection is unable to be cleared by the innate immune response. This branch is made up of two major cell groups: T cells and B cells named after the organ they develop in (T cells in the thymus and B cells in the bone marrow). This branch is highly specific to the pathogen that has infiltrated the body. This high specificity is possible through genetic (VDJ) recombination of the major receptor on these cells (T cell receptor or TCR on T cells and the B cell receptor or BCR on B cells). These adaptive immune cells allow for individuals to fight and clear a diverse range of infections throughout their lifetime. Adaptive immune cells take several days to become activated and differentiate into effector cells, but once the pathogen is cleared, a small pool of memory cells is left to rapidly respond to reinfection. The work of this dissertation focuses on T cell differentiation during acute and chronic viral infection, so we will focus on the T cell for the rest of this introduction.

T cells originate from multipotent hematopoietic stem cells in the bone marrow. These progenitors migrate from to the thymus via the bloodstream, where they undergo maturation. Initial commitment of these multipotent hematopoietic stem cells into the T cell lineage occurs with Notch1 signaling within the thymus. After this, thymic T cells or thymocytes go through several stages of development. The first stage is the $CD3^{-}CD4^{-}CD8^{-}$ or double-negative (DN) stage. These DN cells

are able to still develop into γδ T cells and iNKT cells. The DN stage can be broken down into 4 parts (DN1-4) based on expression of surface molecules CD44, CD25, and Kit. During this stage, the TCRβ receptor undergoes VDJ recombination during the DN2/DN3 stages, and successfully recombined TCRβ thymocytes with a pre-TCRα go on to proliferate during the DN4 stage. The next stage is the $CD3^{+}pT\alpha\beta^{+}CD4^{+}CD8^{+}$ double-positive (DP) stage. During the DP stage, TCRα undergoes VJ recombination. DP cells then undergo positive selection where thymocytes that are able to recognize self-peptide:self-MHC complexes survive and thymocytes that are unable to recognize the peptide:MHC complex undergo apoptosis. DP Thymocytes then undergo negative selection where cells that become too highly activated in response to self-antigen undergo apoptosis. During this time, DP cells stop producing either CD4 or CD8 co-receptor molecules and become single-positive (SP) thymocytes. $CD4^{+}$ SP thymocytes recognized peptide presented on MHC-II, whereas $CD8^{+}$ SP thymocytes recognize peptide presented on MHC-I. SP thymocytes have undergone full thymic maturation and will leave the thymus and move into the periphery.

Once the mature T cells enter the periphery, they circulate through the bloodstream, the lymphoid organs, and the lymphatics. During this time, T cells are naïve in that they have not seen their cognate antigen presented on MHC. In order for T cells to become activated, they require three signals: signal 1 from

TCR stimulation, signal 2 from costimulation through CD28 and/or other costimulatory molecules, and signal 3 from cytokines.

Once a naïve T cells is activated by an antigen presenting cell (APC) presenting cognate antigen on it's MHC, a T cell will undergo activation through the TCR signaling pathway. Upon activation of this pathway, several downstream steps occur leading to hydrolyzation of phosphatidylinositol 4,5 bisphosphate (PIP_2) to generate inositol triphosphate (IP_3) and diacylglycerol (DAG). IP_3 causes release of Ca^{2+} from the endoplasmic reticulum and other intracellular repositories, which in turn causes an influx of extracellular calcium through activation of Ca^{2+}-release-activated Ca^{2+} channels (CRAC) on the plasma membrane. This influx of intracellular calcium leads to activation of Ca^{2+} sensitive nuclear factor of activated T cells (NFAT). DAG activates the mitogen-activated protein kinase (MAPK) signaling pathway as well as the nuclear factor of κ light polypeptide gene enhancer in B cells (NFκB) signaling pathway. Once these signaling pathways have been activated, downstream target genes will become expressed leading to T cell proliferation and differentiation.

$CD8^+$ T Cell Differentiation: Effector versus Memory

Activated $CD8^+$ T cells undergo three major phases during acute infection: clonal expansion, contraction, and memory. During clonal expansion, activated $CD8^+$ T cells rapidly undergo several rounds of division to expand the population of

pathogen-specific $CD8^+$ T cells from ~$1x10^2$-$1x10^3$ cells within the spleen to ~$1x10^6$ cells. These expanded $CD8^+$ T cells gain effector functions and are able to clear infection through release of cytokines such as IFNγ and TNFα, as well as killing infected cells via "the kiss of death." To do this, $CD8^+$ effectors generate holes in the membranes of infected target cells with perforins and release granzymes into the infected cell to induce programmed cell death. Once infection is cleared, $CD8^+$ T cells undergo a contraction phase where around 90% of the population undergoes apoptosis, leaving a small pool of memory $CD8^+$ T cells that survive and continue on for years post infection. These memory $CD8^+$ T cells protect the host from secondary infection with the same pathogen by rapidly responding to reinfection.

Experimental differentiation of effector and memory $CD8^+$ T cells is primarily through expression of the surface markers CD127 (IL-7rα) and KLRG1 (Schluns et al., 2000) (Kaech et al., 2003) (Huster et al., 2004). Terminal effector $CD8^+$ T cells (TECs) are $KLRG1^{hi}$ $CD127^{lo}$, whereas memory percursor $CD8^+$ T cells (MPCs) are $KLRG1^{lo}$ $CD127^{hi}$. Memory cells can be differentiated from effector cells as early as day 7 during LCMV-Armstrong infection using these markers. Effector $CD8^+$ T cells make up the majority of the T cell response, rapidly proliferating in response to activation, whereas memory $CD8^+$ T cells proliferate less, but go on to survive after clearance of infection (Figure 1.1). How $CD8^+$ T cells are able to differentiate into either effector or memory T cells is still not

clear, but there are several potential mechanisms currently under debate in the field.

The first mechanism that was proposed was the separate-precursor model, where memory and effector $CD8^+$ T cells are pre-programmed in the thymus, and an activated $CD8^+$ T cell would differentiate into either an effector T cell or a memory T cell depending on how they were programmed previously. This model was disproven by adoptive transfer experiments where individual naïve $CD8^+$ T cells were barcoded and host mice were infected (Stemberger et al., 2007) (Gerlach et al., 2010). These experiments showed that a single T cell was able to produce both effector and memory T cells in response to infection. These experiments were performed using TCR transgenic cells, so they did not test the role for TCR signal strength in effector/memory differentiation.

Another mechanism that has been proposed is the decreasing-potential model, where repetitive TCR stimulation with cognate antigen and pro-inflammatory cytokines pushes activated $CD8^+$ T cells towards increased proliferation and terminal differentiation to effector T cells. This model is able to explain how a single naïve T cell is able to produce both effector and memory progeny upon activation. Studies that support this model include work by Joshi et al. that show inflammatory cytokine IL-12 promotes T-bet expression during T cell priming and

Figure 1.1. Kinetics of the $CD8^+$ T cell response and proportions of TECs and MPCs in response to acute viral infection

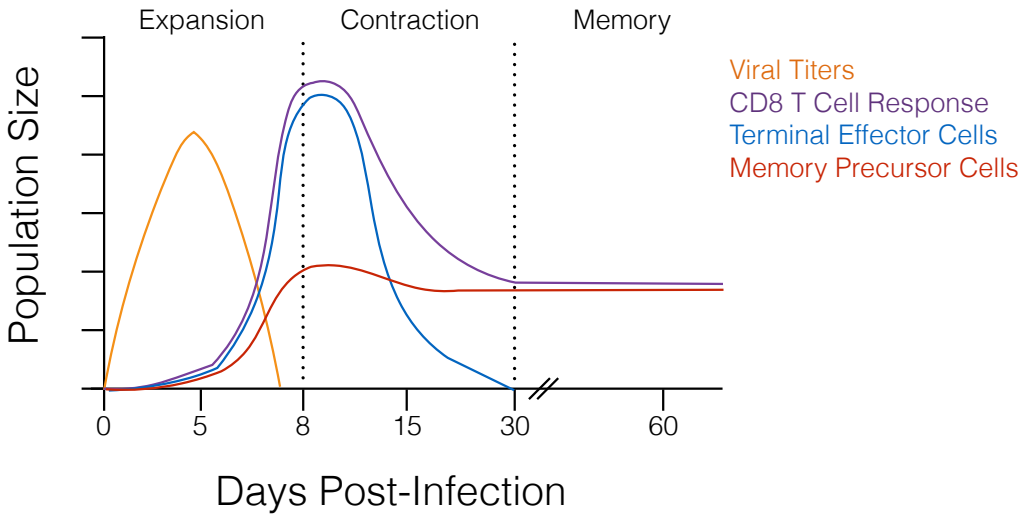

Figure 1.1. Kinetics of the $CD8^+$ T cell response and proportions of TECs and MPCs in response to acute viral infection

During acute viral infection, pathogen-specific $CD8^+$ T cells undergo clonal expansion and clear viral infection. After viral clearance, $CD8^+$ T cells undergo a contraction phase where ~90-95% of the population undergoes apoptosis, and a small pool of pathogen-specific memory cells are left to protect the host from reinfection by the same pathogen. This pool of $CD8^+$ T cells can be broken down into two major groups: terminal effector cells (TECs) and memory precursor cells (MPCs). TECs rapidly proliferate and make up the majority of the population at the peak of the $CD8^+$ T cell response, whereas MPCs proliferate less, but go on to form memory.

terminal effector differentiation in $CD8^+$ T cells in response to LCMV (Joshi et al., 2007). It has also been found that decreasing the length of antigen stimulation a T cell receives during infection (Sarkar et al., 2008) or during vaccination (Badovinac et al., 2005) leads to an increase in the proportion of MPCs, whereas inflammation was shown to reverse the effects seen with decreased antigen stimulation (Badovinac et al., 2005). Early clearance of *Listeria monocytogenes* infection through the use of antibiotics has also shown an increase in the proportion of MPCs compared to TECs, as well as cause a defect in the clonal expansion phase of TECs (Badovinac et al., 2004).

This work also supports the signal-strength model, whereas the intensity of TCR signal strength, costimulation, and inflammatory cytokines can lead to terminal differentiation of activated $CD8^+$ T cells to the effector lineage. The signal-strength model differs from the decreasing-potential model in that intensity of signal strength is more important than the repetitive stimulation of T cells with these signals. The general consensus of the field is that terminal differentiation of effector cells lies between these two models, where both intensity and repetition are able to drive cells to an effector fate.

One final model that also incorporates elements of differentiation through signal strength is the asymmetric cell division model. In this model, differentiation between TECs and MPCs is determined by proximity of the daughter cell to the

APC. Work done by Chang et al. has shown that the daughter cells that arise from the first cell division inherit unequal amounts of proteins that are important for $CD8^+$ T cell differentiation (Chang et al., 2007), with the promixal daughter cell receiving more proteins and cytokine signaling required for terminal effector differentiation (Verbist et al., 2016) and the distal daughter cell receiving more proteins required for memory differentiation (Pollizzi et al., 2016). While it is implausible that the fate of a daughter cell is strictly determined by whether it was proximal or distal to the APC during the first cell division, it is reasonable to believe that these division disparities could affect the ultimate fate of a T cell after several divisions.

Transcriptional Regulation of $CD8^+$ TECs and MPCs

During an acute viral infection, $CD8^+$ T cells differentiate into effector and memory cells, which are critical for clearance of the pathogen and protective immunity from reinfection. These $CD8^+$ T cell fates are regulated through transcriptional programs. Several transcription factors are known to play a role in $CD8^+$ T cell effector differentiation including BATF (Kurachi et al., 2014) (Grusdat et al., 2014) (Godec et al., 2015), T-bet (Intlekofer et al., 2005) (Joshi et al., 2007) (Rao, Li et al., 2010), Blimp-1 (Rutishauser et al., 2009) (Shin et al., 2013) (Xin et al., 2016), and Id2 (Cannarile et al., 2006) (Yang et al., 2011) (Knell et al., 2013) (Omilusik et al., 2010). Inversely, Eomes (Intlekofer et al., 2005) (Rao et al., 2010) (Banerjee et al., 2010), TCF1 (Jeannet et al., 2010) (Zhou et al., 2010),

Id3 (Yang et al., 2011) (Ji et al., 2011), and Runx3 (Wang et al., 2018) have been shown to play a critical role in $CD8^+$ T memory cells. Two major transcription factors, IRF4 and Runx2, are the focus of this dissertation, and our current knowledge of their roles in the immune response will be discussed below.

Interferon Regulatory Factor 4 (IRF4)

IRF4 is a transcription factor that is part of the interferon regulatory factor family. This family of proteins was originally discovered as regulating transcription of IFN-induced genes upon IFNα/β-treatment (Levy, Kessler et al., 1988) (Fu et al., 1990) (Kessler et al., 1990). IRF4 is able to bind to IFN-stimulated response elements (ISRE) or IFNγ-activated sequences (GAS) and activate or repress target genes (Eisenbeis et al., 1995) (Yamagata et al., 1996) (Matsuyama et al., 1995). In addition, IRF4 is able to form complexes with other transcription factors such as PU.1 (Eisenbeis et al., 1995) and BATF (Kurachi et al., 2014) to bind to other DNA-binding sites, allowing for regulation of non-IFN related genes.

IRF4 expression is primarily limited to the immune system, where it has been shown to be expressed in T/B cells (Eisenbeis et al., 1995) (Yamagata et al., 1996), macrophages (Marecki et al., 1999) (Rosenbauer et al., 1999), and dendritic cells (DCs) (Williams et al., 2013) (Schlitzer et al., 2013). In DCs, IRF4's primary role is to promote expression of cytokines that help regulate the $CD4^+$ T cell response. During an asthmatic response, DCs upregulate IRF4, which

promotes T_H2 differentiation in $CD4^+$ T cells through production of IL-10 and IL-33 (Williams & Bevan, 2007). During a *Aspergillus fumigates* fungal infection, a subset of $CD11b^+$ DCs express IRF4 which regulates production of IL-23 (Schlitzer et al., 2013). IL-23 in turn, promotes T_H17 differentiation in $CD4^+$ T cells (Schlitzer et al., 2013) (Gaffen et al., 2014). In macrophages, IRF4 was found to repress H2-L^d MHC-I expression, as well as activate transcription of the IL-1β promoter (Marecki et al., 1999).

IRF4 has a better-defined role in the lymphoid compartment, where it's expression was first discovered in the immune system (Shukla & Lu, 2014). IRF4 is unique to other IRF family members in that it is not upregulated in response to IFN-stimulation, rather it is upregulated through antigen-receptor mediated stimuli, such as IgM and TCR (Matsuyama et al., 1995). In B cells, IRF4 is primarily regulated through the NFκB signaling pathway (Saito et al., 2007), where it plays several critical roles in B cell development and differentiation. IRF4/IRF8 have been shown to play a redundant roll in the pre-B cell stage of development (Lu, 2003) (Ma et al., 2006b) by binding to the Ig κ 3' enhancer (Brass et al., 1996) (Brass et al., 1999) and limiting expansion of the pre-B cell population through inhibition of cell cycling (Ma et al., 2008) (Johnson et al., 2008) (Lazorchak et al., 2006). IRF4 alone also plays an important role in receptor editing (Pathak et al., 2008), class switching (Klein et al., 2006) (Sciammas et al., 2006), and plasma cell development (Sciammas & Davis,

2004) (Sciammas et al., 2006) (Klein et al., 2006) (Benson et al., 2007).

IRF4 plays a major role in T cells. Since IRF4 is upregulated in response to TCR stimulation (Matsuyama et al., 1995), it is present in most T-cell subsets including T_H2, T_H9, T_H17, T_{FH}, and T_{REG} (Huber & Lohoff, 2014). In T_H2 cells, IRF4 has been shown to promote IL-4 production by directly binding to the *Il-4* promoter with it's binding partner NFATc2 (Rengarajan et al., 2002), promote expression of the major T_H2 transcription factor GATA3 (Lohoff et al., 2002), and regulate the expression of *Gfi1*, a transcription factor that is important for IL-2-mediated T_H2 expansion (Tominaga et al., 2003). In T_H9 cells, IL-9 expression is directly correlated to IRF4 expression, and loss of IRF4 in the $CD4^+$ T cell compartment leads to a loss of T_H9 cells during airway inflammation (Staudt et al., 2010). In T_H17 cells, IRF4 regulates *Il-17* and *Il-22* expression to promote T_H17 function. In T_H17-mediated autoimmune models such as experimental autoimmune encephalomyelitis (EAE) (Brüstle et al., 2007) and irritable bowel syndrome (IBS) (Mudter et al., 2008) (Mudter et al., 2011), IRF4 has been shown to play a critical role in disease. In EAE, IRF4 has been shown to be required in $CD4^+$ T cells for disease to occur (Brüstle et al., 2007). In patients with IBS, IRF4 expression directly correlated with IL-17 levels and disease severity (Mudter et al., 2011). In T_{FH} cells, loss of IRF4 leads to a defect in T_{FH} differentiation after immunization with keynote limpet hemocyanin (KLH) (Kwon et al., 2009) as well as after *Leishmania major* infection (Bollig et al., 2012). These defects are attributed to a

defect in *Bcl6* expression, a critical gene that IRF4 also regulates in B cells (Bollig et al., 2012) (Ochiai et al., 2013). IRF4 has also been shown to regulate IL-21, a cytokine required for T_{FH} development (Biswas et al., 2010) (Kwon et al., 2009) (Huber et al., 2008) and could likely be contributing to the T_{FH} defect seen in IRF4 deficient mice. In T_{REG} cells, IRF4 is required for T_{REG} effector function. Loss of IRF4 leads to an increase in the total number of T_{REG} cells; however, IRF4 deficient T_{REGs} have decreased expression of ICOS, an activation marker for T_{REGs}, and IL-10, a cytokine involved in T_{REG} suppressor activity (Zheng et al., 2009) (Cretney et al., 2013).

IRF4 was first identified in having a potential role in $CD8^+$ T cells through a microarray experiment where IRF4 was the most highly downregulated transcription factor in IL-2 inductible T cell kinase (*Itk)*-deficient CD8SP thymocytes compared to WT controls (Berg, unpublished data). Initial studies found that IRF4 was upregulated, but not required, during thymic development (Nayar et al., 2012). *Irf4*$^{-/-}$ $CD8^+$ T cells showed increased levels of innate/memory markers such as CD44, CXCR3, Eomes, and CD122, similar to *Itk*-deficient mice. The authors further showed that dose-dependent inhibition of ITK with the small molecule inhibition, 10n, directly correlated with IRF4 expression levels, providing evidence that IRF4 expression was regulated through ITK (Nayar et al., 2012).

Following this work, four major articles were published, including one in this dissertation, which dissected the role of IRF4 in $CD8^+$ T cell activation, and effector differentiation. In work by Raczkowski et al., the authors found that IRF4-deficient mice were unable to clear *Listeria monocytogenes* infection. They further found this to be a $CD8^+$ T cell intrinsic defect, when adoptively transferred WT $CD8^+$ T cells are able to clear *L. monocytogenes* infection in IRF4-deficient mice. They also showed *Irf4*$^{-/-}$ $CD8^+$ T cells were able to proliferate initially, but were unable to at later stages of activation (Raczkowski et al., 2013). Their work also identified a defect in effector function (Granzyme B protein expression, *Gzk* and *Prf1* mRNA expression, and *in vivo* cytotoxicity) and cytokine production (IFNγ, TNFα, and IL-2 protein expression) in IRF4-deficient $CD8^+$ T cells, as well as a decrease in expression of effector transcription factors Blimp-1, Id2, and T-bet, and an increase in expression of memory transcription factors Bcl6, Eomes, and Id3 (Raczkowski et al., 2013).

In Nayar et al., we observed similar results as Raczkowski et al. in LCMV-Armstrong viral infection as well as Influenza A-PR8 viral infection. *Irf4*$^{-/-}$ *CD4-cre*$^+$ (*Irf4*$^{-/-}$*)* mice were unable to clear LCMV-Armstrong infection, whereas WT and *Irf*$^{+/-}$ *CD4-cre*$^+$ (*Irf4*$^{+/-}$*)* were able to clear infection (Nayar et al., 2014). Similar results were also observed in effector function and cytokine production during LCMV-Armstrong infection (Nayar et al., 2014). This work uniquely showed the effects of graded levels of IRF4 expression through the use of *Irf4*$^{+/-}$ mice, where

we showed haplo-deficiency in the *Irf4* gene lead to a decrease in IRF4 protein expression levels compared to WT cells (Nayar et al., 2014). Graded levels of IRF4 expression showed a graded defect in the $CD8^+$ T effector response, with IRF4 expression inversely correlating with Eomes expression. Graded IRF4 expression directly correlating with total number of GP_{33}-tetramer$^+$ $CD8^+$ T cells at day 8/14 post infection, IFNγ expression, TNFα expression, and IL-2 expression (Nayar et al., 2014). This work also showed that *Irf4*$^{+/-}$ $CD8^+$ T cells have no long term defect in MPCs, a defect that is seen in *Irf4*$^{-/-}$ $CD8^+$ T cells in response to LCMV-Armstrong infection (Nayar et al., 2014) as well as *L. monocytogenes* infection (Raczkowski et al., 2013).

In work by Man et al., the authors showed a similar defect seen in the previous papers, with a defect in the pathogen-specific $CD8^+$ T cell response in *Irf4*$^{-/-}$ mice during Influenza viral infection with the HKx31 strain, as well as during LCMV-Armstrong (WE strain) infection. In their work, the authors showed that there were no early defects in proliferation, but that there was a significant increase in apoptotic markers Annexin V and Caspase3 in *Irf4*$^{-/-}$ $CD8^+$ T cells compared to WT controls (Man et al., 2013). The authors go on to show that there is a defect in proliferation at later stages of activation in Influenza (HKx31) in *Irf4*$^{-/-}$ $CD8^+$ T cells compared to WT controls (Man et al., 2013), similar to results seen in Raczkowski et al. during *L. monocytogenes* infection. They further show that IRF4 protein expression is TCR signaling dependent, using OVA peptides with

single-point amino acid changes which in turn change the affinity of the peptide to the OT-I TCR transgenic $CD8^+$ T cell. They show that IRF4 expression level is directly correlated to the affinity of the OVA-peptide or OVA-peptide variant to the OT-I TCR, and that IRF4 regulates that affinity-driven transcriptional program in $CD8^+$ T cells (i.e. genes that are different between high-affinity peptide and low-affinity peptide) including *Eomes*, *S1pr1*, *Il7r*, and *Ccr2* (Man et al., 2013). Their work further showed that IRF4 regulated aerobic glycolysis in high-affinity effector $CD8^+$ T cells through transcriptional regulation of several metabolic genes (Man et al., 2013).

One final paper by Yao et al. was published in this group of publications looking at the role of IRF4 in $CD8^+$ T cell activation and differentiation. In their work, they showed that mTOR regulated IRF4 expression in activated $CD8^+$ T cells *in vitro* (Yao et al., 2013). This group saw impairment in effector function and proliferation, as was previously shown in (Raczkowski et al., 2013) and (Man et al., 2013), but uniquely showed that proliferation and survival defects seen later during $CD8^+$ T cell differentiation into effector cells was from IRF4 regulating CDK inhibitors *Cdkn2a*, *Cdkn1a*, and *Cdkn1c*, as well as regulating *Bim* expression (Yao et al., 2013). From these manuscripts, the groundwork was laid for how IRF4 is regulated through TCR signal strength, as well as IRF4's role in $CD8^+$ T cell effector differentiation through regulating of proliferation, survival, and effector metabolism.

Runt-Related Transcription Factor 2 (Runx2)

Runx2 is a member of the Runt domain family of transcription factors. Runx2 is primarily studied in the osteogenesis where is it required for osteoblast formation. Haplodeficiency of Runx2 leads to cleidocranial dysostosis (CCD), a disease primarily associated with bone and dental abnormalities (Otto et al., 2002). Complete loss of Runx2 leads to neonatal lethality due to a complete loss of bone formation (Komori, 2018). Runx2 requires binding partner CBFβ in order to bind to DNA. CBFβ does not directly interact with the DNA binding site; however, it enhances Runx-proteins ability to bind to DNA by inducing structural changes that opens the DNA-binding region of the protein (Tahirov et al., 2001) and stabilizes Runx-proteins by protecting them from ubiquitin-mediated degradation (Huang et al., 2001).

Runx2 is known to have several transcription factor binding partners including AP1 (c-Fos and c-Jun) (D'Alonzo et al., 2001), Smad1 and Smad5 (Hanai et al., 1999) (Lee et al., 2000) (Nishimura et al., 2002) (Sowa et al., 2004), Ets1 (Wotton et al., 1994) (Sato et al., 1998), androgen and glucocorticoid receptors (Ning & Robins, 1999), Dlx5 (Shirakabe et al., 2001) (Hassan et al., 2004), Hes1 (McLarren et al., 2000), and Oct-1 (Inman et al., 2005). Runx2 is often times found as part of a large transcriptional complex, and many of these heterodimeric binding partners are believed to be important in regulating this function. In

osteoblasts, Runx2 regulates osteoblast differentiation at multiple stages. Runx2 promotes osteoblast differentiation in pluripotent mesenchymal stem cells during the early stages of osteoblast differentiation by promoting expression of α2(I) collagen, osteopontin, and bone sialoprotein (BSP) (Ducy et al., 1999) (Harada et al., 1999) (Lee et al., 2000). Later Runx2 blocks osteoblast differentiation at the late stages of osteoblast maturation through repression of these same target genes (Ducy et al., 1999). This flip in regulation indicates a likely role for transcriptional binding partners regulating Runx2 activating/repressive functions during osteoblast differentiation.

Runx2 also plays a critical role in proliferation and cell cycle regulation in osteoblasts. Runx2 is upregulated in osteoblasts during the G_0/G_1 phase of cell cycle, and downregulated in the $S/G_2/M$ phases (Pratap et al., 2003). Further, loss of Runx2 leads to an increase in proliferation of osteoblasts, that is inhibited by reintroduction of Runx2 (Pratap et al., 2003). Loss of Runx2 expression in MEFs also leads to spontaneous immortalization and tumorigenesis (Kilbey et al., 2007) (Zaidi et al., 2007), indicating a critical role for Runx2 in the regulation of cell cycle and transformation. While Runx2 controls differentiation and proliferation as a result of its transcriptional regulation, Runx2 is also modulated through post-transcriptional regulation. Runx is primarily post-transcriptionally regulated through intracellular localization and phosphorylation.

Runx2 transcriptional activity is dependent on its localization to subnuclear foci. This localization is dependent on the nuclear matrix targeting sequence (NMTS) region of the Runx2 protein (Kanno et al., 1998) (Zeng et al., 1997) (Zeng et al., 1998), and the NMTS is required for Runx2-dependent transactivation (Zaidi et al., 2001). Loss of the NMTS results in loss recruitment of Runx2 to nuclear foci (Harrington, 2002), and failure to develop mineralized tissue due to maturational arrest of osteoblasts (Choi et al., 2001).

Phosphorylation of Runx2 is another post-translational modification is known to regulate Runx2 downstream activity. In vascular endothelial cells, Insulin-like growth factor-1 (IGF-1) activates MAPK/ERK pathways through PI3K and increases Runx2 phosphorylation and binding to OSE2 (Qiao et al., 2004). Mechanical stress has also been shown to activate MAPK/ERK, increase Runx2 phosphorylation, and increase expression of osteoblast genes (Ziros et al., 2002) (Kanno et al., 2007). Fibroblast growth factor-2 (FGF-2), an activator of bone growth *in vivo*, activates osteocalcin mRNA expression by increasing p-ERK1/2 which in turn phosphorylated Runx2. Use of ERK1/2 phosphorylation inhibitor, U0126, blocked FGF-2 mediated Runx2-phosphorylation (Xiao et al., 2002). Runx2 transcriptional activity can also be repressed by phosphorylation of serine residues S104 and S451, which inhibits heterodimerization with it binding partner CBFβ (Wee et al., 2002).

Very little work has been done elucidating the role of Runx2 in the immune system. Work from Sawai et al showed that Runx2 expression was required in plasmacytoid dendritic cells (pDCs) for migration out of the bone marrow, and that this defect was CCR5 mediated (Sawai et al., 2013), further work showed that this retention was also regulated by Runx2-mediated inhibition of CXCR4 (Chopin et al., 2016). Within the T cell population, Vaillant et al showed that Runx2 was expressed during the DN stage of thymic development, and that enforced expression of Runx2 lead to block of thymocyte development at the TCRβ-selection stage (Vaillant et al., 2002). These Runx2-enforced DN cells went on to become $CD4^{-}CD8^{+}TCR^{-}$ immature single positive thymocytes (ISPs), which were more sensitive to TGFβ-induced proliferation (Vaillant et al., 2002).

Two previous studies have hinted at the role of Runx2 in $CD8^{+}$ T cell memory. The first is an immunological genome project resource paper that analyzed the transcriptome throughout infection to determine transcriptional factors with effector or memory transcriptional profiles. This work found Runx2 was a predicted activator/repressor during $CD8^{+}$ T cell response to infection (Best et al., 2013). The second study was performed by Hu et al, where they collected 386 gene expression profiles from naïve, effector, and memory $CD8^{+}$ T cells from 35 GEO datasets and generated a genome-wide regulatory network (Hu & Chen, 2013). In this network, they identified Runx2 as a highly-ranked transcription factor important for regulating $CD8^{+}$ T cell memory. They further showed that

Sox4 and Eomes, but not TCF1, bound to the promoter region of Runx2 in 2C T cells. Interestingly, they did not find any differences in memory formation in retroviral overexpression or shRNA knockdown of Runx2 in 2C T cells activated *in vitro* (Hu & Chen, 2013). With this limited information of Runx2 in the immune system, we sought to determine how loss of Runx2 in the T cell compartment led to a defect in the total number of pathogen-specific $CD8^+$ T memory cells.

Acute LCMV-Armstrong versus Chronic LCMV-Clone 13

Lymphocytic Choriomeningitis Virus (LCMV) is a group V ambisense single strand RNA (ssRNA) virus from the *Arenaviridae* family of viruses. LCMV contains 2 RNA strands, a long and short strand. The long strand encodes the RNA-dependent RNA polymerase as well as a zinc finger binding Z protein, whereas the short strand encodes the glycoprotein (GP) precursor that gets cleaved into GP1 and GP2 as well as the nucleoprotein (NP). LCMV was first isolated in 1933 from monkeys in St. Louis by Charles Armstrong, for whom the strain was named (Welsh & Seedhom, 2008).

LCMV has been a model viral infection for studying the immune response for decades. This is because LCMV has many features that make it a promising candidate for study. The receptor LCMV uses to enter a host cell, α-dystroglycan receptor, is a ubiquitous protein that is expressed across many different species, making propagation of the virus simple. LCMV is a naturally occurring infection in

mice. This allows us to look at the normal *in vivo* response to infection in an animal model that shares many similarities with humans. LCMV is also a non-cytolytic virus, which means that any response that is occurring, cell death or otherwise, is being generated by the immune response, and not through viral-mediated cell death. Another reason LCMV is a strong candidate for viral infection studies is that there are acute and chronic viral strains of LCMV, with 5 gene mutations between acute LCMV-Armstrong and chronic LCMV-Clone 13 leading to two amino acid difference (Matloubian et al.,1993). Because of this, LCMV has become a staple viral infection used in studying *in vivo* viral infection responses in mouse models.

LCMV-Armstrong: An Acute Viral Infection

LCMV-Armstrong is an acute viral infection in mice. LCMV-Armstrong elicits a strong $CD8^+$ T cell response where the majority of the response is compromised of a two immunodominant epitopes (GP_{33-41}, $NP_{396-404}$) (Basler et al., 2004) (Probst et al., 2003) (Tewari et al., 2004) (van der Most et al., 1998) as well as several subdominant epitopes (Kotturi et al., 2007). The peak of the $CD8^+$ T cell response occurs around day 8 post-infection, and clearance of virus occurs between day 7-9 post-infection. The $CD8^+$ T cell response is required for viral clearance in LCMV-Armstrong infection, whereas the $CD4^+$ T cell response is dispensable (Matloubian et al., 1994). $CD8^+$ TECs and MPCs can be differentiated by flow cytometry starting at day 8 post-infection, when CD127

expression can be visualized by fluorescent antibody staining. LCMV-Armstrong generates a typical TEC and MPC response, which was characterized above, unlike LCMV-Clone 13, which generates an exhausted $CD8^+$ T cell population.

LCMV-Clone 13: Chronic Viral Infection

LCMV-Clone 13 varies from LCMV-Armstrong by 5 nucleotides and by 2 amino acids, GP1 (F260L) and L-polymerase (K1076Q) (Sullivan et al., 2011). Of these two amino acid substitutions, only GP1 (F260L) is believed to be responsible for persistent infection in mice. The F260L mutation in the GP1 receptor causes increased binding affinity for cellular receptor, α-dystroglycan, which is highly expressed on dendritic cells (Cao et al., 1998) (Sevilla et al., 2000) (Smelt et al., 2001). The point mutation allows LCMV-Clone 13 to displace extracellular matrix proteins and facilitate virus-receptor interaction (Kunz et al., 2001). This increased binding affinity to α-dystroglycan on dendritic cells also inhibits dendritic cell mediated T-cell anti-viral functions (Sevilla et al., 2000) (Smelt et al., 2001) which lead to viral persistence in the host and T cell exhaustion.

$CD8^+$ T Cell Exhaustion

T cell exhaustion is a unique state that T cells differentiate into during chronic stimulation. T cell exhaustion occurs often during chronic infection (Zajac et al., 1998) (Gallimore et al., 1998) or cancer (Lee et al., 1999) and is characterized by a decrease in effector function, an increase in inhibitory receptors, and eventual

deletion of pathogen-specific cells (Figure 1.2) (Zajac et al., 1998) (Wherry et al., 2003) (Moskophidis et al., 1993). Exhaustion is directly correlated with TCR signal strength, with immunodominant epitopes undergoing clonal deletion and sub-immunodominant epitopes becoming the major $CD8^+$ T cell response during chronic viral infection (Wherry et al., 2003). Exhausted $CD8^+$ T cells are unable to form a memory population (Wherry et al., 2004), and require epitope-specific TCR signals in order for long-term maintenance to occur (Shin et al., 2007).

Immunoregulation is a critical part of T cell exhaustion. The two major negative regulators during LCMV-clone 13 infection are cell surface inhibitory receptors and soluble factors. Inhibitory receptors play a critical role in self-tolerance and the prevention of autoimmunity (Freeman et al., 2006). Inhibitory receptors are expressed transiently during $CD8^+$ T cell activation, however, prolonged expression of inhibitory receptors is a hallmark of T cell exhaustion (Barber et al., 2005). The major inhibitory receptors known to play a critical role in $CD8^+$ T cell exhaustion are PD-1 (CD279), LAG-3, 2B4 (CD244), CD160, TIM-3, and CTLA-4. PD-1 affects $CD8^+$ T cell survival and proliferation (Petrovas et al., 2006) (Petrovas et al., 2007) (Blackburn et al., 2008a) (Blackburn et al., 2010), whereas LAG-3 affects $CD8^+$ T cell proliferation alone (Workman et al., 2004). The role of 2B4 and CD160 is not well defined during $CD8^+$ T cell exhaustion; however the number of inhibitory receptors expressed by the same $CD8^+$ T cell directly correlates with severity of exhaustion (Blackburn et al., 2008b).

Figure 1.2. Graded loss of function in CD8$^+$ T cell exhaustion during chronic viral infection

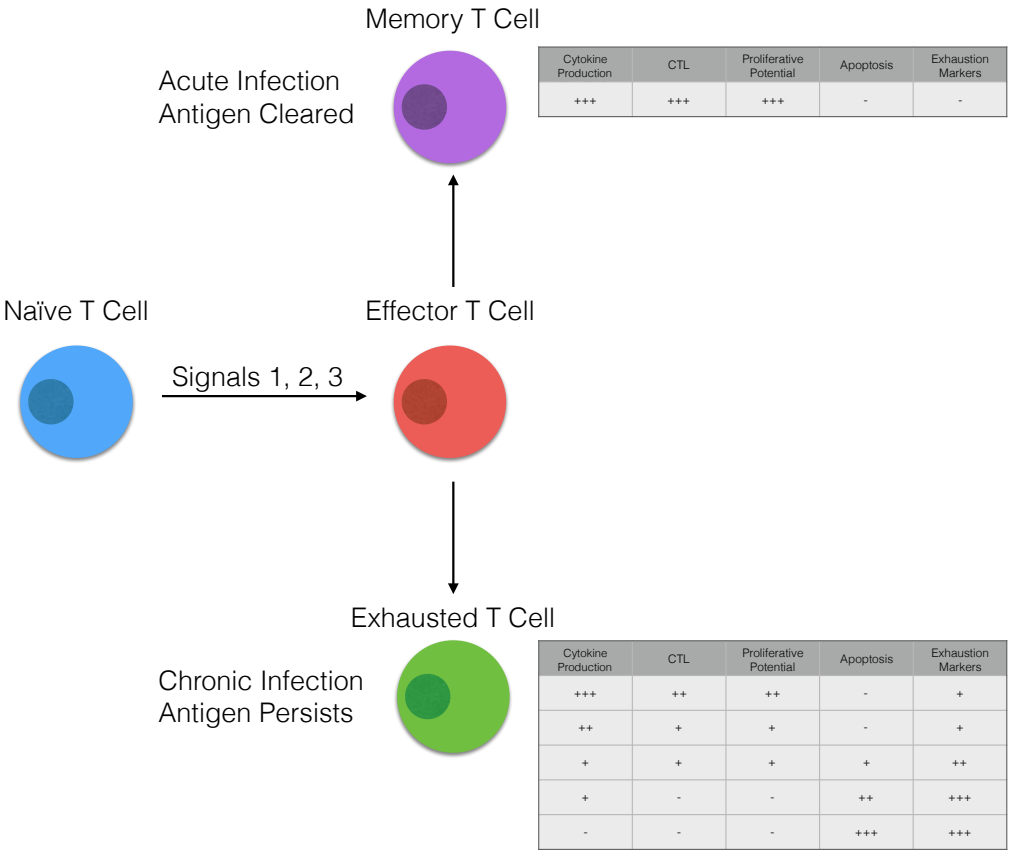

Cytokine Production	CTL	Proliferative Potential	Apoptosis	Exhaustion Markers
+++	+++	+++	-	-

Cytokine Production	CTL	Proliferative Potential	Apoptosis	Exhaustion Markers
+++	++	++	-	+
++	+	+	-	+
+	+	+	+	++
+	-	-	++	+++
-	-	-	+++	+++

Figure 1.2. Graded loss of function in $CD8^+$ T cell exhaustion during chronic viral infection

During infection with a virus, naïve pathogen-specific $CD8^+$ T cells become activated, clonally expand, and differentiate into effector $CD8^+$ T cells. Effector T cells are able to produce cytokines such as IFNγ and TNFα, and perform cytotoxic activities on infected host cells. Clearance of pathogen allows for formation of $CD8^+$ T cell memory. These memory cells produce high levels of IFNγ, TNFα, and IL-2, and are able to rapidly respond to reinfection by proliferating and performing effector functions. During chronic viral infection where antigen is not cleared, $CD8^+$ T cells differentiate into exhausted T cells. Exhausted $CD8^+$ T cells slowly lose the ability to produce cytokines, proliferate, or perform effector functions as they become more exhausted. They also express more inhibitory exhaustion markers (i.e. PD-1, 2B4, LAG-3, CD160) and undergo apoptosis as they become more exhausted.

Two major immunregulatory cytokines known to play a critical role during LCMV-clone 13 infection are IL-10 and TGFβ. IL-10 is produced by $CD4^+$ T cells and dendritic cells during LCMV-clone 13 infection (Brooks et al., 2006b) (Ejrnaes et al., 2006). Blockade of IL-10 has been shown to increase viral control and enhance T cell responses during LCMV-clone 13 infection (Brooks et al., 2006b) (Ejrnaes et al., 2006). TGFβ has also been shown to suppress $CD8^+$ T cell functionality during chronic viral infection, and blocking TGFβ signaling pathways in $CD8^+$ T cells leads to increased functionality and prevention of severe exhaustion in $CD8^+$ T cells (Tinoco et al., 2009).

Exhausted $CD8^+$ T cells are transcriptionally unique from TECs and MPCs, and are believed to be their own differentiation state (Wherry et al., 2007). Future work understanding transcriptional regulation of exhaustion in $CD8^+$ T cells will be critical for treatment of chronic infections and cancer systems where exhaustion occurs.

Thesis Objectives

ITK is a major downstream signaling component of the TCR signaling pathway. ITK is the first component downstream of TCR signaling that is not required for T cell activation; however, loss of ITK leads to sub-optimal T cell activation with a decrease in Ca^{2+} flux and DAG production. As a result ITK-deficient mice generate an innate-like population of $CD8^+$ T cells in response to LCMV-

Armstrong infection. To understand how sub-optimal TCR signaling impacted the transcriptional profile of these cells, we performed a microarray comparing ITK-deficient CD8SP thymocytes to WT controls. The most highly upregulated transcription factor in ITK-deficient cells was Runx2, whereas the most highly upregulated transcription factor in WT cells was IRF4. These results indicated that TCR signal strength positively regulated IRF4 expression levels, and TCR signal strength repressed Runx2 expression levels in $CD8^+$ T cells. Both IRF4 and Runx2 are upregulated upon activation of $CD8^+$ T cells; however, IRF4 is upregulated early after TCR signaling, whereas Runx2 is upregulated later during the clonal expansion phase and continues to stay upregulated through the memory phase of the $CD8^+$ T cell response. IRF4 was also chosen for our study because previous work in B cells indicated that IRF4 was upregulated in proportion to BCR signal intensity, and regulated differentiation of various B cell subsets upon activation. **Based on these data, we hypothesized that the strength of TCR signaling regulated IRF4 expression in activated $CD8^+$ T cells, as well as positively regulating $CD8^+$ T cell differentiation during viral infection. Due to the memory-like phenotype of ITK-deficient cells and the expression pattern of Runx2, we also hypothesized that Runx2 regulated $CD8^+$ T cell memory during viral infection.** These hypotheses have been addressed in this thesis in the following three chapters:

Chapter III: Graded Levels of IRF4 Regulate $CD8^+$ T Cell Differentiation and

Expansion during Acute LCMV Armstrong Infection: This chapter tests the hypothesis that TCR signal strength through affinity of peptide to TCR and peptide dose regulate expression levels of IRF4 in $CD8^+$ T cells, which in turn regulates the magnitude of the $CD8^+$ T cell effector response during LCMV-Armstrong infection.

Chapter IV: IRF4 Regulates the Ratio of Eomesodermin to T-bet in $CD8^+$ T Cells Responding to Persistent LCMV Infection: Results from chapter III indicated that IRF4 expression was regulated by TCR signal strength, and that IRF4 expression levels regulated the magnitude of the $CD8^+$ T cell response. One way IRF4 did this is through regulation of the transcription factors T-bet and Eomes. An optimal ratio of Eomes to T-bet is required for viral clearance during LCMV-Clone 13 infection, however, how this balance is maintained is not well understood. This chapter tests the hypothesis that IRF4 regulates the levels of T-bet to Eomes during LCMV-Clone 13 infection, and that a haplodeficiency in IRF4 will lead to a defect in viral clearance through skewed T-bet to Eomes ratios.

Chapter V: Runx2 is Required for Long-Term Persistence of Antiviral $CD8^+$ T Memory Cells during Acute LCMV-Armstrong Infection: This chapter tests the hypothesis that Runx2-deficiency will impact the pathogen-specific $CD8^+$ memory response during LCMV-Armstrong infection, and that Runx2 is inversely

correlated to TCR signal strength, and is potentially repressed by IRF4.

Chapter II:

Materials and Methods

Mice

Mice were bred and housed in specific pathogen-free conditions at the University of Massachusetts Medical School (UMMS) in accordance with institutional animal care and use committee guidelines.

Chapter III:

Irf4$^{fl/fl}$ *CD4-Cre*$^{+}$ and OT-I *Rag1*$^{-/-}$ *Irf4*$^{fl/fl}$ *CD4-Cre*$^{+}$ have been described previously (Nayar et al., 2012) (Klein et al., 2006). P14 *TCRα*$^{-/-}$ were purchased from Taconic Farms (Germantown, New York). *Irf4*$^{+/+}$ *CD4-Cre*$^{+}$, *Irf4*$^{+/fl}$, and *Irf4*$^{+/+}$ were used as wild-type (WT) controls.

Chapter IV:

Irf4$^{fl/fl}$ and *Eomes*$^{fl/fl}$ mice have been described previously (Klein et al., 2006) (Y. Zhu et al., 2010). *CD4-Cre*$^{+}$ transgenic mice were a gift from Joonsoo Kang (UMMS). *Irf4*$^{fl/fl}$ mice were crossed to *CD4-Cre*$^{+}$ transgenic mice at UMMS to generate *Irf4*$^{fl/fl}$ *CD4-Cre*$^{+}$ mice. P14 TCR transgenic TCRα$^{-/-}$ used for in-vitro studies were purchased from Taconic Farms (Germantown, New York) and crossed to *Irf4*$^{fl/fl}$ *CD4-Cre*$^{+}$ mice at UMMS. P14 TCR transgenic mice used for *in vivo* studies were a gift from Susan Kaech (Yale), and were crossed to *Irf4*$^{fl/fl}$ *CD4-cre*$^{+}$ mice to generate P14 *Irf4*$^{+/fl}$ *CD4-cre*$^{+}$ mice. *Eomes*$^{fl/fl}$ mice were purchased from The Jackson Labs (Maine) and crossed to *Irf4*$^{+/fl}$ *CD4-Cre*$^{+}$ at UMMS. *Irf4*$^{+/+}$ and *Irf4*$^{+/+}$ *CD4-Cre*$^{+}$ mice were used as WT controls.

Chapter V:

C57BL/6J mice were purchased from Jackson (Bar Harbor, ME) and bred in house. OT-I TCR transgenic *Rag2*$^{-/-}$ mice were purchased from Taconic Bioscience (Germantown, NY) and bred in house. *Runx2*$^{fl/fl}$ mice were a gift from Dr. Amjad Javed (University of Alabama at Birmingham) (H. Chen et al., 2011). *CD4-cre*$^{+}$ transgenic mice were a gift from Dr. Joonsoo Kang (UMMS). P14 TCR transgenic mice were a gift from Susan Kaech (Yale), and were crossed to *Runx2*$^{fl/fl}$ *CD4-cre*$^{+}$ transgenic mice. *Runx2*$^{+/+}$ and *Runx2*$^{+/+}$ *CD4-cre*$^{+}$ mice were used as WT controls. *Irf4*$^{+/fl}$ *CD4-cre*$^{+}$ and *Irf4*$^{fl/fl}$ *CD4-cre*$^{+}$ mice have been described previously (Nayar et al., 2012) (Klein et al., 2006).

Virus and Infections

Chapter III:

For virus infections, LCMV-Armstrong GP_{33} and F6L variants were injected i.p. at $5x10^4$ PFU, unless otherwise specified. For adoptive transfers, splenocytes from P14 WT CD45.1^{+}CD45.2^{+}, P14 *Irf4*$^{+/fl}$ CD45.2^{+}, OT-I WT CD45.1^{+}, or OT-I *Irf4*$^{+/fl}$CD45.2^{+} mice were stained with Abs to CD8α and Vα2 to determine the proportions of P14 or OT I cells, and equal numbers of WT and *Irf4*$^{+/fl}$ cells were mixed. Total P14 cells (2,000, 20,000, or 1,000,0000) were transferred i.v. into WT or CD45.1^{+} hosts 1 day prior to infection.

Chapter IV:

LCMV-clone 13 stocks were propagated in baby hamster kidney 21 cells at UMMS (Welsh & Seedhom, 2008) and were generously provided by Dr. Raymond M. Welsh and amplified by us. Adult male mice (6–9 weeks old) were infected with an exhausting dose, $2x10^6$ PFU of LCMV-clone 13 i.v. For adoptive transfers, $1x10^4$ WT or *Irf4*$^{+/fl}$ P14 cells were i.v. transferred into WT *CD4-Cre*+ host mice one day prior to infection.

Chapter V:

Adult male mice (7-11 weeks old) were infected with LCMV-Armstrong at $5x10^4$ PFU i.p. For rechallenge, mice were infected with LCMV-Clone 13 at $2x10^6$ PFU i.v. LCMV-Armstrong and LCMV-Clone 13 were graciously provided by Dr. Raymond Welsh (UMMS). For co-adoptive transfers, splenocytes from P14 WT CD4-cre$^+$ CD90.1$^+$ CD90.2$^+$ and P14 *Runx2*$^{fl/fl}$ CD4-cre$^+$ CD90.1$^+$ were stained with antibodies to CD8α and Vα2 to determine proportions of P14 cells, and equal numbers of WT and *Runx2*$^{fl/fl}$ cells were mixed. 10,000 P14 cells were transferred i.v. into CD90.2$^+$ host mice 1 day prior to infection.

Viral Titers

Chapter III:

Spleens were harvested at day 8 postinfection (p.i.), homogenized in media and stored at -80°C.

Chapter IV:

Sera, livers and kidneys were harvested from infected mice at the indicated time points post-infection (p.i.). Organs were homogenized in one ml of complete RPMI media and stored at -80°C. LCMV-clone 13 virus titers were determined by plaque assays as previously described (Welsh & Seedhom, 2008).

Chapter V:

Spleens and fat pads were harvested 9 days post LCMV Armstrong infection. For rechallenge, kidneys and livers were harvested 4 days post LCMV Clone 13 infection. Organs were homogenized in 1ml RPMI media and stored at -80°C. Plaque assays were performed as described previously (Welsh & Seedhom, 2008).

Cell Culture

Chapter III:

Lymph node cells from P14 WT and P14 *Irf4*$^{+/fl}$ mice were mixed with equal numbers of WT CD45.1 splenocytes and stimulated with $GP_{33–41}$ epitope (GP_{33}) or F6L peptides for 24, 48, and 72 hours. Cells were harvested and analyzed for IRF4, Eomes, and TCF1 expression by intracellular staining. For cytokine production, splenocytes from infected mice were stimulated with GP_{33}, GP_{276},

and NP_{396} peptide for 5 hours in the presence of 1 mg/ml GolgiStop and 1 mg/ml GolgiPlug, and Abs to CD107a and CD107b.

Chapter IV:

Lymph node cells from P14 WT, P14 *Irf4*$^{+/fl}$ or P14 *Irf4*$^{fl/fl}$ mice were mixed with equal numbers of WT CD45.1 splenocytes and stimulated with $GP_{33–41}$ or F6L peptides for 24, 48, and 72 hours. Cells were harvested and analyzed for T-bet and Eomes expression by intracellular staining. For cytokine staining, cells were stimulated *ex vivo* with 1µg/ml $GP_{276-286}$ or GP_{33-41} peptide for 5 hours at 37°C.

Chapter V:

Splenocytes from OT-I TCR transgenic mice were stimulated with OVA, T4, or G4 peptide with indicated doses for 72 hours. Cells were harvested and analyzed for Runx2, Eomes, and CD44 expression by intracellular staining. For cytokine experiments, IFNβ and IL-12 were purchased from R&D Systems (Minneanapolis, MN). IL-7 and IL-15 were purchased from Peprotech (Rocky Hill, NJ). OVA, T4, and G4 peptides were purchased from 21st Century Biochemicals (Marlborough, MA). Imiquimod was purchased from invivogen (San Diego, CA). LPS was purchased from Sigma (St. Louis, MO). Splenocytes from *Irf4*$^{+/+}$ CD4-cre^{+}, *Irf4*$^{+/fl}$ CD4-cre^{+}, and *Irf4*$^{fl/fl}$ CD4-cre^{+} mice were isolated and plated with platebound anti-CD3 /CD28 for 72 hours. Cells were harvested and analyzed for Runx2, Eomes, and CD44 expression by intracellular staining. For cytokine

production, splenocytes from infected mice were stimulated with GP_{33-41}, $GP_{276-286}$, and $NP_{396-404}$ peptide for 4 hours in the presence of 1µg/ml GolgiStop and 1µg/ml GolgiPlug, and antibodies to CD107a and CD107b. GP_{33-41}, $GP_{276-286}$, and $NP_{396-404}$ peptides were generously provided by Dr. Raymond Welsh (UMMS) and generated by Keith Daniels.

Antibody and H2-D^b Tetramer Staining

Chapter III:

Antibodies binding to the following were purchased:

CD45.2 (V500) and TNFα (APC-Cy7) were purchased from BD Biosciences (San Jose, CA). KLRG1 (FITC), Eomes (PE), CD107a (PE), CD107b (PE), CD27 (PE), CD127 (PE-Cy5), CD127 (PerCP-Cy5.5), T-bet (PerCP-Cy5.5), IFNγ (PerCP-Cy5.5), Eomes (PerCP-efluor710), CD45.1 (PECy7), KLRG1 (PE-Cy7), T-bet (PE-Cy7), IRF4 (Alexa Fluor 647), CD44 (Alexa Fluor 700), CD62L (APC-eFluor780), CD44 (eFluor450), KLRG1 (eFluor450), IFNγ (eFluor450), CD90.2 (APC-eFluor780), CD45.1 (APC-eFluor780), IL-2 (PerCP-Cy5.5) were purchased from eBioscience (San Diego, CA). CD8α (PE-TexasRed), granzyme B (PE), granzyme B (APC), Live-Dead-Violet, Live-Dead-Aqua and goat-anti-rabbit IgG (Alexa Fluor 647) and (Alexa Fluor 488) were purchased from Life Technologies (Grand Island, NY). $H2D^b$-GP_{33} monomers were prepared at the University of Massachusetts Medical School; LCMV-specific ($H2D^b$-NP_{396} and $H2D^b$-GP_{276}) monomers were obtained from the NIH Tetramer Core Facility (Atlanta, GA).

Intracellular TCF1 staining was performed using rabbit-anti-mouse TCF1 (Cell Signaling Technology, Danvers, MA), followed by staining with goat-anti-rabbit secondary (Life Technologies). Samples were analyzed on an LSRII flow cytometer (BD Biosciences), and data were analyzed using FlowJo (Tree Star).

Chapter IV:

Antibodies to the following were purchased:

Eomes (PE), CD244.2 (PE), T-bet (PerCP-Cy5.5), Eomes (PerCP-eFluor710), CD223 (PerCP-eFlour710), TNFα (PerCP-eFluor710), T-bet (PE-Cy7), IFNγ (eFluor450), IL-2 (APC), and CD279 (APC) were purchased from eBioscience (San Diego, CA). CD160 (PE-CF594) was purchased from BD (Billerica, MA). CD8α (PE-TexasRed), Granzyme B (PE), Live/Dead Fixable Aqua Dead Cell Stain Kit were purchased from Life Technologies (Grand Island, NY). $H2D^b$-GP_{33} monomers were prepared at UMMS; LCMV-specific $H2D^b$-GP_{276} and $H2D^b$-GP_{33} monomer were obtained from the NIH Tetramer Core Facility (Atlanta, GA). Single cell suspensions from spleens were prepared, RBC lysed and F_c receptors were blocked using supernatant from 2.4G2 hybridomas. Cells were stained with $H2D^b$-GP_{276} or $H2D^b$-GP_{33} tetramers prior to staining with cell-surface antibodies. For cytokine staining, cells were stimulated *ex vivo* with 1µg/ml $GP_{276-286}$ or GP_{33-41} peptide for 5 hours at 37°C. LCMV peptides $GP_{276-286}$ (SGVENPGGYCL), GP_{33-41} (KAVYNFATC) and F6L (KAVYN- LATC) were synthesized and HPLC purified by 21st century Biochemicals (Marlboro, MA). Peptides were ~90% pure.

Intracellular cytokine staining was performed using BD Cytofix/CytopermTM Fixation/Permeabilization Solution kit. Intracellular transcription factor staining was performed using eBioscience Foxp3/transcription factor staining kit, as per manufacturer's instructions, unless specified. All samples were analyzed on an LSRII flow cytometer (BD Biosciences), and data were analyzed using FlowJo (Tree Star).

Chapter V:

Antibodies to the following were purchased:

CD127 (FITC), Bcl2 (PE), Bcl6 (PE), IRF4 (PE), CD8α (PE-eFluor 610), TNFα (PerCP-eFluor 710), Eomes (PerCP-eFluor 710), CD122 (PerCP-eFluor 710), T-bet (Pe-Cy7), CD44 (PE-Cy7 and Alexa Fluor 700), KLRG1 (PE-Cy7 and eFluor 450), IFNγ (eFluor 450), IL-2 (APC), Vα2 (APC), CD27 (APC-eFluor 780), and CD90.2 (APC-eFluor 780) antibodies were purchased from eBioscience (San Diego, CA). CD107a (FITC), CD107b (FITC), CD62L (FITC), 7-AAD, AnnexinV (PE), and CD90.1 (V500) were purchased from BD (Billerica, MA). Antibodies to Granzyme B (PE), Live/Dead Violet, Live/Dead Aqua, and Goat α Rabbit (Alexa Fluor 647) were purchased from LifeTech (Grand Island, NY). H2-D^b GP_{33-41}, H2-D^b $GP_{276-286}$, H2-D^b $NP_{396-404}$ monomers were obtained from the NIH Tetramer Core Facility (Atlanta, GA). Runx2 and TCF1 antibodies were purchased from Cell Signaling Technologies (Danvers, MA). Single cell suspensions from spleens, bone marrow, lymph nodes, lung, and liver were prepared, RBC lysed,

and Fc receptors were blocked using supernatant from 2.4G2 hybridomas. Lymphocytes were isolated from lung and liver using Lympholyte-M (CedarLane; Burlington, NC), and perfusion was performed on mice to prevent contamination of blood lymphocytes in these preparations. Cells were stained with H2-D^b GP_{33-41}, H2-D^b $GP_{276-286}$, and H2-D^b $NP_{396-404}$ tetramers prior to staining with cell surface antibodies. For cytokine staining, cells were stimulated *ex vivo* with 1ug/ml GP_{33-41}, $GP_{276-286}$, or $NP_{396-404}$ for 4 hours at 37°C. Intracellular cytokine staining was performed using BD Cytofix/Cytoperm™ Fixation/Permeabilization Solution kit. Intracellular transcription factor staining was performed using eBioscience FoxP3/transcription factor staining kit. Samples were analyzed on the LSRII flow cytometer (BD Bioscience), and data was analyzed on FlowJo (Tree Star).

LCMV-Specific Antibody Titers

To quantify LCMV-specific antibody titers, high-binding 96 well flat bottom ELISA plates (Corning) were coated overnight at room temperature with cell lysate from LCMV-clone 13 infected BHK21 cells. Plates were washed, blocked and three-fold serial dilutions of serum samples were plated. Plates were washed again and incubated with horseradish peroxidase labeled goat anti-mouse IgG detection antibody (Bethyl labs) and developed using 3,3',5,5'-Tetra-methylbenzidine substrate. The reaction was quenched 0.18M H_2SO_4 ELISA stop solution (Bethyl Labs) and the optical density (OD) was measured at 450nm

using an Emax Endpoint ELISA microplate reader (Molecular Devices). LCMV-specific antibody titers were determined by end-point titer method and two times the mean OD of uninfected control sera was used as the cut-off.

Statistical Analysis

Chapters III, V:

All data are represented as mean ± SEM. Statistical significance is indicated by $^{ns}p > 0.05$, $^{*}p \leq 0.05$, $^{**}p \leq 0.01$, $^{***}p \leq 0.001$, and $^{****}p \leq 0.0001$, based on unpaired student *t* test.

Chapter IV:

All data are represented as mean ± SEM. Statistical significance is indicated by $^{ns}p > 0.05$, $^{*}p \leq 0.05$, $^{**}p \leq 0.01$, $^{***}p \leq 0.001$, and $^{****}p \leq 0.0001$, based on unpaired student *t* test. For outlined day 112-114 samples, statistical significance is indicated by $p ≤ 0.05 and $$p ≤ 0.01. Statistical analysis was performed using unpaired t test with Welch's correction, ordinary one-way ANOVA using Tukey's multiple comparison test or Log-rank (Mantel-Cox) test as indicated in the figure legend.

Chapter III: Graded Levels of IRF4 Regulate CD8$^+$ T Cell Differentiation and Expansion during acute LCMV Armstrong infection

Attributions and Copyright Information

The data described in this chapter were published in the Journal of Immunology in 2014.

Graded Levels of IRF4 Regulate $CD8^+$ T Cell Differentiation and Expansion, but not Attrition, in Response to Acute Virus Infection

Ribhu Nayar, Elizabeth Schutten, Bianca Bautista, Keith Daniels, Amanda L Prince, Megan Enos, Michael A Brehm, Susan L Swain, Raymond M Welsh, and Leslie J Berg

Specific Contribution to Figures: Ribhu Nayar performed, designed, and analyzed all experiments described in figure 3.1 through 3.12. Elizabeth Schutten performed and analyzed experiments described in figure 3.3, 3.5, 3.7-9, 3.12.

Oral consent was received from Ribhu Nayar to include work from this manuscript in the dissertation.

Introduction

In response to acute infections, $CD8^+$ T cells undergo priming, differentiation, and expansion to generate robust effector responses that are required for Ag clearance (Williams & Bevan, 2007) (Kaech & Wherry, 2007). At the termination of the response, the majority of these effector $CD8^+$ T cells die by apoptosis, whereas a small population of efficient memory T cells survives. These memory $CD8^+$ T cells are primed for rapid proliferation and effector functions upon reinfection.

The magnitude and quality of the $CD8^+$ T cell response to an infection is influenced by many factors, including the affinity of TCR-peptide/MHC interactions, the Ag load, costimulatory molecule expression, and the inflammatory cytokine environment. Differences in TCR affinity do not affect the initial activation of Ag-specific $CD8^+$ T cells, but at later time points, T cells with the highest affinity for the Ag dominate the response (Zehn et al., 2009). Similarly, Ag load does not influence the numbers of $CD8^+$ T cells at the early expansion phase but does regulates the size of the overall response at the peak of infection (Badovinac et al., 2002) (Mercado et al., 2000) (Prlic et al., 2006). To date, the molecular mechanisms linking TCR affinity and Ag density to the magnitude of the $CD8^+$ T response have not been characterized.

$CD8^+$ T cell responses to acute infections are also regulated by variations in transcription factor expression. High expression of T-bet and Blimp-1 drive the

differentiation of primed $CD8^+$ T cells into terminal effectors, whereas T cell factor 1 (TCF1) and Eomesodermin (Eomes) are important for the generation and maintenance of memory cells (Rutishauser et al., 2009) (Joshi et al., 2007) (Kallies et al., 2009) (Zhou et al., 2010) (Banerjee et al., 2010) (Jeannet et al., 2010). Although the cytokine milieu influences the transcription factor profile of activated $CD8^+$ T cells (Joshi et al., 2007) (Cui et al., 2011), how these different molecular programs are initially established is not known.

The transcription factor IRF4 is upregulated by BCR and TCR signaling (Matsuyama et al., 1995) (Eisenbeis et al., 1995). In B cells, different levels of IRF4 regulate differentiation to Ab-secreting plasma cells versus germinal center cells (Sciammas et al., 2006). In T cells, IRF4 is required for the differentiation of helper $CD4^+$ T cell subsets, functional regulatory T cells, and effector and innate like $CD8^+$ T cells (Mittrücker et al., 1997) (Lohoff et al., 2002) (Rengarajan et al., 2002) (Staudt et al., 2010) (Brüstle et al., 2007) (Huber et al., 2012) (Chung et al., 2009) (Zheng et al., 2009) (Cretney et al., 2011) (Nayar et al., 2012). Furthermore, IRF4 was initially found to be required for normal T cell responses to acute lymphocytic choriomeningitis virus (LCMV) infection (Mittrücker et al., 1997). However, the role of IRF4 in $CD8^+$ T cell differentiation to acute infections has not been characterized in detail, and importantly, the regulation of this process by distinct levels of IRF4 has not been investigated. In this study, we show that variations in Ag dose or in the affinity of TCR–peptide/MHC interactions lead to different levels of IRF4 expression in $CD8^+$ T cells. In turn,

these differences regulate the magnitude of the $CD8^+$ T cell response to acute virus infection at the peak of the infection without having any substantial effect on $CD8^+$ T cell attrition. Eomes and TCF1 expression are highly sensitive to distinct levels of IRF4, whereas the effects of IRF4 on T-bet expression are dependent on the nature of the infection. These data indicate that IRF4 is a key factor that links signals from the TCR to the transcriptional programming of $CD8^+$ T cells.

Results

The strength of TCR signaling regulates the levels and duration of transcription factor expression

The expression of IRF4 is upregulated in naive T cells by TCR signaling (Matsuyama et al., 1995). This response is dependent on the activation of the Tec kinase Itk (Nayar et al., 2012). To determine whether the levels of IRF4 were affected by the strength of TCR signaling to stimulation by natural ligands, P14 TCR transgenic TCRα$^{-/-}$ (hereafter referred to as P14 WT) CD8^{+} T cells (Pircher et al., 1989) were stimulated in vitro, and IRF4 levels were examined by intracellular staining. The P14 TCR recognizes the GP_{33} of LCMV bound to H2-D^{b}. A single amino acid substitution from phenylalanine to leucine at position six generates a lower affinity peptide ligand, F6L (Gronski et al., 2004). F6L–H2-D^{b} complexes display ~5-fold reduction in the equilibrium dissociation constant (K_D) for binding to the P14 TCR, and 100- to 1,000- fold reduction in functional avidity.

P14 T cells were stimulated with the high-affinity GP_{33} peptide and the lower affinity F6L variant. At 24 hours, both populations of cells expressed similar amounts of IRF4. However, high IRF4 expression was sustained at 48 and 72 hours post-stimulation in cells stimulated with GP_{33} peptide, whereas cells stimulated with F6L peptide showed declining IRF4 as early as 48 hours post-activation (Figure 3.1A). Histograms showing IRF4 staining on IRF4-deficient P14 T cells (*Irf4*$^{fl/fl}$) stimulated with the GP_{33} peptide are included as negative

Figure 3.1. Variations in TCR affinity and Ag dose upregulate IRF4, Eomes, and TCF1 to different levels

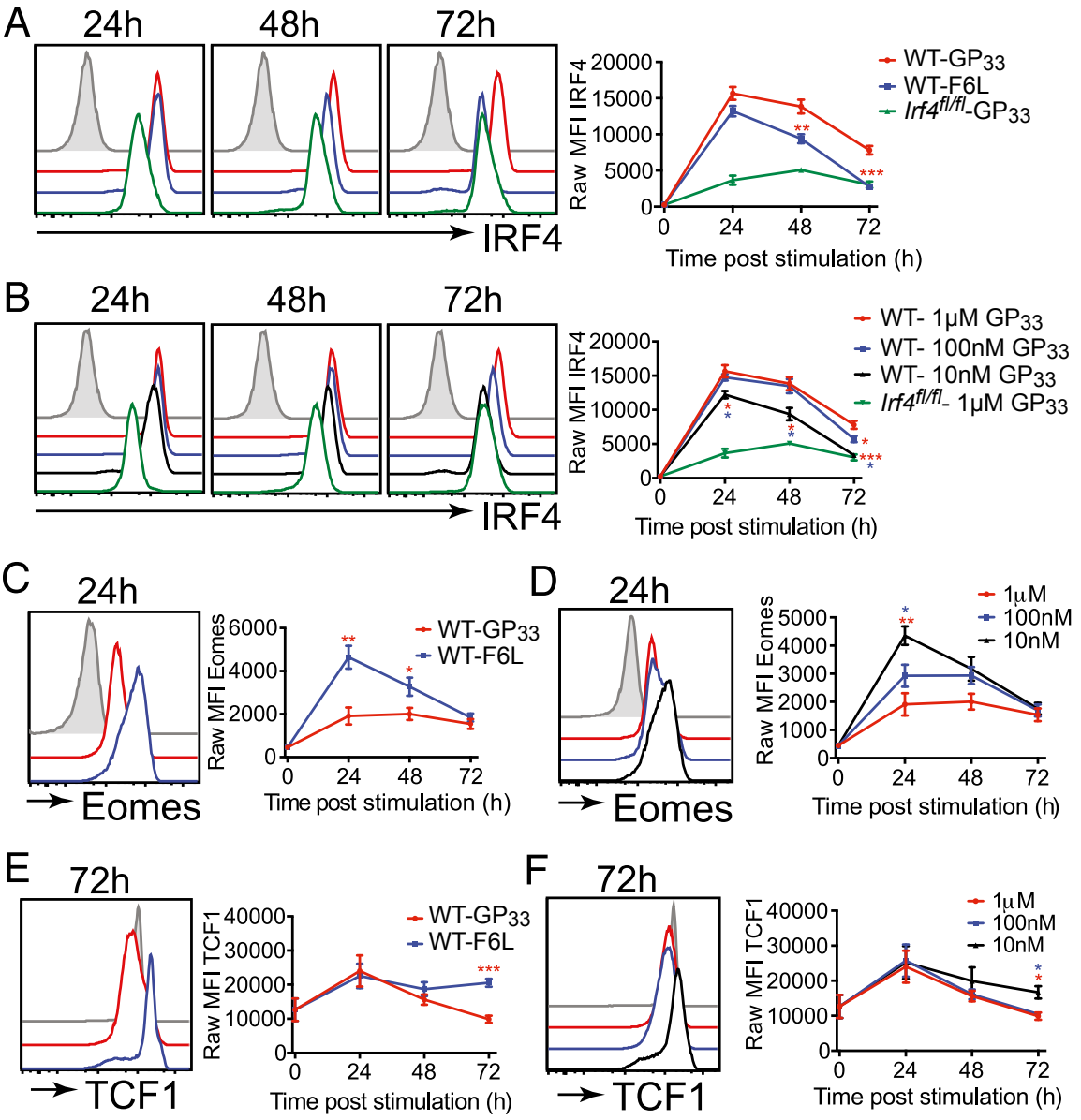

Figure 3.1: Variations in TCR affinity and Ag dose upregulate IRF4, Eomes, and TCF1 to different levels

P14 WT and P14 *Irf4*$^{fl/fl}$ were stimulated *in vitro*. At 0, 24, 48, and 72 hours, cells were stained and analyzed for IRF4, Eomes, and TCF1 expression. Histograms show gated live CD8^{+}CD45.2^{+} CD44^{hi} T cells. Gray histograms show staining on direct *ex vivo* CD8^{+}CD45.2^{+} P14 WT cells. P14 *Irf4*$^{fl/fl}$ cells stimulated with 1mM GP_{33} peptide are included as negative staining controls for IRF4 expression. Data are representative of four independent experiments. Graphs are compilations of raw MFI of gated live CD8^{+}CD45.2^{+}CD44^{hi} T cells. **(A, C,** and **E)** P14 WT T cells were stimulated with 1mM GP_{33} or F6L peptide. *, significant differences in MFI of WT cells stimulated with GP_{33} versus F6L ligands. **(B, D,** and **F)** P14 WT cells were stimulated with the indicated doses of GP_{33} peptide. **(B)** 1mM and 100nM stimulation conditions were significantly different for IRF4 100nM at all time points. **(D)** 10nM stimulation was significantly different from 1mM and 100nM at 24 hours. **(F)** 10nM stimulation was significantly different from 1mM and 100nM at 72 hours. *$p \leq 0.05$, **$p \leq 0.01$, ***$p \leq 0.001$.

controls. Alterations in peptide dose also impacted IRF4 expression. As shown, higher doses of GP_{33} peptide (1mM and 100nM) induced strong IRF4 expression at 24 and 48 hours post-stimulation relative to the 10nM stimulation condition (Figure 3.1B). By 72 hours, differences in IRF4 levels were observed between each of the peptide doses, with the highest peptide dose leading to the most sustained IRF4 expression (Figure 3.1B). These data indicate that expression of IRF4 is transient and is regulated by the strength of TCR stimulation.

In $CD8^+$ T cells, IRF4 negatively regulates the expression of Eomes: a transcription factor that is required for the maintenance of memory cells post-infection (Banerjee et al., 2010) (Nayar et al., 2012). As shown in Figure 3.1C, stimulation with the lower affinity F6L peptide resulted in higher Eomes expression, correlating with its reduced IRF4 expression. Similar results were seen with diminishing doses of GP_{33} peptide (Figure 3.1D). Eomes expression in $CD8^+$ T expression at 72 hours, 10nM stimulation was significantly different from 1mM and cells is positively regulated by the transcription factor, TCF1 (Zhou et al., 2010). As shown in Figure 3.1E, stimulation with GP_{33} or F6L peptide resulted in similar TCF1 expression 24 hours post-activation; however, at later time points, TCF1 remained highest in cells stimulated with the lower affinity F6L ligand. A similar pattern was seen with the lowest dose of GP_{33} peptide (Figure 3.1F). Taken together, these data demonstrate that varying TCR signal strength, either by changes in TCR-MHC/peptide affinity or dose, leads to distinct expression patterns of three key transcription factors in $CD8^+$ T cells.

Figure 3.2. *Irf4* regulates Eomes and TCF1 expression in a dose-dependent manner

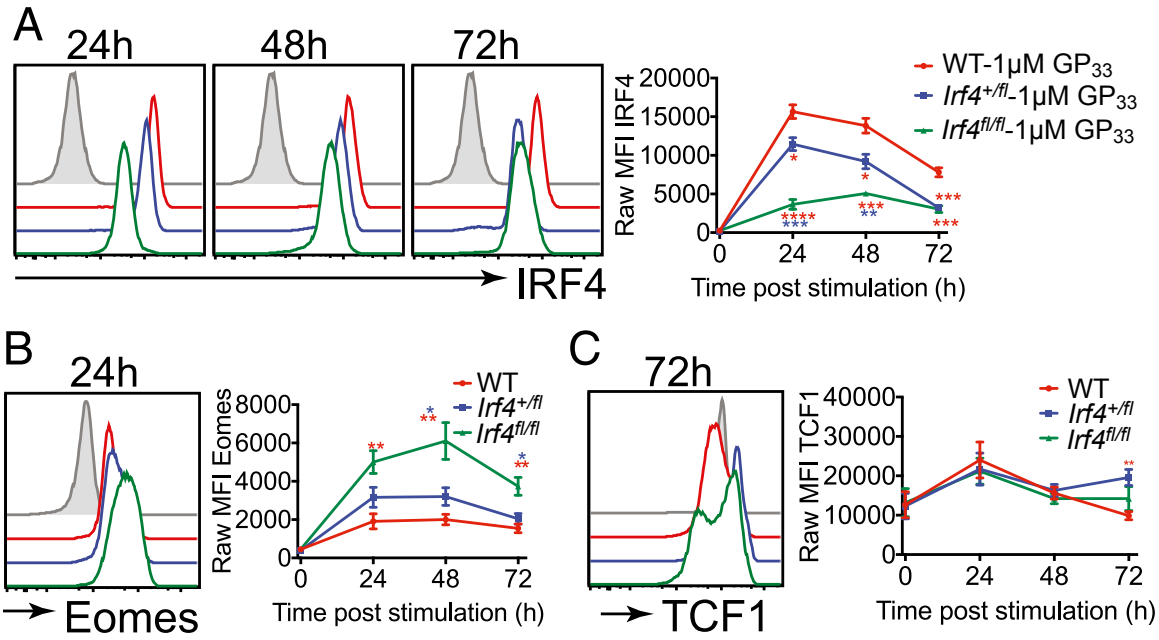

Figure 3.2: *Irf4* regulates Eomes and TCF1 expression in a dose-dependent manner

(A–C) P14 WT, P14 *Irf4*$^{+/fl}$, and P14 *Irf4*$^{fl/fl}$ cells were stimulated with 1mM GP_{33} peptide for the indicated time points, and cells were stained and analyzed for IRF4, Eomes, and TCF1 expression. Histograms show gated live CD8^{+}CD45.2^{+}CD44^{hi} T cells. Gray histograms show staining on direct ex vivo CD8^{+}CD45.2^{+} P14 WT cells. Data are representative of four independent experiments. Graphs are compilations of raw MFI of gated live CD8^{+}CD45.2^{+}CD44^{hi} T cells. **(A)** IRF4 expression was significantly different between all genotypes at 24 and 48 hours and between P14 WT and P14 *Irf4*$^{+/fl}$ cells and P14 WT and P14 *Irf4*$^{fl/fl}$ cells at 72 hours. **(B)** P14 WT and P14 *Irf4*$^{fl/fl}$ cells were significantly different at all time points, whereas P14 *Irf4*$^{+/fl}$ and P14 *Irf4*$^{fl/fl}$ cells were significantly different at 48 and 72 hours. **(C)** TCF1 expression was significantly different between P14 WT and P14 *Irf4*$^{+/fl}$ cells at 72 hours. *p ≤ 0.05, **p ≤ 0.01, ***p ≤ 0.001, ****p ≤ 0.0001.

To determine whether IRF4 regulated the expression of Eomes and/or TCF1, we used P14 T cells with one or two alleles of Irf4 deleted (*Irf4*$^{+/fl}$ x *CD4-Cre* and *Irf4*$^{fl/fl}$ x *CD4-Cre*, referred to as *Irf4*$^{+/fl}$ and *Irf4*$^{fl/fl}$, respectively). For these studies, P14 WT, P14 *Irf4*$^{+/fl}$, and P14 *Irf4*$^{fl/fl}$ T cells were stimulated in vitro with GP_{33} peptide. As expected, WT cells expressed the highest levels of IRF4, whereas *Irf4*$^{+/fl}$ cells expressed intermediate levels of IRF4 relative to *Irf4*$^{fl/fl}$ and WT cells 24 and 48 hour time points (Figure 3.2A); furthermore, this pattern of expression showed a striking similarity to that seen following stimulation of WT P14 T cells with the lower affinity F6L ligand or with lower doses of GP_{33} peptide (compare Figure 3.2A with Figure 3.1A-B). Eomes expression inversely correlated with IRF4 levels; P14 *Irf4*$^{fl/fl}$ cells expressed the highest levels of Eomes, with *Irf4*$^{+/fl}$ T cells expressing intermediate levels of Eomes compared with WT cells (Figure 3.2B). TCF1 expression was elevated in *Irf4*$^{fl/fl}$ and *Irf4*$^{+/fl}$ cells at the 72 hour time point relative to the WT samples with *Irf4*$^{+/fl}$ cells expressing the highest levels of TCF1 (Figure 3.2C). These data indicate that a complete or heterozygous deficiency in *Irf4* leads to lower expression of IRF4, and in turn, this alteration changes the expression patterns of Eomes and TCF1 in stimulated $CD8^+$ T cells.

Figure 3.3. Reduced gene dosage of *Irf4* limits CD8$^+$ T cell clonal expansion at the peak of the response without affecting attrition (GP_{33})

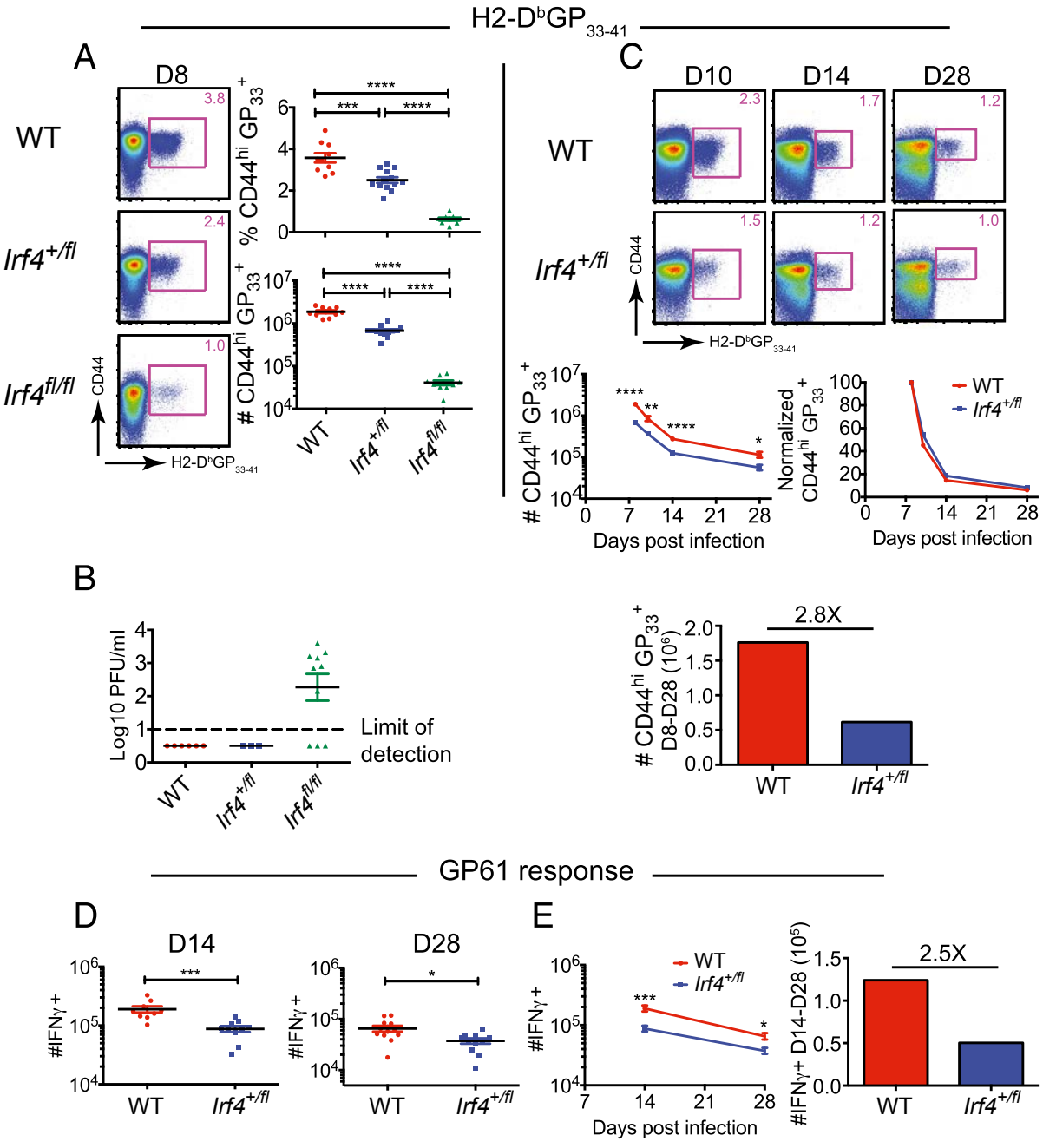

Figure 3.3. Reduced gene dosage of *Irf4* limits CD8$^+$ T cell clonal expansion at the peak of the response without affecting attrition (GP_{33})

Splenocytes from LCMV-infected WT, *Irf4*$^{+/fl}$, and *Irf4*$^{fl/fl}$ mice were analyzed at days 8, 10, 14, and 28 p.i. **(A)** Dot plots show CD44 versus H2 D^b-GP_{33} tetramer staining on gated live CD8$^+$ T cells. Graphs on right show a compilation of percentages and numbers from day 8 p.i. **(B)** LCMV titers in spleen at day 8 p.i. Dotted line indicates limit of detection. **(C)** Dot plots show CD44 versus H2 D^b-GP_{33} tetramer staining on gated live CD8$^+$ T cells at indicated time points post-infection. Graphs show the compilation of total numbers of CD44^{hi} GP_{33}-specific T cells **(left)** and proportions of CD44^{hi} GP_{33}–specific T cells at each time point normalized to the numbers at day 8 **(right)**. The graph below shows the differences in the numbers of CD44^{hi} GP_{33}–specific T cells between days 8 and 28 p.i. (i.e., average number day 8 - average number day 28) for each genotype; the number on the graph indicates the fold difference in the average numbers of WT cells lost between days 8 and 28 relative to the loss of *Irf4*$^{+/fl}$ cells. Data are from two or more independent experiments with at least six mice per group per time point. **(D)** Splenocytes from LCMV-infected WT and *Irf4*$^{+/fl}$ mice at days 14 and 28 p.i. were stimulated for 5 hours with GP61 peptide and analyzed for IFNγ expression. Graphs show a compilation of data indicating the numbers of IFNγ–producing cells at day 14 **(left)** and day 28 **(right)** p.i. **(E)** Graphs show the average numbers at days 14 and 28 p.i. to indicate the rate of attrition **(left)**; bar graph indicates the loss of GP61-specific cells at day 14 versus day 28 p.i.

(right); the number on the bar graph indicates the fold difference in the average numbers of WT cells lost between days 8 and 28 relative to the loss of *Irf4*$^{+/fl}$ cells. *p ≤ 0.05, **p ≤ 0.01, ***p ≤ 0.001, ****p ≤ 0.0001.

Figure 3.4. Reduced gene dosage of *Irf4* limits CD8$^+$ T cell clonal expansion at the peak of the response without affecting attrition (GP_{276}/NP_{396})

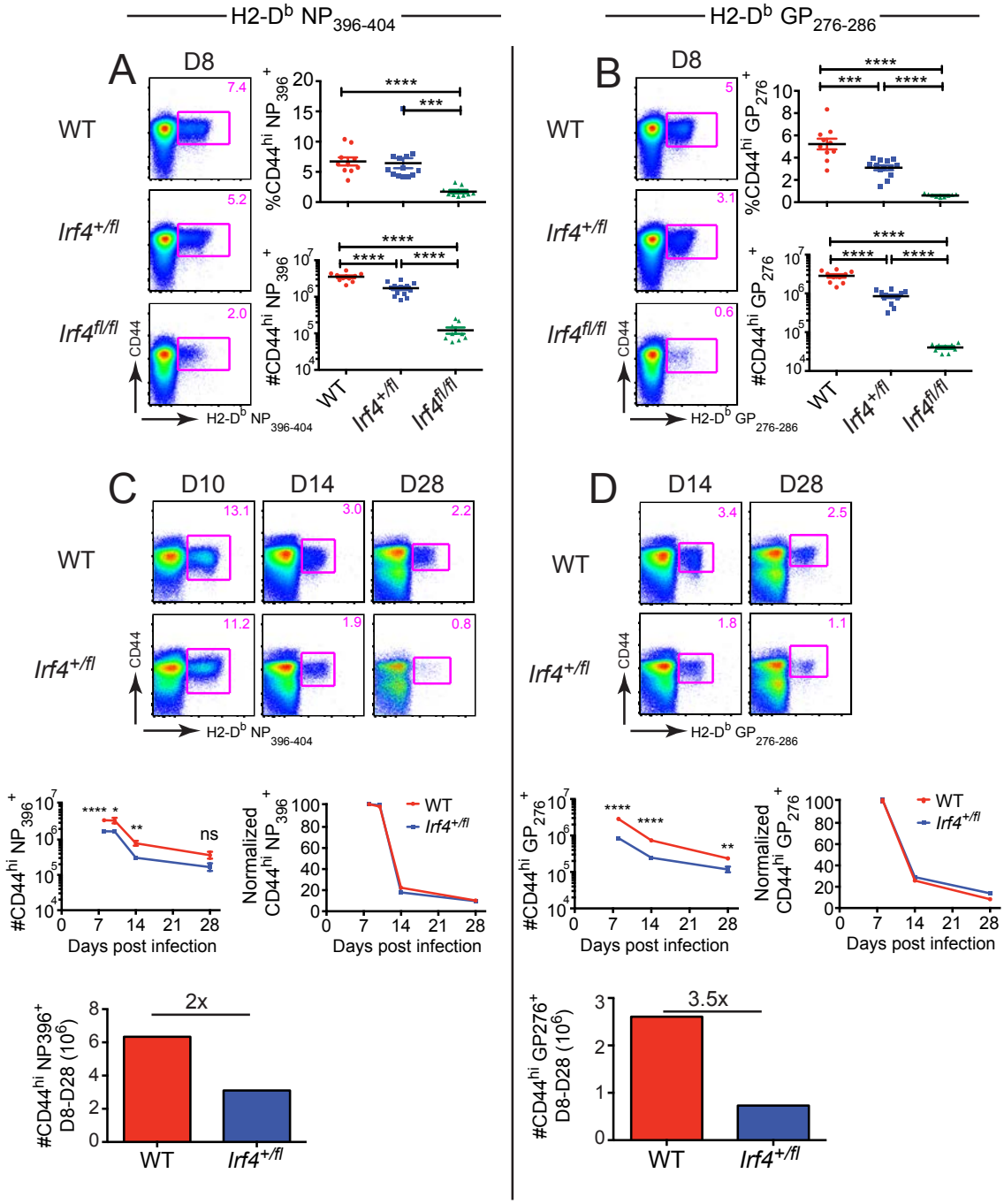

Figure 3.4: Reduced gene dosage of *Irf4* limits CD8$^+$ T cell clonal expansion at the peak of the response without affecting attrition (GP_{276}/NP_{396})

Splenocytes from LCMV-GP_{33}-infected WT, *Irf4*$^{+/fl}$, and *Irf4*$^{fl/fl}$ mice were analyzed at day 8, 10, 14 and 28 post-infection. Dot plots show CD44 vs H2 D^b-NP_{396} **(A)** or CD44 vs H2 D^b-GP_{276} **(B)** tetramer staining on gated live CD8$^+$ T cells on day 8 p.i.. Graphs on right show a compilation of percentages and numbers from day 8 p.i. Dot plots show CD44 vs H2 D^b-NP_{396} **(C)** or CD44 vs H2 D^b-GP_{276} **(D)** tetramer staining on gated live CD8$^+$ T cells from the indicated timepoints p.i. Graphs show compilations of the total numbers of virus-specific T cells **(left)**, the numbers of virus-specific T cells at later timepoints normalized to the numbers present at day 8 p.i **(right)**. The graph below shows the differences in the numbers of CD44^{hi} GP_{33}-specific T cells between day 8 and day 28 p.i (i.e., average # day 8 – average # day 28) for each genotype; the number on the graph indicates the fold difference in the average numbers of WT cells lost between day 8 and day 28 relative to the loss of *Irf4*$^{+/fl}$ cells. Data are from 2 or more independent experiments with at least 6 mice per group per timepoint.

A heterozygous deficiency in Irf4 reduces virus-specific CD8$^+$ T cell clonal expansion

To elucidate the role of graded IRF4 expression during polyclonal CD8$^+$ T cell differentiation *in vivo*, WT, *Irf4*$^{+/fl}$, and *Irf4*$^{fl/fl}$ mice were infected with LCMV-Armstrong. Responses to three LCMV epitopes (i.e., H2-D^b/GP$_{33-41}$, H2-D^b/NP$_{396-404}$, and H2-D^b/GP$_{276-286}$ [hereafter referred to as GP$_{33}$, NP$_{396}$, and GP$_{276}$]) were examined using MHC–peptide tetramers. At the peak of the response (i.e., day 8 p.i.) the magnitude of the CD8$^+$ T cell response depended on the gene dosage of *Irf4*. WT CD8$^+$ T cells mounted the most robust response, followed by *Irf4*$^{+/fl}$, and then *Irf4*$^{fl/fl}$ cells (Figure 3.3A, 3.4A-B). Enumeration of viral titers by plaque assay indicated that all WT (5 of 5) and *Irf4*$^{+/fl}$ (3 of 3) mice had cleared the virus, whereas only 30% of *Irf4*$^{fl/fl}$ (3 of 10) mice had cleared LCMV by day 8 p.i. These data indicated that modest reductions in IRF4 expression did not interfere with viral clearance but that a minimal level of IRF4 was required for sterilizing immunity to LCMV (Figure 3.3B). As our in vitro studies showed reduced IRF4 expression levels following activation of WT versus *Irf4*$^{+/fl}$ P14 T cells, these initial infection experiments indicated that even modest differences in the magnitude of IRF4 expression had a profound effect on the clonal expansion of virus-specific CD8$^+$ T cells.

Reduced levels of IRF4 do not affect the kinetics of CD8$^+$ T cell expansion or attrition

The reduced numbers of virus specific *Irf4*$^{+/fl}$ cells at day 8 p.i. could be attributed to delayed kinetics of *Irf4*$^{+/fl}$ CD8$^+$ T cell expansion relative to the WT cells. On the basis of previous data indicating a regulatory T cell defect in *Irf4*$^{fl/fl}$ mice that disrupts normal T cell homeostasis (Zheng et al., 2009), studies of *Irf4*$^{fl/fl}$ mice were not included in the subsequent analyses. Instead, we focused on a comparison of WT versus *Irf4*$^{+/fl}$ T cell responses to understand the effect of partial loss of IRF4 expression on CD8$^+$ T cell differentiation. Examination of WT and *Irf4*$^{+/fl}$ CD8$^+$ T cell populations at later time points following LCMV-Armstrong infection indicated that the peak response for both WT and *Irf4*$^{+/fl}$ CD8$^+$ T cells was at day 8 p.i; by day 10 p.i., both populations had started to contract (Figure 3.3C, 3.4C-D). Following antigen clearance, the majority of CD8$^+$ T cells undergo attrition by apoptosis and form a small but stable pool of memory cells (Kaech & Wherry, 2007) (Williams & Bevan, 2007). Examination of virus-specific CD8$^+$ T cells at days 14 and 28 p.i. confirmed that this pattern was observed for both WT and *Irf4*$^{+/fl}$ CD8$^+$ T cells. However, by day 28 p.i., the differences in the numbers of WT and the *Irf4*$^{+/fl}$ CD8$^+$ T cells were quite modest, and no longer significant for one of the three epitopes examined (Figure 3.3C, 3.4C-D). Normalization of virus- specific CD8$^+$ T cell numbers to the peak of the response indicated that loss of one allele of *Irf4* did not change the kinetics of the CD8$^+$ T response nor did it affect the rate of CD8$^+$ T cell contraction. Thus, in comparison with the

numbers of virus-specific T cells present at the peak of the response, greater numbers of WT $CD8^+$ T cells were lost between days 8 and 28 p.i. relative to *Irf4*$^{+/fl}$ $CD8^+$ T cells (Figure 3.3C, 3.4C-D). Therefore, not only did WT cells undergo more robust expansion than the *Irf4*$^{+/fl}$ $CD8^+$ T cells, the WT cells also underwent more extensive contraction.

We also examined the $CD4^+$ T cell response to LCMV- Armstrong in infected WT and *Irf4*$^{+/fl}$ mice. Similar to our findings for $CD8^+$ T cells, analysis of GP_{61} epitope–specific $CD4^+$ T cells at days 14 and 28 p.i. indicated a defect in *Irf4*$^{+/fl}$ $CD4^+$ T cell expansion relative to the WT cells (Figure 3.3D). Furthermore, consistent with our analysis of the $CD8^+$ T cell response, we found that greater numbers of WT GP_{61}-epitope–specific $CD4^+$ T cells were lost between days 14 and 28 p.i. relative to *Irf4*$^{+/fl}$ $CD4^+$ T cells (Figure 3.3E).

Taken together, these data suggest that the effects of reduced IRF4 expression are a general feature of $CD8^+$ T cell responses to viral infections and furthermore are impacting $CD4^+$ T cell responses as well. We conclude that different amounts of IRF4 expression during T cell priming regulate the magnitude of the peak antiviral T cell response without affecting the kinetics of the response or the rate of attrition following Ag clearance.

Reduced gene dosage of Irf4 regulates effector cytokine expression

To assess $CD8^+$ T cell effector functions following virus infection, splenocytes from LCMV-Armstrong–infected WT, *Irf4*$^{+/fl}$, and *Irf4*$^{fl/fl}$ mice were examined at days 8 and 28 p.i. for IFNγ, TNFα, and IL-2 expression. As expected, the gene dosage of *Irf4* strongly correlated with the numbers of IFNγ–producing $CD8^+$ T cells (Figure 3.5, 3.6A-B). No differences in the frequencies of TNFα–producing $CD8^+$ T cells as a proportion of $IFN\gamma^+$ $CD8^+$ T cells were observed at day 8 p.i. when comparing WT and *Irf4*$^{+/fl}$ mice; however, *Irf4*$^{fl/fl}$ mice showed a substantial reduction in the relative proportion of this double cytokine-producing subset. Furthermore, at day 28 p.i., the median fluorescence intensity (MFI) of TNFα staining and the frequencies of TNFα/IFNγ double-producers and IFNγ/TNFα/IL-2 triple-producers were significantly decreased in *Irf4*$^{+/fl}$ mice compared with WT controls. Analyses of granzyme B expression and degranulation as assessed by CD107a and CD107b staining revealed no differences between any of the genotypes at either time point. Overall, these data indicate that reduced expression of IRF4 leads to an impaired ability of virus-specific $CD8^+$ T cells to produce cytokines other than IFNγ as the cells transition into a long-term memory population.

Levels of IRF4 expression selectively impact the short-lived $CD8^+$ effector cell population

In response to acute infections, $CD8^+$ T cells undergo clonal expansion and

differentiation to terminal effector cells (TEC; KLRG1^{hi}CD127^{lo}) and memory-precursor cells (MPC; KLRG1^{lo}CD127^{hi}). Examination of these populations revealed that reduced IRF4 expression had a more substantial impact on the numbers of virus-specific TEC compared with MPC for each population (Figure 3.7A, 3.8A, 3.9A). Specifically, at day 8 p.i., *Irf4*$^{+/fl}$ mice had a 2.5- to 4.4-fold reduction in numbers of TEC versus a 1.4- to 2.0-fold reduction in MPC numbers over the three epitopes examined. Furthermore, despite the increase in MPC percentages among virus-specific CD8$^+$ T cells in *Irf4*$^{+/fl}$ mice at early times post-infection (days 8, 10, and 14 p.i.), the absolute numbers of MPCs in these mice were decreased. Because the numbers of TEC are much greater than the numbers of MPC, these data indicate that diminished TEC populations are largely responsible for the decrease in the total magnitude of the CD8$^+$ T cell effector response in *Irf4*$^{+/fl}$ mice. Interestingly, by day 28 p.i., WT and *Irf4*$^{+/fl}$ mice had comparable numbers of virus-specific CD8$^+$ T cells, and no significant differences in the numbers of MPC were observed for two of the three viral epitopes examined. Consistent with these data, examination of virus-specific effector (T_{EM}) and central (T_{CM}) memory populations at day 28 p.i. showed only a modest reduction in the numbers of T_{EM} in *Irf4*$^{+/fl}$ compared with WT mice and no differences in the numbers of T_{CM} cells between the two genotypes (Figure 3.7B, 3.8B, 3.9B). These data indicate that reduced IRF4 expression is regulating the expansion phase of the T cell response but not impacting the generation of long-lived virus-specific CD8$^+$ T cells.

Figure 3.5. Lower expression of IRF4 impairs production of effector cytokines at day 28 post-infection (GP_{33})

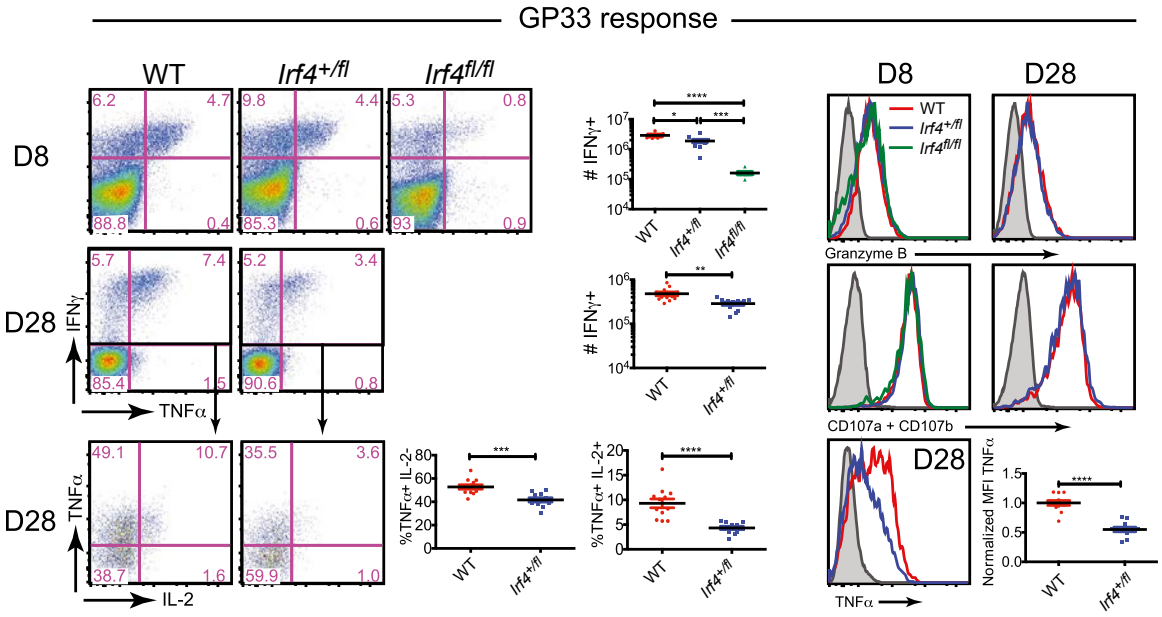

Figure 3.5. Lower expression of IRF4 impairs production of effector cytokines at day 28 post-infection (GP_{33})

Splenocytes from LCMV-GP_{33}–infected WT, *Irf4*$^{+/fl}$, and *Irf4*$^{fl/fl}$ mice from days 8 and 28 p.i. were stimulated for 5 hours with GP_{33} peptide and analyzed for IFNγ, TNFα, IL-2, granzyme B, and CD107a + CD107b. Dot plots show IFNγ versus TNFα staining on gated live $CD8^+CD44^{hi}$ T cells, and for day 28 p.i., $IFN\gamma^+$ cells were analyzed for TNFα versus IL-2 staining. Graphs show a compilation of numbers of $IFN\gamma^+$ cells from days 8 and 28 p.i., and percentage of $TNF\alpha^+IL\text{-}2^-$ and percentage of $TNF\alpha{+}IL\text{-}2^+$ on gated $IFN\gamma^+$ cells at day 28 p.i. On the right, histograms show granzyme B, CD107a + CD107b, and TNFα staining; gray histograms show staining on naive $CD8^+$ T cells from uninfected WT mice; the graph shows a compilation of MFIs of TNFα staining at day 28 p.i. normalized to WT samples in each experiment. Data are representative of three independent experiments with at least five mice per group per time point. *$p \leq 0.05$, **$p \leq 0.01$, ***$p \leq 0.001$, ****$p \leq 0.0001$.

Figure 3.6. Lower expression of IRF4 impairs production of effector cytokines at day 28 post-infection (GP_{276}/NP_{396})

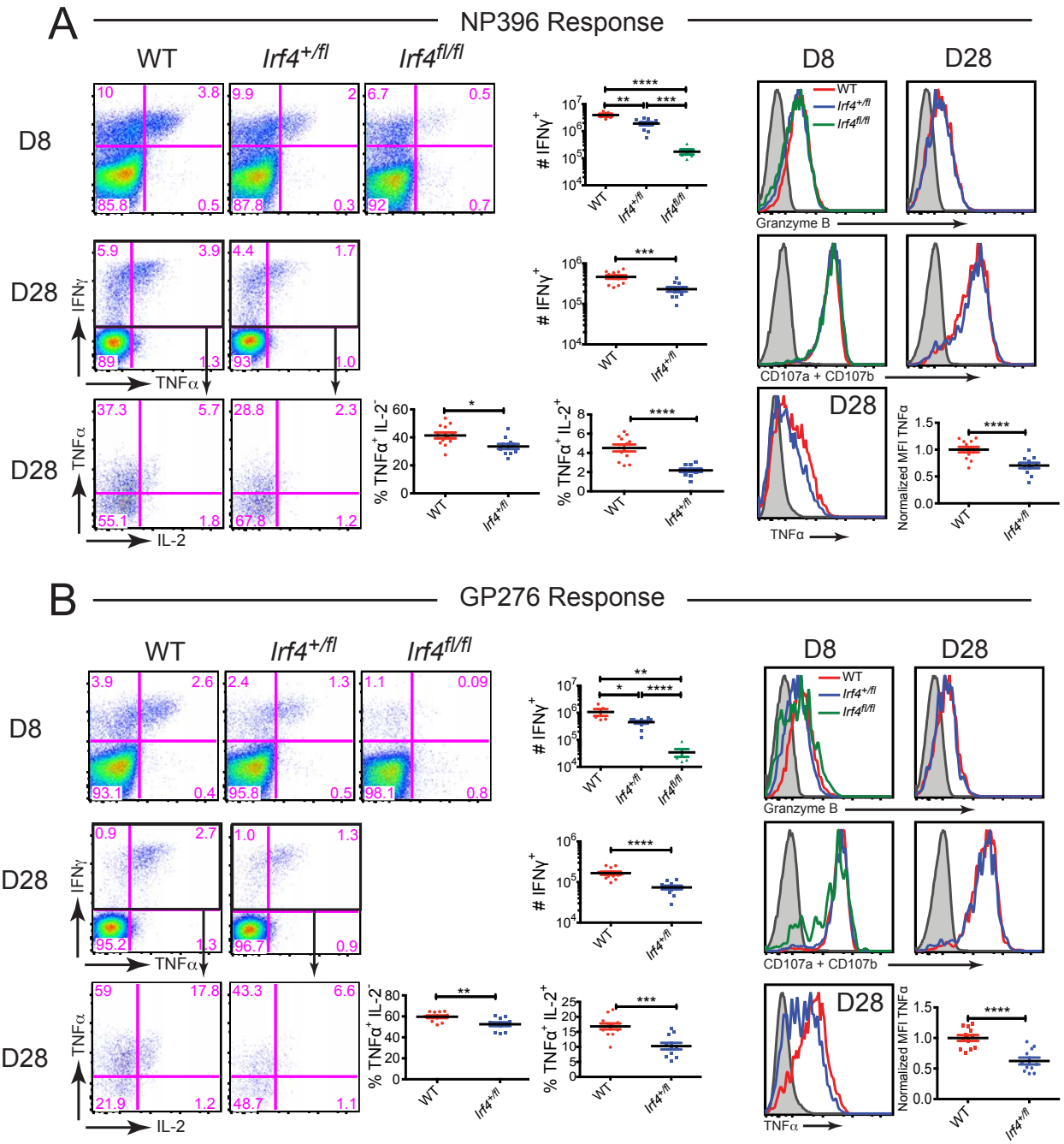

Figure 3.6: Lower expression of IRF4 impairs production of effector cytokines at day 28 post-infection (GP_{276}/NP_{396})

Splenocytes from LCMV-GP_{33}-infected WT, *Irf4*$^{+/fl}$ and *Irf4*$^{fl/fl}$ mice were analyzed at day 8, 10, 14 and 28 p.i. for NP_{396} **(A)** and GP_{276} **(B)** epitope-specific responses. Data are organized as outlined in the legend for Figure 3.5.

Figure 3.7. Differences in IRF4 expression regulate the nature of CD8$^+$ T cell differentiation (GP_{33})

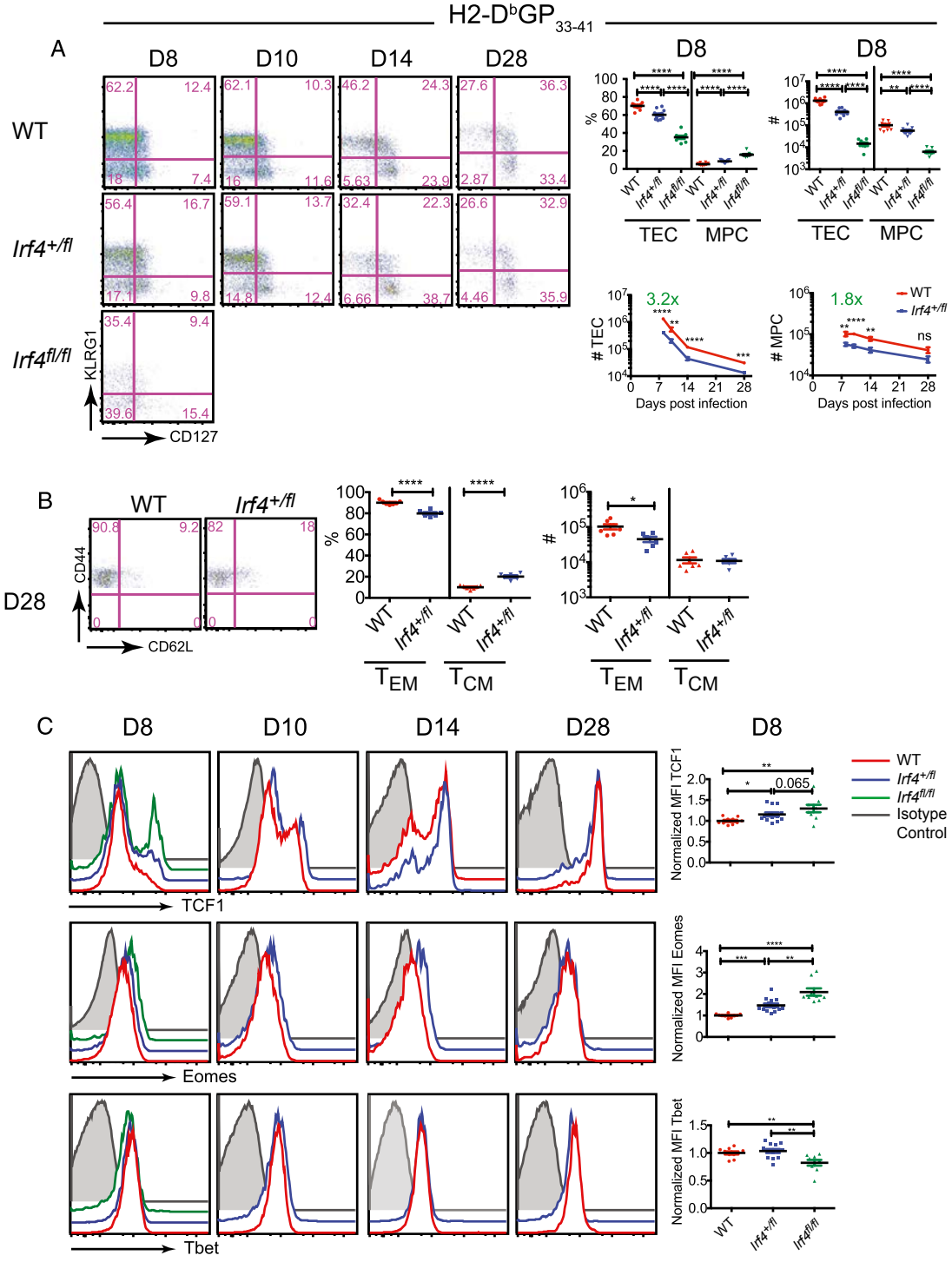

Figure 3.7: Differences in IRF4 expression regulate the nature of $CD8^+$ T cell differentiation (GP_{33})

Splenocytes from LCMV-GP_{33}–infected WT, *Irf4*$^{+/fl}$ and *Irf4*$^{fl/fl}$ mice were analyzed at days 8, 10, 14, and 28 p.i. **(A)** Dot plots show KLRG1 versus CD127 staining on $CD44^{hi}$ H2 D^b-GP_{33} tetramer–positive live $CD8^+$ T cells. Graphs show compilations of the percentages and numbers of $KLRG1^{hi}CD127^{lo}$ (TEC) and $KLRG1^{lo}CD127^{hi}$ (MPC) populations. Numbers on time-course graphs indicate the relative difference in TEC or MPC numbers between WT and *Irf4*$^{+/fl}$ mice at day 8 p.i. **(B)** Dot plots show CD44 versus CD62L staining on $CD44^{hi}$ H2 D^b-GP_{33} tetramer–positive live $CD8^+$ T cells at day 28 p.i. Graphs show compilations of the percentages and numbers of $CD44^{hi}CD62L^{lo}$ (T_{EM}) and $CD44^{hi}CD62L^{hi}$ (T_{CM}) populations. **(C)** Histograms show TCF1, Eomes, and T-bet staining on $CD44^{hi}$ H2 D^b-GP_{33} tetramer–positive live $CD8^+$ T cells. Graphs show compilations of MFI of transcription factor staining at day 8 p.i., normalized to WT samples in each experiment. Data are representative of two or more independent experiments with n ≥ 6 mice per time point. *p ≤ 0.05, **p ≤ 0.01, ***p ≤ 0.001, ****p ≤ 0.0001.

Figure 3.8. Differences in IRF4 expression regulate CD8$^+$ T cell differentiation (NP_{396})

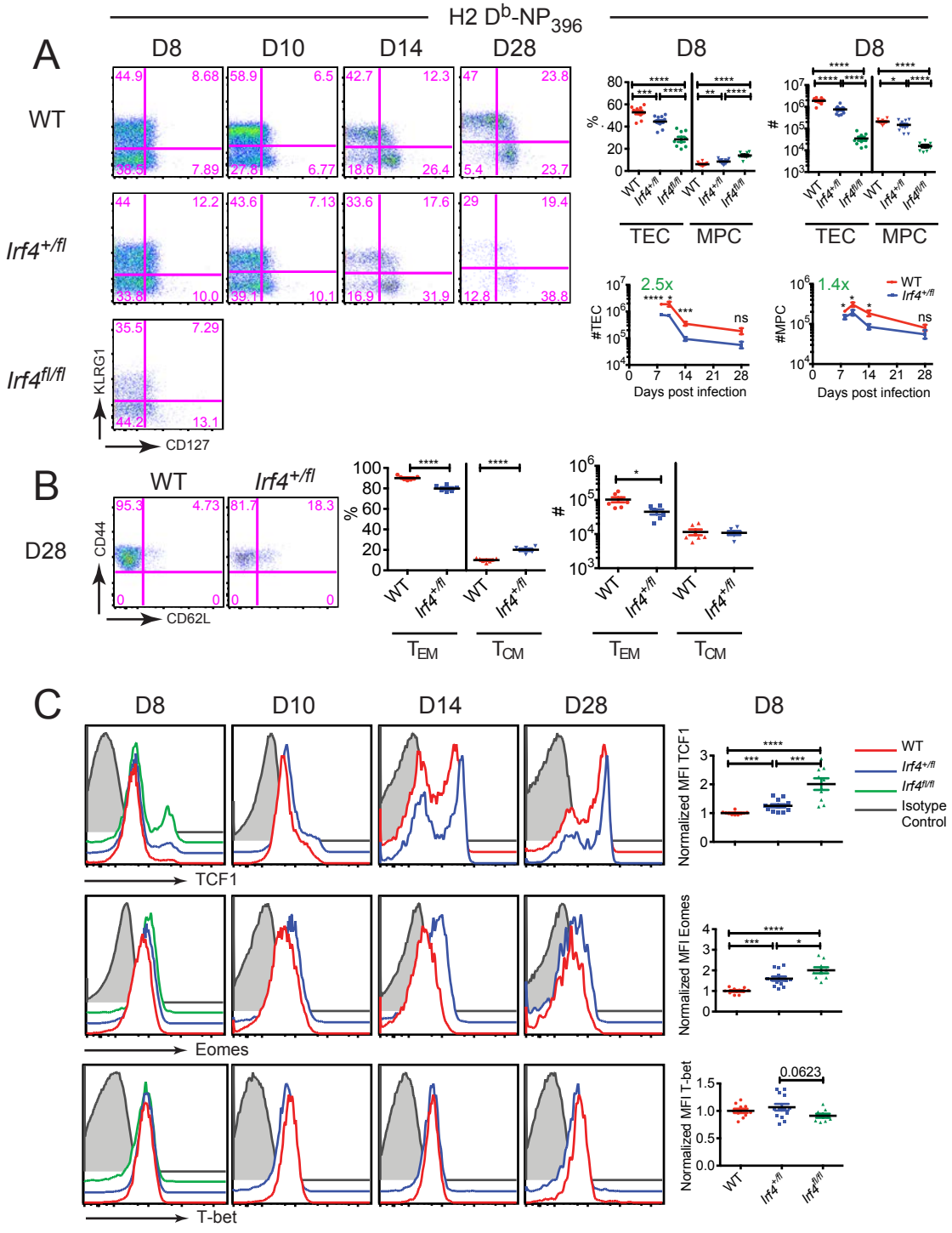

Figure 3.8: Differences in IRF4 expression regulate $CD8^+$ T cell differentiation (NP_{396})

Splenocytes from LCMV-GP_{33}-infected WT, *Irf4*$^{+/fl}$, and *Irf4*$^{fl/fl}$ mice were analyzed at day 8, 10, 14 and 28 p.i. for NP_{396} epitope-specific responses. Data are organized as outlined in the legend for Figure 3.7.

Figure 3.9. Differences in IRF4 expression regulate CD8$^+$ T cell differentiation (GP_{276})

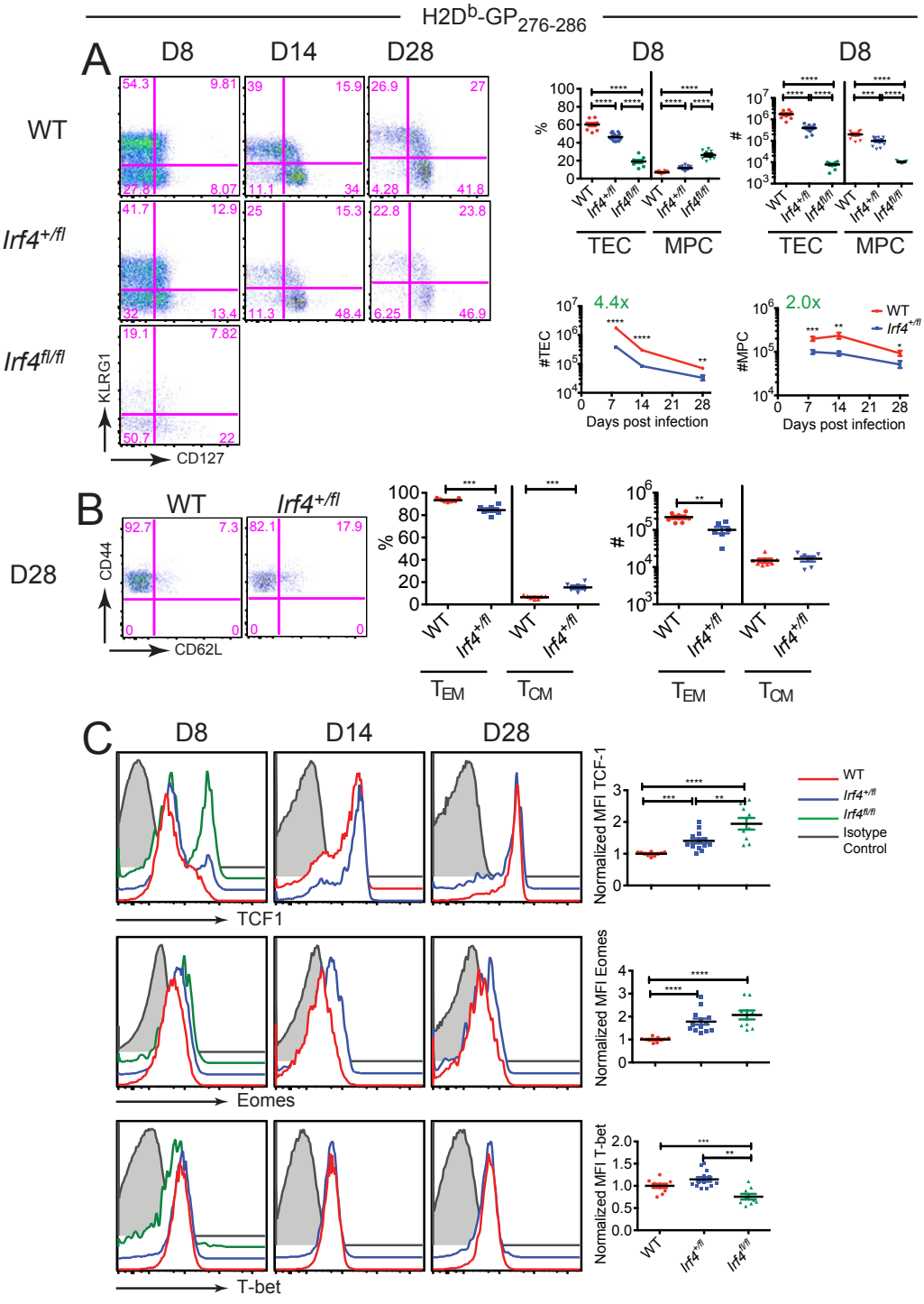

Figure 3.9: Differences in IRF4 expression regulate $CD8^+$ T cell differentiation (GP_{276})

Splenocytes from LCMV-GP_{33}-infected WT, *Irf4*$^{+/fl}$, and *Irf4*$^{fl/fl}$ mice were analyzed at day 8, 14 and 28 p.i. for GP_{276} epitope-specific responses. Data are organized as outlined in the legend for Figure 3.7.

Differential role for IRF4 in regulating TCF1, Eomes, and T-bet expression

Virus-specific $CD8^+$ T cell differentiation is regulated by the expression of transcription factors such as TCF1, Eomes, and T-bet at day 8 p.i (Banerjee et al., 2010) (Intlekofer et al., 2005) (Jeannet et al., 2010) (Joshi et al., 2007) (Zhou et al., 2010). Consistent with our *in vitro* stimulation data, LCMV-specific $Irf4^{fl/fl}$ cells expressed the highest levels of TCF1 and Eomes, $Irf4^{+/fl}$ cells had intermediate levels, and WT cells had the lowest levels of both factors. In contrast, the expression of T-bet was reduced in $Irf4^{fl/fl}$ cells compared with WT, but no differences were observed in T-bet levels when comparing WT and $Irf4^{+/fl}$ cells (Figure 3.7C, 3.8C, 3.9C). These data indicated that TCF1 and Eomes expression were more sensitive to modest changes in IRF4 levels than was T-bet expression, indicating an IRF4 dose-dependent variation in the regulation of these key transcription factors. At later time points post-infection, differences in Eomes and TCF1 levels in virus-specific $Irf4^{+/fl}$ versus WT cells were less uniform across the three epitope-specific populations, although in general, $Irf4^{+/fl}$ cells tended to express higher levels of these factors than WT cells at days 10 and 14 p.i.; however, by day 28 p.i., no further differences were observed between $Irf4^{+/fl}$ and WT cells. Consistent with the transient nature of IRF4 expression and the data presented above, these results confirm that variations in IRF4 expression levels have the greatest impact at the peak of the virus-specific $CD8^+$ T cell response and are not generally altering the long-lived population of virus-specific $CD8^+$ T cells found at day 28 p.i.

Cell-intrinsic role for IRF4 in regulating the magnitude of the $CD8^+$ effector T cell response

To assess whether the altered virus-specific $CD8^+$ T cell response seen in *Irf4*$^{+/fl}$ versus WT mice was due to differences intrinsic to the $CD8^+$ T cells, we performed adoptive transfer experiments. This approach also allowed us to examine whether activation of P14 T cells *in vivo* with an LCMV variant expressing the lower affinity F6L ligand would phenocopy the results of reducing IRF4 expression by a heterozygous deficiency in the *Irf4* gene. We first established that activation of P14 cells with LCMV expressing the GP_{33} epitope results in higher IRF4 expression relative to P14 cells activated in response to LCMV-F6L infection. $1*10^6$ congenically marked WT P14 ($CD45.1^+CD45.2^+$) cells were transferred into naive WT ($CD45.2^+$) hosts. One day later, mice were infected with $1*10^5$ PFU LCMV-Armstrong expressing either the WT GP_{33} epitope (LCMV-GP_{33}) or the mutant F6L epitope (LCMV-F6L). Previous studies showed that the single amino acid substitution in the LCMV-F6L virus has no impact on viral replication or viral clearance when compared with LCMV-GP_{33} (Gronski et al., 2004). As expected, at day 3 p.i., P14 cells activated with LCMV-GP_{33} expressed higher levels of IRF4 relative to P14 cells activated in response to the F6L epitope (Figure 3.10A). These data were consistent with the results seen upon *in vitro* stimulation of WT P14 cells with the GP_{33} and F6L ligands (Figure 3.1A).

To assess the cell-intrinsic role of reduced TCR stimulation, either alone or in combination with reduced IRF4 expression, in regulating the $CD8^+$ T cell response, congenically marked WT P14 ($CD45.1^+CD45.2^+$) and *Irf4*$^{+/fl}$ P14 ($CD45.2^+$) cells were mixed 1:1 and transferred into naive WT ($CD45.1^+$) hosts (Figure 3.10B). When analyzed at day 8 p.i., we observed a substantially greater proportion of WT P14 cells relative to the *Irf4*$^{+/fl}$ P14 population, indicating differential expansion of the two populations (Figure 3.10C-D). This trend was observed when a total of 2,000 or 20,000 P14 cells were transferred as a 1:1 mixture of the two genotypes. Strikingly, infection with the LCMV-F6L virus reduced the overall expansion of both WT and *Irf4*$^{+/fl}$ P14 cells but maintained the competitive advantage of the WT over the *Irf4*$^{+/fl}$ cells (Figure 3.10D). These findings indicate that the decreased expansion of P14 cells in response to LCMV-F6L relative to LCMV-GP_{33} is highly correlated with decreased IRF4 expression. Thus, these data suggest that variable upregulation of IRF4 in $CD8^+$ T cells is responsible for the effect of TCR signal strength on the magnitude of the peak effector response, as reported previously (Zehn et al., 2009). More detailed analyses of the P14 populations were performed with mice receiving 20,000 transferred P14 cells prior to infection, because this provided a greater number of cells for analysis. Examination of TEC versus MPC subsets among the P14 populations indicated that the graded magnitude of the response seen among the four experimental groups could be largely attributed to differences in the expansion of P14 TEC (Figure 3.11A). This was affected by changes in IRF4

expression because of deletion of one *Irf4* allele or by infecting mice with an LCMV variant expressing only a lower affinity ligand for the P14 TCR, or both. In contrast, the MPC populations were largely unaffected by loss of one functional *Irf4* allele. Regardless of the virus used, *Irf4*$^{+/fl}$ P14 cells expressed higher total levels TCF1 because of the increased proportions of TCF1^{+} cells among the *Irf4*$^{+/fl}$ P14 populations (Figure 3.11B). However, similar to our observations regarding the MPC population, the absolute numbers of TCF1^{+} cells were not affected by a heterozygous deficiency in *Irf4* (Figure 3.11B). This is in contrast to a recent report showing a ~2-fold decrease in *tcf7* mRNA in *in vitro*-activated *Irf4*-deficient OT-I CD8^{+} T cells (Man et al., 2013). This discrepancy could arise from differential priming of CD8^{+} T cells *in vivo* in response to a virus infection versus that occurring when T cells are activated *in vitro*; alternatively, the differences seen might arise from differences in the time points examined in our *ex vivo* analysis versus that used for the *in vitro* stimulation studies. Nonetheless, consistent with previous data (Xinyuan Zhou et al., 2010), we found that higher TCF1 expression in *Irf4*$^{+/fl}$ P14 cells correlated with enhanced Eomes expression in these cells (Figure 3.11C). In contrast, we observed no differences in the expression of T-bet when comparing WT to *Irf4*$^{+/fl}$ P14 cells (Figure 3.11C).

The costimulatory molecule CD27 is important for survival of CD8^{+} effector and memory cells (Peperzak et al., 2010); interestingly, we found increased expression of CD27 on *Irf4*$^{+/fl}$ P14 cells than WT P14 cells (Figure 3.11C). This finding is consistent with our observation that, following the peak of the antiviral

Figure 3.10. Cell-intrinsic requirement for IRF4 in regulating the magnitude of CD8$^+$ T cell responses

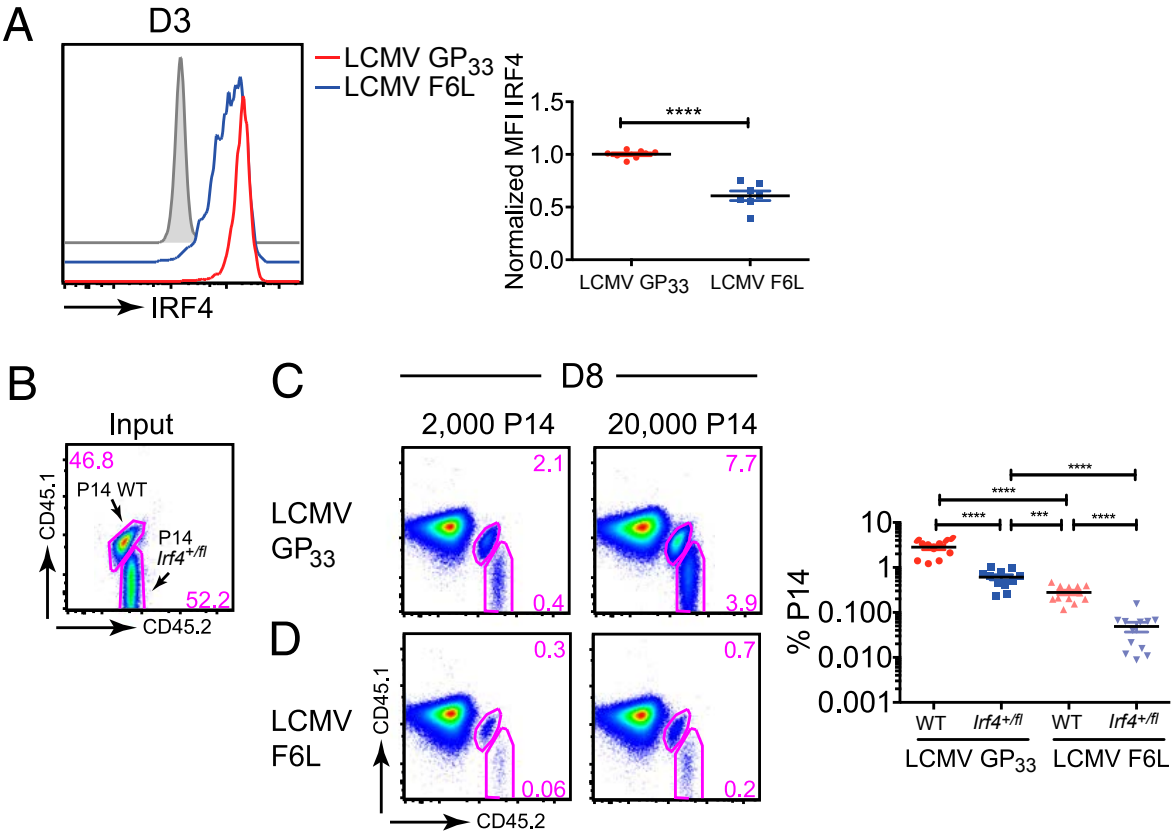

Figure 3.10: Cell-intrinsic requirement for IRF4 in regulating the magnitude of $CD8^+$ T cell responses

(A) A total of $1x10^6$ P14 WT ($CD45.1^+CD45.2^+$) cells were transferred into $CD45.2^+$ hosts 1 day prior to infection with $1x10^5$ PFU LCMV-GP_{33} or LCMV-F6L virus. Histograms show IRF4 staining on gated live $CD8^+$ $CD44^{hi}$ P14 cells; the gray histogram represents IRF4 staining on naive $CD8^+$ $CD44^{lo}$ cells. The graphs below show compilations of MFI for IRF4 staining normalized to the LCMV-GP_{33} infection in each experiment. **(B–D)** A total of 2,000 or 20,000 P14 cells comprising a 1:1 mix of P14 WT ($CD45.1^+CD45.2^+$) and P14 $Irf4^{+/fl}$ ($CD45.2^+$) were transferred into $CD45.1^+$ congenic hosts 1 day prior to infection with LCMV-GP_{33} or LCMV-F6L, and splenocytes were analyzed on day 8 p.i. Dot plots show CD45.1 versus CD45.2 staining on input cell mixture **(B)** or on gated live $CD8^+$ $CD44^{hi}$ from mice infected with LCMV-WT **(C)** or LCMV-F6L **(D)**. Graph shows a compilation of percentages of P14 WT and P14 $Irf4^{+/fl}$ populations from mice receiving 2000 P14 cells. Data are representative of more than or equal to three independent experiments. ***$p \leq 0.001$, ****$p \leq 0.0001$

response, *Irf4*$^{+/fl}$ cells undergo less cell death than their WT counterparts. To address this possibility further, we examined Bcl2 expression. As shown, the loss of one allele of *Irf4* and/or infection with LCMV-F6L resulted in enhanced expression of the pro-survival molecule Bcl2 in P14 cells (Figure 3.11D). This increase could be mainly attributed to higher Bcl2 expression in the *Irf4*$^{+/fl}$ versus the WT P14 MPC population (Figure 3.11D). Taken together, these data are consistent with the greater survival potential of *Irf4*$^{+/fl}$ P14 cells relative to WT and provide an explanation for the reduced numerical attrition of virus-specific *Irf4*$^{+/fl}$ CD8^{+} T cells observed (Figure 3.3C, 3.1C-D). Finally, these data also indicate that the differences in the clonal expansion and differentiation of virus specific effector CD8^{+} T cells observed upon infection of intact WT and *Irf4*$^{+/fl}$ mice were due to a CD8^{+} T cell–intrinsic requirement for high levels of IRF4; furthermore, these differences mainly arose from the variable expansion of the short-lived effector cells.

Differential T cell expansion is driven by variations in the levels of IRF4 expressed in competing T cell populations

The data described above establish a CD8^{+} T cell-intrinsic requirement for IRF4. During polyclonal T cell responses, Ag-specific T cells compete for Ag and inflammatory cytokines. To test whether variations in IRF4 expression levels between competing T cell populations could result in variable T cell expansion,

Figure 3.11. *Irf4* haplo-deficiency selectively impairs terminal effector CD8$^+$ T cell numbers and alters transcription factor, CD27 and Bcl2 expression

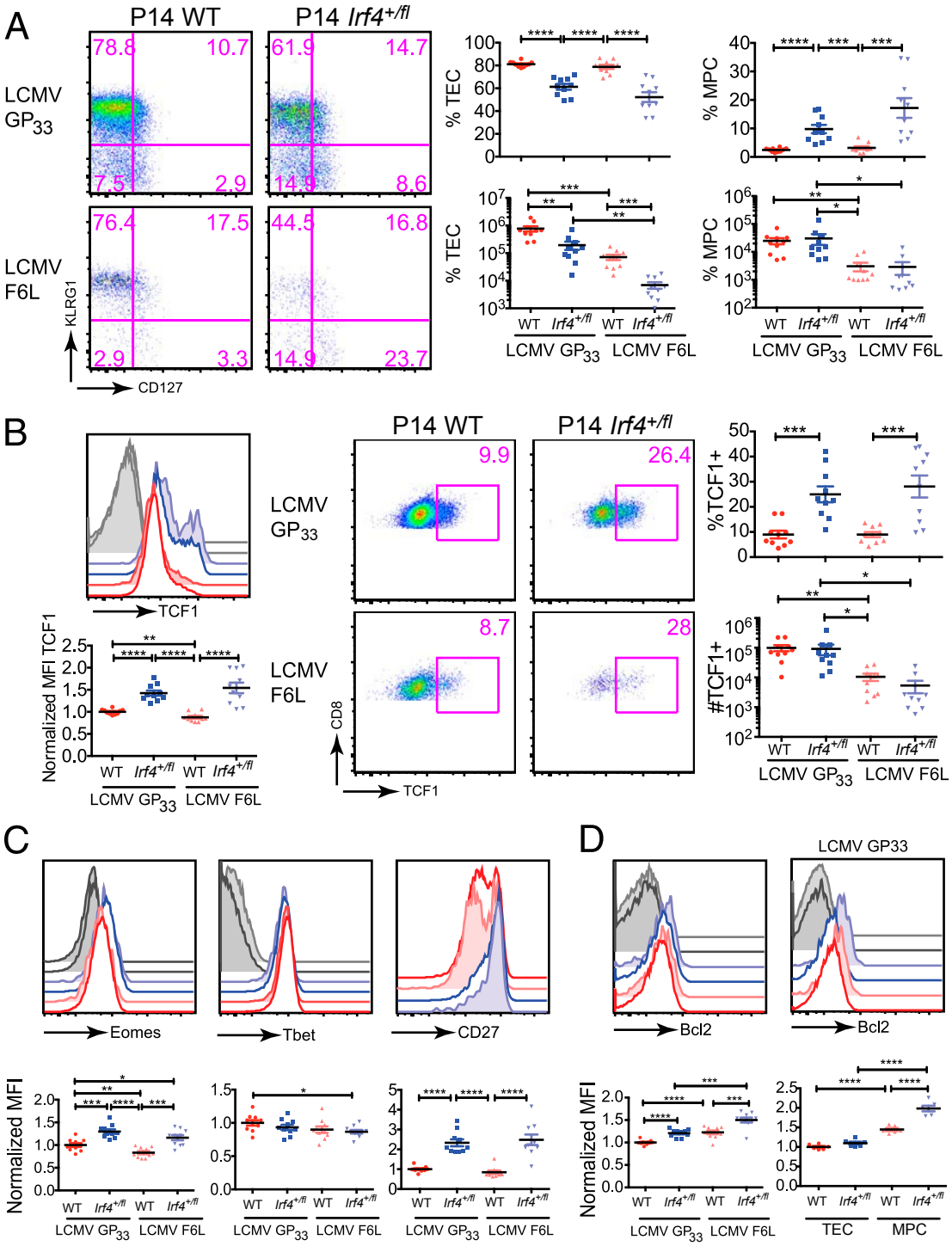

Figure 3.11: *Irf4* haplo-deficiency selectively impairs terminal effector CD8$^+$ T cell numbers and alters transcription factor, CD27 and Bcl2 expression

A total of 20,000 P14 cells comprising a 1:1 mix of P14 WT (CD45.1$^+$CD45.2$^+$) and P14 Irf4$^{+/fl}$ (CD45.2$^+$) were transferred into CD45.1$^+$ congenic hosts 1 day prior to infection with LCMV-GP$_{33}$ or LCMV-F6L, and splenocytes were analyzed on day 8 p.i. **(A)** Dot plots show KLRG1 versus CD127 staining on gated live CD8$^+$CD44^{hi} P14 populations. Graphs show compilations of percentages and numbers of TEC and MPC populations for each genotype. **(B)** The histogram shows TCF1 expression on gated live CD8$^+$CD44^{hi}P14$^+$ cells. Open histograms, LCMV-WT responding cells; shaded histograms, LCMV-F6L responding cells. Colors are as indicated in graphs. The graph below shows the compilation of TCF1 MFI normalized to WT cells responding to LCMV-WT virus in each experiment. Dot plots show CD8 versus TCF1 staining on gated live CD8$^+$CD44^{hi} P14 cells. The graphs at the right show compilations of percentages and absolute numbers of CD8$^+$TCF1$^+$ population for each genotype. **(C)** Histograms show Eomes, T-bet, and CD27 staining on CD8$^+$CD44^{hi} P14 cells of each genotype, and the graphs below show compilations of MFI for each stain normalized to WT cells responding to LCMV-WT virus in each experiment. **(D)** Left histogram shows Bcl2 staining on gated live CD8$^+$ CD44^{hi} P14 populations from LCMV-WT responding cells (open histograms) and LCMV-F6L responding cells (shaded histograms). Colors are as indicated in the graph. The graph below shows the compilation of Bcl2 MFI normalized to WT cells responding to LCMV-

WT virus in each experiment. Right histogram shows Bcl2 staining on gated live $CD8^{+}CD44^{hi}$ P14 TEC (open histograms) and MPC (shaded histograms) populations from LCMV-GP_{33}–infected mice. Colors are as indicated in graphs. The graph below shows the compilation of Bcl2 MFI normalized to WT TEC samples for each experiment. Data are representative of two to three independent experiments. *$p \leq 0.05$, **$p \leq 0.01$, ***$p \leq 0.001$, ****$p \leq 0.0001$.

we transferred WT P14 T cells into either WT or *Irf4*$^{+/fl}$ host mice and infected them with LCMV-GP_{33} or LCMV-F6L virus. Our findings thus far predicted that, in the case where WT P14 cells were responding in a host where all endogenous T cells are *Irf4*$^{+/fl}$, the WT P14 cells should show an enhanced response relative to their response in a WT host environment. In contrast, we reasoned that the WT P14 cells should show an impaired response following infection with LCMV-F6L in a WT host; however, we predicted that this response should improve if the WT P14 cells are transferred into *Irf4*$^{+/fl}$ hosts, thereby providing the WT P14 cells with an advantage based on two functional alleles of *Irf4*.

As shown in Figure 3.12A, the data from these experiments supported our predictions. A single population of WT P14 T cells was transferred into either WT or *Irf4*$^{+/fl}$ hosts, which were then infected with either LCMV-GP_{33} or LCMV-F6L. We found that WT P14 cells contributed more dominantly to the response to LCMV-GP_{33} when the endogenous T cell population was *Irf4*$^{+/fl}$ cells, in contrast to their contribution when responding in a WT host. Alternatively, the WT P14 cells contributed little to the response to LCMV-F6L when present in a WT host, but this response could be greatly improved by transferring these cells into an *Irf4*$^{+/fl}$ host, where the endogenous T cell response was handicapped in IRF4 expression. These data indicate that the contribution of an individual virus-specific $CD8^+$ T cell population to the overall response is not simply regulated by the levels of IRF4 expressed in those cells, but also is determined by the levels of IRF4 expressed in competing T cell populations present in the same individual.

On the basis of these data, we speculated that the $CD8^+$ T cells forming the most robust response to an acute infection would express the highest levels of IRF4, thus accounting for the predominance of these populations at the peak of the response. In acute LCMV infections, $CD8^+$ T cell responses to GP_{33} and NP_{396} epitopes are immunodominant whereas those to GP_{276} are subdominant (van der Most et al., 1998). Because the expression of IRF4 is transient in nature, we were unable to detect differences in IRF4 expression in these populations during the polyclonal response to LCMV-Armstrong. However, we did observe that the magnitude and kinetics of upregulation of TCF1, a target repressed by IRF4, were different between the epitope-specific populations. GP_{276}-specific cells expressed the highest levels of TCF1, followed by GP_{33}-specific cells, and then NP_{396}-specific cells, suggesting lower IRF4 expression in GP_{276}-specific cells and the highest expression in NP_{396}-specific cells (Figure 3.12B). Because TCF1 also regulates the differentiation of T_{EM} to T_{CM} (Zhou et al., 2010), these data provide further mechanistic support for the observation that GP_{276}-specific $CD8^+$ T cells are the earliest subset to form T_{CM} in response to LCMV-Armstrong, whereas NP_{396}-specific T cell population are the slowest (Sarkar et al., 2007). These results show that variations in IRF4 expression can modulate the relative proportions of different virus-specific T cell populations recognizing the same epitope and suggest that differences observed in the expansion of polyclonal T cell responses to different epitopes may be driven by differential upregulation of IRF4.

Figure 3.12. Ability to express higher levels of IRF4 provides a competitive advantage to Ag-specific CD8^{+} T cells

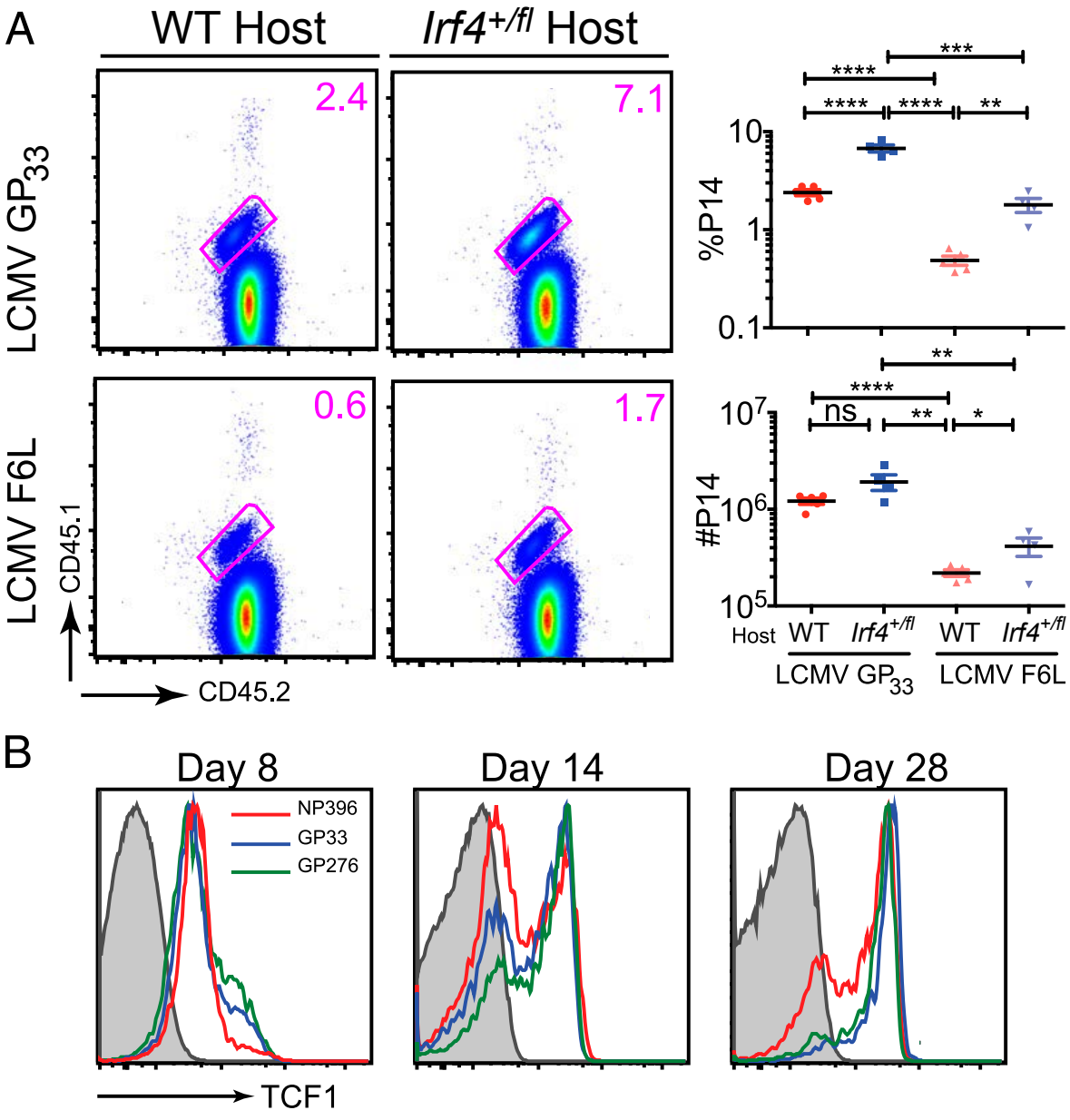

Figure 3.12: Ability to express higher levels of IRF4 provides a competitive advantage to Ag-specific $CD8^+$ T cells

(A) A total of 1000 P14 WT ($CD45.1^+CD45.2^+$) T cells were transferred into WT or $Irf4^{+/fl}$ hosts ($CD45.2^+$) 1 day prior to infection with LCMV-GP_{33} or LCMV-F6L, and splenocytes were analyzed at day 8 p.i. Dot plots show CD45.1 versus CD45.2 staining on gated live $CD8^+$ $CD44^{hi}$ cells. Graphs show a compilation of percentages of P14 WT populations. Data are representative of two independent experiments with more than or equal to four mice per group. **(B)** Splenocytes from LCMV-GP_{33}-infected WT mice were analyzed at days 8, 14, and 28 p.i. Histograms show TCF1 staining of $CD44^{hi}$ $H2D^b$-NP_{396}, -GP_{33}, and -GP_{276} tetramer–positive live $CD8^+$ T cells; gray histograms represent isotype control staining. *$p \leq 0.05$, **$p \leq 0.01$, ***$p \leq 0.001$, ****$p \leq 0.0001$.

Discussion

The adaptive immune system protects us from pathogens by mounting a strong primary response, and then retaining protective cells that form immunological memory. The recognition of pathogens by $CD8^+$ T cells occurs via interactions of the TCR with peptide/MHC complexes. This process not only allows for activation of pathogen-specific T cells, but also for the selection of high affinity $CD8^+$ T cell clones from the pool of responding T cells (Zehn et al., 2009). Although even brief Ag exposure is sufficient to induce a programmed proliferative burst of effector $CD8^+$ T cell (Kaech & Ahmed, 2001) (van Stipdonk et al., 2001), the ultimate magnitude of the response is nonetheless proportional to the overall Ag load (Badovinac et al., 2002) (Mercado et al., 2000) (Prlic et al., 2006). These findings indicate that TCR signaling contributes to the programming of the $CD8^+$ T cell response during the short period of initial Ag exposure.

The data presented in this study, along with two recent reports (Man et al., 2013) (Yao et al., 2013), demonstrate that the transcription factor, IRF4, is a central component in translating the strength of TCR signaling into the magnitude of the $CD8^+$ T cell response to infection. Man et.al. examined the response of OT-I $CD8^+$ T cell to infections with Influenza A virus expressing different affinity variants of the OVA peptide. This study showed that decreasing the TCR signal strength resulted in lower IRF4 expression in OT-I cells both *in vitro* and *in vivo*, and dramatic differences in the numbers of OT-I $CD8^+$ T cells at the peak of the

response, a phenotype similar to that observed for IRF4-deficient $CD8^+$ T cells responding to infection. Yao et.al. also showed that IRF4 expression was dependent on the strength of TCR signaling *in vitro*, and that loss of IRF4 expression resulted in a diminished polyclonal $CD8^+$ T cell response at the peak of the infection. Consistent with these two studies, we found that upregulation of IRF4 in P14 TCR transgenic $CD8^+$ T cells was also dependent on the affinity and the dose of the stimulating peptide. Further, reduced expression of IRF4 was also observed following *in vitro* stimulation of *Irf4* haplodeficient P14 T cells compared with WT. Similar to the findings of Man et al., we also found a dose-dependent decrease in $CD8^+$ T cell expansion upon loss of one or both alleles of *Irf4*, a phenomenon that could be phenocopied using an LCMV variant expressing a lower affinity ligand for the P14 TCR. Taken together, these studies provide strong support for the conclusion that levels of IRF4 are tightly regulated by the strength of TCR signaling and, in turn, regulate the magnitude of the $CD8^+$ T cell response to infection.

Most importantly, we show that modest variations in the levels of IRF4 expression, such as those achieved by a heterozygous deficiency in *Irf4*, are sufficient to have a dramatic impact on the peak expansion of virus-specific $CD8^+$ T cells. In our studies, reduced IRF4 expression decreased the maximum numbers of Ag-specific $CD8^+$ T cells by 2- to 3-fold and, furthermore, had a greater impact on the numbers of terminal effector cells compared with the memory precursor cells. These data provide a mechanistic explanation for

previous studies demonstrating that shortening the duration of Ag exposure decreases the total $CD8^+$ T cell response and in particular the size of the TEC compartment, without affecting the number of MPCs (Badovinac et al., 2002) (Prlic et al., 2006) (Joshi et al., 2007).

Our studies also showed that, following virus clearance and the bulk of the T cell attrition, there was virtually no impact on the numbers of Ag-specific T cells remaining, regardless of their ability to express high levels of IRF4. This latter finding is strikingly similar to the observations of Bevan and colleagues (Zehn et al., 2009) in their elegant study examining the response of OT-I T cells to strains of *Listeria monocytogenes* expressing different affinity variants of the OVA peptide. In this study, dramatic differences in the peak expansion of OT-I T cells were seen following activation by *Listeria* strains expressing the different OVA variants; however, following bacterial clearance, few differences were found in the numbers of long-term surviving OT-I memory T cells. A likely explanation for these data are that the higher affinity OVA variants induced higher levels of IRF4 than did the lower affinity variants, thus accounting for the relative response of the OT-I T cells to each bacterial strain. Furthermore, because the expression of IRF4 is transient in nature, the effects of different levels of IRF4 are limited to $CD8^+$ T cell priming and the peak expansion phase but not thereafter. We also found increased expression pro-survival factors, CD27 and Bcl2, in P14 *Irf4* haplosufficient cells, consistent with a greater survival potential of these cells relative to WT. These data provide a potential mechanism to account for the

findings of Bevan and colleagues, that ligands representing a broad range of TCR affinities generated relatively similar numbers of memory T cells, despite the dramatic differences in T cell expansion at the peak of the response (Zehn et al., 2009).

Inflammatory cytokines produced during an infection also increase TCR activation by sustaining phosphorylation of ZAP-70 and phospholipase Cγ (Richer et al., 2013). Because the activation of phospholipase Cγ, as well as the levels of IRF4 expression are *Itk* dependent (Nayar et al., 2012) (Berg et al., 2005), it is possible that factors such as cytokines also may help sustain IRF4 expression, which may lead to an overall enhancement in the TEC response. For instance, IL-12 enhances the expression of T-bet (Takemoto et al., 2006), another transcription factor that positively regulates the size of the TEC compartment (Joshi et al., 2007). Because the expression of T-bet was more dependent on IRF4 following infection with influenza A than LCMV, it is possible that IRF4 also functions to integrate signals from the TCR and cytokines to dictate the magnitude of the $CD8^+$ T cell response.

Another transcription factor, Blimp1, also plays a central role in terminal effector cell differentiation. Blimp1-deficient $CD8^+$ T cells have higher expression of TCF1 and Eomes transcripts and lower expression of T-bet mRNA (Rutishauser et al., 2009) (Kallies et al., 2009). Three recent studies found a role for IRF4 in Blimp-1 expression in $CD8^+$ T cells (Man et al., 2013) (Yao et al., 2013) (Raczkowski et

al., 2013). In our study, we find a dose-dependent effect of IRF4 levels on the expression of TCF1 and Eomes in $CD8^+$ T cells responding to infection. These observations not only confirm our previous data that IRF4 is a negative regulator of Eomes expression (Nayar et al., 2012) but also suggest that regulation of Eomes is more complex and possibly involves multiple transcription factors functioning in a temporal manner. Taken together, these data indicate that IRF4 is a central component of this transcriptional program and that the magnitude of IRF4 upregulation during $CD8^+$ T cell priming is a critical determinant of the outcome of the response.

Our data also provide a potential explanation for observations regarding the variable expansion, as well as the varying kinetics, of $CD8^+$ T cell responses to different viral epitopes. For instance, polyclonal $CD8^+$ T cells responses to LMCV epitopes GP_{33} and NP_{396} form the dominant response, whereas those to GP_{276} are subdominant (van der Most et al., 1998), suggesting that IRF4 expression is higher in the former populations. This possibility would fit with our data showing that the response of IRF4-sufficient P14 T cells in an *Irf4*$^{+/fl}$ host following LCMV infection gives the P14 cells a substantial competitive advantage over the endogenous response, compared with those same cells responding in a WT host. Because of the transient nature of IRF4 expression during T cell priming, we were unable to directly test this hypothesis on the polyclonal T cell response to LCMV. However, we did observe that the levels of TCF1, a downstream target of IRF4, were different between the different epitope-specific populations. TCF1

is also important for the conversion of T_{EM} to T_{CM} cells (Zhou et al., 2010). Because LCMV GP_{276}–specific cells convert to T_{CM} earlier than NP_{396}-specific cells following acute infection (Sarkar et al., 2007), these data are consistent with a lower level of IRF4 expression in the GP_{276}- specific subset. In further support of this hypothesis, *Irf4*$^{+/fl}$ $CD8^+$ T cells also convert to T_{CM} more rapidly than WT T cells. Thus, differences in the magnitude and/or duration of IRF4 expression may be one factor that could account for observed differences in the responses of $CD8^+$ T cells to distinct viral epitopes. Overall, our findings, along with those of others, demonstrate that variations in the levels of IRF4 expressed during T cell priming fine-tune the size and quality of the pathogen-specific adaptive immune response.

Chapter IV: IRF4 Regulates the Ratio of T-bet to Eomesodermin in $CD8^+$ T cells responding to persistent LCMV infection

Attributions and Copyright Information

The data described in this chapter were published in PLoS ONE in 2015.

IRF4 Regulates the Ratio of T-Bet to Eomesodermin in CD8+ T Cells Responding to Persistent LCMV Infection

Ribhu Nayar*, Elizabeth Schutten*, Sonal Jangalwe, Philip A Durost, Laurie L Kenney, James M Conley, Keith Daniels, Michael A Brehm, Raymond M Welsh, and Leslie J Berg

* indicates equal contribution by both authors

Specific Contribution to Figures: Ribhu Nayar and I performed, designed, and analyzed all experiments described in figure 4.1 through 4.10. Sonal Jangalwe performed the ELISA shown in figure 4.5E.

Oral consent was received from Ribhu Nayar to include work from this manuscript in the dissertation.

Introduction

Acute virus infections are characterized by the formation of robust $CD8^+$ T cell effector responses followed by the generation of immunological memory. Both $CD8^+$ effector T cells as well as $CD8^+$ memory cells produce a variety of cytokines and cytotoxic molecules, and have high proliferative capacity (Kaech & Cui, 2012). In contrast, during chronic viral infections, high viral loads cause $CD8^+$ T cell exhaustion that is characterized by hierarchal loss of effector functions and eventual deletion of antigen-specific cells (Wherry et al., 2003) (Fuller & Zajac, 2003) (Mueller & Ahmed, 2009). The remaining virus-specific $CD8^+$ T cells lose the ability to make IFNγ, TNFα, and IL-2, and up-regulate high levels of inhibitory receptors such as PD-1 and LAG-3. Eventually the cells become completely dysfunctional and are deleted by apoptosis (Wherry et al., 2003). T cell exhaustion was initially thought to be a viral immune evasion mechanism, but recent studies have indicated that it serves to protect the host from T cell-mediated immunopathology (Zajac et al., 1998) (Cornberg et al., 2013).

Many factors regulate T cell exhaustion. The expression of the immuno-suppressive cytokine IL-10 and inhibitory co-receptors like PD-1 enhance T cell exhaustion, whereas help from $CD4^+$ T cells aids in the restoration of $CD8^+$ T cell function (Brooks et al., 2006a) (Barber et al., 2005) (Matloubian et al., 1994)

(Aubert et al., 2011). Persistent T cell signaling due to high viral loads and increased MHC-I presentation is detrimental as well as beneficial during chronic infection. Increased antigen presentation results in reduced numbers and impaired function of anti-viral $CD8^+$ T cells; however, loss of this interaction also leads to poor viral control (Mueller & Ahmed, 2009). Antigen is also required for the long-term maintenance of virus-specific cells during chronic infections, as these cells do not undergo homeostatic proliferation in response to IL-7 and IL-15; instead, they require viral antigen (Wherry et al., 2004) (Shin et al., 2007).

In the presence of a persistent infection, exhausted $CD8^+$ T cells were found as two distinct subsets, one subset expressing high levels of the transcription factor, T-bet, and the other subset expressing high levels of the related transcription factor, Eomesodermin (Eomes). Further, Paley, et.al. showed that, in response to antigenic stimulation, $T\text{-bet}^{hi}$ cells give rise to $Eomes^{hi}$ cells. $T\text{-bet}^{hi}$ cells were found to be less exhausted and exhibited higher proliferative rates in response to antigen, while the $Eomes^{hi}$ cells were more exhausted, but exhibited greater cytotoxic activity than the $T\text{-bet}^{hi}$ cells. Both subsets were essential for viral control, as loss of either transcription factor resulted in viral persistence (Paley et al., 2012). These data indicated that optimal expression of T-bet and Eomes and the presence of both $CD8^+$ T cell subsets were both essential for efficient viral control. However, the pathway that regulates the differentiation of antigen-

specific T cells into these subsets, and whether a specific ratio of the two subsets is critical for viral control, are not known.

IRF4 is a pleiotropic transcription factor that regulates a myriad of functions in a wide variety of cell populations (Huber & Lohoff, 2014). Recently, others and we have shown that levels of IRF4 in $CD8^+$ T cells are regulated by the strength of TCR signaling. Thus, robust expression of IRF4 is important for maximal $CD8^+$ T cell expansion in response to acute viral infections (Nayar et al., 2014) (Yao et al., 2013) (Man et al., 2013) (Raczkowski et al., 2013) (Grusdat et al., 2014). When IRF4 levels are reduced by a haplo-deficiency of the *Irf4* gene, the magnitude of the $CD8^+$ T cell response is dramatically impaired. The decreased numbers of virus-specific T cells are accounted for by a reduction in terminal effector cells (TEC; $KLRG1^{hi}CD127^{lo}$) without a significant effect on the numbers of memory precursor cells (MPC, $KLRG1^{lo}CD127^{hi}$) (Nayar et al., 2014). These studies also highlighted a role for IRF4 in the expression of key transcription factors T-bet and Eomes, important for differentiation and maintenance of TEC and MPC populations, respectively, during acute infections (Nayar et al., 2014) (Yao et al., 2013) (Man et al., 2013) (Raczkowski et al., 2013) (Grusdat et al., 2014) (Joshi et al., 2007) (Banerjee et al., 2010).

Here we show that TCR signal strength maintains an optimal balance of T-bet to Eomes, and that this process is regulated by the levels of IRF4 expressed.

Reduced expression of IRF4 skews this ratio in the favor of Eomes during infection with LCMV-clone 13, resulting in reduced differentiation of T-bet^{+} Eomes^{-} precursors and impaired viral control. Reducing Eomes expression in Irf4 heterozygous mice re-establishes the protective balance of T-bet to Eomes, restores differentiation of T-bet^{+} Eomes^{-} precursors, and ultimately rescues defective viral clearance. These data indicate a critical role for IRF4 in regulating T cell exhaustion by balancing the relative expression of T-bet and Eomes during chronic infection. Overall, these findings demonstrate that reduced differentiation of the T-bet^{+} Eomes^{-} CD8^{+} T cell population impairs viral clearance, whereas a partial reduction in Eomes expression can restore viral control during persistent LCMV-clone 13 infections.

Results

TCR signal strength via IRF4 regulates the ratio of T-bet and Eomesodermin in activated CD8$^+$ T cells

To understand the role of TCR signal strength in the differentiation of CD8$^+$ T cell subsets, we utilized P14 TCR transgenic TCRa$^{-/-}$ cells (hereafter referred to as P14 WT), that respond to the lymphocytic choriomeningitis virus (LCMV) GP_{33-41} epitope (GP_{33}) bound to H2-D^b; additionally, P14 WT cells respond to a lower affinity 'F6L' peptide variant of GP_{33-41}, containing a single amino acid substitution from phenylalanine to leucine at the sixth position of the peptide. This alteration leads to a 5-fold decrease in the affinity of the P14 TCR for the F6L-H2-D^b complex relative to GP_{33-41}- H2-D^b, and as a consequence, a 100-1000-fold reduction in functional avidity(Gronski et al., 2004). P14 WT T cells were stimulated *in vitro* and then examined for T-bet (Figure 4.1A) and Eomes (previously published in (Nayar et al., 2014)) expression by intracellular staining. At 24hr post-stimulation, P14 WT T cells stimulated with the high affinity GP_{33} epitope, expressed a higher T-bet to Eomes ratio relative to cells stimulated with the lower affinity F6L epitope (Figure 4.2A). A similar trend was also observed when P14 cells were stimulated with decreasing doses of the GP_{33} peptide. These data indicate that variations in TCR signal strength, such as those achieved by varying the affinity of the peptide-MHC for the TCR or by varying the

dose of stimulating peptide, affect the relative expression levels of these key transcription factors.

The transcription factor IRF4 is upregulated in $CD8^+$ T cells in a graded manner in response to variations in TCR signal strength. Furthermore, IRF4 is known to be a negative regulator of Eomes and a positive regulator of T-bet expression in $CD8^+$ T cells (Nayar et al., 2014) (Yao et al., 2013) (Man et al., 2013) (Raczkowski et al., 2013) (Nayar et al., 2012) (Huber et al., 2012). To determine if alterations in IRF4 expression affect the relative up-regulation of T-bet and Eomes, we compared P14 WT T cells to P14 $TCRa^{-/-}$ cells lacking one or two functional alleles of *Irf4* (*Irf4*$^{+/fl}$ *X CD4-Cre* and *Irf4*$^{fl/fl}$ *X CD4-Cre*; referred to as P14 *Irf4*$^{+/fl}$ and P14 *Irf4*$^{fl/fl}$, respectively). In response to stimulation with the GP_{33} peptide, P14 WT cells expressed the highest T-bet to Eomes ratio, while P14 *Irf4*$^{+/fl}$ cells showed a reduced T-bet to Eomes ratio, and P14 *Irf4*$^{fl/fl}$ cells exhibited the lowest T-bet to Eomes ratio (Figure 4.2A). This pattern was observed at all time points examined (Figure 4.2B-C). Furthermore, no alterations in the ratio of T-bet to Eomes expression was observed when P14 *Irf4*$^{fl/fl}$ cells were stimulated with varying doses of GP_{33} peptide (Fig 4.2D-F). These data indicate that the strength of TCR signaling via IRF4 regulates the relative expression of T-bet and Eomes in $CD8^+$ T cells.

Figure 4.1. IRF4 regulates T-bet expression levels in stimulated CD8^{+} T cells at 72 hours post stimulation

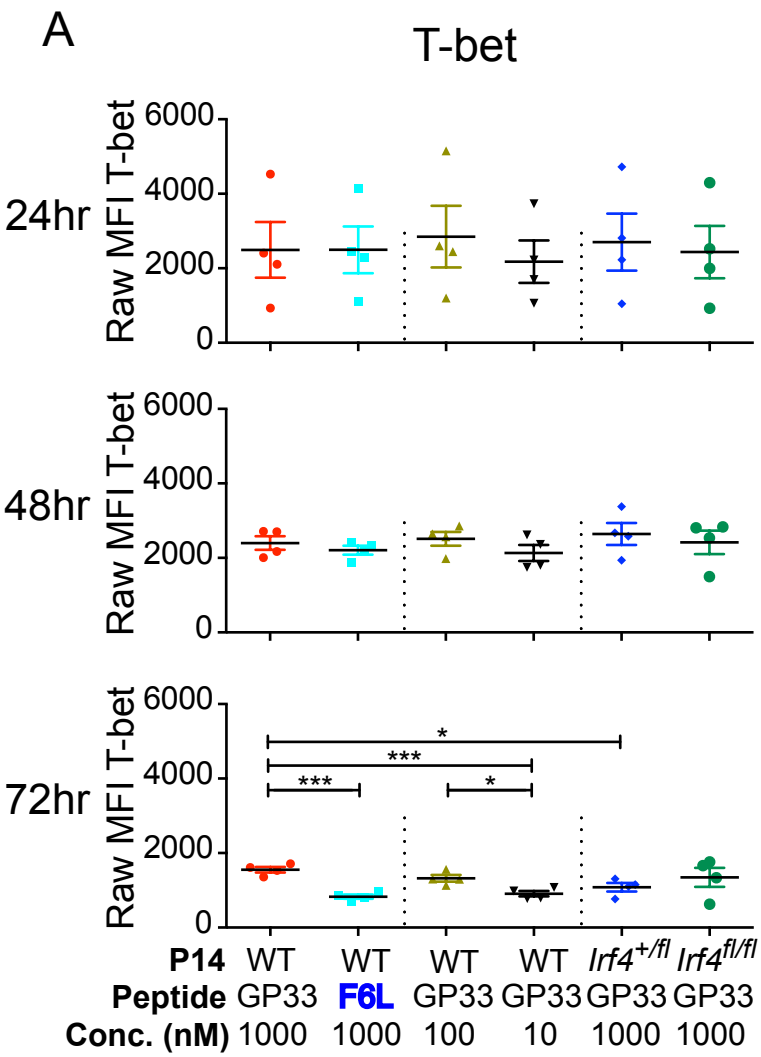

Figure 4.1: IRF4 regulates T-bet expression levels in stimulated $CD8^+$ T cells at 72 hours post stimulation

P14 WT, P14 *Irf4*$^{+/fl}$ or P14 *Irf4*$^{fl/fl}$ cells were stimulated with the indicated concentrations of GP_{33} and F6L peptides *in vitro*. At 24, 48, and 72 hours, cells were stained and analyzed for T-bet expression. The graphs show the raw MFIs for T-bet at each time-point. Data were generated from gated live $CD8^+CD45.2^+CD44^{hi}$ T cells analyzed in four independent experiments.

Figure 4.2. IRF4 regulates the T-bet to Eomesodermin ratio in stimulated CD8$^+$ T cells

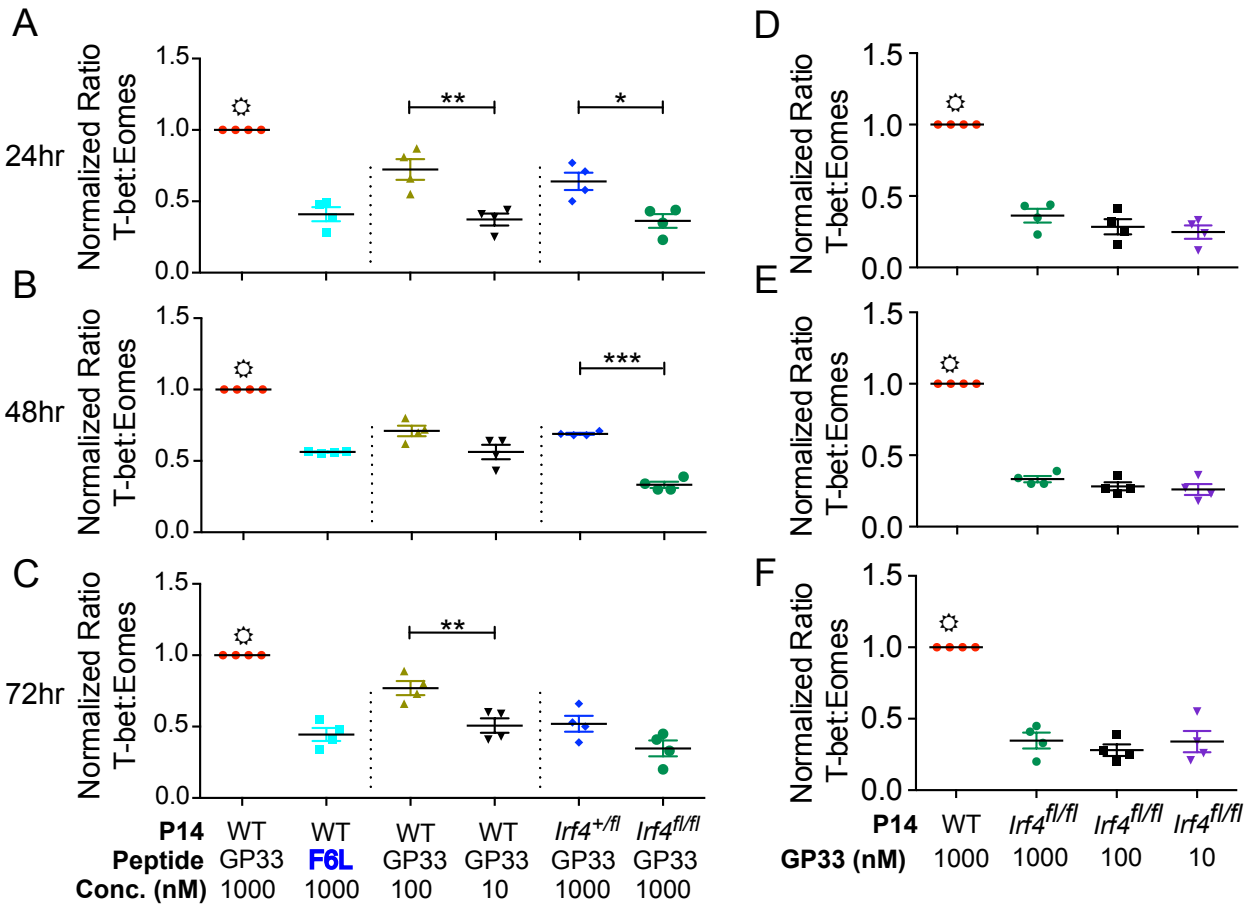

Figure 4.2: IRF4 regulates the T-bet to Eomesodermin ratio in stimulated $CD8^+$ T cells

P14 WT, P14 *Irf4*$^{+/fl}$ or P14 *Irf4*$^{fl/fl}$ cells were stimulated with the indicated concentrations of GP_{33} and F6L peptides *in vitro*. At **(A, D)** 24, **(B, E)** 48, or **(C, F)** 72 hours, cells were stained and analyzed for T-bet and Eomes expression. The graphs show compilations of the ratios of MFIs for T-bet relative to Eomes, each normalized to the value for 1μM GP_{33}-stimulated cells at each time-point. Data were generated from gated live $CD8^+CD45.2^+CD44^{hi}$ T cells analyzed in four independent experiments. ☼, denotes statistically significant difference between 1μM GP_{33}-stimulated cells and all other sample groups on the graph as determined by unpaired t test with Welch's correction.

Levels of IRF4 regulate CD8$^+$ T cell differentiation into T-bet$^+$ Eomes$^-$ and T-bet$^-$ Eomes$^+$ subsets in response to LCMV Cl13 infection

The data described thus far indicated a critical role of IRF4 in maintaining the balance of T-bet and Eomes *in vitro*. To determine whether the levels of IRF4 regulate the relative expression of T-bet and Eomes *in vivo*, WT, *Irf4*$^{+/fl}$ *X CD4-Cre* and *Irf4*$^{fl/fl}$ *X CD4-Cre* mice (henceforth referred to as *Irf4*$^{+/fl}$ and *Irf4*$^{fl/fl}$, respectively) were infected with an exhausting dose of LCMV-clone 13. Due to the defects in regulatory T cell populations in *Irf4*$^{fl/fl}$ mice, CD4$^+$ and CD8$^+$ T cell populations are activated in *Irf4*$^{fl/fl}$ mice even in the absence of infection (Nayar et al., 2012) (Zheng et al., 2009). As a result, we focused on understanding how modest reductions, rather than a complete loss of IRF4 expression, impacted the protective response to persistent virus infection.

Virus specific responses to H2-D^b/GP$_{276–286}$ and H2-D^b/GP$_{33–41}$ were examined using MHC-peptide tetramers. At day 8 post-infection, *Irf4*$^{+/fl}$ and *Irf4*$^{fl/fl}$ mice had reduced proportions and numbers of virus-specific CD8$^+$ T cells compared to WT mice, consistent with previous studies of acute virus infections in these mice (Figure 4.3A and 4.4A) (Nayar et al., 2014) (Yao et al., 2013) (Man et al., 2013) (Raczkowski et al., 2013) (Grusdat et al., 2014). At day 12 post-infection, WT and *Irf4*$^{+/fl}$ had similar levels of virus in their sera, whereas *Irf4*$^{fl/fl}$ mice showed slightly reduced control of the virus infection (Figure 4.3B). Analysis of T-bet and Eomes expression in the virus-specific CD8$^+$ T cells indicated that WT cells had

the highest T-bet to Eomes ratio, followed by *Irf4*$^{+/fl}$ CD8^{+} T cells, and then *Irf4*$^{fl/fl}$ cells (Figure 4.3C and 4.4B).

In response to LCMV-clone 13 infection, anti-viral CD8^{+} T cells differentiate into T-bet^{+} Eomes^{-} precursors that give rise to T-bet^{-} Eomes^{+} progeny in response to antigenic stimulation (Paley et al., 2012). Examination of these subsets at day 8 p.i. indicated an IRF4 dose-dependent defect in the differentiation of these populations. *Irf4*$^{+/fl}$ mice exhibited a significant decrease in the numbers and proportions of the T-bet^{+} Eomes^{-} precursors with a concomitant increase in the differentiation to T-bet^{+} Eomes^{+} cells (Figure 4.3D and 4.4C). These double positive cells could potentially be an intermediate population that differentiates into T-bet^{-} Eomes^{+} cells later during infection. As the viral titers are not different between WT and *Irf4*$^{+/fl}$ at day 12 p.i. (Figure 4.3B), these data indicate an inherent defect in the differentiation of CD8^{+} T cells expressing lower levels of IRF4. The differentiation of the *Irf4*$^{fl/fl}$ cells into T-bet^{+} Eomes^{-} and T-bet^{+} Eomes^{+} populations was severely compromised, likely accounting for the increased viral titers in the *Irf4*$^{fl/fl}$ mice. These data indicate that IRF4 regulates the relative expression of T-bet and Eomes and therefore may impact the differentiation of T-bet^{+} Eomes^{-} precursors into T-bet^{-} Eomes^{+} progeny early during persistent LCMV infection. Further, high levels of IRF4 are required for robust expansion of virus-specific T-bet^{+} Eomes^{-} effector CD8^{+} T cells and viral control at early times post-infection.

Figure 4.3 *Irf4* gene dosage regulates CD8^{+} T cell clonal expansion in response to LCMV-clone 13 infection and the differentiation of T-bet^{hi} and Eomes^{hi} subsets (GP$_{276}$)

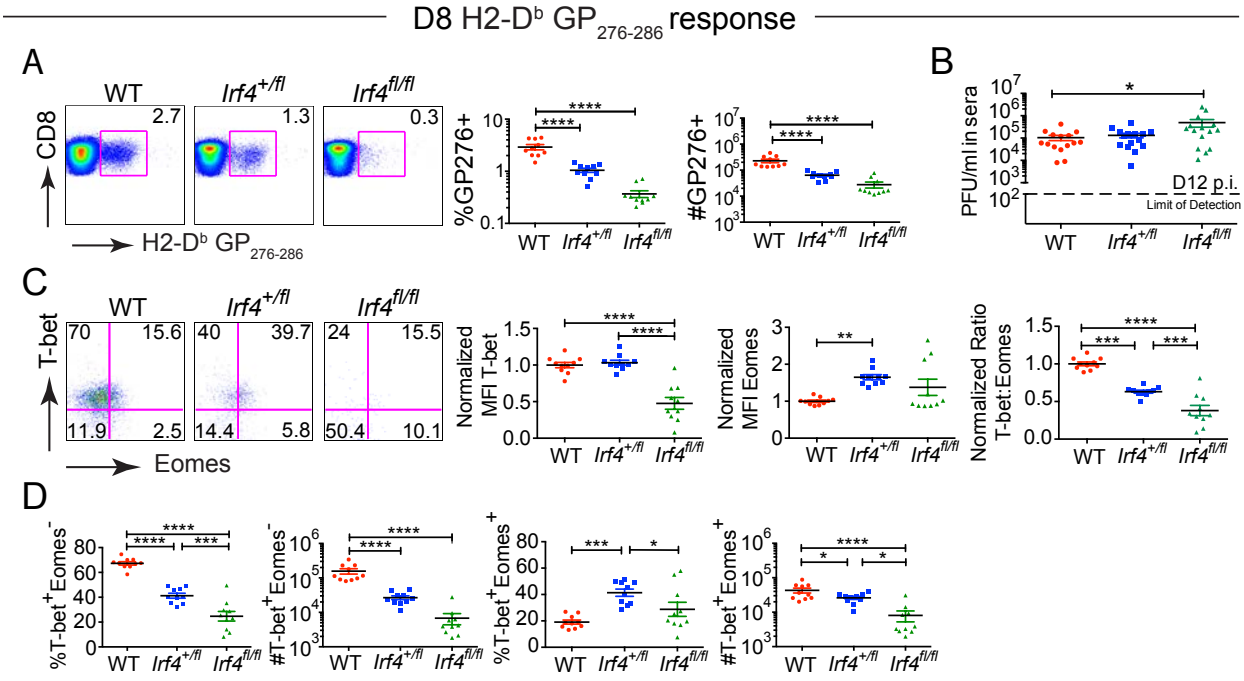

Figure 4.3: *Irf4* gene dosage regulates $CD8^+$ T cell clonal expansion in response to LCMV-clone 13 infection and the differentiation of T-bet^{hi} and $Eomes^{hi}$ subsets (GP_{276})

(A) Splenocytes from LCMV-clone 13-infected WT, $Irf4^{+/fl}$ and $Irf4^{fl/fl}$ mice were harvested at day 8 p.i. and stained with a viability dye, LCMV-specific H2-D^b-GP_{276} tetramer, and antibodies to CD8, T-bet and Eomes. Dot plots show CD8 versus H2-D^b-GP_{276} tetramer staining (left). Graphs show compilations of proportions and numbers from day 8 p.i. (right). Each data point represents an individual mouse and data are a compilation of three independent experiments. **(B)** LCMV-clone 13 titers in serum at day 12 post-infection. Dotted line indicates limit of detection. Each data point represents an individual mouse and data are a compilation of four independent experiments. **(C)** Representative dot plots show T-bet vs Eomes staining on gated $CD8^+$ live H2-D^b-GP_{276} specific cells at D8 p.i (left). Graphs show the MFI of T-bet and Eomes, each normalized to the average of WT samples for live $CD8^+$ H2-D^b-GP_{276} specific cells, and the ratio of normalized MFIs for T-bet relative to Eomes (right). Each data point represents an individual mouse and data are a compilation of three independent experiments. **(D)** Graphs show compilations of proportions and numbers of T-bet^+ $Eomes^-$ and T-bet^+ $Eomes^+$ cells. Each data point represents an individual mouse and data are a compilation of three independent experiments. Significant differences determined by Ordinary one-way ANOVA using Tukey's multiple comparison test.

Figure 4.4. *Irf4* gene dosage regulates CD8^{+} T cell clonal expansion in response to LCMV-clone 13 infection as well as the differentiation of T-bet^{hi} and Eomes^{hi} subsets (GP$_{33}$)

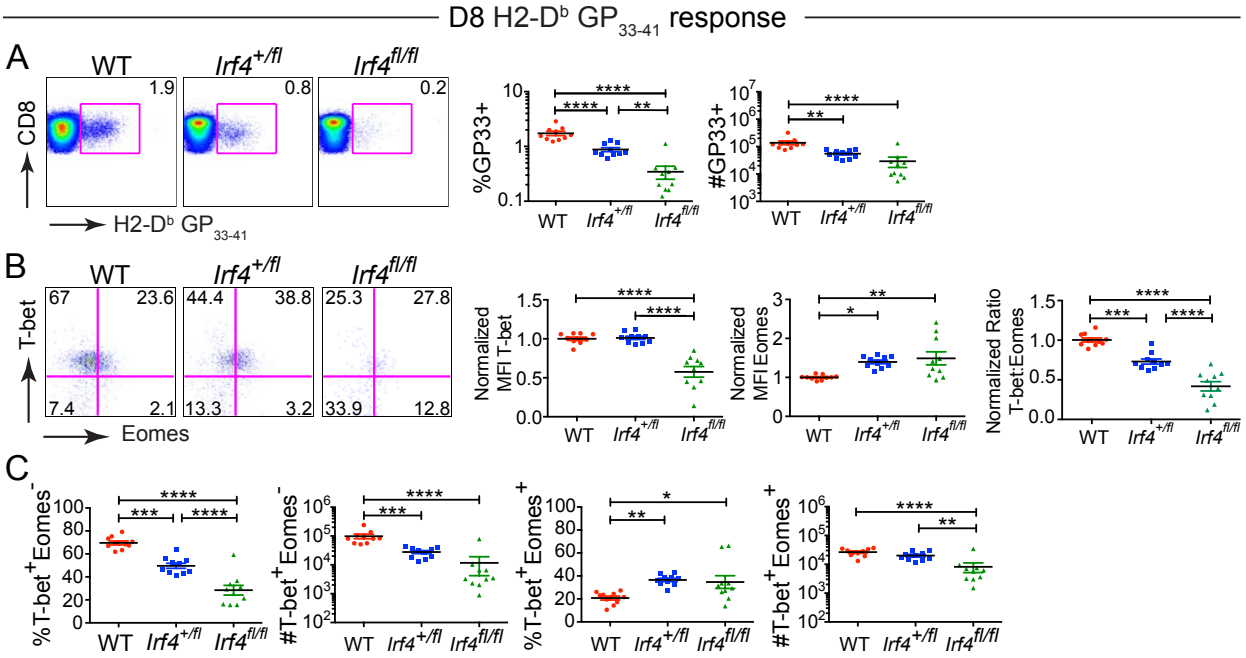

Figure 4.4: *Irf4* gene dosage regulates $CD8^+$ T cell clonal expansion in response to LCMV-clone 13 infection as well as the differentiation of T-bet^{hi} and $Eomes^{hi}$ subsets (GP_{33})

(A) Splenocytes from LCMV-clone 13-infected WT, $Irf4^{+/fl}$ and $Irf4^{fl/fl}$ mice were harvested at day 8 p.i. and stained with a viability dye, LCMV-specific $H2D^b$-GP_{33} tetramer, and antibodies to CD8, T-bet and Eomes. Dot plots show CD8 versus $H2\text{-}D^b$-GP_{33} tetramer staining. Graphs show compilations of proportions and numbers from day 8 post-infection (right). **(B)** Representative dot plots show T-bet vs Eomes staining on gated $CD8^+$ live $H2\text{-}D^b$-GP_{33} specific cells at day 8 p.i. Graphs show the MFI of T-bet and Eomes each normalized to the average of WT samples in each experiment for live $CD8^+$ $H2\text{-}D^b$-GP_{33} specific cells, and the ratio of normalized MFIs for T-bet relative to Eomes. **(C)** Graphs show compilations of proportions and numbers of T-bet^+ $Eomes^-$ and T-bet^+ $Eomes^+$ cells. Each data point represents an individual mouse and data are a compilation of three independent experiments; significant differences determined by Ordinary one-way ANOVA using Tukey's multiple comparison test.

WT levels of IRF4 are required to maintain the balance of T-bet to Eomesodermin expression during persistent infection

In activated T cells, the expression of IRF4 is regulated by the strength of TCR signaling via the mTOR pathway; furthermore, mTOR signaling is suppressed during chronic infection by signaling through the inhibitory receptor PD-1 (Nayar et al., 2014) (Yao et al., 2013) (Man et al., 2013) (Nayar et al., 2012) (Staron et al., 2014). To test the importance of IRF4 expression levels at later timepoints during the persistent infection, we examined $CD8^+$ T cell responses to LCMV-clone 13 at day 21-24 p.i. At this time point, we observed reduced proportions of virus-specific T cells in the spleens of *Irf4*$^{+/fl}$ mice compared to WT mice; however, absolute numbers were not significantly different (Figure 4.5A, D). As expected, *Irf4*$^{fl/fl}$ mice had significant reductions in both the proportions and numbers of both subsets of virus-specific $CD8^+$ T cells.

Examination of T-bet and Eomes expression in virus-specific $CD8^+$ T cells at day 21-24 p.i. with LCMV-clone 13 indicated that for both of the LCMV epitopes examined, virus-specific *Irf4*$^{+/fl}$ $CD8^+$ T cells exhibited an altered T-bet to Eomes ratio relative to WT cells (Figure 4.5C, E). This skewed ratio resulted in reduced differentiation of T-bet$^+$ Eomes$^-$ and increased differentiation of T-bet$^-$ Eomes$^+$ populations in *Irf4*$^{+/fl}$ mice relative to WT mice (Figure 4.5C, E and 4.6A, C). High viral titers have been implicated in the excessive proliferation and eventual

Figure 4.5. Persistent reduction in virus-specific T-bet^{+} Eomes^{-} CD8^{+} T cells in LCMV-clone 13-infected *Irf4*$^{+/fl}$ mice

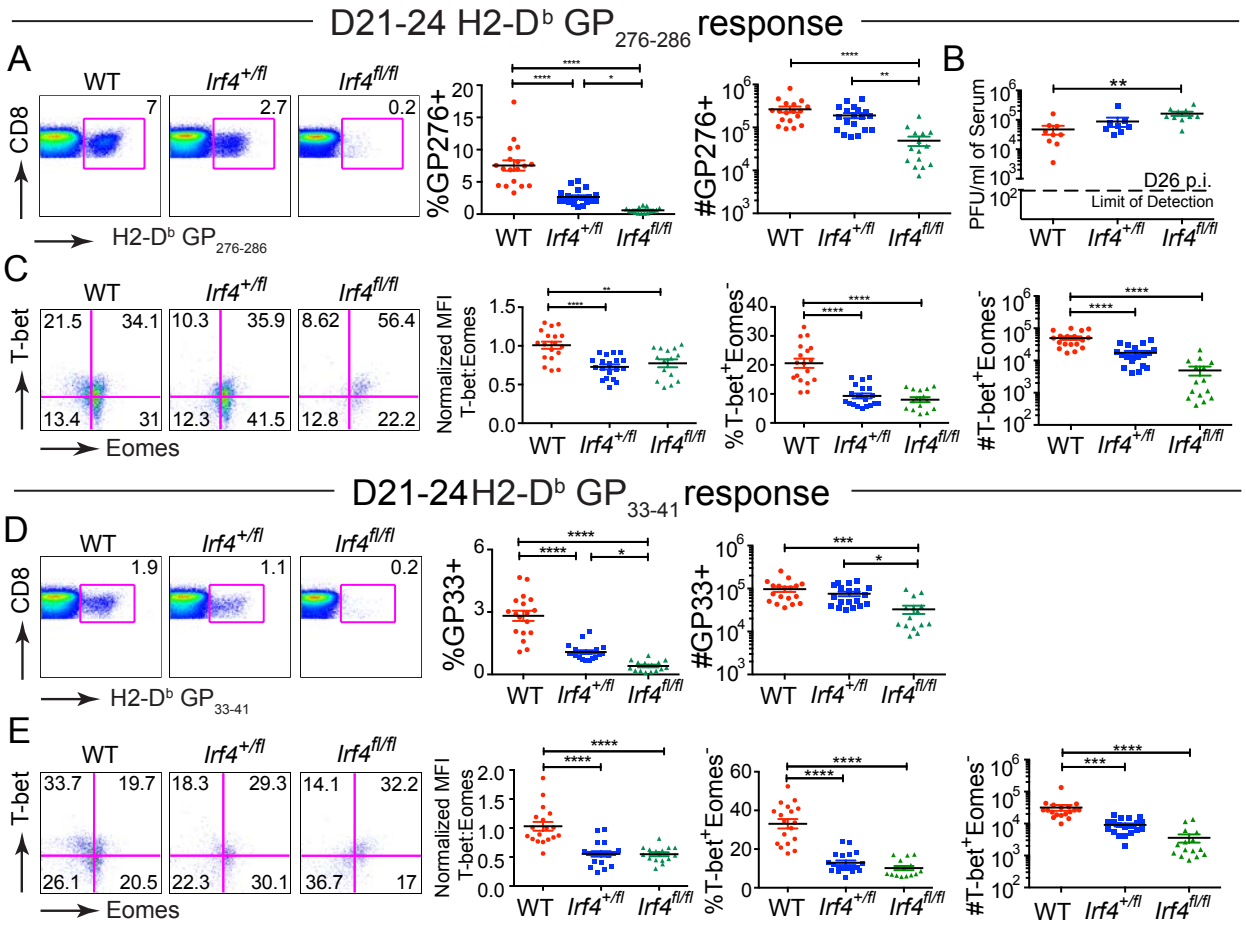

Fig 4.5. Persistent reduction in virus-specific T-bet^{+} Eomes^{-} CD8^{+} T cells in LCMV-clone 13-infected *Irf4*$^{+/fl}$ mice

(A, D) Splenocytes from LCMV-clone 13-infected WT, *Irf4*$^{+/fl}$ and *Irf4*$^{fl/fl}$ mice were were harvested at day 21-24 p.i. and stained with a viability dye, LCMV-specific H2-D^{b}-GP$_{276}$ and H2D^{b}-GP$_{33}$ tetramers, and antibodies to CD8, T-bet and Eomes. Dot plots show CD8 versus H2-D^{b}-GP$_{276}$ **(A)** or H2-D^{b}-GP$_{33}$ **(D)** tetramer staining (left). Graphs show compilations of proportions and numbers from day 21-24 p.i. (right). Each data point represents an individual mouse and data are a compilation of five independent experiments. **(B)** LCMV-clone 13 titers in serum at day 26 post-infection. Dotted line indicates limit of detection. Each data point represents an individual mouse and data are a compilation of two independent experiments. **(C, E)** Dot plots show T-bet vs Eomes staining on live CD8^{+} H2-D^{b}-GP$_{276}$ **(C)** or H2-D^{b}-GP$_{33}$ **(E)** tetramer positive cells (left). Graph shows the ratio of MFIs of T-bet relative to Eomes, each normalized to the average value of WT samples (middle). Graphs show a compilation of proportions and numbers of T-bet^{+} Eomes^{-} cells for each population (right). Each data point represents an individual mouse and data are a compilation of five independent experiments. Significant differences determined by Ordinary one-way ANOVA using Tukey's multiple comparison test.

Figure 4.6. *Irf4* gene dosage regulates the proportions of virus-specific CD8$^+$ T cells during persistent LCMV-clone 13 infection

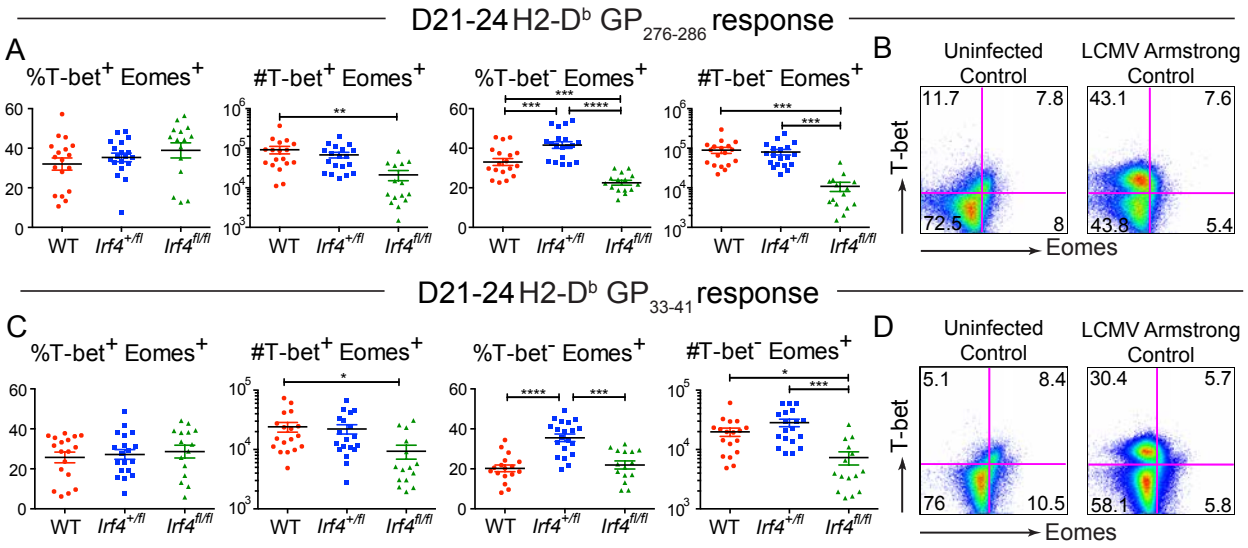

Figure 4.6: *Irf4* gene dosage regulates the proportions of virus-specific CD8$^+$ T cells during persistent LCMV-clone 13 infection

Splenocytes from LCMV-clone 13 infected WT, *Irf4*$^{+/fl}$ and *Irf4*$^{fl/fl}$ mice were harvested between day 21-24 p.i. and stained with a viability dye, LCMV-specific H2-D^b-GP$_{276}$ and H2D^b-GP$_{33}$ tetramers, and antibodies to CD8, T-bet and Eomes. **(A, C)** Graphs show the numbers and proportions of T-bet$^+$ Eomes$^+$ (left) and T-bet$^-$ Eomes$^+$ (right) populations. Each data point represents an individual mouse and data are compilations of five independent experiments; significant differences determined by Ordinary one-way ANOVA using Tukey's multiple comparison test. **(B, D)** Dot plots of uninfected control and LCMV Armstrong infected control used to determine gating of T-bet versus Eomes for each tetramer stained subset.

conversion of the T-bet^{hi} CD8^{+} T cell population into Eomes^{hi} CD8^{+} T cell population in patients with chronic HCV infection (Paley et al., 2012) (Popescu et al., 2014). However, at day 26 p.i., we observed no difference in serum virus titers between *Irf4*$^{+/fl}$ and WT mice, indicating that the altered CD8^{+} T cell populations were not simply a reflection of differences in viral load (Figure 4.5B). These data indicate that a modest reduction in IRF4 expression leads to impaired generation of T-bet^{+} Eomes^{-} virus-specific CD8^{+} T cells at later timepoints of the persistent infection.

Intrinsic role of IRF4 in regulating the balance of T-bet to Eomesodermin expression in CD8^{+} T cells responding to LCMV-clone 13 infection

To address whether differences in IRF4 expression were regulating the balance of T-bet to Eomes by acting in virus-specific CD8^{+} T cells, we performed adoptive transfer experiments. P14 WT or P14 *Irf4*$^{+/fl}$ CD8^{+} T cells were transferred into congenic hosts, and recipients were infected with LCMV-clone 13. Beginning at day 10 p.i., we observed that a proportion of recipients receiving WT P14 cells were succumbing to the infection, a response not seen in recipients that received P14 *Irf4*$^{+/fl}$ cells (Figure 4.7A). Analysis of viral titers in the sera of the surviving mice at D15 p.i. indicated that 75% of recipients receiving WT P14 cells had viral titers <7.5x10^{4}, whereas for recipients receiving P14 *Irf4*$^{+/fl}$ cells, this value was 2.9x10^{5}; however, the means of the two datasets were not significantly different. Based on previous studies showing that fatality from LCMV-clone 13 infection

Figure 4.7. Cell-intrinsic role of IRF4 in regulating the balance of T-bet to Eomesodermin expression in CD8$^+$ T cells responding to LCMV-clone 13 infection

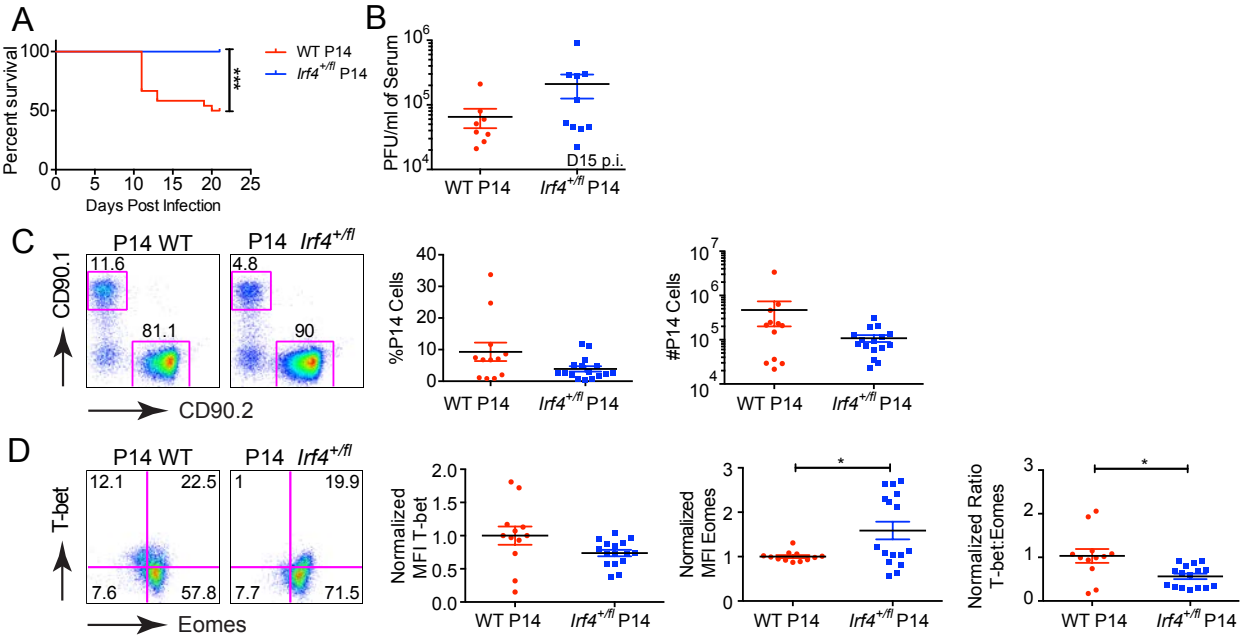

Figure 4.7: Cell-intrinsic role of IRF4 in regulating the balance of T-bet to Eomesodermin expression in CD8$^+$ T cells responding to LCMV-clone 13 infection

1 x 10^4 CD90.1 WT P14 cells or CD90.1 *Irf4*$^{+/fl}$ P14 cells were transferred into CD90.2 CD4-Cre$^+$ host mice and one day later recipients were infected with LCMV-clone 13. **(A)** Survival curve showing percent survival of recipient mice that received either WT or *Irf4*$^{+/fl}$ P14 cells over 22 days. Data are a compilation of three independent experiments. **(B)** Serum was harvested from recipient mice at day 15 post infection and virus titers were determined by plaque assay. Each data point represents an individual mouse and data are a compilation of two independent experiments. **(C)** Dot plots show CD90.1 (transferred cells) versus CD90.2 (host cells) staining on gated live CD8$^+$ T cells (left). Graphs show compilations of proportions and numbers of transferred P14 cells at day 22 post-infection (right). Each data point represents an individual mouse and data are a compilation of three independent experiments. **(D)** Dot plots show T-bet versus Eomes staining on gated live CD90.1$^+$ CD8$^+$ T cells (left). Graphs show the normalized MFI of T-bet and Eomes, each normalized to the average of P14 WT transferred samples and the ratio of the normalized MFIs for T-bet relative to Eomes, (right). Each data point represents an individual mouse and data are a compilation of three independent experiments. Statistical analysis was determined by Log-rank (Mantel-Cox) test **(A)** or unpaired t test with Welch's correction **(B-D)**.

results from excessive T cell responses leading to immunopathology (Cornberg et al., 2013), these data suggest a more robust effector response of WT compared to *Irf4*$^{+/fl}$ P14 cells to the LCMV-clone 13 infection, consistent with previous observations (Grusdat et al., 2014).

To examine the P14 cells directly, surviving mice were analyzed at day 22 p.i.. At this timepoint, we recovered fewer P14 *Irf4*$^{+/fl}$ cells from recipient mice compared to WT P14 cells (Figure 4.7C). Examination of these cells for T-bet and Eomes expression showed that WT P14 cells had increased levels of T-bet and reduced levels of Eomes relative to P14 *Irf4*$^{+/fl}$ cells, resulting in higher T-bet to Eomes ratio in the WT P14 cells (Figure 4.7D). Overall, these data indicate that the magnitude of IRF4 expression in virus-specific CD8^{+} T cells regulates their expansion, as well as the relative expression of T-bet and Eomes in response to LCMV-clone 13.

WT levels of IRF4 are essential for optimal control of persistent virus infection

While modest reductions in the levels of IRF4 were inconsequential for early control of virus replication through day 26 p.i. long-term studies revealed that *Irf4*$^{+/fl}$ mice had a defect in controlling the persistent virus infection. Relative to WT mice, a lower proportion of *Irf4*$^{+/fl}$ mice controlled LCMV-clone 13 infection in the kidney, liver and serum when examined more than 100 days p.i. (Figure

Figure 4.8. High expression of IRF4 is essential for long-term control of LCMV-clone 13

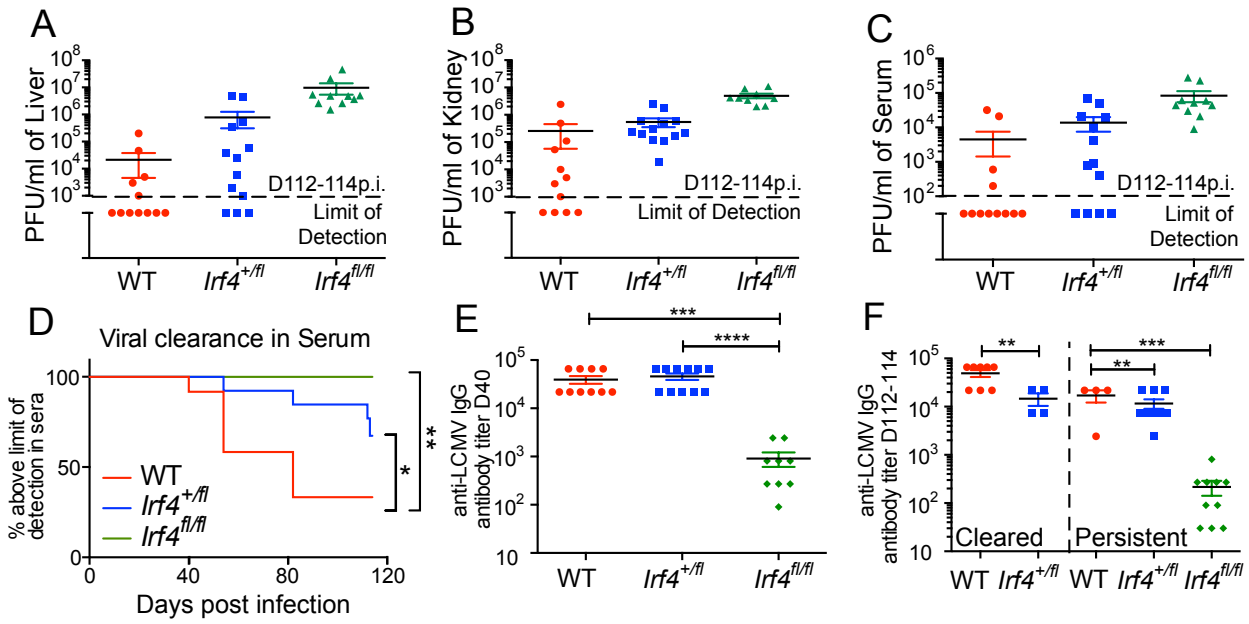

Figure 4.8: High expression of IRF4 is essential for long-term control of LCMV-clone 13

Kidney **(A)**, livers **(B)**, and sera **(C)** were harvested from LCMV-clone 13 infected WT, *Irf4*$^{+/fl}$ and *Irf4*$^{fl/fl}$ mice between day 112-114 post-infection and virus titers were determined by plaque assay. Dotted line indicates the limit of detection. Each data point represents an individual mouse and data are a compilation of three independent experiments. **(D)** Serum was harvested from infected mice at various timepoints post-infection. Graph indicates the proportion of mice with viral titers above the limit of detection over time. Data are a compilation of three independent experiments; significant differences were determined by Log-rank (Mantel-Cox) test. **(E)** Anti-LCMV IgG antibody titers in sera at day 40 p.i. Each data point represents an individual mouse and data are a compilation of three independent experiments; significant differences determined by Ordinary one-way ANOVA using Tukey's multiple comparison test. **(F)** Anti-LCMV IgG antibody titers in sera at day 112-114 p.i. Data are segregated based on serum viral titers; at left are mice with undetectable virus in their sera (cleared) and at right are mice with persistent serum virus titers (persistent). Each data point represents an individual mouse and data are a compilation of three independent experiments; significant differences determined by unpaired t test with Welch's correction (cleared) and Ordinary one-way ANOVA using Tukey's multiple comparison test (persistent).

4.8A-C). In addition, enumeration of viral titers in sera over time indicated that the kinetics of viral control were slower for *Irf4*$^{+/fl}$ mice than WT mice (Figure 4.8D). As expected, *Irf4*$^{fl/fl}$ mice exhibited the highest viral titers and a complete impairment in viral control (Figure 4.8A-D).

IRF4 is also important for the differentiation of CD4$^+$ T_{FH} cells that regulate plasma cell differentiation. As previous studies have shown that during LCMV infection reduced antibody responses lead to virus persistence (Bergthaler et al., 2009) (Thomsen et al., 1996), we considered whether the slower kinetics of virus control in *Irf4*$^{+/fl}$ mice could be accounted for by reduced anti-LCMV antibody titers. Analysis of LCMV-specific IgG antibody titers at day 40 p.i. indicated that *Irf4*$^{fl/fl}$ mice were impaired in antibody production, consistent with the requirement for IRF4 in T_{FH} differentiation (Figure 4.8E). However, we observed no difference in antibody titers between WT and *Irf4*$^{+/fl}$ mice, supporting a CD8$^+$ T cell-intrinsic defect in viral control in *Irf4*$^{+/fl}$ mice. We then analyzed virus-specific antibody titers at day 112-114 p.i., a timepoint at which the majority of WT mice were controlling the infection. When antibody data were segregated so that WT and *Irf4*$^{+/fl}$ mice were compared based on whether they had detectable virus in their sera (Figure 4.8C), we found slightly reduced antibody titers in *Irf4*$^{+/fl}$ mice that were controlling the virus relative to WT mice in this group (Figure 4.8F). However, no difference in antibody titers between the two genotypes of mice were seen for those that still had persistent virus replication in their sera. These

data indicate that high levels of IRF4 expression are essential for optimal long-term control of the persistent LCMV-clone 13 infection, and that differences in viral control are not correlated with differences in anti-viral antibody titers.

Examination of virus-specific $CD8^+$ T cells at day 112-114 p.i. showed no significant differences in their numbers of virus-specific $CD8^+$ T cells in *Irf4*$^{+/fl}$ mice compared to WT controls (Figure 4.9A, D). Nonetheless, consistent with our observation from day 8 and day 21-24 p.i., virus-specific *Irf4*$^{+/fl}$ $CD8^+$ T cells at day 112-114 p.i. exhibited reduced T-bet to Eomes ratio relative to WT cells (Figure 4.10A, C). This skewed ratio resulted in higher proportions and numbers of T-bet$^+$ Eomes$^-$ virus-specific $CD8^+$ T cells in WT mice relative to *Irf4*$^{+/fl}$ mice (Figure 4.9B, E). When the data from the WT mice were segregated according to viral titers, we found that WT mice that had not controlled LCMV-clone 13 infection at this time point, appeared as outliers and had proportions and numbers of T-bet$^+$ Eomes$^-$ virus-specific $CD8^+$ T cells comparable to *Irf4*$^{+/fl}$ mice (Figure 4.9B, E). These findings are consistent with the conclusion that persistent antigen is essential for conversion of T-bet$^+$ Eomes$^-$ cells into T-bet$^-$ Eomes$^+$ progeny (Paley et al., 2012).

Control of persistent LCMV-clone 13 infection has been associated with high numbers of T-bet$^+$ virus-specific $CD8^+$ T cells that lack expression of the

Figure 4.9. The proportions of T-bet^{+} Eomes^{-} cells correlate with viral control at late timepoints of LCMV-clone 13 infection

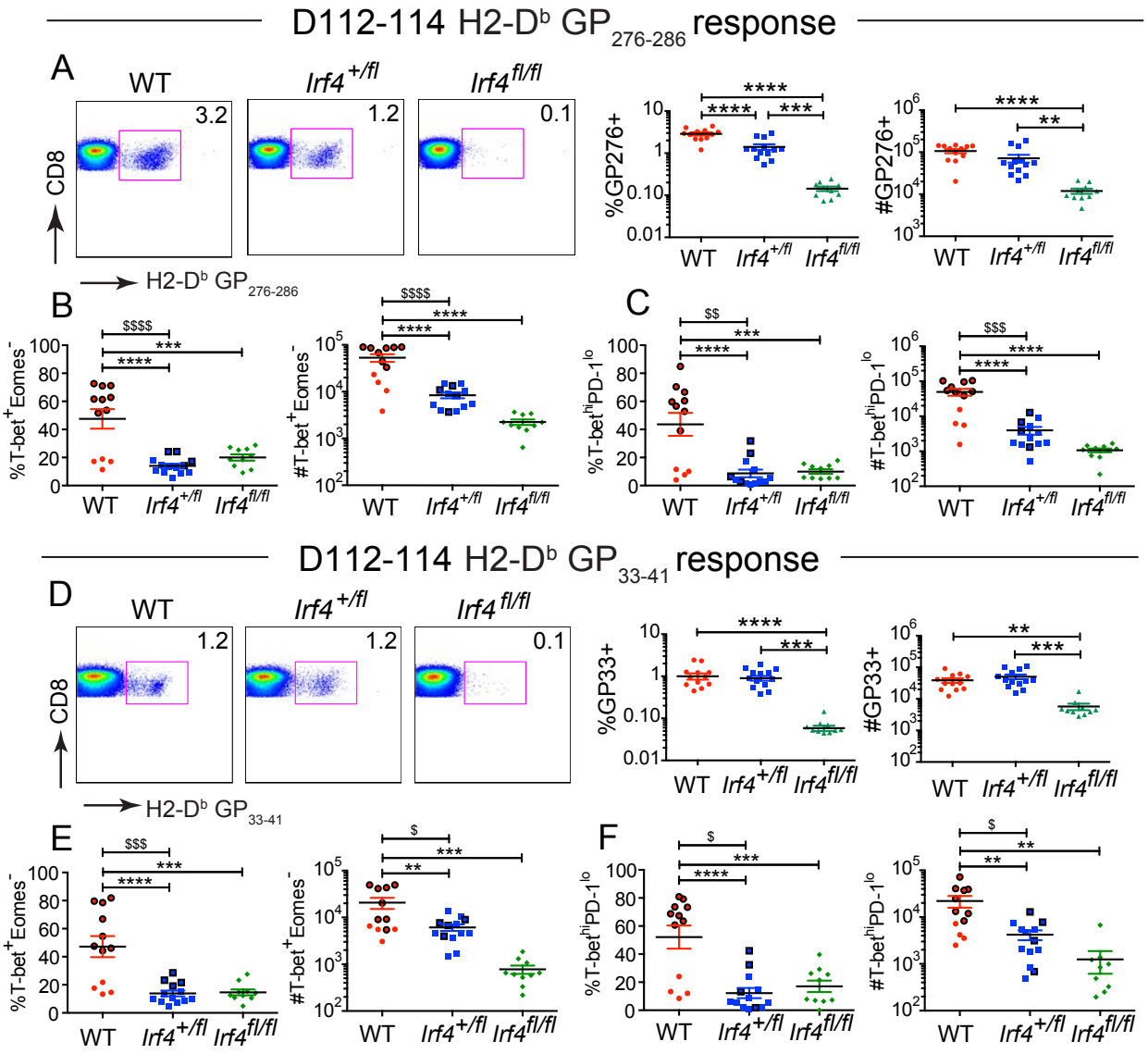

Figure 4.9: The proportions of T-bet^{+} Eomes^{-} cells correlate with viral control at late timepoints of LCMV-clone 13 infection

(A, D) Splenocytes from LCMV-clone 13-infected WT, *Irf4*$^{+/fl}$ and *Irf4*$^{fl/fl}$ mice were stained with a viability dye, LCMV-specific H2-D^{b}-GP$_{276}$ and H2D^{b}-GP$_{33}$ tetramers, and antibodies to CD8, T-bet and Eomes, and analyzed between day 112-114 p.i. Dot plots show CD8 versus H2-D^{b}-GP$_{276}$ **(A)** or CD8 vs H2D^{b}-GP$_{33}$ **(D)** tetramer staining on live CD8^{+} T cells. Graphs show compilations of proportions and numbers of tetramer-specific cells from day 112-114 post infection. **(B, E)** Graphs show compilations of the numbers and proportions of T-bet^{+} Eomes^{-} H2-D^{b}-GP$_{276}$ **(B)** or H2-D^{b}-GP$_{33}$ **(E)** specific cells. **(C, F)** Graphs show compilations of the numbers and proportions of T-bet^{hi} PD-1^{lo} H2-D^{b}-GP$_{276}$ **(C)** or H2-D^{b}-GP$_{33}$ **(F)** specific cells. Symbols outlined in bold represent mice with undetectable titers of virus in sera at day 112-114 p.i. Each data point represents an individual mouse and data are a compilation of three independent experiments; significant differences determined by Ordinary one-way ANOVA using Tukey's multiple comparison test. $ denotes statistically significant difference between WT and *Irf4*$^{+/fl}$ samples when analyzing only mice with undetectable serum viral titers (bold outlined symbols). Significant differences between outlined samples were determined by unpaired t test with Welch's correction.

Figure 4.10. Clearance of LCMV-clone 13 leads to increased T-bet to Eomesodermin ratios

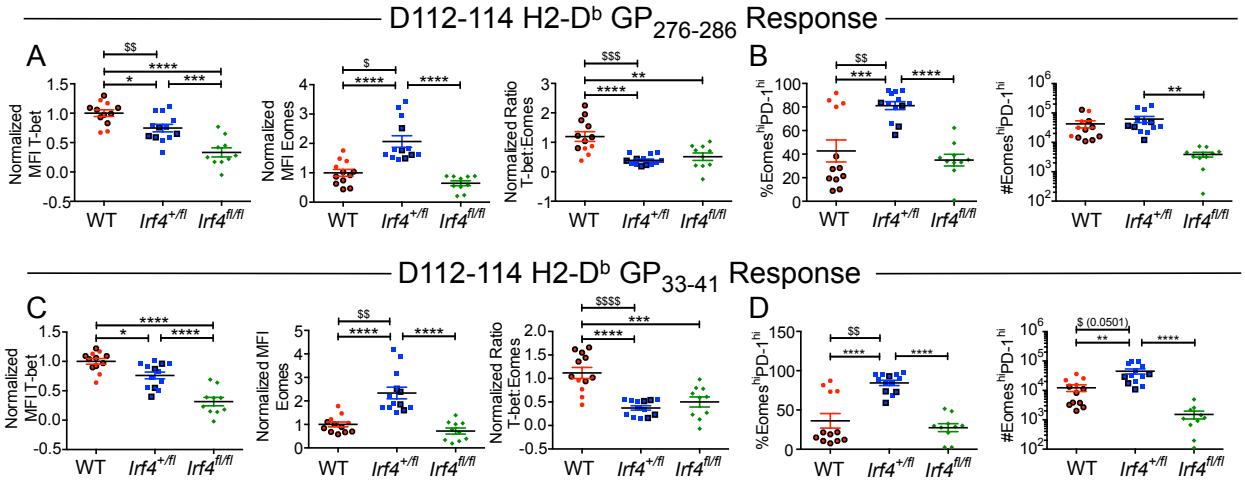

Figure 4.10: Clearance of LCMV-clone 13 leads to increased T-bet to Eomesodermin ratios

Splenocytes from LCMV-clone 13-infected WT, *Irf4*$^{+/fl}$ and *Irf4*$^{fl/fl}$ mice were stained with a viability dye, LCMV-specific H2-D^{b}-GP$_{276}$ and H2D^{b}-GP$_{33}$ tetramers, and antibodies to CD8, T-bet and Eomes, and analyzed between day 112-114 p.i. Graphs show the MFI of T-bet and Eomes each normalized to the average of WT samples, and the ratio of normalized MFIs for T-bet relative to Eomes, for live CD8^{+} H2-D^{b}-GP$_{276}$ **(A)** and H2-D^{b}-GP$_{33}$ **(C)** specific cells. Graphs show compilations of the numbers and proportions of Eomes^{hi} PD-1^{hi} H2-D^{b}-GP$_{276}$ **(B)** or H2-D^{b}-GP$_{33}$ **(D)** specific cells. Each data point represents an individual mouse and data are a compilation of three independent experiments; significant differences determined by Ordinary one-way ANOVA using Tukey's multiple comparison test. Symbols with bold outlines represent mice whose serum viral titers were below the limit of detection at day 112-114 p.i.. $ denotes statistically significant difference between WT and *Irf4*$^{+/fl}$ samples when analyzing only mice with undetectable serum viral titers (bold outlined symbols). Significant differences between bold outlined samples were determined by unpaired t test with Welch's correction.

exhaustion marker, PD-1 (Paley et al., 2012). When analyzed at day 112-114 p.i., we observed increased proportions and numbers of T-bet^{hi} PD-1^{lo} cells in WT mice relative to *Irf4*$^{+/fl}$ and *Irf4*$^{fl/fl}$ mice infected with LCMV-clone 13 (Figure 4.9C, F). However, as with the analysis of T-bet^{+} Eomes^{-} cells, the T-bet^{hi} PD-1^{lo} population in WT mice that had not cleared the virus by this timepoint appeared more similar to that of the *Irf4*$^{+/fl}$ cells. These data suggest that the proportions and numbers of T-bet^{hi} PD-1^{lo} CD8^{+} T cells may be more closely associated with viral control than with IRF4 expression levels. Similar findings are evident from analysis of Eomes^{+} PD-1^{hi} CD8^{+} T cell proportions and numbers at this timepoint (Figure 4.10B, D).

Reducing Eomes expression improves viral control in LCMV-clone 13-infected *Irf4*$^{+/fl}$ mice

The data presented above indicated that LCMV-clone 13-infected *Irf4*$^{+/fl}$ mice have a lower T-bet to Eomes ratio than WT mice in their virus-specific CD8^{+} T cells at all time points investigated post-infection. Since optimal expression of both of these factors is essential for viral control, we considered whether manipulation of this ratio in favor of T-bet would restore protective CD8^{+} T cell responses in *Irf4*$^{+/fl}$ mice, leading to improved viral control. To address this, *Irf4*$^{+/fl}$ mice were crossed to Eomes$^{+/fl}$ mice to generate *Irf4*$^{+/fl}$ Eomes$^{+/fl}$ *CD4-Cre* mice (henceforth referred to as *Irf4*$^{+/fl}$ Eomes$^{+/fl}$ mice). These compound heterozygotes

were infected with LCMV-clone 13, along with WT, *Irf4*$^{+/fl}$, and Eomes$^{+/fl}$ mice and analyzed at day 77-82 p.i.

We first observed higher proportions of GP_{276}-specific T cells in the spleens of WT mice relative to the other three genotypes. Analysis of absolute cell numbers indicated that WT mice had more GP_{276}-specific CD8^{+} T cells than did Eomes$^{+/fl}$ or *Irf4*$^{+/fl}$ Eomes$^{+/fl}$ mice; in addition, *Irf4*$^{+/fl}$ Eomes$^{+/fl}$ mice had significantly fewer cells than did *Irf4*$^{+/fl}$ mice (Figure 4.11A). In contrast, the proportions of GP_{33}-specific CD8^{+} T cells were similar between all four genotypes with only modest differences in the absolute numbers of these virus-specific CD8^{+} T cell populations (Figure 4.11C).

Analysis of the levels of T-bet and Eomes in virus-specific CD8^{+} T cells between day 77-82 p.i. indicated that the *Irf4*$^{+/fl}$ and the compound heterozygotes had lower T-bet expression relative to WT, as would be expected due to the role of IRF4 in positively regulating T-bet expression (Figure 4.11B, D) (Nayar et al., 2014) (Yao et al., 2013) (Man et al., 2013) (Kurachi et al., 2014). The expression of Eomes was higher in the *Irf4*$^{+/fl}$ cells relative to *Irf4*$^{+/fl}$ Eomes$^{+/fl}$ cells, indicating that the heterozygous deficiency in Eomes was able to reduce Eomes protein expression in *Irf4*$^{+/fl}$ cells (Figure 4.11B, D). In addition, *Irf4*$^{+/fl}$ Eomes$^{+/fl}$ cells showed normalized ratios of T-bet to Eomes expression levels that were comparable to those seen in WT cells. Furthermore, the re-establishment of the

Figure 4.11. *Irf4-Eomes* compound haplodeficiency restores the T-bet to Eomes ratios in virus-specific CD8$^+$ T cells

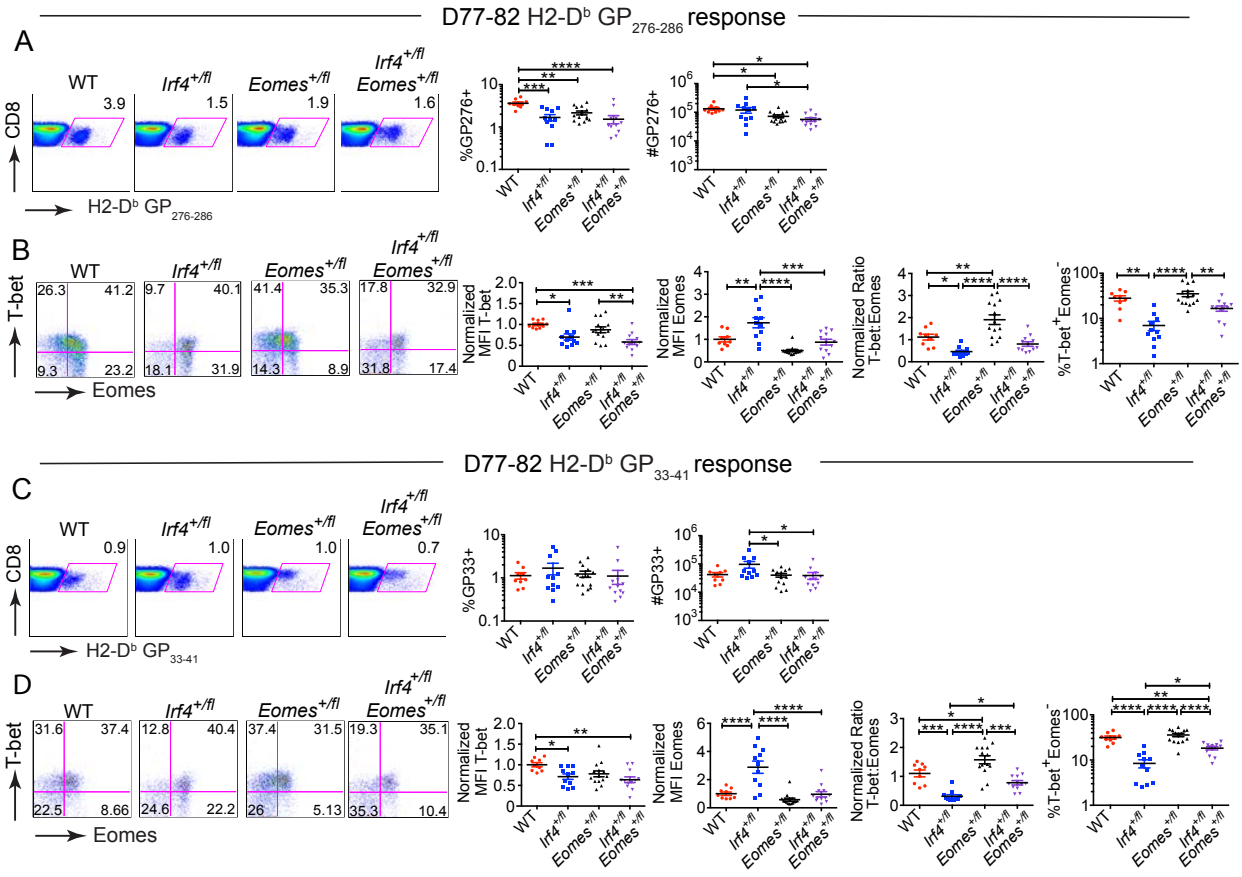

Figure 4.11: *Irf4-Eomes* compound haplodeficiency restores the T-bet to Eomes ratios in virus-specific CD8$^+$ T cells

Splenocytes from LCMV-clone 13 infected WT, *Irf4*$^{+/fl}$, Eomes$^{+/fl}$ and *Irf4*$^{+/fl}$Eomes$^{+/fl}$ mice were stained with a viability dye, LCMV-specific H2-D^b-GP$_{276}$ and H2D^b-GP$_{33}$ tetramers, and antibodies to CD8, T-bet and Eomes and analyzed between D77-82 p.i. **(A, C)** Dot plots show CD8 vs H2-D^b-GP$_{276}$ **(A)** or CD8 vs H2D^b-GP$_{33}$ **(C)** tetramer staining on live CD8$^+$ T cells. Graphs show compilations of proportions and numbers of virus-specific CD8$^+$ T cells. **(B, D)** Dot plots show T-bet vs Eomes staining of H2-D^b-GP$_{276}$ **(B)** or H2-D^b-GP$_{33}$ **(D)** specific cells. Graphs show the MFI of T-bet and Eomes each normalized to average value for WT samples in each experiment, and the ratio of normalized MFIs for T-bet relative to Eomes, and the compilation of proportions of T-bet$^+$ Eomes$^-$ cells for each virus-specific subset. Each data point represents an individual mouse and data are a compilation of three independent experiments; significant differences determined by Ordinary one-way ANOVA using Tukey's multiple comparison test.

WT T-bet to Eomes ratio was also accompanied by increased proportions of T-bet^{+} Eomes^{-} GP_{33}-specific cells in *Irf4*$^{+/fl}$ Eomes$^{+/fl}$ mice compared to those found in *Irf4*$^{+/fl}$ mice (Fig 4.11D).

To test the functional consequences of the restored T-bet to Eomes ratio and increased differentiation of the T-bet^{+} Eomes^{-} virus-specific CD8^{+} T cell population in *Irf4*$^{+/fl}$ Eomes$^{+/fl}$ mice, we examined the viral titers in these mice between days 77-82 p.i. This analysis showed a significantly higher titer of virus in the kidneys of *Irf4*$^{+/fl}$ mice compared to the other three genotypes analyzed (Figure 4.12A). Additionally, in contrast to the *Irf4*$^{+/fl}$ mice, virus was efficiently cleared from livers and sera of WT, Eomes$^{+/fl}$, and *Irf4*$^{+/fl}$ Eomes$^{+/fl}$ mice at this timepoint (Figs 4.12B-C). Finally, we observed no difference in the kinetics of virus clearance when comparing WT to *Irf4*$^{+/fl}$ Eomes$^{+/fl}$ mice (Fig 4.12D). These data demonstrate that reducing Eomes expression in *Irf4*$^{+/fl}$ mice restores a protective balance of T-bet to Eomes levels, leading to improved protective T cell responses to this persistent virus infection

To determine whether these mice showed differences in T cell exhaustion, we examined expression of 2B4, CD160, LAG-3, and PD-1 on virus-specific cells. At this timepoint, *Irf4*$^{fl/fl}$ cells showed a marked reduction in 2B4 expression relative to all other genotypes, and *Irf4*$^{+/fl}$ cells had higher PD-1 expression relative to WT cells (Figure 4.13B, 4.14B). While WT mice exhibited higher

Figure 4.12. *Irf4-Eomes* compound haplodeficiency restores virus control during persistent LCMV-clone 13 infection

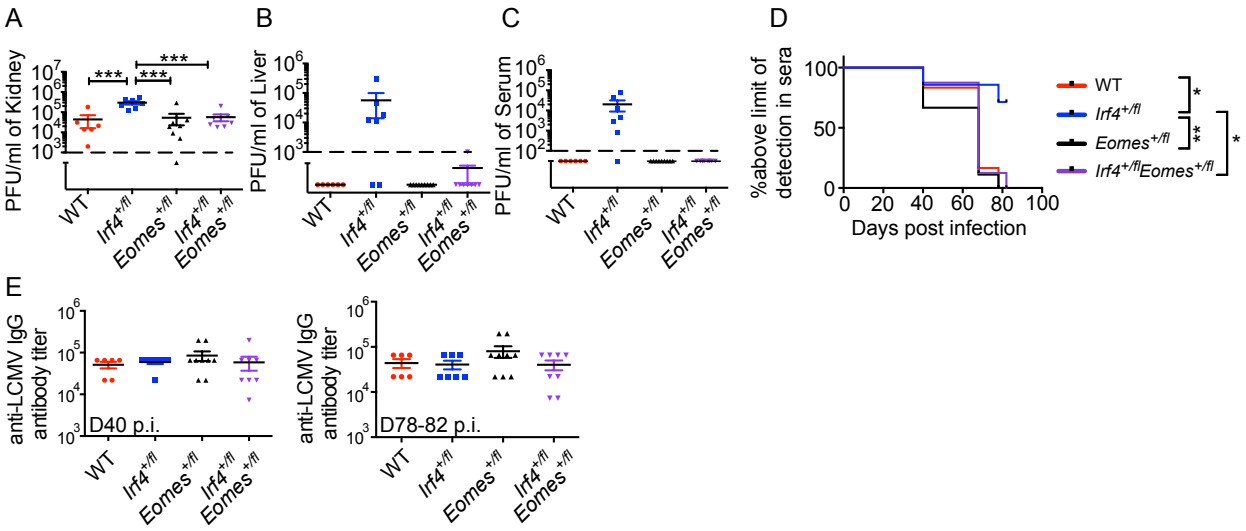

Figure 4.12: *Irf4-Eomes* compound haplodeficiency restores virus control during persistent LCMV-clone 13 infection

Kidney **(A)**, livers **(B)**, and sera **(C)** were harvested from LCMV-clone 13 infected WT, *Irf4*$^{+/fl}$, Eomes$^{+/fl}$ and *Irf*$^{+/fl}$Eomes$^{+/fl}$ mice between day 77-82 post infection and virus titers were determined by plaque assay. Dotted lines indicate the limit of detection. Each data point represents an individual mouse and data are compilations of two independent experiments. **(D)** Serum was harvested from infected mice at various timepoints post infection. Graph indicates the proportion of mice with viral titers above the limit of detection in serum over time. Each data point represents an individual mouse and data are compilation of two independent experiments; significant differences as determined by Ordinary one-way ANOVA using Tukey's multiple comparison test **(A)** and Log-rank (Mantel-Cox) test **(D)**. **(E)** Anti-LCMV IgG antibody titers in sera at day 40 and day 78-82 p.i. were determined. For day 40 timepoint, data points corresponding to 3 WT and 4 *Irf4*$^{+/fl}$ mice were previously shown in Fig 4.8E. Each data point represents an individual mouse and data are a compilation of two independent experiments; significant differences determined by Ordinary one-way ANOVA using Tukey's multiple comparison test.

Figure 4.13. Compound haplo-deficiency of *Irf4* and *Eomes* does not alter exhaustion marker expression, cytokine production, or effector function in H2-D^b-GP$_{276}$ specific cells

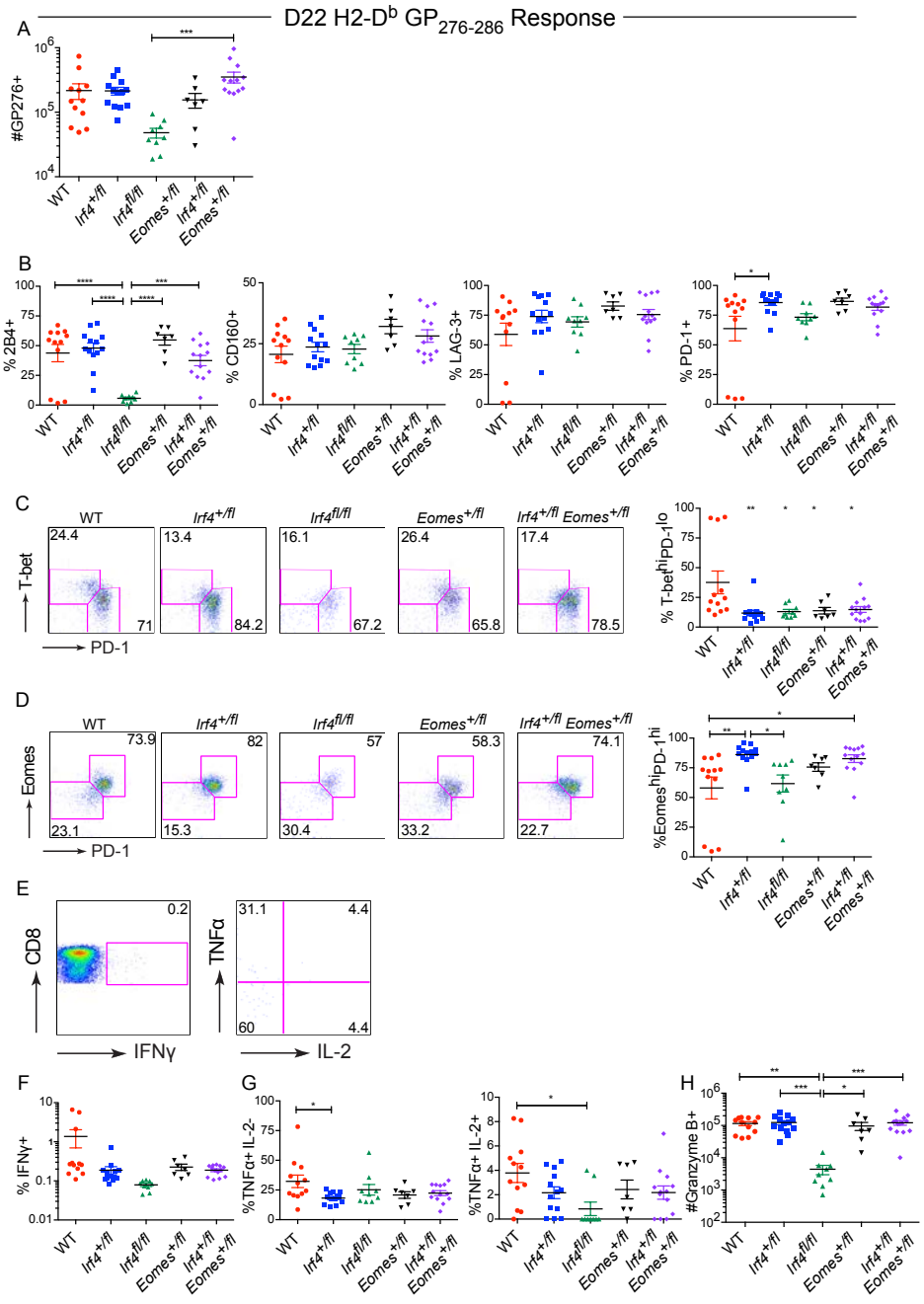

Figure 4.13: Compound haplo-deficiency of *Irf4* and *Eomes* does not alter exhaustion marker expression, cytokine production, or effector function in H2-D^b-GP$_{276}$ specific cells

Splenocytes from LCMV-clone 13-infected WT, *Irf4*$^{+/fl}$, *Irf4*$^{fl/fl}$, *Eomes*$^{+/fl}$ and *Irf4*$^{+/fl}$*Eomes*$^{+/fl}$ mice were stained with a viability dye, LCMV-specific H2-D^b-GP$_{276}$ tetramers, and antibodies to CD8, T-bet, Eomes, 2B4, CD160, LAG-3, PD-1, and granzyme B and analyzed at day 22 p.i. **(A)** Number of H2-D^b-GP$_{276}$ specific cells at day 22 p.i. **(B)** Graphs show the proportions of 2B4-, CD160-, LAG-3-, and PD-1-positive H2-D^b-GP$_{276}$ specific cells at day 22 p.i. **(C)** Dot plots show T-bet versus PD-1 staining on H2-D^b-GP$_{276}$ specific CD8$^+$, live cells. Graph shows the proportions of T-bet^{hi} PD-1^{lo} H2-D^b-GP$_{276}$ CD8$^+$ specific cells. * Indicates statistically significant differences relative to WT samples. **(D)** Dot plots show Eomes versus PD-1 staining on H2-D^b-GP$_{276}$ specific, CD8$^+$, live cells. Graph shows proportions of Eomes^{hi} PD-1^{hi} H2-D^b-GP$_{276}$ CD8$^+$ specific cells. **(E-H)** Splenocytes from LCMV-clone 13-infected WT, *Irf4*$^{+/fl}$, *Irf4*$^{fl/fl}$, *Eomes*$^{+/fl}$ and *Irf4*$^{+/fl}$ *Eomes*$^{+/fl}$ mice were isolated at day 22 p.i. and stimulated with GP$_{276}$ peptide, stained with a viability dye and antibodies to CD8, IFNγ, TNFα and IL-2.

(E) Dot plots show representative staining of WT CD8$^+$ live cells (CD8 versus IFNγ) and gated IFNγ$^+$ CD8$^+$ live cells (TNFα versus IL-2). **(F)** Graph shows the proportions of IFNγ$^+$ cells gated on CD8$^+$ live cells for each genotype. **(G)** Graphs show the proportions of TNFα$^+$ IL-2$^-$ (left) and TNFα$^+$ IL-2$^+$ (right) cells gated on IFNγ$^+$ CD8$^+$ live cells for each genotype. **(H)** Graph shows the numbers of

Granzyme B^+ H2-D^b-GP_{276} $CD8^+$ live cells for each genotype. Each data point represents an individual mouse and data are compilations of three independent experiments; significant differences were determined by Ordinary one-way ANOVA using Tukey's multiple comparison test.

Figure 4.14. Compound haplo-deficiency of *Irf4* and *Eomes* does not alter exhaustion marker expression, cytokine production, or effector function in H2-D^{b}-GP$_{33}$ specific cells

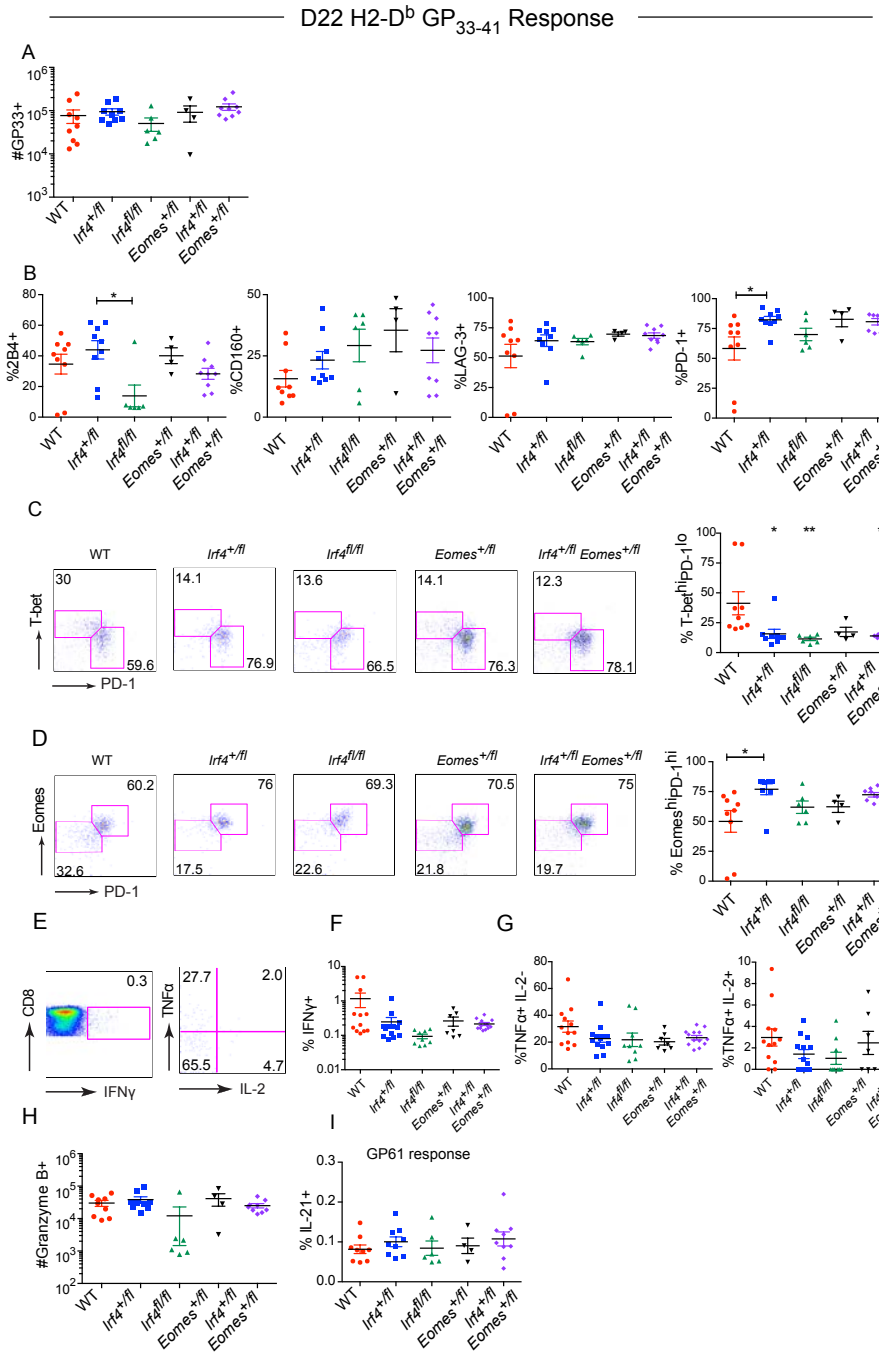

Figure 4.14: Compound haplo-deficiency of *Irf4* and *Eomes* does not alter exhaustion marker expression, cytokine production, or effector function in H2-D^b-GP$_{33}$ specific cells

Splenocytes from LCMV-clone 13-infected WT, *Irf4*$^{+/fl}$, *Irf4*$^{fl/fl}$, *Eomes*$^{+/fl}$ and *Irf4*$^{+/fl}$*Eomes*$^{+/fl}$ mice were stained with a viability dye, LCMV-specific H2-D^b-GP$_{33}$ tetramers, and antibodies to CD8, T-bet, Eomes, 2B4, CD160, LAG-3, PD-1, and granzyme B and analyzed at day 22 p.i. **(A)** Number of H2-D^b-GP$_{33}$ specific cells at day 22 p.i. **(B)** Graphs show the proportions of 2B4-, CD160-, LAG-3-, and PD-1-positive H2-D^b-GP$_{33}$ specific cells at day 22 p.i. **(C)** Dot plots show T-bet versus PD-1 staining on H2-D^b-GP$_{33}$ specific, CD8$^+$, live cells. Graph shows the proportions of T-bet^{hi} PD-1^{lo} H2-D^b-GP$_{33}$ CD8$^+$ specific cells. * Indicates statistically significant differences relative to WT samples. **(D)** Dot plots show Eomes versus PD-1 staining on H2-D^b-GP$_{33}$ specific, CD8$^+$, live cells. Graph shows proportions of Eomes^{hi} PD-1^{hi} H2-D^b-GP$_{33}$ CD8$^+$ specific cells. **(E-H)** Splenocytes from LCMV-clone 13-infected WT, *Irf4*$^{+/fl}$, *Irf4*$^{fl/fl}$, *Eomes*$^{+/fl}$ and *Irf4*$^{+/fl}$ *Eomes*$^{+/fl}$ mice were isolated at day 22 p.i. and stimulated with GP$_{33}$ peptide, stained with a viability dye and antibodies to CD8, IFNγ, TNFα, and IL-2. **(E)** Dot plots show representative staining of WT CD8$^+$ live cells (CD8 versus IFNγ) and gated IFNγ$^+$ CD8$^+$ live cells (TNFα versus IL-2). **(F)** Graph shows the proportions of IFNγ$^+$ cells gated on CD8$^+$ live cells for each genotype. **(G)** Graphs show the proportions of TNFα$^+$ IL-2$^-$ (left) and TNFα$^+$ IL-2$^+$ (right) cells gated on IFNγ$^+$ CD8$^+$ live cells for each genotype. **(H)** Graph shows the numbers of Granzyme

B^+ H2-D^b-GP_{33} specific $CD8^+$ live cells for each genotype. Each data point represents an individual mouse and data are compilations of two **(A-D,H-I)** or three **(E-G)** independent experiments; significant differences were determined by Ordinary one-way ANOVA using Tukey's multiple comparison test.

proportions of T-bet^{hi} PD-1^{lo} and lower proportions of Eomes^{hi} PD-1^{hi} populations relative to *Irf4*$^{+/fl}$ mice, we did not observe any differences between *Irf4*$^{+/fl}$ and *Irf4*$^{+/fl}$ Eomes$^{+/fl}$ cells (Figure 4.13C, D and 4.14C, D). Overall, these data indicate that differences in viral control are unlikely to be due to differential expression of exhaustion markers.

We next examined cytokine production by virus-specific CD8^{+} T cells from WT, *Irf4*$^{+/fl}$, *Irf4*$^{fl/fl}$, Eomes$^{+/fl}$, and *Irf4*$^{+/fl}$ Eomes$^{+/fl}$ mice at day 22 p.i. *Ex-vivo* stimulation of splenocytes from infected with GP_{276} or GP_{33} peptide showed few cells capable of producing IFNγ, and little evidence of multi-functional T cells in any of the mice (Figure 4.13E, F and 4.14E, F). We also failed to observe a difference in Granzyme B expression between any of the genotypes, with the exception of *Irf4*$^{fl/fl}$ cells (Figure 4.13H and 4.14H), arguing against a difference in cytotoxic activity between WT, *Irf4*$^{+/fl}$, Eomes$^{+/fl}$, and *Irf4*$^{+/fl}$ Eomes$^{+/fl}$ mice at this timepoint.

To determine whether *Irf4*$^{+/fl}$ Eomes$^{+/fl}$ produced higher levels of anti-viral antibodies compared to *Irf4*$^{+/fl}$ mice, we examined anti-LCMV IgG titers at day 40 and day 78-82 p.i. with LCMV-clone 13. No differences in anti-viral antibody titers were observed in this analysis (Figure 4.12E), consistent with the comparable proportions of IL-21-producing GP61-specific CD4^{+} T cells in these mice (Figure 4.14I).

Discussion

$CD8^+$ T cell exhaustion is commonly observed during persistent infections and cancers (Wherry, 2011). Although a number of cell extrinsic factors such as the presence of the immune-suppressive cytokine IL-10, absence of help from $CD4^+$ T cells, and high viral loads have been implicated in inducing exhaustion, a clear understanding of the $CD8^+$ T cell intrinsic molecular mechanisms is still lacking (Mueller & Ahmed, 2009) (Doering et al., 2012). The role of several transcription factors, such as Blimp-1, T-bet, and Eomes have been examined during chronic infection (Paley et al., 2012) (Shin et al., 2009) (Kao et al., 2011). Blimp-1 is highly expressed in exhausted $CD8^+$ T cells and its expression correlates with greater expression of exhaustion markers. Yet, *Blimp-1* knockouts have a defect in controlling LCMV-clone 13 infections relative to WT mice, whereas mice haplo-deficient for *Blimp-1* are more proficient at controlling the infection. These data indicate that varying levels of Blimp-1 regulate distinct transcriptional modules in exhausted $CD8^+$ T cells, and that levels of Blimp-1 that are too high or too low are detrimental to the immune response (Shin et al., 2009). Similarly, the expression of T-bet and Eomes segregate into $T\text{-bet}^{hi}$ and $Eomes^{hi}$ populations during persistent infections. Even though both proteins are T-box transcription factors and function redundantly early in LCMV Armstrong infection, loss of either protein results in impaired control of LCMV-clone 13 infections likely due to the different gene networks they regulate during LCMV-clone 13 infections (Paley et al., 2012) (Doering et al., 2012). Together these data demonstrate that efficient

control of LCMV-clone 13 requires an optimal level of each of these transcription factors. Interestingly, mice lacking Blimp-1, T-bet, or Eomes have no defect in clearing acute LCMV Armstrong infections, yet are impaired in controlling LCMV-clone 13 (Banerjee et al., 2010) (Rutishauser et al., 2009) (Intlekofer et al., 2007). Here we find that IRF4 joins this group of transcription factors, as reduced expression of IRF4 leads to persistence of LCMV-clone 13 infection, but does not affect clearance of LCMV Armstrong (Nayar et al., 2014).

Despite the fact that the function of $Tbet^{hi}$ and $Eomes^{hi}$ subsets is well defined, the factors regulating the differentiation of anti-viral $CD8^+$ T cells into these subsets is not known. We explored the role of TCR signaling via IRF4 in the relative expression of T-bet and Eomes and the differentiation of T-bet^+ $Eomes^-$ and T-bet^- $Eomes^+$ subsets during chronic LCMV infection. We find that the balance of these two transcription factors is dependent on the strength of TCR signaling and reduction in the affinity or the dose of the stimulating ligand resulted in lowering of this ratio. Molecularly, the relative levels of T-bet and Eomes were dependent on the magnitude of IRF4 expression, and reduced IRF4 expression, such as those achieved by haplo-deficiency of *Irf4*, resulted in skewing of this ratio in the favor of Eomes, both *in vitro* and *in vivo*. Previous studies have demonstrated that IRF4, together with its binding partner, BATF, directly bind to the both the *T-bet* and *Eomes* loci in effector $CD8^+$ T cells,

indicating a direct role of IRF4/BATF in regulating the expression of these two genes (Man et al., 2013) (Kurachi et al., 2014).

The most severe consequence of the altered T-bet to Eomes ratio was the reduced differentiation of T-bet^{+} Eomes^{-} precursors, and long-term viral persistence in *Irf4*$^{+/fl}$ mice. IRF4 regulates multiple pathways such as proliferation, metabolism, and expression of effector cytokines in anti-viral CD8^{+} T cells (Yao et al., 2013) (Man et al., 2013). Thus, it is likely that defects in any of these pathways could contribute to impaired viral clearance in *Irf4*$^{+/fl}$ mice rather than the lower T-bet to Eomes ratio. To directly test the importance of T-bet to Eomes ratio, we reduced Eomes expression in *Irf4*$^{+/fl}$ mice by generating *Irf4*$^{+/fl}$ *Eomes*$^{+/fl}$ mice. These compound heterozygotes had lower Eomes expression relative to *Irf4*$^{+/fl}$ mice, exhibited no alteration in the T-bet to Eomes ratio relative to WT cells, and showed enhanced differentiation of T-bet^{+} Eomes^{-} cells relative to *Irf4*$^{+/fl}$ mice. Consequently, *Irf4*$^{+/fl}$ *Eomes*$^{+/fl}$ mice were indistinguishable from WT mice in terms of viral clearance from multiple organs. These data, to the best of our knowledge, are the first to test the importance of relative expression of T-bet and Eomes in LCMV-clone 13 viral control.

Another consequence of reduced T-bet to Eomes ratio was the altered differentiation of T-bet^{hi} and Eomes^{hi} populations in *Irf4*$^{+/fl}$ mice. Using T-bet and Eomes knockout mice, Paley et al. showed that both T-bet^{hi} and Eomes^{hi} subsets

are important for viral control (Paley et al., 2012). However, it is not known if reduced differentiation of one population over the other affects viral clearance. Our studies suggest that reduced differentiation of T-bet^{+} Eomes^{-} population in *Irf4*$^{+/fl}$ mice is detrimental to efficient viral control, and that increasing this population in *Irf4*$^{+/fl}$ *Eomes*$^{+/fl}$ mice restores viral control. Consistent with this observation, lower proportions of CD8^{+} T-bet^{+} Eomes^{-} cells are observed in lung transplant recipients with relapsed CMV infection relative to controllers (Popescu et al., 2014). A recent study showed that loss of FoxO1 results in higher levels of T-bet and lower levels of Eomes, thus biasing CD8^{+} T cell differentiation to the T-bet^{hi} subset. Interestingly, the *FoxO1* deficient mice were also defective in viral control (Staron et al., 2014). Together these data underscore the importance of previous observations that both subsets of CD8^{+} T cells, the T-bet^{hi} and the Eomes^{hi} populations, play unique and essential functions during anti-viral immune responses to LCMV-clone 13 (Paley et al., 2012). Further, these data support our conclusion that balanced differentiation of T-bet^{+} Eomes^{-} and T-bet^{-} Eomes^{+} subsets are important for viral control.

Recently, we and others have shown that the levels of IRF4 regulate the magnitude of CD8^{+} T cell expansion during acute infections (Nayar et al., 2014) (Yao et al., 2013) (Man et al., 2013) (Raczkowski et al., 2013) (Grusdat et al., 2014). Similar to that seen with acute infections, we find here that the levels of IRF4 also regulate the magnitude of the CD8^{+} T cell response to LCMV-clone 13

at day 8 post infection. Furthermore, the increased numbers of virus-specific cells in WT mice relative to *Irf4*$^{+/fl}$ mice also resulted in a significant increase in the numbers of Tbet^{+} Eomes^{-} cells at this timepoint. Somewhat surprisingly, total virus-specific CD8^{+} T cell numbers were not different between WT and *Irf4*$^{+/fl}$ mice at day 22 p.i., nor were they different at later timepoints examined. Therefore, we speculate that this early difference in the magnitude of the CD8^{+} T cell response may be responsible for the ultimate ability of WT, but not *Irf4*$^{+/fl}$ mice to clear LCMV clone 13.

Chapter V: Runx2 is Required for Long-Term Persistence of Antiviral $CD8^+$ T Memory Cells during Acute LCMV-Armstrong Infection

Attributions and Copyright Information

The data described in this chapter were published in ImmunoHorizons in 2018.

The transcription factor Runx2 is required for long-term persistence of antiviral $CD8^+$ memory T cells

Elizabeth Olesin, Ribhu Nayar, Priya Saikumar-Lakshmi, and Leslie J Berg

Specific Contribution to Figures: I performed, designed, and analyzed all experiments described in Figure 5.1 through Figure 5.12. Ribhu Nayar helped perform experiments in Figure 5.2 through Figure 5.4. Priya Saikumar-Lakshmi helped perform experiments in Figure 5.4.

Introduction

The T cell response to acute viral infections has been well characterized at the cellular level. Following infection, a robust pathogen-specific $CD8^+$ T cell response is observed, and within 1-2 weeks post-infection, the pathogen is cleared from the infected host. This early effector phase includes the proliferation and differentiation of cytotoxic effector T cells, a process that is dependent on inflammatory cytokines produced by innate immune cells, and on the presentation of viral peptides on host antigen-presenting-cells (APCs) (Mempel et al., 2004) (Wherry & Ahmed, 2004) (Kaech & Cui, 2012). After viral clearance, the majority of the effector CD8+ T cell population will undergo apoptosis, a process that continues for many weeks post-pathogen clearance (Zhou et al., 2012). Ultimately, the host retains a small pool of pathogen-specific memory T cells that provide rapid protection upon secondary infection (Cui & Kaech, 2010).

During an acute anti-viral response, the pool of activated $CD8^+$ T cells is not homogeneous. Based on differential expression of surface markers, such as KLRG1 and CD127, virus-specific $CD8^+$ T cells can be classified as $KLRG1^{hi}$ $CD127^{lo}$ terminal effector cells (TECs) and $KLRG1^{lo}$ $CD127^{hi}$ memory precursor cells (MPCs) (Kaech et al., 2003). TECs rapidly proliferate in response to infection, make up the majority of the $CD8^+$ effector response, and undergo apoptosis after clearance of the infection. MPCs proliferate less than TECs, but go on to survive and undergo homeostatic proliferation after the infection is

eliminated (Kaech et al., 2003) (Joshi & Kaech, 2008). Several transcription factors have been shown to play critical roles in the relative differentiation of TECs versus MPCs during acute viral infection. These include IRF4 (Nayar et al., 2012) (Raczkowski et al., 2013) (Man et al., 2013) (Yao et al., 2013) (Nayar et al., 2014), BATF (Kurachi et al., 2014) (Grusdat et al., 2014) (Godec et al., 2015), T-bet (Sullivan et al., 2003) (Intlekofer et al., 2005) (Joshi et al., 2007) (Rao et al., 2010), Blimp-1 (Rutishauser et al., 2009) (Shin et al., 2013) (Xin et al., 2016), and Id2 (Cannarile et al., 2006) (Yang et al., 2011) (Knell et al., 2013) (Omilusik et al., 2010), which regulate TEC differentiation and effector cell function. In contrast, Eomesodermin (Eomes) (Intlekofer et al., 2005) (Rao et al., 2010) (Banerjee et al., 2010) , TCF1 (Jeannet et al., 2010) (Zhou et al., 2010), Id3 (Yang et al., 2011) (Ji et al., 2011), and Runx3 (Wang et al., 2018) are all required for $CD8^+$ T cell memory formation and homeostasis.

Here we show that a member of the Runt-related transcription factor family (RUNX), Runx2, is also important for regulating the long-term persistence of $CD8^+$ memory T cells following acute LCMV Armstrong infection. Runx2, like the other RUNX factors, contains a runt DNA binding domain, and pairs with CBFβ to bind to DNA (Tahirov et al., 2001). Runx2 functions primarily in bone development, where it is required for osteoblast generation (Komori, 2018) and bone formation (Choi et al., 2001).

Runx1 and Runx3 have well-characterized roles in T cells, including important functions during T_{REG} development (Kitoh et al., 2009), T_H1 skewing (Naoe et al.,

2007), and $CD8^+$ T cell differentiation (D. Wang et al., 2018) (Cruz-Guilloty et al., 2009). In contrast, no clear function for Runx2 in T cells has been identified, although an earlier study showed that ectopic overexpression of Runx2 in thymocytes perturbed T cell development at the $CD4^-CD8^-$ stage (Vaillant et al., 2002). A genome-wide regulatory network generated by Hu et al. also suggested that Runx2 may play a role in $CD8^+$ T cell memory (Hu & Chen, 2013). Using mice carrying floxed alleles of Runx2 crossed to CD4-cre, we find no apparent defects in T cell development or T cell homeostasis under steady-state conditions. However, following infection with LCMV-Armstrong, we identify a $CD8^+$ T cell-intrinsic defect in the development and persistence of virus-specific MPCs. This correlates with our findings that Runx2 expression levels in activated $CD8^+$ T cells are enhanced by TLR and memory cytokine stimulation, but inhibited by IRF4 expression. Together, these data identify Runx2 as an important mediator of virus-specific memory T cells following resolution of infection by LCMV-Armstrong.

Results

Loss of Runx2 in T cells leads to a defect in pathogen-specific CD8$^+$ MPCs during LCMV Armstrong Infection

To circumvent the neonatal lethality of a germline deficiency in Runx2, we generated mice that lacked Runx2 only in T cells. To this end, *Runx2*$^{fl/fl}$ mice (Chen et al., 2011) were crossed to the CD4-cre$^+$ transgenic line (Nayar et al., 2014) (Nayar et al., 2012) (hereafter referred to as *Runx2*$^{fl/fl}$ mice). *Runx2*$^{fl/fl}$ mice showed no apparent defect in thymic T cell development or in peripheral T cells compared to *Runx2*$^{+/+}$ CD4-cre$^+$ controls (hereafter called WT mice) (Figure 5.1A-C). Additionally, *Runx2*$^{fl/fl}$ mice exhibited no abnormalities in their numbers or proportions of CD8$^+$ CD44^{hi} and CD8$^+$ CD44^{lo} T cells within the spleen (Figure 5.1D).

To assess the function of Runx2 in anti-viral T cell responses, we infected WT and *Runx2*$^{fl/fl}$ mice with 5x10^4 PFU LCMV-Armstrong I.P. and harvested spleens at day 9 (the peak of the CD8$^+$ T cell response), day 14 (the attrition phase), and day 28 (the memory phase) post-infection (Figure 5.2). Compared to WT mice, *Runx2*$^{fl/fl}$ mice had no alterations in the numbers of H2-D^b GP$_{33\text{-}41}$ tetramer-specific cells (GP$_{33}$) at days 9 and 14 post-infection, but did show reduced numbers of virus-specific cells at day 28 post-infection (Figure 5.2A-B). Similar results were observed for H2-D^b GP$_{276\text{-}286}$ specific cells (GP$_{276}$) and H2-D^b

Figure 5.1. No major differences are observed in thymus and spleen of *Runx2*$^{fl/fl}$ mice

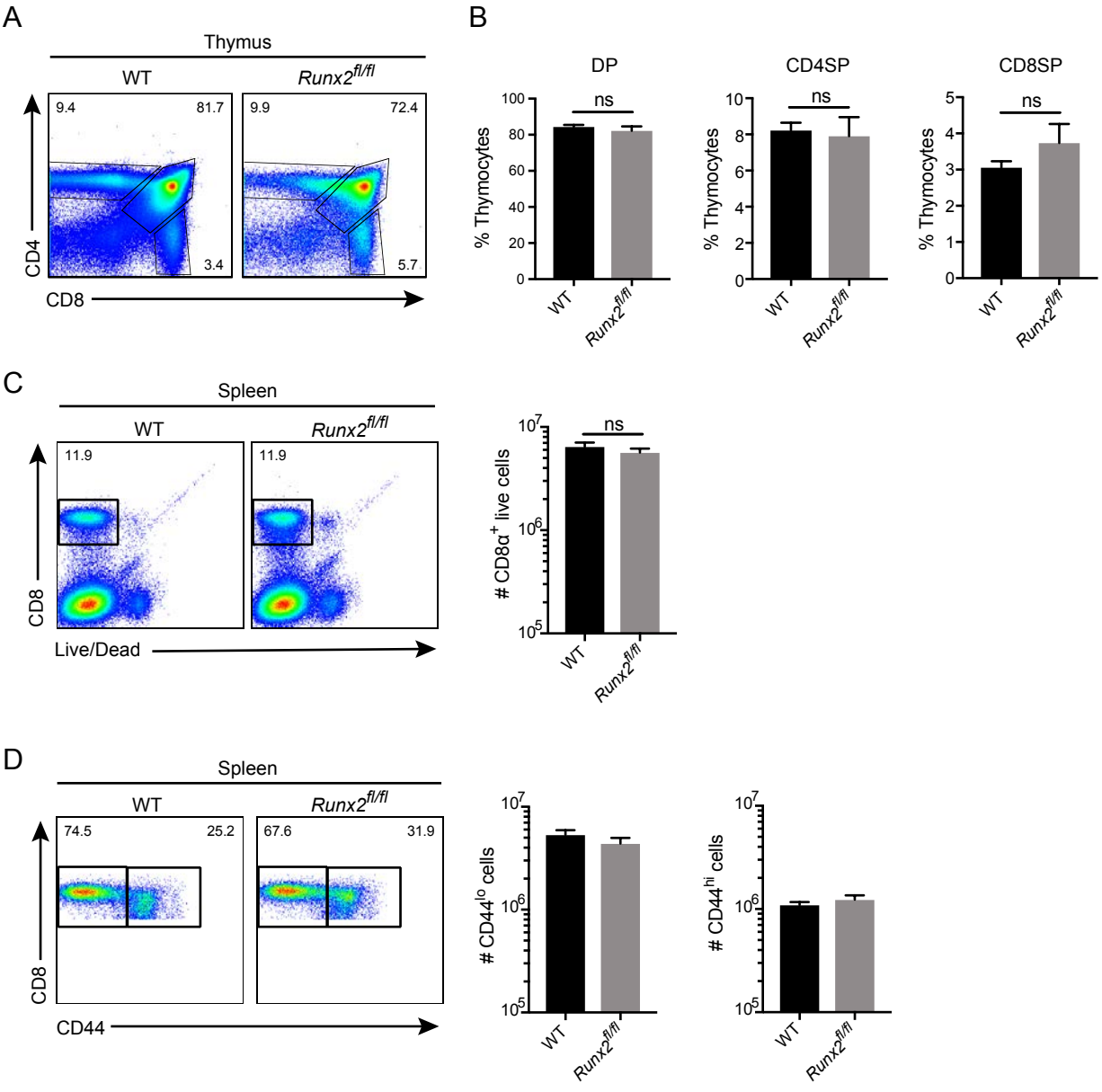

Figure 5.1: No major differences are observed in thymus and spleen of *Runx2$^{fl/fl}$* mice

(A) Thymocytes were isolated from WT or *Runx2$^{fl/fl}$* and stained with antibodies to CD4 and CD8. Dot-plots show CD4 versus CD8 staining. **(B)** Percentages of DP thymocytes (left), CD4SP thymocytes (center), and CD8SP thymocytes (right) in WT and *Runx2$^{fl/fl}$* mice are shown. **(C)** Splenocytes from WT and *Runx2$^{fl/fl}$* mice were stained analyzed for CD8 versus live/dead staining (left); numbers of live CD8^{+} cells are shown at right. **(D)** WT and *Runx2$^{fl/fl}$* splenocytes were stained for CD8 versus CD44 (left) and absolute numbers of CD8^{+} CD44^{lo} (center) and CD8^{+} CD44^{hi} (left) cells are shown. Data are representative of 3 independent experiments with a total of 9-12 mice per group. Mean ± SEM.

Figure 5.2. Loss of Runx2 in the T cell compartment leads to a defect in the number of CD8$^+$ MPCs during LCMV Armstrong infection without any major impact on CD8$^+$ TECs

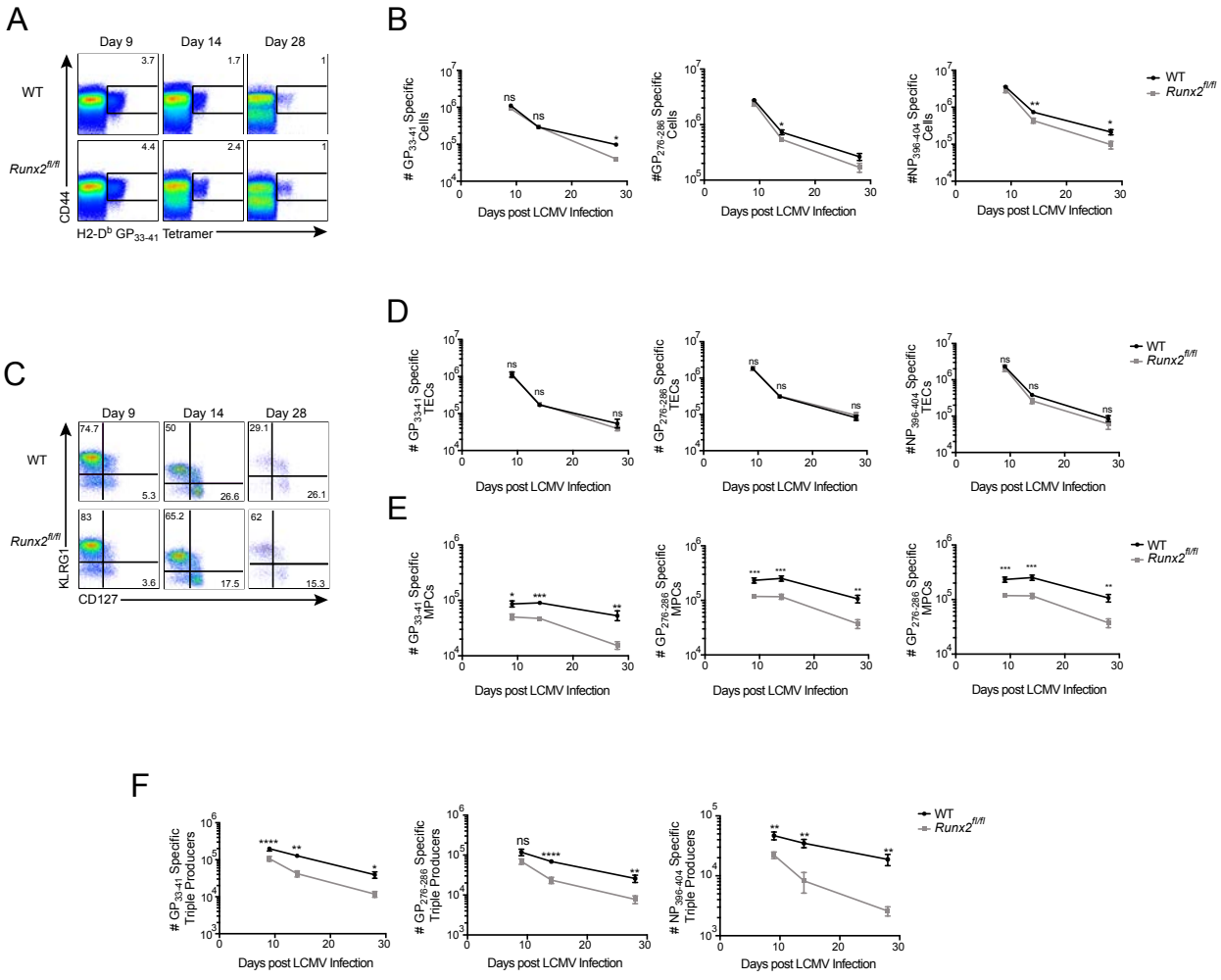

Figure 5.2: Loss of Runx2 in the T cell compartment leads to a defect in the number of CD8$^+$ MPCs during LCMV Armstrong infection without any major impact on CD8$^+$ TECs

WT and *Runx2$^{fl/fl}$* mice were infected with LCMV-Armstrong, and analyzed on day 9, 14, and 28 post-infection. **(A)** Gated CD8α$^+$ splenocytes were stained for H2-D^b GP$_{33-41}$ tetramer and CD44. **(B)** Compilation of data shows total number of H2-D^b GP$_{33-41}$ (left), H2-D^b GP$_{276-286}$ (center), and H2-D^b NP$_{396-404}$ (right) specific splenocytes in WT versus *Runx2$^{fl/fl}$* mice at day 9, 14, and 28 post infection. **(C)** KLRG1 vs CD127 staining of WT and *Runx2$^{fl/fl}$* CD8α$^+$ CD44^{hi}, H2-D^b GP$_{33-41}$ tetramer$^+$ splenocytes at days 9, 14, and 28 post infection. **(D-E)** Total number of H2-D^b GP$_{33-41}$ (left), H2-D^b GP$_{276-286}$ (center), and H2-D^b NP$_{396-404}$ (right) specific TECs **(D)** and MPCs **(E)** in WT versus *Runx2$^{fl/fl}$* mice at day 9, 14, and 28 post infection. **(F)** Cells were restimulated with H2-D^b GP$_{33-41}$ (left), H2-D^b GP$_{276-286}$ (center), or H2-D^b NP$_{396-404}$ (right) peptide for 4 hours *in vitro.* Total number of H2-D^b GP$_{33-41}$ (left), H2-D^b GP$_{276-286}$ (center), and H2-D^b NP$_{396-404}$ (right) IFNγ$^+$, TNFα$^+$, IL-2$^+$ splenocytes (triple producers) in WT versus *Runx2$^{fl/fl}$* CD8α$^+$, CD44^{hi} cells at day 9, 14, and 28 post LCMV Armstrong infection. Data are from 9 independent experiments with a total of 9-12 mice per group per timepoint. Mean ± SEM.

$NP_{396-404}$ specific cells (NP_{396}), indicating the defect at day 28 post-infection in the $CD8^+$ T cells was not an epitope-specific phenotype (Figure 5.2B).

These results suggested a potential defect in the virus-specific MPC population in LCMV-Armstrong infected *Runx2*$^{fl/fl}$ mice. To assess this possibility, we examined tetramer-positive $CD8^+$ T cells for KLRG1 and CD127 expression at each timepoint post-infection. This analysis revealed a defect in the total number of GP_{33}, GP_{276}, and NP_{396} MPCs in *Runx2*$^{fl/fl}$ mice compared to controls at all 3 timepoints tested; in contrast, no differences were found in the virus-specific TEC populations in this comparison (Figures 5.2C-E). Functional memory cells are able to produce IFNγ, TNFα, and IL-2, and this poly-functionality is an indicator of a robust memory population (Slifka & Whitton, 2000). Comparisons of cytokine production by virus-specific WT and *Runx2*$^{fl/fl}$ $CD8^+$ T cells revealed a significant reduction in the total numbers of triple cytokine-producing cells when T cells lacked Runx2 expression (Figures 5.2F). These data indicated that the reduced numbers of tetramer-positive $CD8^+$ T cells in LCMV-Armstrong infected *Runx2*$^{fl/fl}$ mice was due to a defect in the memory T cell population.

As mentioned above, *Runx2*$^{fl/fl}$ mice showed no reduction in virus-specific TEC numbers compared to WT mice at days 9, 14, or 28 post-LCMV infection. We also observed only modest defects in Granzyme B expression and no defects in CD107a+b expression at day 9 post-infection in *Runx2*$^{fl/fl}$ mice (Figure 5.3A-B).

Figure 5.3. Loss of Runx2 in the T cell compartment has no major effect on CD8$^+$ T cell antiviral effector function

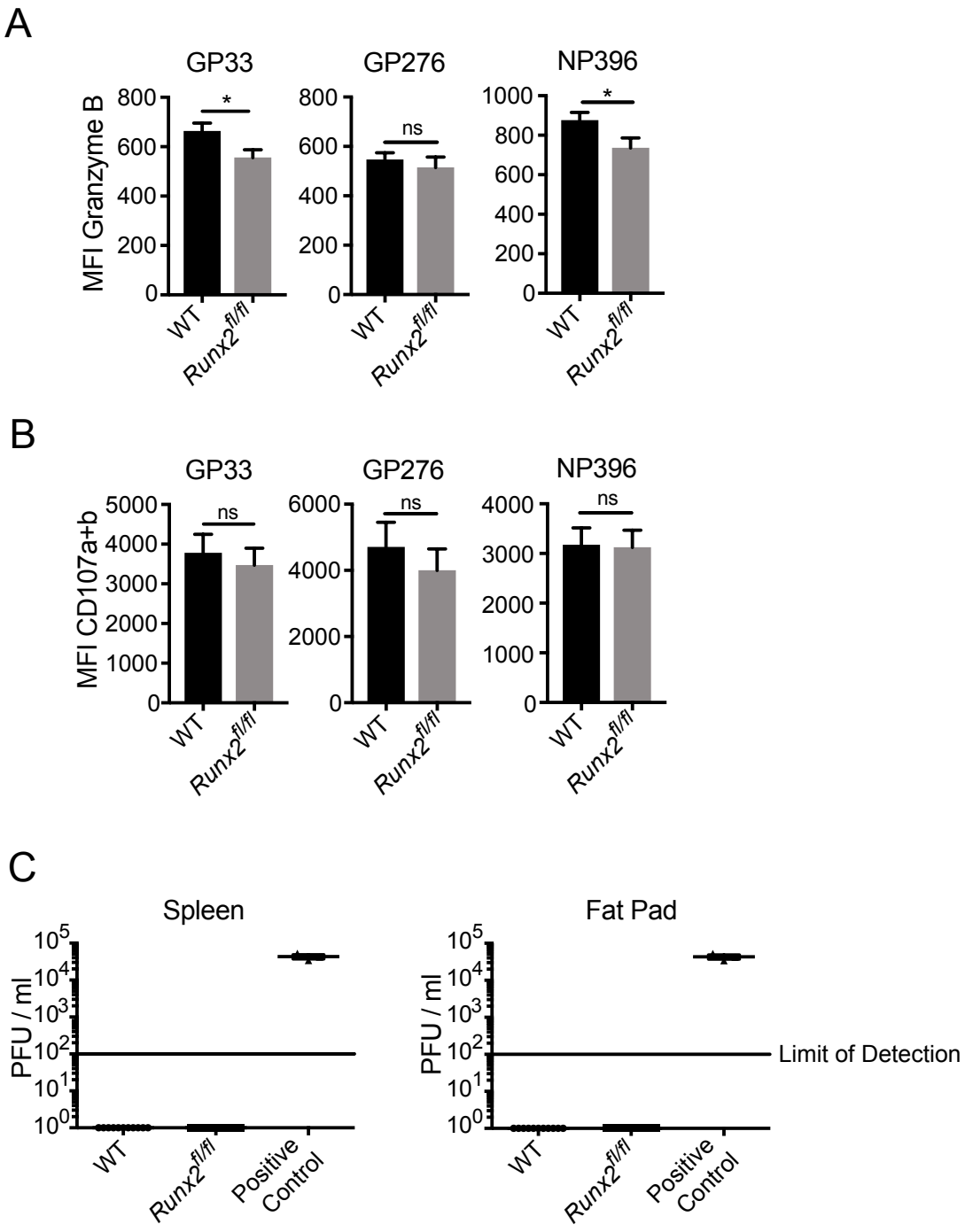

Figure 5.3: Loss of Runx2 in the T cell compartment has no major effect on CD8^{+} T cell antiviral effector function

(A) MFI of Granzyme B in WT versus *Runx2*$^{fl/fl}$ cells day 9 post infection. Cells were restimulated *in vitro* for 4h with GP_{33-41} peptide, $GP_{276-286}$ peptide, or $NP_{396-404}$ peptide and stained for intracellular Granzyme B. **(B)** MFI of CD107a+b in WT versus *Runx2*$^{fl/fl}$ cells day 9 post infection. Cells were restimulated *in vitro* for 4h with GP_{33-41} peptide, $GP_{276-286}$ peptide, or $NP_{396-404}$ peptide and stained for CD107a+b. **(C)** PFU/ml LCMV virus in spleen or fat pad of WT versus *Runx2*$^{fl/fl}$ at day 9 post infection. Positive control shows LCMV-Armstrong stock solution. Mean ± SEM.

These results suggested there were no defects in anti-viral effector cell functions when T cells lacked Runx2. Analysis of viral clearance in LCMV-Armstrong-infected WT versus *Runx2*$^{fl/fl}$ mice confirmed this supposition (Figure 5.3C).

Based on these data, we considered whether virus-specific CD8$^+$ T cell subsets might express different levels of Runx2. To test this, we infected WT C57/BL6 mice with LCMV-Armstrong and harvested spleens at day 9 post-infection. Runx2 protein levels were examined in CD8$^+$ MPCs and TECs specific for three viral epitopes. While Runx2 was upregulated in both subsets of virus-specific cells relative to the levels present in naïve CD8$^+$ T cells, we observed increased levels of Runx2 in the MPCs compared to the TECs for each of the epitopes tested (Figure 5.4A). These results indicated that Runx2 is upregulated within all activated CD8$^+$ T cells, but is higher within the MPC population than in the TEC subset.

To further assess potential molecular differences between WT and *Runx2*$^{fl/fl}$ anti-viral CD8$^+$ T cells, we examined the expression levels of several transcription factors that are important for TEC and MPC differentiation and function. This analysis revealed that at days 14 and 28 post-infection, *Runx2*$^{fl/fl}$ CD8$^+$ T cells expressed lower levels of Eomesodermin and TCF1 compared to WT T cells, consistent with the reduced numbers of MPC in these mice. In contrast, expression of T-bet, a factor associated with CD8$^+$ effector function, was not

Figure 5.4. Runx2 is upregulated in MPCs compared to TECs, and loss of Runx2 leads to a defect in MPC differentiation TFs Eomes and TCF1

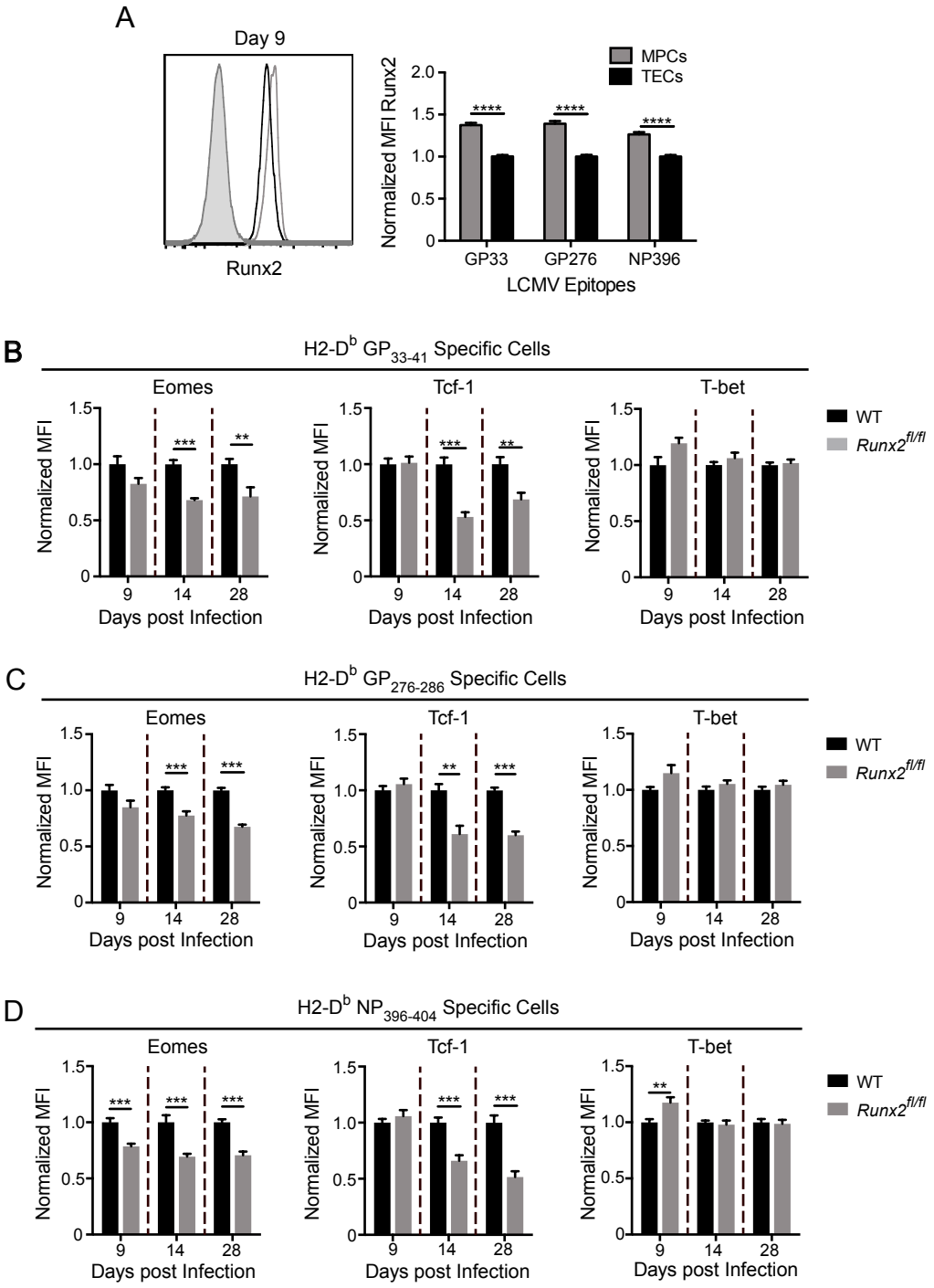

Figure 5.4: Runx2 is upregulated in MPCs compared to TECs, and loss of Runx2 leads to a defect in MPC differentiation TFs Eomes and TCF1

(A) WT C57/BL6 mice were infected with LCMV-Armstrong and analyzed on day 9 post-infection for Runx2 expression levels in $CD8\alpha^{+}$, $CD44^{hi}$ H2-D^{b} GP_{33-41}, $GP_{276-286}$, and $NP_{396-404}$ specific MPCs versus TECs. **(B-D)** Normalized MFI of Eomes, TCF1, and T-bet in **(B)** H2-D^{b} GP_{33-41}, **(C)** H2-D^{b} $GP_{276-286}$, and **(D)** H2-D^{b} $NP_{396-404}$ tetramer-specific WT versus *Runx2*$^{fl/fl}$ splenocytes were analyzed at day 9,14, and 28 post LCMV Armstrong infection by staining for Eomes, TCF1 or T-bet. Data show normalized MFI for transcription factor staining in gated $CD8\alpha^{+}$, $CD44^{hi}$ **(B)** H2-D^{b} GP_{33-41}, **(C)** H2-D^{b} $GP_{276-286}$, or **(D)** H2-D^{b} NP_{396-}404 cells. Samples were normalized to average MFI value for each protein in the WT samples in each experiment. Data from **(A)** are from 2 independent experiments with a total of 12 mice. Data from **(B-D)** are from 3 independent experiments with a total of 9-12 mice per group. Mean ± SEM.

Figure 5.5. Loss of Runx2 does not increase apoptosis of virus-specific TEC or MPCs following LCMV Armstrong infection

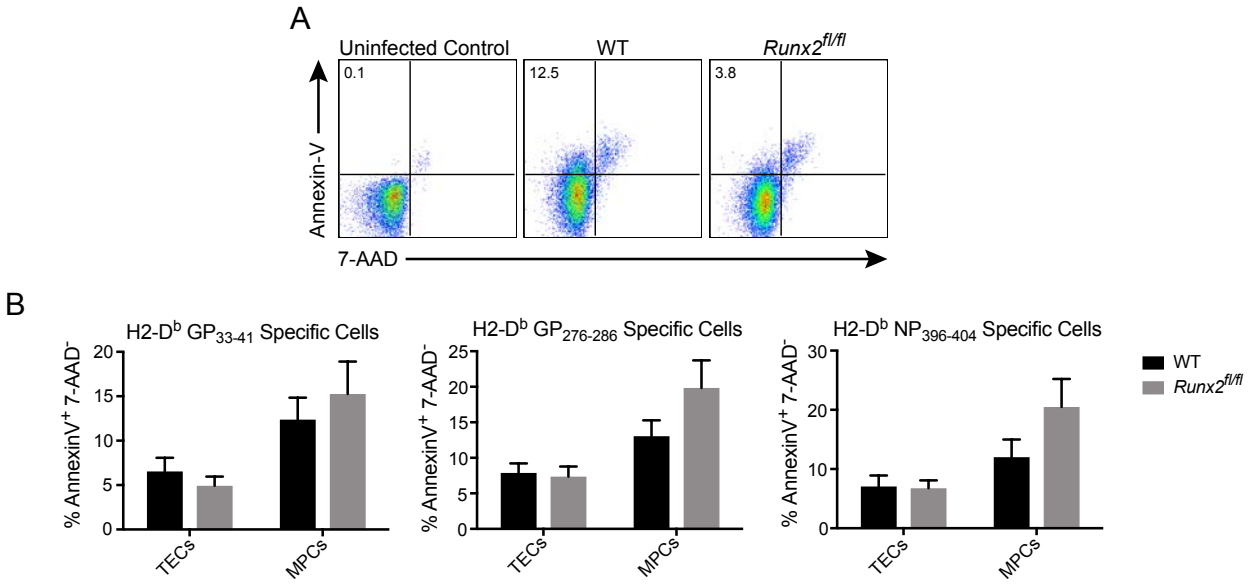

Figure 5.5: Loss of Runx2 does not increase apoptosis of virus-specific TEC or MPCs following LCMV Armstrong infection

WT and *Runx2*$^{fl/fl}$ mice were infected with LCMV-Armstrong and splenocytes were isolated 10 days post-infection. (A) Cells were analyzed for Annexin-V and 7-AAD staining as shown. (B) Percentage of AnnexinV^{+} 7-AAD^{-} TECs and MPCs among each virus-specific population, including H2-D^{b} GP$_{33-41}$, H2-D^{b} GP$_{276-286}$, and H2-D^{b} NP$_{396-404}$ tetramer specific cells in WT and *Runx2*$^{fl/fl}$ mice. Samples are gated on CD8α^{+}, CD44^{hi}, tetramer^{+} cells. Data are from 2 independent experiments with a total of 8 mice per group. Mean ± SEM.

altered between WT and *Runx2*$^{fl/fl}$ cells (Figure 5.4B-D), consistent with previous results indicating no defect in CD8$^+$ effector function (Figure 5.3).

We next considered whether the loss of MPCs in LCMV-Armstrong infected *Runx2*$^{fl/fl}$ mice were due to Runx2 promoting apoptosis in MPCs. However, examination of splenocytes from LCMV-Armstrong infected WT or *Runx2*$^{fl/fl}$ mice at day 10 post-infection failed to show a significant increase in apoptosis of virus-specific CD8$^+$ T cells in the absence of Runx2 (Fig 5.5A-B). Taken together, these results indicated that Runx2 is regulating an alternative aspect of memory CD8$^+$ T cell persistence, such as homeostatic proliferation, rather than survival.

Loss of pathogen-specific CD8$^+$ memory T cells is due to a CD8$^+$ T cell-intrinsic deficiency in Runx2

To determine whether the loss of LCMV-specific Runx2-deficient CD8$^+$ memory T cells was caused by an intrinsic loss of Runx2 in the CD8$^+$ T cells, we performed adoptive transfer experiments. WT and *Runx2*$^{fl/fl}$ mice were crossed to the P14 TCR transgenic line that expresses a TCR specific for the GP_{33} epitope of LCMV. WT (CD90.1$^+$ CD90.2$^+$) and *Runx2*$^{fl/fl}$ (CD90.1$^+$) P14 cells were co-transferred into CD90.2$^+$ host mice at a 1:1 mixture (Figure 5.6A), and recipients were infected with LCMV-Armstrong the following day. Four weeks later, donor cells were examined in the spleens of infected mice. As shown in Figure 5.6, *Runx2*$^{fl/fl}$ P14 cells were significantly reduced in numbers relative to WT P14 cells (Figure

5.6B). Assessment of TEC and MPC subsets showed that both populations of *Runx2*$^{fl/fl}$ P14 cells were reduced in numbers compared to their WT counterparts, but a more dramatic reduction was observed in the *Runx2*$^{fl/fl}$ MPC subset, where WT P14 cells outnumbered *Runx2*$^{fl/fl}$ P14 cells by a 23-fold margin (Figure 5.6C). Examination of several proteins associated with MPC differentiation and survival, including Eomesodermin, TCF1, CD27, CD122, Bcl-2, showed reduced expression by *Runx2*$^{fl/fl}$ P14 cells relative to WT P14 cells at this timepoint. Surprisingly, this was not the case for Bcl-6, which was upregulated in *Runx2*$^{fl/fl}$ cells compared to WT controls (Figure 5.6D). We also assessed cytokine production by WT and *Runx2*$^{fl/fl}$ P14 cells at day 28 post-infection, and observed markedly fewer triple-cytokine producing cells amongst the *Runx2*$^{fl/fl}$ P14 cells relative to WT P14 cells (Figure 5.6E). Overall, these data demonstrate that the defect in memory CD8$^+$ T cell persistence in *Runx2*$^{fl/fl}$ mice following LCMV-Armstrong infection is a CD8$^+$ T cell-intrinsic phenotype. Mean ± SEM.

Runx2-dependent CD8$^+$ memory T cell loss does not impair the recall response to LCMV

To determine whether the defect in numbers of *Runx2*$^{fl/fl}$ CD8$^+$ memory T cells would impact the recall response, we rechallenged LCMV-Armstrong-infected WT and *Runx2*$^{fl/fl}$ mice with LCMV-clone 13. Initially, WT and *Runx2*$^{fl/fl}$ mice were

Figure 5.6. Loss of pathogen-specific T cell memory is due to the absence of Runx2 in CD8$^+$ T cells

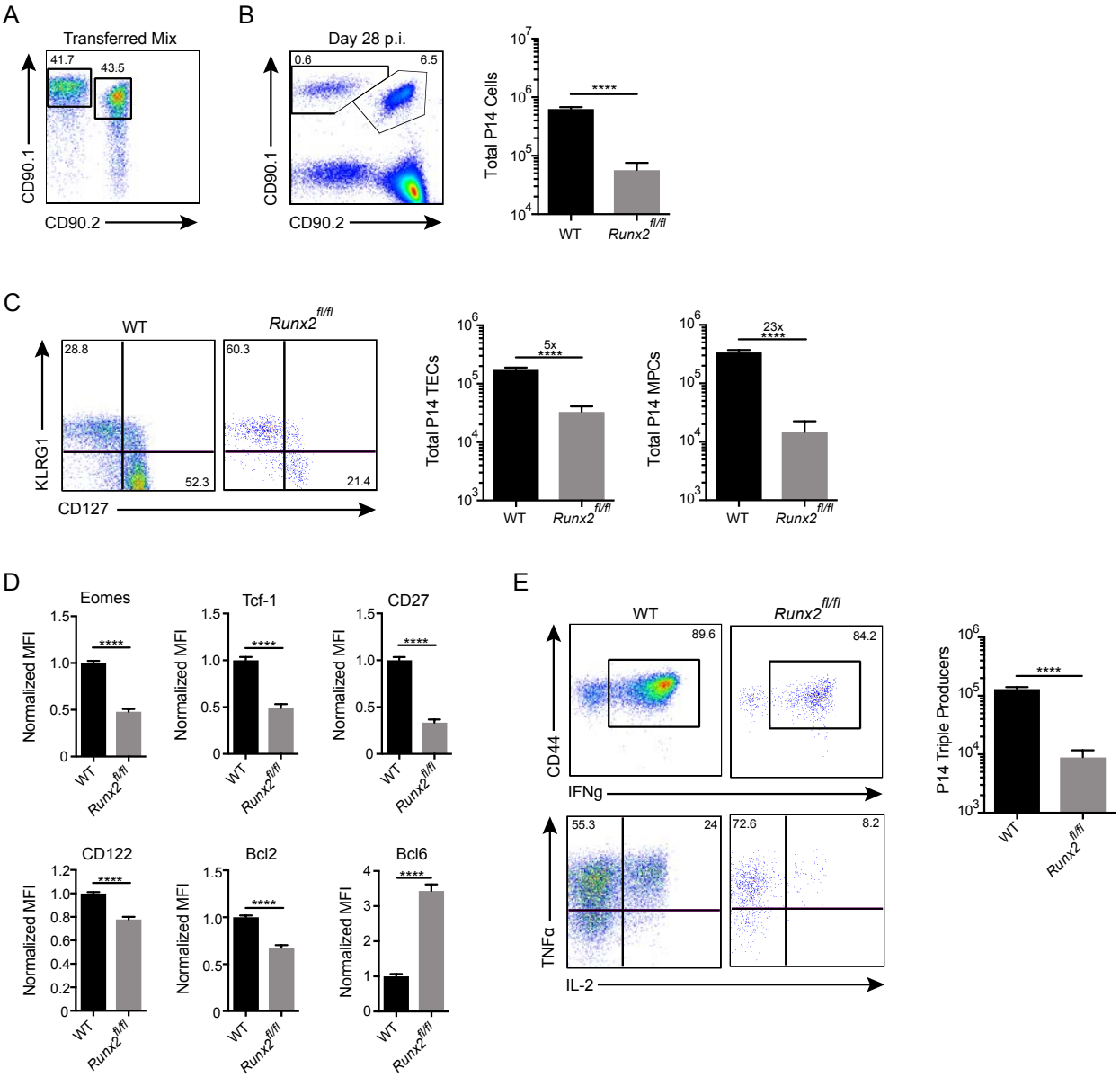

Figure 5.6: Loss of pathogen-specific T cell memory is due to the absence of Runx2 in CD8$^+$ T cells

WT P14 (CD90.1$^+$/CD90.2$^+$) and *Runx2$^{fl/fl}$* P14 cells (CD90.1$^+$) were mixed 1:1 and transferred into WT (CD90.2$^+$) recipients. **(A)** Mixture of donor T cells prior to transfer. **(B)** One day after transfer, recipient mice were infected with LCMV-Armstrong, and splenocytes were analyzed on day 28 post-infection. WT P14 (CD90.1$^+$/CD90.2$^+$) and *Runx2$^{fl/fl}$* P14 cells (CD90.1$^+$) cells are shown (left) and the total numbers of WT P14 and *Runx2$^{fl/fl}$* P14 splenocytes day 28 post-infection were compiled (right). **(C)** Cells were stained for KLRG1 and CD127 and donor populations were gated on (left); total numbers of WT P14 and *Runx2$^{fl/fl}$* P14 TECs (middle) and MPCs (left) in host mice at day 28 post infection are shown. **(D)** Normalized expression of Eomes, TCF1, CD27, CD122, Bcl2, and Bcl6 at day 28 post-infection. MFI are normalized to the average of WT P14 cells analyzed in each sample. **(E)** Cells were restimulated with GP_{33-41} peptide for 4 hours *in vitro*, and stained for intracellular IFNγ, TNFα, and IL-2 as shown (left). Total numbers of H2-D^b GP_{33-41} specific IFNγ$^+$, TNFα$^+$, IL-2$^+$ splenocytes (triple producers) in WT versus *Runx2$^{fl/fl}$* P14 cells at day 28 post LCMV Armstrong infection are shown (right). Data are from 2 independent experiments with a total of 9 mice. Mean ± SEM.

infected with LCMV-Armstrong, and 90 days after infection, mice were rechallenged with a high dose of LCMV-Clone 13. Prior to rechallenge, we examined the surviving populations of virus-specific $CD8^+$ T cells and found reduced numbers of tetramer-positive cells in *Runx2*$^{fl/fl}$ mice compared to controls; furthermore, *Runx2*$^{fl/fl}$ mice had a more substantial deficit in the $CD62L^{hi}$ than the $CD62L^{lo}$ subset of each epitope-specific memory T cell population (Figure 5.7A-D). Four days after rechallenge, we observed substantial expansion of the both WT and *Runx2*$^{fl/fl}$ virus-specific memory cells. This robust recall response was observed for all three viral epitopes tested (Figure 5.8A-B). A careful examination of TECs and MPCs showed no significant differences in either population when comparing WT to *Runx2*$^{fl/fl}$ mice (Figure 5.8C). We also found no differences in viral clearance between WT and *Runx2*$^{fl/fl}$ at day 4 post-rechallenge (Figure 5.8D). Phenotypic and functional analysis of the cells after rechallenge showed few significant differences between virus-specific WT and *Runx2*$^{fl/fl}$ cells (Figure 5.9A-C). These results indicate that the loss of memory T cells seen in *Runx2*$^{fl/fl}$ mice does not impair their protective response to secondary challenge.

Based on these data, we considered whether the reduced numbers of virus-specific memory $CD8^+$ T cells seen in the spleens of *Runx2*$^{fl/fl}$ mice might be due to altered migration of these cells to other tissues, rather than to an absolute

Figure 5.7 Runx2 deficiency leads to a significant loss of CD62L^{hi} memory CD8 T cells at a late memory timepoint

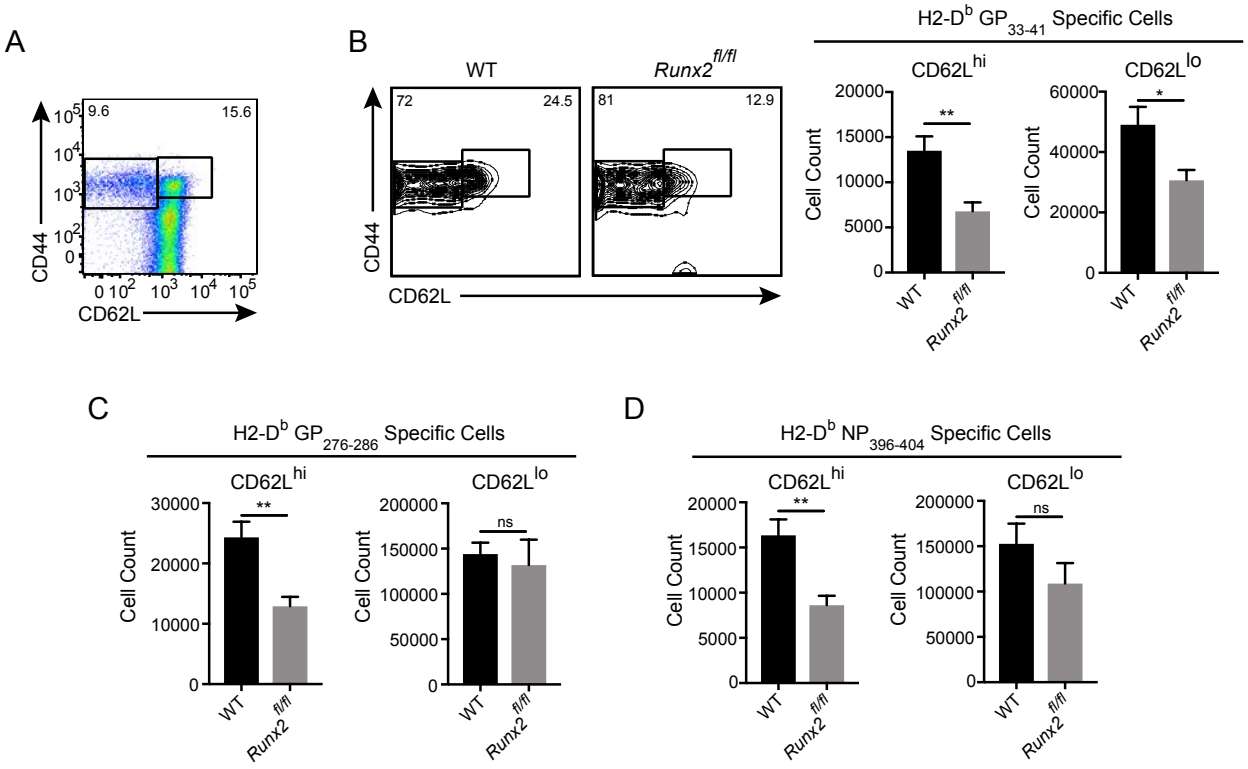

Figure 5.7 Runx2 deficiency leads to a significant loss of CD62L^{hi} memory CD8 T cells at a late memory timepoint

WT and *Runx*$^{fl/fl}$ mice were infected with LCMV-Armstrong, and then 90 days later spleens were harvested for staining. **(A)** Dot-plot shows CD62L^{hi} and CD62L^{lo} cells from an uninfected control to indicate gating strategy. **(B)** Splenocytes were analyzed on day 90, prior to secondary challenge, for CD44^{hi} CD62L^{hi} staining (gated H2-D^{b} GP$_{33-41}$ tetramer^{+} CD8^{+} cells) (left), as well as total numbers of CD62L^{hi} cells (center) and CD62L^{lo} cells (right). **(C)** Total numbers of CD62L^{hi} (left) and CD62L^{lo} (right) H2-D^{b} GP$_{276-286}$ specific cells at day 90 post-primary infection. **(D)** Total numbers of CD62L^{hi} (left) and CD62L^{lo} (right) H2-D^{b} NP$_{396-286}$ specific cells day 90 post-primary infection. Data are from 3 independent experiments with a total of 12 mice per group. Mean ± SEM.

Figure 5.8. Runx2 deficiency in T cells does not impair proliferation of pathogen-specific CD8 T cells or viral clearance during recall response to LCMV-Clone 13

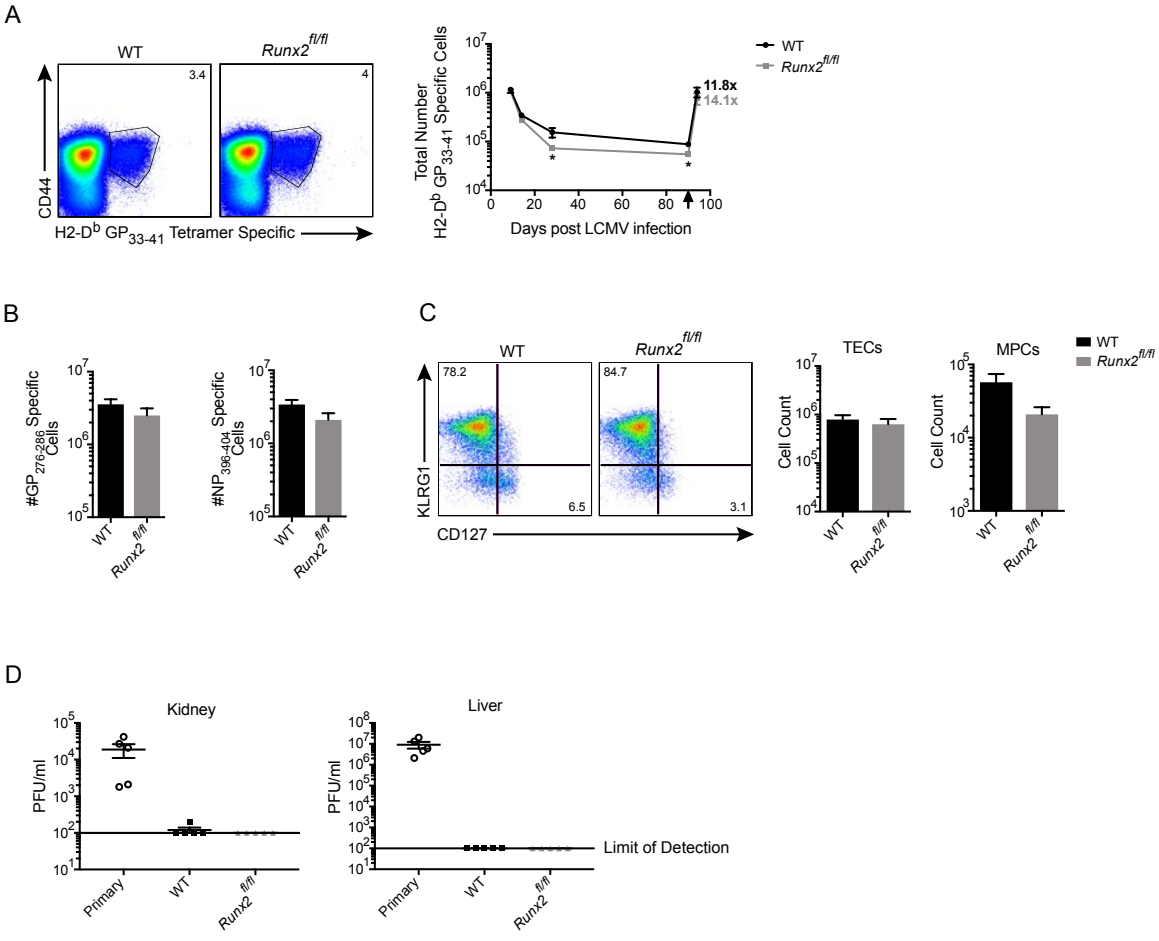

Figure 5.8. Runx2 deficiency in T cells does not impair proliferation of pathogen-specific CD8 T cells or viral clearance during recall response to LCMV-Clone 13

WT and *Runx2*$^{fl/fl}$ mice were infected with LCMV-Armstrong, and on day 90 post-infection were rechallenged with a high dose of LCMV-clone 13. **(A)** H2-D^{b} GP$_{33-41}$ tetramer^{+} CD8^{+} CD44^{hi} staining is shown on day 4 post-rechallenge (left). Timecourse of virus-specific cells including day 4 post LCMV-clone 13 rechallenge is shown (right). **(B)** Total numbers of GP$_{276-286}$ (left) and NP$_{396-404}$ (right) specific cells 4 days after LCMV Clone 13 rechallenge. **(C)** H2-D^{b} GP$_{33-41}$ specific CD8^{+} cells were stained for KLRG1 and CD127 at day 4 post LCMV-clone 13 rechallenge (left), and total cell numbers of H2-D^{b} GP$_{33-41}$ specific TECs (center) and MPCs (right) were quantified. **(D)** Plaque assay of LCMV titers in kidney and liver on day 4 post LCMV-clone 13 rechallenge. Data are from 2 independent experiments with a total of 5 mice per group. Mean ± SEM.

Figure 5.9. Runx2 deficiency in T cells does not impair transcriptional profile of pathogen-specific CD8 T cells during recall response to LCMV-Clone 13

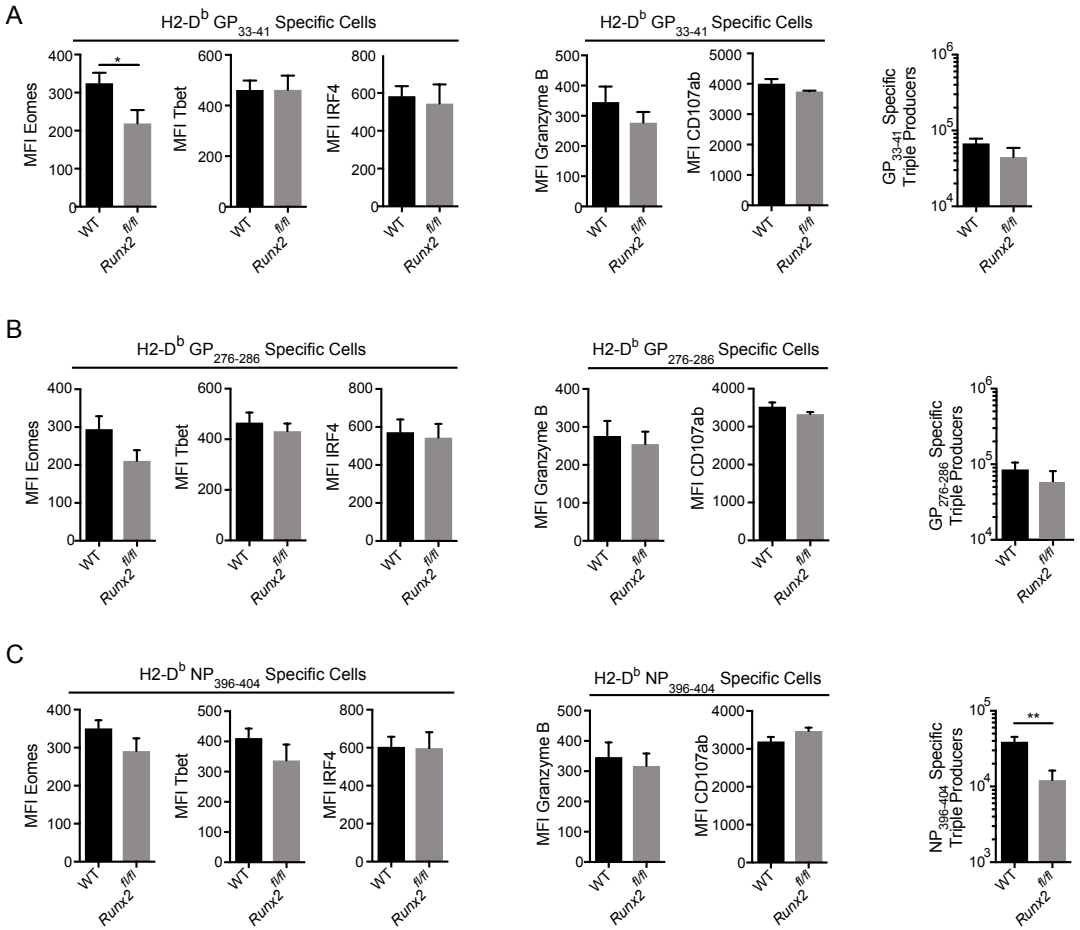

Figure 5.9: Runx2 deficiency in T cells does not impair transcriptional profile of pathogen-specific CD8 T cells during recall response to LCMV-Clone 13

WT and *Runx2*$^{fl/fl}$ mice were infected with LCMV-Armstrong, and on day 90 post-infection were rechallenged with a high dose of LCMV-clone 13. **(A-C)** MFI of Eomes, T-bet, IRF4, Granzyme B, CD107a+b, and total number of triple producers on day 4 after LCMV Clone 13 rechallenge for **(A)** H2-D^{b} GP_{33-41}, **(B)** H2-D^{b} $GP_{276-286}$, and **(C)** H2-D^{b} $NP_{396-404}$ tetramer specific cells . Intracellular cytokine staining was performed after a 4 hour GP_{33-41} peptide stimulation *in vitro*. Data from LCMV-clone 13 rechallenge are from 2 independent experiments with a total of 5 mice per group. Mean ± SEM.

reduction in the total memory cell population. This hypothesis was suggested by a previous study that showed loss of Runx2 in the plasmacytoid dendritic cell compartment led to a retention of the cells in the bone marrow (Chopin et al., 2016). To test this, we examined several organs for pathogen-specific $CD8^+$ T cells 14 days post-primary infection with LCMV-Armstrong. As shown, we found significantly fewer LCMV-specific memory $CD8^+$ T cells in nearly all organs examined, and for each of the viral epitopes assessed (Figure 5.10A-C). These data indicate that the reduced numbers of splenic *Runx2*$^{fl/fl}$ LCMV-specific memory $CD8^+$ T cells is not due to enhanced homing or retention of these cells to or in other organs.

Runx2 expression is regulated by TLR4/TLR7 signals and cytokine signaling pathways *in vitro*

Previous work has shown a role for TLR signaling in $CD8^+$ T cell memory formation (Quigley et al., 2009) (Mercier et al., 2009). We next wanted to determine if Runx2 expression in activated $CD8^+$ T cells was regulated by TLR signaling *in vitro*. To determine the optimal day post stimulation to look at Runx2 expression, we isolated splenocytes from P14 TCR transgenic mice and looked for Runx2 expression up to 5 days post stimulation with GP_{33} peptide. We found that Runx2 was upregulated by day 3 post-stimulation, and remained elevated through day 5 (Figure 5.11A); however, cell death increased dramatically starting day 4 post infection (Figure 5.11B). We therefore chose seventy-two hours post

Figure 5.10 Loss of Runx2 leads to a defect in MPCs in multiple organ compartments after LCMV-Armstrong infection

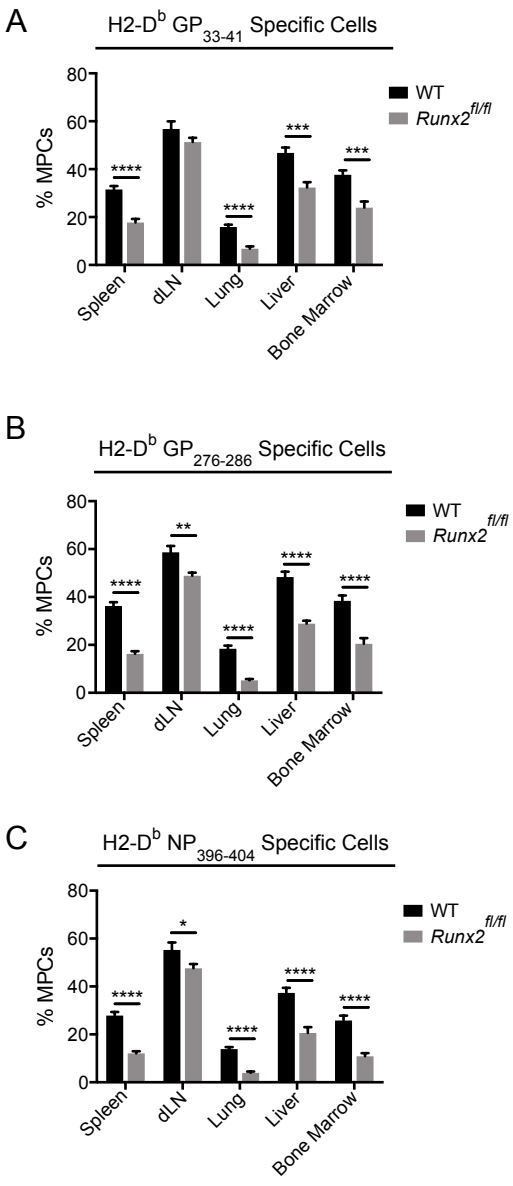

Figure 5.10 Loss of Runx2 leads to a defect in MPCs in multiple organ compartments after LCMV-Armstrong infection

(A-C) Spleen, lymph node, lung, liver, and bone marrow lymphocytes were isolated on day 14 post primary infection with LCMV-Armstrong. Frequencies of **(A)** H2-D^b GP_{33-41}, **(B)** H2-D^b $GP_{276-286}$, and **(C)** H2-D^b $NP_{396-404}$ specific MPCs in tissues from infected WT versus *Runx2*$^{fl/fl}$ mice are shown. Data are from 3 independent experiments with a total of 9-10 mice per group. Mean ± SEM.

Figure 5.11. TLR and cytokine signaling enhance Runx2 expression *in vitro*

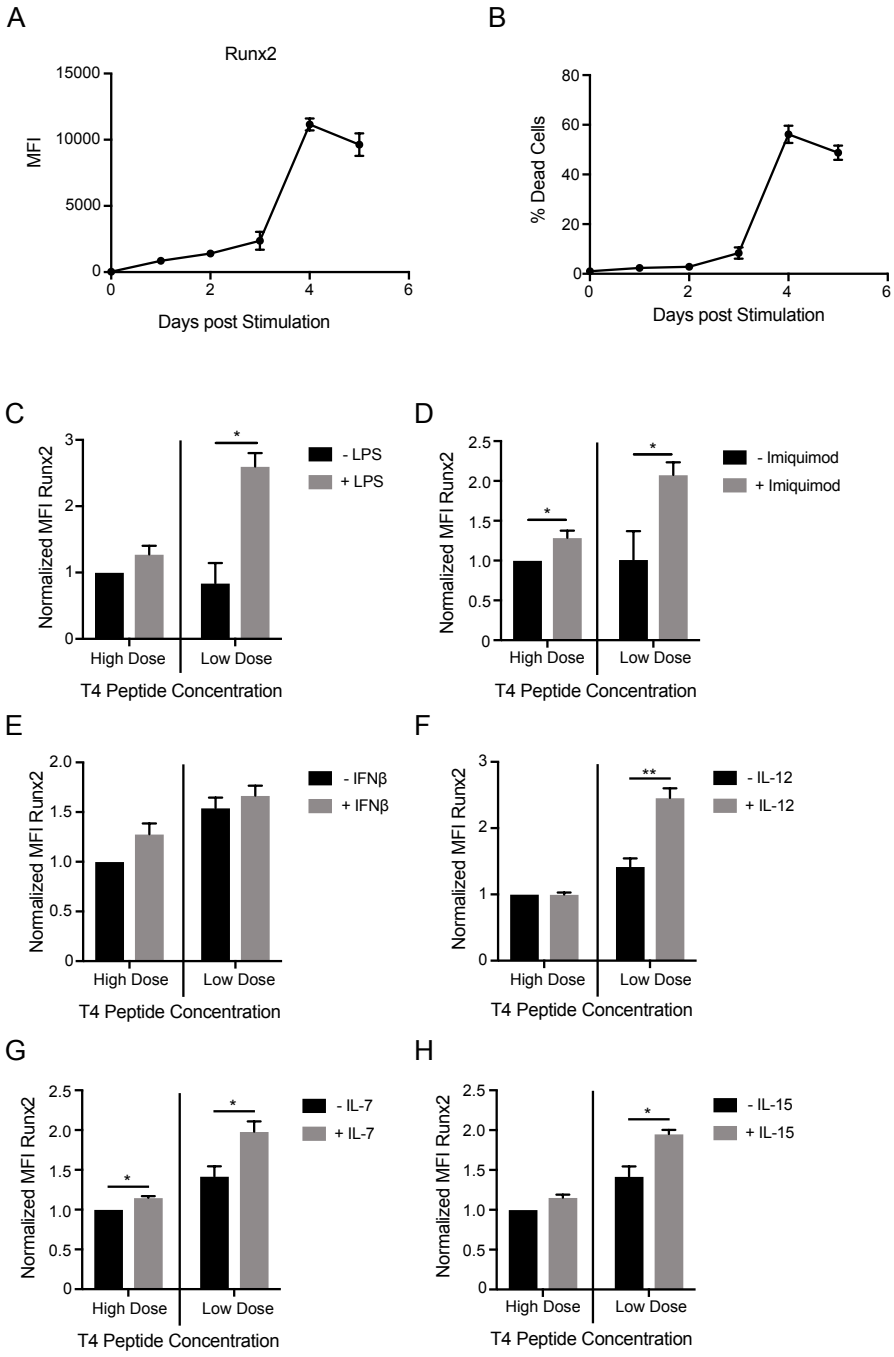

Figure 5.11: TLR and cytokine signaling enhance Runx2 expression *in vitro*

(A) Runx2 expression and **(B)** cell death in P14 splenocytes stimulated with GP_{33-41} peptide (1uM) and IL-2 supernatants. Each day, cells were analyzed for Runx2 and cell death by flow cytometry. Graphs show MFI of Runx2 staining **(A)** and percentages of dead cells **(B)**. **(C-H)** OT-I TCR transgenic splenocytes were isolated and cultured *in vitro* with high (100nM) or low **(C-D** 0.4nM**) (E-H** 0.8nM**)** doses of T4 peptide, in the presence or absence of **(C)** LPS, **(D)** Imiquimod, **(E)** IFNβ, **(F)** IL-12, **(G)** IL-7, **(H)** IL-15. Cultures also contained 20ng recombinant IL-2 **(C-D)**, or supernatants from IL-2 producer cells **(E-H)**. Samples were stained for Runx2 72 hours post stimulation. Graphs show MFI of Runx2 staining normalized to signal in OT-I cells stimulated with high dose T4 peptide in the absence of cytokine or TLR agonist. Data are representative of 3-5 experiments. Mean ± SEM.

stimulation as the optimal timepoint for assessing Runx2 expression accompanied by minimal cell death *in vitro*. To test the role of TLR agonists on Runx2 expression we isolated splenocytes from OT-I TCR transgenic *Rag2*$^{-/-}$ mice, stimulated OT-I T cells with high or low concentrations of the lower affinity OVA peptide variant SIITFEKL (T4), and incubated with or without TLR agonists LPS (Figure 5.11C) or Imiquimod (Figure 5.11D). We found that Runx2 was upregulated in cells treated with either TLR agonist at both high and low T4 peptide doses, but this upregulation was more dramatic when cells were stimulated with the low peptide dose.

Previous work from M. Mescher and colleagues has shown that type-I IFN and IL-12 regulate memory CD8^{+} T cell development in several viral and intracellular bacterial infection systems (Agarwal et al., 2009) (Xiao et al., 2009). These findings prompted us to assess whether type-I IFN or IL-12 was contributing to the high expression of Runx2 in CD8^{+} T cells stimulated in the presence of TLR agonists. We stimulated OT-I T cells with either high or low concentration of T4 peptide, and incubated cells with or without IFNβ (Figure 5.11E) or IL-12 (Figure 5.11F). We found treatment with IFNβ had no significant effect on Runx2 expression, while treatment with IL-12 led to increased Runx2 expression at the lower peptide dose. These results suggest a direct effect of IL-12 on T cells. Furthermore, the fact that IFNβ had no direct effect on T cells suggests that the enhanced Runx2 upregulation observed when stimulation cultures were treated

with TLR agonists might be acting via upregulation of costimulatory molecules on splenic antigen-presenting cells (APCs).

We also tested additional cytokines known to be important in homeostatic proliferation and survival of memory cells for their effects on Runx2 expression. Splenocytes from OT-I TCR transgenic mice were isolated and stimulated with high or low doses of the T4 peptide. Cultures were supplemented with or without IL-7 (Figure 5.11G) or IL-15 (Figure 5.11H), and analyzed at day 3 post-stimulation. These studies demonstrated that both IL-7 and IL-15 promoted increased expression of Runx2 when T cells were activated with weak TCR stimulation.

Together, these data show that TLR signaling, most likely in APCs, and stimulation of T cells with cytokines known to be important in $CD8^+$ T cell memory development and homeostasis, enhance Runx2 upregulation; interestingly, these cytokine and TLR agonist signals have the greatest impact in T cells activated with weaker strength of TCR signaling.

Runx2 expression is regulated by TCR signaling pathways in activated $CD8^+$ T cells *in vitro*

From our TLR and cytokine data, we found that OT-I cells stimulated with low concentrations of T4 peptide expressed higher levels of Runx2 than cells stimulated with a higher concentration of peptide (Figure 5.11). These data suggested an important role for TCR signal strength in controlling Runx2

expression levels. Previous studies have shown an important inverse correlation between TCR signal strength and the development of $CD8^+$ MPCs after infection (Kaech & Cui, 2012) (Restifo & Gattinoni, 2013). To assess more comprehensively a role for TCR signal strength in regulating Runx2 expression, we performed experiments using extensive dose ranges of three peptides recognized by the OT-I TCR. For these studies OT-I cells were stimulated with APCs plus varying concentrations of the highly potent SIINFEKL (N4) peptide, the medium potency (T4), or the low potency SIIGFEKL (G4) peptide. These experiments clearly revealed an inverse correlation between peptide dose and Runx2 expression (Figure 5.12A). Similar results were also observed for Eomes expression (Figure 5.12B). As expected, CD44 upregulation showed a positive correlation with peptide dose (Figure 5.12C).

These findings suggested that the transcription factor IRF4 might regulate Runx2 expression. This possibility was suggested by our previous studies showing that IRF4 is upregulated to different levels based on TCR signal strength, and further, that IRF4 is a negative regulator of Eomes expression (Nayar et al., 2012) (Nayar et al., 2014). To test this possibility, we stimulated WT, *Irf4*$^{+/fl}$ *CD4-cre*$^+$, and *Irf4*$^{fl/fl}$ *CD4-cre*$^+$ (hereby referred to as *Irf4*$^{+/fl}$ and *Irf4*$^{fl/fl}$ respectively) naïve $CD8^+$ T cells with αCD3/CD28 for 72 hours and examined Runx2 expression. As shown, we observed a significant increase in Runx2 expression in stimulated *Irf4*$^{fl/fl}$ $CD8^+$ T cells compared to WT or *Irf4*$^{+/fl}$ cells (Figure 5.12D). Consistent with

Figure 5.12. Runx2 expression inversely correlates with TCR signal strength and Irf4 expression levels

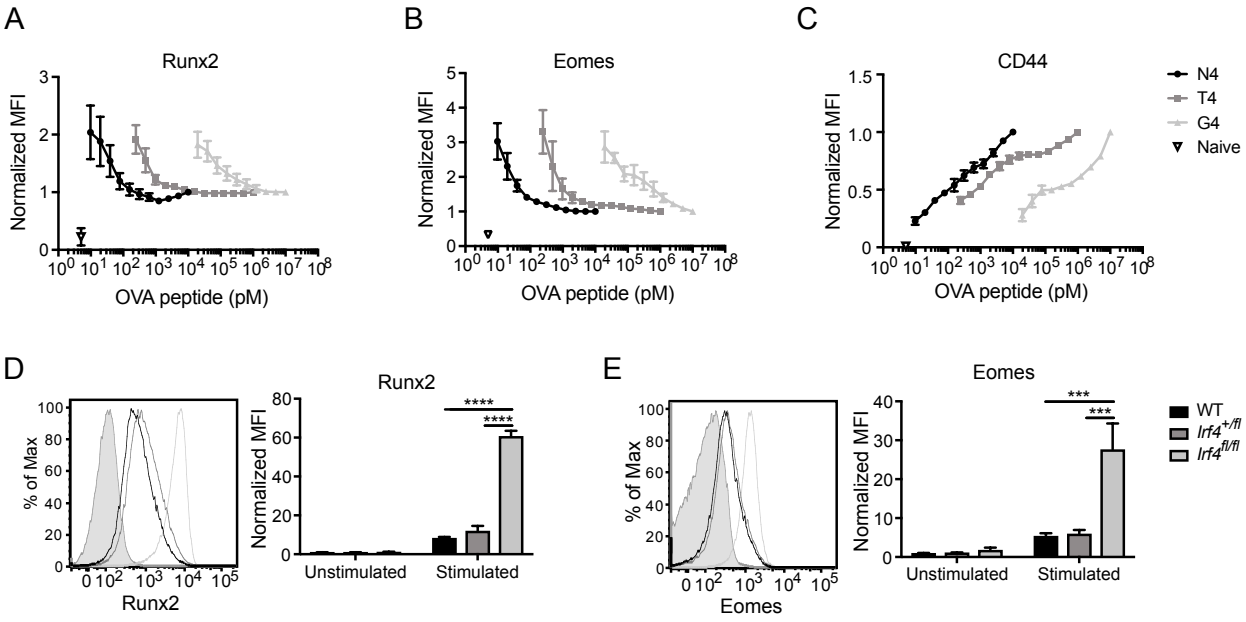

Figure 5.12. Runx2 expression inversely correlates with TCR signal strength and Irf4 expression levels

(A-C) OT-I TCR transgenic splenocytes were isolated and cultured *in vitro* with various doses of N4, T4, or G4 peptide in the presence of supernatants from IL-2-secreting cells. After 72h, OT-I cells were stained for **(A)** Runx2, **(B)** Eomes, and **(C)** CD44. Graphs show MFI of Runx2, Eomes, or CD44 staining normalized to signal in OT-I cells stimulated with 10nM N4 peptide. **(D-E)** $CD8^+$ T cells were isolated from splenocytes of WT, $Irf4^{+/fl}$, or $Irf4^{fl/fl}$ mice, and plated with αCD3/28 plus IL-2 supernatants. Cells were harvested 72h after stimulation and stained for Runx2 **(D)** or Eomes **(E)**. Filled histograms shows staining in naïve WT OT-I cells. Graphs at right show compilations of data normalized to WT unstimulated control. Data are representative of 3-5 experiments. Mean ± SEM.

previously published data, similar results were observed for Eomes (Figure 5.12E). Together these results indicate that Runx2 is more highly expressed when $CD8^+$ T cells are stimulated with low levels of antigen, and that IRF4 is a negative regulator of Runx2 and Eomes expression following $CD8^+$ T cell activation.

Discussion

A key aspect of the adaptive immune response is the generation of long-term memory cells that provide rapid and robust protection upon secondary exposure to an infecting pathogen. Improving memory $CD8^+$ T cell responses is currently a focus of many vaccine efforts, whereas inhibition of memory T cell responses is an ongoing challenge in the development of therapies to treat autoimmune diseases. Thus, there is a need to understand in more detail the molecular mechanisms regulating memory T cell development and persistence.

Our studies identified Runx2 as an important factor in the maintenance of long-term memory $CD8^+$ T cells. However, we found that Runx2 was not necessary for anti-viral effector function, or for robust recall responses to secondary challenge. These features of the $CD8^+$ T cell response to infection in *Runx2*$^{fl/fl}$ mice show striking resemblance to previous studies examining the consequences of a deficiency in IL-15 or IL-15Rα (Lodolce et al., 1998) (Ma et al., 2006a). In these earlier studies, IL-15 signaling was found to be essential for long-term memory $CD8^+$ T cell homeostasis and self-renewal. We observed that IL-15 stimulation of $CD8^+$ T cells in vitro promoted enhanced Runx2 upregulation only under conditions of weak TCR stimulation. These findings suggest the possibility that *in vivo* tonic TCR signals plus IL-15 are functioning to maintain memory cells in part through the upregulation of Runx2. Consistent with this possibility, IL-15 is thought to promote memory T cell homeostatic proliferation,

rather than memory cell survival (Becker et al., 2002) (Schluns et al., 2002) (Goldrath et al., 2002) (Burkett et al., 2003) (Rubinstein et al., 2008), a function that aligns well with data demonstrating that Runx2 overexpression in thymocytes promotes uncontrolled cellular proliferation leading to lymphomagenesis (Vaillant et al., 1999).

We also found that Runx2 expression levels are enhanced by weak, rather than strong, TCR signal intensity, likely due to negative regulation by the transcription factor IRF4. This pattern mirrors that of Eomes, another transcription factor associated with long-term memory $CD8^+$ T cell maintenance (Banerjee et al., 2010). Along with weak TCR signaling, cytokines that promote memory T cell formation and signals that activate APCs, also promote enhanced Runx2 upregulation. These data further strengthen an association of Runx2 expression with optimal formation of long-lived memory $CD8^+$ T cells (Cui & Kaech, 2010) (Restifo & Gattinoni, 2013).

Determining the precise mechanism underlying the loss of memory $CD8^+$ T cells in the absence of Runx2 has remained. Early on, studies using microarrays were performed to identify differentially expressed genes between WT and *Runx2*$^{fl/fl}$ $CD8^+$ T cells. Cells isolated from LCMV-Armstrong infected mice and analyzed directly *ex vivo* failed to yield informative gene targets of Runx2 regulation; similar uninformative results were obtained when comparing WT and *Runx2*$^{fl/fl}$

$CD8^+$ T cells stimulated in vitro (data not shown). This prompted us to consider alternative mechanisms for Runx2 function, such as a change in rRNA transcription and processing, based on the known role for Runx2 in regulating this pathway in osteoblasts (Ali et al., 2012); these studies also failed to identify a function for Runx2 in $CD8^+$ T cells (data not shown). One additional possibility is that Runx2 is affecting memory formation through regulation of chromatin accessibility, a known function of Runx3 in $CD8^+$ T cells (D. Wang et al., 2018). Runx family members have been shown to have redundant roles $CD4^+$ T_{REG} cells; thus the most robust alterations are observed in the absence of Cbfβ, the binding partner for all three Runx proteins (Rudra et al., 2009). Future studies examining $CD8^+$ T cell memory using Cbfβ-deficient T cells may be informative in this regard. Alternatively, Runx2 may function intermittently in memory $CD8^+$ T cells, during short time windows when memory cells associate with stromal cells in lymphoid organs and receive homeostatic TCR and IL-15/IL-7 signals. Capturing the cells during these brief interactions may be required to identify the specific genes and/or pathways regulated by Runx2 in memory $CD8^+$ T cells.

Chapter VI: Discussion

IRF4 and $CD8^+$ Effector T Cell Differentiation during Acute LCMV-Armstrong Infection

The adaptive immune system protects us from pathogens by generating a strong Ag-specific response, which forms a small population of memory cells capable of rapidly responding to reinfection. $CD8^+$ T cells are able to recognize pathogens through their TCR via Ag presented on MHC-I on APCs. This process allows for T cells to be selected based on affinity to Ag, as well as allowing for high-affinity T cell clones to be activated in response to Ag stimulation (Badovinac et al., 2002).

Work from chapter three of this dissertation as well as from (Raczkowski et al., 2013), (Man et al., 2013), and (Yao et al., 2013) have shown a major role for the transcription factor IRF4 in regulating the level of activation of $CD8^+$ T cells in response to TCR signal strength during pathogen infection. (Man et al., 2013) determined the role of IRF4 during Influenza A viral infection using viruses that expressed OVA peptides of various affinities to the OT-I TCR. This study found that IRF4 expression levels directly correlated with TCR signal strength (i.e. antigen affinity to the OT-I TCR), and the difference in TCR signal strength corresponded with an effect on the total number of $CD8^+$ OT-I cells at the peak of the $CD8^+$ T cell response. (Yao et al., 2013) found similar results, where TCR signal strength directly correlated with IRF4 expression and the total number of effector $CD8^+$ T cells in response to Infuenza A infection. Consistent with these

two studies, we found that IRF4 expression levels directly correlated with peptide affinity to Ag in P14 TCR transgenic $CD8^+$ cells. We also found that IRF4 expression levels were decreased in IRF4 haplodeficient $P14^+$ T cells stimulated *in vitro* compared to WT controls. Using this system, we looked at the effects of decreasing levels of IRF4 expression in WT, $Irf4^{+/fl}$, and $Irf4^{fl/fl}$ $CD8^+$ T cells during LCMV Armstrong infection, and found that lower levels of IRF4 corresponded to lower levels of pathogen-specific $CD8^+$ T effector cells at the peak of response. Similar results were observed in adoptively transferred WT P14 cells in hosts infected with WT and F6L variant LCMV-Armstrong. From our work and others, there is strong evidence that levels of IRF4 are regulated by TCR signal strength, and in turn, IRF4 regulates the magnitude of the $CD8^+$ T cell effector response.

We also show that modest variation in IRF4 levels, through use of $Irf4^{+/fl}$ mice can lead to significant decrease in the total number of $CD8^+$ T cells at the peak of the $CD8^+$ T cell response. We further show that this decrease in IRF4 expression primarily impacts the TEC population, while only have minor effects on the MPC population, indicating that levels of IRF4 primarily impacts the effector population, while having no major impact on the memory population. These results parallel work from Zehn et al, where use of a *Listeria*-OVA model with several OVA peptide variant strains found that peptide affinity directly correlated with the total number of cells at the peak of the $CD8^+$ T cell response, but found no defects on

the surviving memory populations for any of the peptide variants (Zehn et al., 2009).

From our work and others, it is clear that IRF4 is regulated by TCR signal strength, but it is unknown whether other signals, such as pro-inflammatory cytokines, may potentially affect IRF4 expression. We found that IRF4 protein expression was quickly upregulated after TCR signaling and peaked at 24 hours post stimulation *in vitro*. After 24 hours, expression quickly went down in WT GP_{33-41} peptide stimulated WT P14 TCR transgenic $CD8^+$ T cells. Future studies looking into the potential role of pro-inflammatory cytokines in regulating either intensity of the IRF4 peak, or duration of IRF4 expression, would be a potential avenue of interest. Work from Richer et al has show that inflammatory cytokines are able to enhance TCR signaling by sustaining phosphorylation of ZAP-70 and phospholipase Cγ (Richer et al., 2013). Phospholipase Cγ activation and IRF4 expression are both ITK dependent, so it is possible that cytokines could help sustain IRF4 expression (Berg et al., 2005) (Nayar et al., 2012). Previous studies have shown an important role for pro-inflammatory cytokine IL-12 in regulation of T-bet expression (Takemoto et al., 2006) (Joshi et al., 2007). T-bet is another transcription factor that promotes $CD8^+$ effector T cell differentiation, indicating that pro-inflammatory cytokines are able to regulate transcription factors required for $CD8^+$ T effector cell fate. Besides known roles of pro-inflammatory cytokines in regulation of other TEC transcription factors, IRF4 has also been shown to be

regulated by cytokine stimulation in $CD4^+$ T cells (Gomez-Rodriguez et al., 2016), where ITK-deficient $CD4^+$ T cells are able to increase expression of IRF4 through IL-2 stimulation or constitutively active STAT5. This study further showed that STAT5 bound directly to the *Irf4* promoter region, demonstrating a mechanism for increasing IRF4 levels in weakly activated $CD4^+$ T cells (Gomez-Rodriguez et al., 2016). Further work studying the potential role of inflammatory cytokines on IRF4 expression intensity and duration in $CD8^+$ T cells may help advance our understanding of how signaling outside of TCR signal strength can regulate the effector fate in $CD8^+$ T cells.

While IRF4's role in downstream regulation of effector cell fate has been intensely studied (Raczkowski et al., 2013) (Yao et al., 2013) (Man et al., 2013) (Nayar et al., 2014), future work looking into which downstream components of the TCR signaling pathway regulate IRF4 expression, and how they regulate the graded levels of IRF4 expression requires further study. The three major downstream pathways of the TCR signaling complex are MAPK, NFκB, and calcium signaling/NFAT. Previous studies have indicated that MAPK and NFκB show a more digital response to TCR stimulation. MAPK signaling is activated through binding of RasGRP to diacylglycerol (DAG) followed by phosphorylation via protein kinase c (PKC) at the plasma membrane. Activated RasGRP can then bind with SOS (Das et al., 2009), increasing GTPase activity of RasGTP and causing a positive feedback loop of the MAPK signaling pathway (Das et al.,

2009). This turns graded signaling into a digital signaling response, allowing for and “ON” or “OFF” switch for target genes of the MAPK pathway (Das et al., 2009) (Altan-Bonnet & Germain, 2005). NFκB signaling has also been shown to be digital in nature in Jurkat cells, where IκBα degredation showed a digital response, even with graded levels of TCR signaling (i.e. varying doses of α-CD3 antibody) (Kingeter et al., 2010). Calcium signaling on the other hand is highly graded and dependent on TCR signal strength (Chen et al., 2010) (Christo et al., 2015). IRF4 expression has been previously shown to be regulated by NFκB (Grumont & Gerondakis, 2000), but more work needs to be done to understand the roles of MAPK pathway and calcium signaling on IRF4 expression (Figure 6.2). Future work studying these pathways and how they regulate graded expression of IRF4 is important for fully understanding how the TCR signaling pathway regulates $CD8^+$ T cell activation and differentiation.

One final potential point of interest would be determining the role of IRF4 in immunodominance of T cell epitopes. During LCMV-Armstrong infection, two major epitopes (GP_{33-41} and $NP_{396-404}$) dominate the $CD8^+$ T cell response, while several subdominant epitopes ($GP_{276-286}$, GP_{34-41}, etc.) also form a small pool of the $CD8^+$ T cell response (van der Most et al., 1998). Future work studying the potential role of IRF4 signal strength in regulating which populations become immunodominant or subdominant during infection would be interesting to look into. It would unfortunately be very challenging since IRF4 is upregulated early

Figure 6.1. Graded IRF4 expression is potentially regulated through multiple TCR signaling pathways

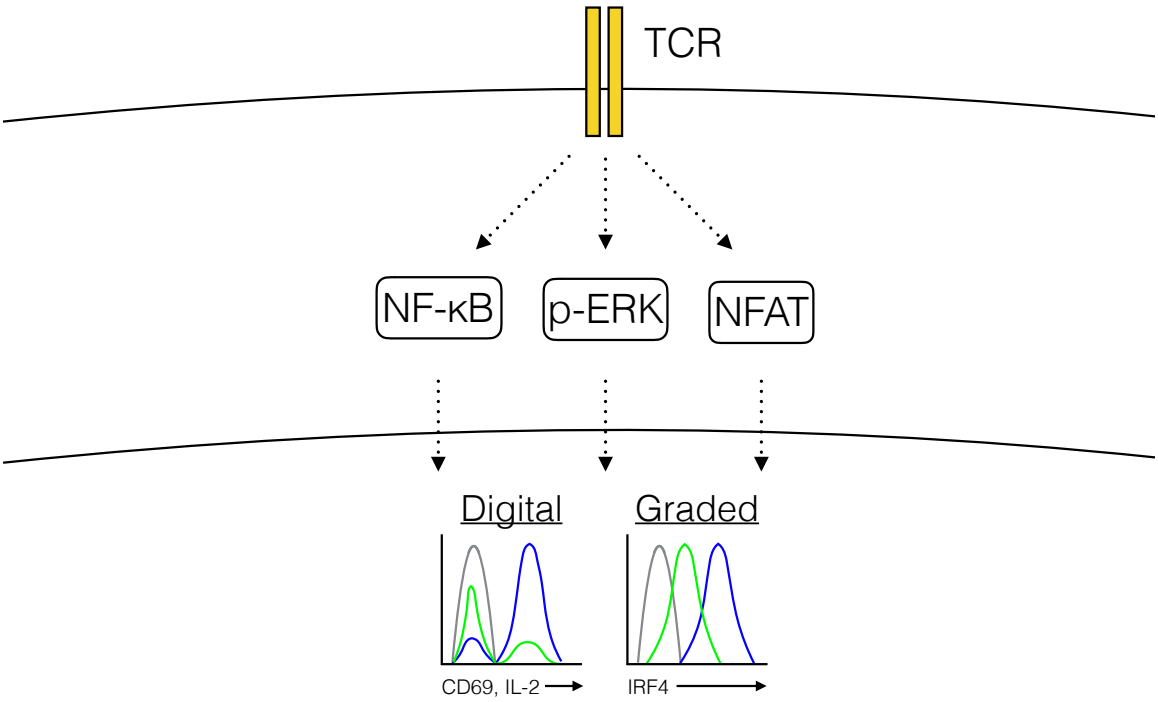

Figure 6.1. Graded IRF4 expression is potentially regulated through multiple TCR signaling pathways

Activation of the TCR leads to downstream signaling of three major pathways: MAPK, NFκB, and calcium signaling/NFAT. Previous work shows that the MAPK and NFκB signaling pathways likely act in a digital manner, with genes either being switched “ON” or “OFF”, whereas calcium signaling has been shown to be important for graded signaling in response to varying levels of TCR signal strength. We hypothesize that graded IRF4 expression is likely occurring through the calcium signaling/NFAT pathway.

after activation, prior to clonal expansion, when the average number of epitope-specific cells is ~100-1000 in the entire spleen. Issues from low cell numbers would also be compounded by the fact that $CD8^+$ T cells are not activated at the exact same time during viral infection in a host, so variability in APC-T cell interactions would also lead to further issues. Testing this theory would likely require *in vitro* work using TCR transgenic cells of pathogen-specific TCRs to synchronize activation of pathogen-specific T cells, as well as have enough pathogen-specific cells for experimental analysis.

Through this work and others, IRF4 has been shown to be a critical component of $CD8^+$ T cell differentiation into the TECs during acute viral and bacterial infection. IRF4 has been shown to be important for regulating proliferation, survival, and expression of transcription factors critical for memory and effector differentiation. Future studies elucidating how TCR signaling regulates graded levels of IRF4, as well as how IRF4 can regulate which populations of pathogen-specific cells become the dominant response in the $CD8^+$ T cell population are interesting directions to further tease apart IRF4 in the $CD8^+$ T cell.

IRF4 and $CD8^+$ T Cell Exhaustion during Chronic LCMV-Clone 13 Infection

$CD8^+$ T cell exhaustion is a commonly observed phenotype during persistent viral infections and cancers (Wherry, 2011). T cell exhaustion is believed to be a mechanism to prevent complications from severe immunopathology (Shin et al.,

2017). There are several extrinsic factors that have been identified in regulating $CD8^+$ T cell exhaustion including increased levels of the immunosuppressive cytokine IL-10, loss of help from $CD4^+$ T cells, and high viral loads (Mueller & Ahmed, 2009) (Doering et al., 2012). The role of Blimp-1, T-bet, and Eomes have been examined during chronic infection (Paley et al., 2012) (Shin et al., 2009) (Kao et al., 2011). These transcription factors have known roles in $CD8^+$ T cell differentiation and effector function during acute viral infection. Blimp-1 is upregulated in exhausted $CD8^+$ T cells during LCMV-clone 13 infection, and increases in Blimp-1 expression correlated with an increased is exhaustion markers PD-1, LAG3, 2B4, and CD160 (Haina Shin et al., 2009). Blimp-1-deficient mice were unable to control LCMV-clone 13 infection compared to WT controls; however, Blimp-1 haplodeficient mice were able to more rapidly control LCMV-clone 13 infection compared to WT control (Shin et al., 2009). These results indicated a sort of Goldilocks effect with Blimp-1 expression levels where Blimp-1 expression that was too high or too low had a detrimental effect on the $CD8^+$ T cell response. Similar results have been observed for T-bet and Eomes during LCMV clone-13 infection. During LCMV-clone 13 infection, the $CD8^+$ T cell response is divided into T-bet^{hi} and $Eomes^{hi}$ populations. Even though T-bet and Eomes are both T-box transcription factors and function redundantly early during acute LCMV-Armstrong infection, loss of either protein results in an impaired ability to control LCMV-clone 13 infection (Paley et al., 2012). This is likely due to the different gene networks they regulate during LCMV-clone 13 infection

(Doering et al., 2012). Together these data demonstrate that control of LCMV-clone 13 infection requires optimal regulation of these major transcription factors. Our work in Chapter IV implicates IRF4 as another transcription factor that requires optimal control in order for chronic viral clearance to occur. Blimp-1, T-bet, Eomes, and IRF4 all require optimal expression in order for viral clearance to occur during LCMV-clone 13 infection. This phenotype is unique to the chronic infection model. Loss of these transcription factors during LCMV-Armstrong infection does not affect clearance of virus from the host.

The function of T-bet^{hi} and Eomes^{hi} CD8^{+} T cell subsets during chronic viral infection has been well studied (Paley et al., 2012); however, how differentiation of these subsets is transcriptionally regulated is not understood. In our work in chapter IV, we explored the role of TCR signal strength via graded levels of IRF4 in the relative expression of T-bet and Eomes as well as the differentiation of T-bet^{hi} and Eomes^{hi} subsets during chronic LCMV-clone 13 infection. We found that levels of IRF4 expression directly regulated the ratio of T-bet^{hi} and Eomes^{hi} populations, with decreasing levels of IRF4 leading towards an increase in the proportion of Eomes^{hi} cells both *in vitro* and *in vivo.* Previous work has demonstrated that IRF4, along with it's binding partner BATF, directly bind to the *Tbet* and *Eomes* loci in effector CD8^{+} T cells, showing a direct role of IRF4/BATF in regulating T-bet and Eomes expression (Man et al., 2013) (Kurachi et al., 2014).

The largest defects in the altered ratios of T-bet and Eomes in *Irf4*$^{+/fl}$ mice was the reduced differentiation of T-bet^{hi} precursors, and the reduced ability to clear viral infection. T-bet^{hi} cells have a lower ability to proliferate and have decreased cytotoxicity compared to Eomes^{hi} cells; however, they seed the Eomes^{hi} pool and are critical for viral clearance (Paley et al., 2012). IRF4 regulates multiple pathways, such as proliferation, metabolism, and expression of effector cytokines in antiviral CD8^{+} T cells during acute viral infection (Man et al., 2013) (Yao et al., 2013) so it is also possible that any defects in these pathways could contribute to impaired viral clearance in *Irf4*$^{+/fl}$ mice. To directly test the importance of the T-bet to Eomes ratio, we reduced the expression of Eomes in the *Irf4*$^{+/fl}$ mice by generating *Irf4*$^{+/fl}$ *Eomes*$^{+/fl}$ mice. These compound heterozygotes had lower Eomes expression compared to *Irf4*$^{+/fl}$ mice, exhibited similar Eomes to T-bet ratios as WT controls, and showed similar levels of T-bet^{hi} precursor cells compared to WT controls. *Irf4*$^{+/fl}$ *Eomes*$^{+/fl}$ mice were able to clear viral infection from multiple organs at a similar rate to WT controls. These results showed that Eomes overexpression, defects in viral clearance, and defects in T-bet^{hi} ratios in *Irf4*$^{+/fl}$ mice could be rescued by compound *Irf4*$^{+/fl}$ *Eomes*$^{+/fl}$ mice.

Another consequence of the reduced T-bet to Eomes ratio in *Irf4*$^{+/fl}$ mice was the altered differentiation of T-bet^{hi} and Eomes^{hi} populations. Using T-bet and Eomes knockout mice, Paley et al showed that loss of either the T-bet^{hi} or Eomes^{hi}

population is detrimental to viral control (Paley et al., 2012); however, it is not known whether reduced levels of one population over the other affects viral control. Our work suggests that reduced differentiation of T-bet^{hi} populations in *Irf4*$^{+/fl}$ mice is detrimental to efficient viral control. Consistent with this observation, lower proportions of T-bet^{hi} CD8^{+} T cells are observed in lung transplant recipients with relapsed CMV infection relative to CMV controllers (Popescu et al., 2014). Loss of FoxO1 results in higher levels of T-bet and lower levels of Eomes, thus biasing CD8^{+} T cell differentiation towards T-bet^{hi} subsets during chronic LCMV-clone13 infection (Staron et al., 2014). Interestingly, FoxO1-deficient mice are also unable to clear chronic viral infection (Staron et al., 2014). These data support our conclusion that balanced differentiation of T-bet^{hi} and Eomes^{hi} subsets are important for viral control.

Levels of IRF4 are known to regulate the magnitude of the effector CD8^{+} T cell response during acute infection (Raczkowski et al., 2013) (Man et al., 2013) (Yao et al., 2013) (Grusdat et al., 2014) (Nayar et al., 2014). We observed that IRF4 regulated the magnitude of the CD8^{+} T cells response to LCMV-clone 13 infection at day 8 post infection. Furthermore, the increased numbers of viral-specific CD8^{+} T cell numbers were not different between WT and *Irf4*$^{+/fl}$ mice at day 22 post infection or at later timepoints examined. Therefore, it is also possible that this early difference in the magnitude of the CD8^{+} T cell response

may be responsible for the ultimate ability of WT mice, but not *Irf4*$^{+/fl}$ mice, to be able to clear LCMV-clone 13 infection.

Runx2 and CD8$^+$ T Cell Memory during Acute LCMV-Armstrong Infection

CD8$^+$ T cell memory is a critical component of the immune response. It allows the host to be protected from reinfection of the same pathogen. CD8$^+$ T cell memory formation is a critical component of vaccine development, allowing protection against deadly pathogens a host has not previously encountered by eliciting an immune response against pathogen-specific antigens. CD8$^+$ T cell memory also has a dark side. Self-reactive CD8$^+$ T cells can recognize a host cell component as a foreign antigen and generate a strong CD8$^+$ T cell response against that population forming a memory pool, which can be reactivated leading to autoimmunity.

Understanding how CD8$^+$ T cells differentiate into memory cells is critical for biomedical research advancement. With this knowledge we could manipulate CD8$^+$ T cells towards a memory phenotype, such as in the case of vaccination, where an increased CD8$^+$ T memory cell pool is highly desired to help protect against infection. We could also manipulate activated CD8$^+$ T cells away from differentiating into a memory cell, such as the case with autoimmunity and CAR-T cell therapy, where the memory pool could cause damage to the host.

The work discussed in Chapter V of this dissertation shows an important role for the transcription factor Runx2 in $CD8^+$ T cell memory. Runx2 is an interesting candidate for $CD8^+$ T memory cell targeted therapies because loss of Runx2 in the $CD8^+$ T cell population has no major effect on the $CD8^+$ TEC response during LCMV infection. *Runx2*$^{fl/fl}$ mice are still able to clear infection at day 9 post infection as WT mice, and there are no major defects seen in the total number of pathogen-specific TECs, as well as effector molecules GranzymeB and CD107a+b for the three epitopes tested. Viral kinetics were not tested, so the rate of viral clearance may vary between WT and *Runx2*$^{fl/fl}$ mice. This makes Runx2 a strong candidate for translational therapies, such as CAR-T cells, where effector function is critical for clearance of cancer cells from the host, while memory function can be destructive and lead to autoimmunity.

Runx2$^{fl/fl}$ show a striking resemblance to IL-15 and IL15rα-deficient mice. IL-15-deficient mice are able to mount a strong $CD8^+$ T effector response against LCMV-Armstrong infection with no defect in proportions of pathogen-specific cells early after infection clearance; however, IL-15-deficient mice have a decrease in the proportion of pathogen-specific cells at memory time points compared to WT controls (Becker et al., 2002). Similar results are observed in IL-15-deficient mice during VSV infection (Schluns et al., 2002). These results are similar to what we see with *Runx2*$^{fl/fl}$ mice during LCMV-Armstrong infection. IL-

15-deficient mice are also able to elicit a strong recall response during reinfection (Becker et al., 2002), similar to what we have seen with *Runx2*$^{fl/fl}$ mice. CD8^{+} T memory cell loss in IL-15-deficient and *Runx2*$^{-/-}$ mice is similar in that there is not a complete loss of the MPC population, rather, a significant decrease in the total number of MPCs. This is likely due to the fact that MPCs in an IL-15-deficient mouse are able to survive, however, they do not homeostatically proliferate (Becker et al., 2002). Another potential mechanism for this phenotype is that IL-7 and IL-15 have been shown to perform similar functions in CD8^{+} T cell memory survival and homeostatic proliferation (Goldrath et al., 2002) allowing a decreased amount of CD8^{+} MPCs to survive and continue during the memory phase of infection off of IL-7 stimulation alone. Further work examining the effects of IL-15 on homeostatic proliferation of *Runx2*$^{-/-}$ MPCs would further help to shed light on the potential role of IL-15 in Runx2-mediated MPC defects seen during LCMV-Armstrong infection.

One potential mechanism for IL-15 regulating Runx2 transcriptional control is through phosphorylation of Runx2. Work from Li et al. has shown that phosphorylated extracellular signal-regulated kinase 1/2 (p-ERK1/2) is critical for phosphorylation of Runx2 in osteoblasts (Y. Li et al., 2012). They further show that Runx2 phosphorylation is required for transcription of Runx2 downstream target genes (Y. Li et al., 2012) (Ge et al., 2012). Stimulation of the IL-15 receptor leads to downstream activation of three major signaling pathways: the

STAT3/STAT5 signaling pathway, Atk/PKB anti-apoptotic pathway, and the MAPK/ERK signaling pathway. From this information, one hypothesis is that IL-15 regulates Runx2 dependent MPC genes through phosphorylation of Runx2 via the MAPK/ERK pathway (Figure 6.2). This hypothesis would also explain the results observed from two microarray experiments performed *ex vivo* and *in vitro*. For the *ex vivo* experiments, congenically marked WT and *Runx2*$^{fl/fl}$ P14 TCR transgenic cells were co-adoptively transferred into a host mouse. Mice were then infected with LCMV-Armstrong and six days later, cells were sorted and RNA was isolated from WT and *Runx2*$^{fl/fl}$ populations. There was no difference observed in transcription between WT and *Runx2*$^{fl/fl}$ cells. Similar results were observed for WT and *Runx2*$^{fl/fl}$ P14 cells stimulated *in vitro* with GP_{33} peptide. If Runx2 downstream transcription was regulated by Runx2 phosphorylation via the MARK/ERK pathway, no differences in transcription would be observed between WT and *Runx2*$^{fl/fl}$ $CD8^+$ T cells *ex vivo* because only a small minority of MPCs actively receive IL-15 signaling at any given time, and no difference would be observed *in vitro* because the cells were not treated with IL-15.

This hypothesis requires further studies looking into p-Runx2 levels in response to IL-15 signaling in $CD8^+$ MPCs. If there is confirmed regulation of Runx2 phosphorylation via IL-15 signaling, it would be ideal to look for transcriptional differences between WT and *Runx2*$^{fl/fl}$ P14 MPCs stimulated with IL-15. To help tease apart which IL-15 downstream target genes are regulated by Runx2, IL-15-

Figure 6.2. IL-15 regulates expression of Runx2 target genes through p-ERK1/2 mediated Runx2 phosphorylation

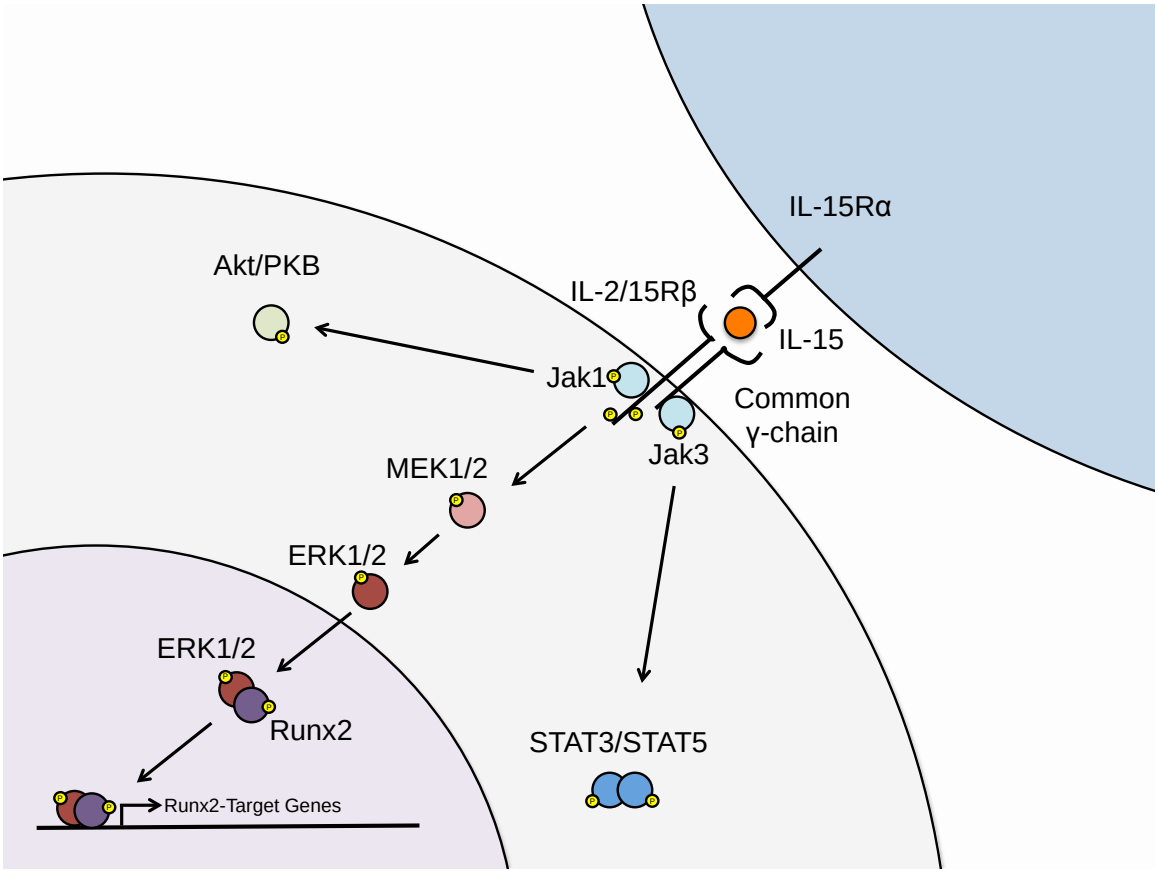

Figure 6.2. IL-15 regulates expression of Runx2 target genes through p-ERK1/2 mediated Runx2 phosphorylation

Hypothetical model for transcriptional regulation of Runx2 target genes via phosphorylation of Runx2. Runx2 requires phosphorylation in order for transcription of downstream target genes. Runx2 phosphorylation could potentially be regulated through the IL-15 signaling pathway via p-ERK1/2. This model would explain defect seen in MPC population in *Runx2*$^{fl/fl}$ CD8^{+} T cells during LCMV-Armstrong infection as well as the fact that no transcriptional differences are observed between WT and *Runx2*$^{fl/fl}$ CD8^{+} P14 cells.

deficient or IL-15Rα-deficient P14 MPCs could also be included in transcriptional studies. MAPK/ERK inhibitors such as U0126 could be used to help dissect the role of IL-15 mediated p-ERK expression in Runx2 phosphorylation. It would also be valuable to look into the potential role of IL-7 signaling and p-Runx2, since stimulation of the IL-7 receptor also leads to downstream MAPK/ERK signaling.

Our work also demonstrated that Runx2 expression inversely correlated with TCR signal strength, with TCR signaling on the cusp of activating T cells leading to the strongest expression of Runx2. Similar results were observed for another major memory transcription factor, Eomes. We further showed that loss of IRF4 in $CD8^+$ T cells lead to a significant increased in Runx2 expression. This work agrees with previous models showing that TCR signal strength intensity helps to regulate effector and memory differentiation in activated $CD8^+$ T cells during infection, with lower TCR signal strength leading towards a memory fate and higher TCR signal strength leading towards an effector fate. Future work studying the effects of TCR signal strength *in vivo* on Runx2 expression and memory formation would be interesting. The LCMV-Armstrong F6L mutant strain could be used to identify differences in Runx2 expression in P14 TCR transgenic cells between WT and F6L mutant infection, where the F6L mutant has a lower affinity for the P14 TCR.

Future work looking into the role of inflammatory cytokines known to regulate effector and memory fate in $CD8^+$ T cells in regulating levels of Runx2 would also be interesting. We performed *in vitro* stimulations of WT P14 cells treated with various cytokines and looked for differences in Runx2 expression. While we found that pro-inflammatory cytokine IL-12 suppressed Runx2 expression, further work looking at the *in vivo* role of inflammatory cytokines in Runx2 expression during LCMV-Armstrong infection would be interesting to determine whether Runx2 is regulated via TCR signal strength alone, or also by pro-inflammatory cytokines.

Determining the precise mechanism of Runx2 downstream signaling that regulated the MPC defect during LCMV-Armstrong infection has eluded us. We initially performed microarrays to determine transcriptional differences between WT and *Runx2*$^{fl/fl}$ P14 cells *ex vivo* from LCMV-Armstrong infection as well as during *in vitro* stimulation; however, no transcriptional differences were observed in either experimental setting. This led us to consider alternative mechanisms of Runx2 function in MPCs.

Runx2 has been shown to bind to histone deacylase 1 (HDAC1) and downregulate rRNA transcription through acetylation of the protein upstream binding factor (UBF) in osteoblasts (Ali et al., 2012). In this way, Runx2 can globally repress translation of mRNA into protein, while having no impact on

transcription. It is known that effector cells are more transcriptionally active compared to memory cells (Best et al., 2013) (Chang et al., 2014), and this post-transcriptional regulation of mRNA translation could be another step to help keep MPCs more quiescent and push them towards the memory fate. However, we found no difference in pre-rRNA transcription between WT and *Runx2*$^{fl/fl}$ P14 cells. This led us to believe that Runx2 was likely not regulating MPCs through globally repressing translation of mRNA to protein.

One additional possibility is that Runx2 is affecting memory formation through the regulation of chromatin accessibility, a known role of Runx3 in T cells (Wang et al., 2018). In this work, authors found a significant increase in Runx2 and Runx3 binding motifs in open regions of the chromosome in MPCs compared to naïve cells (Wang et al., 2018). The authors saw no major defect in MPCs with Runx2 shRNA knockdown, but the shRNA knockdown had a very partial defect on Runx2 protein expression, only really showing that partial loss of Runx2 had no major defect on MPC formation during LCMV infection (Wang et al., 2018). The authors further show that the most dramatic loss of MPCs during LCMV infection occurred with shRNA knockdown of CBFβ, the binding partner of all Runx proteins (Wang et al., 2018). Runx family proteins have been shown to have redundant roles in $CD4^+$ T_{REG} cells (Rudra et al., 2009), and thus could explain why knockdown of the CBFβ binding partner led to the most dramatic phenotype. Runx2 and Runx3 could be playing redundant roles in regulating Memory cell

chromatin accessibility. To further test this hypothesis, ATAC-seq would need to be performed on WT versus *Runx2*$^{fl/fl}$ P14 MPCs from LCMV-Armstrong infection. This would help us determine if Runx2 was enabling accessibility of chromatin required for memory cells. Future studies looking at the role of CBFβ in MPC formation would also be important for determining whether Runx2 and Runx3 are playing redundant roles in regulating chromosome accessibility for MPCs. Runx1 and Runx3 have known roles in CD8$^+$ T cell effector function and differentiation, so *Cbfβ*$^{fl/fl}$ mice with an inducible cre (ex. tamoxifen-cre), may be required to help tease apart this mechanism.

From this work it is clear that Runx2 is playing a role in MPCs during LCMV-Armstrong infection, and loss of Runx2 leads to a defect in the total number of MPCs. Although we have been unable to determine the downstream mechanisms of Runx2 within the CD8$^+$ MPC population, we have several potential hypotheses as to how this may be occurring, and directions for future studies. From our work it is clear that, while Runx2 is regulated inversely from TCR signal strength (in a similar fashion as other memory transcription factors), it is not playing the conventional role of a transcription factor in MPCs. This work is a critical addition to the field. While Runx2 may seem like another transcription factor to add to the list of many that regulate memory differentiation and function in CD8$^+$ T cells, Runx2 has shown a potential uniqueness, in that it does not regulate transcription in MPC steady state. We hypothesize that it likely requires

IL-15 signaling to phosphorylate Runx2, thus allowed downstream transcription of target genes to occur. Our other major hypothesis is that it is required for chromatin accessibility of MPC related genes. Both of these functions are relatively unique and uncommon among known memory transcription factors, and would make it an interesting candidate for targeted therapies once these mechanisms have been fully elucidated.

IRF4 and Runx2: Major Regulators of $CD8^+$ T Cell Effector and Memory

From our work we have determined inverse roles for the transcription factors IRF4 and Runx2 in $CD8^+$ T cell effector and memory differentiation. IRF4 is transiently expressed early after T cell activation, and plays a critical role in the $CD8^+$ T cell effector response. Runx2 expression is upregulated later after T cell activation; around 3 days post stimulation *in vitro* and remains upregulated for the life of the $CD8^+$ T cell. In chapter V, we determined that IRF4 was able to repress Runx2 expression in activated $CD8^+$ T cells. This could be potentially caused by direct repression of Runx2 by IRF4. IRF4 has also been shown to bind directly to the Runx2 promoter in activated $CD8^+$ T cells (Kurachi et al., 2014). From these results, we generated a model of $CD8^+$ T cell differentiation during $CD8^+$ T cell activation (Figure 6.3) where repression of Runx2 by IRF4 potentially regulates memory cell differentiation. In our model, IRF4 expression, which has been shown to be positively regulated by TCR signal strength (Nayar et al., 2014) as well as by proinflammatory cytokines, represses Runx2 expression,

Figure 6.3 Model of IRF4 and Runx2-mediated terminal effector versus memory cell fate during acute viral infection

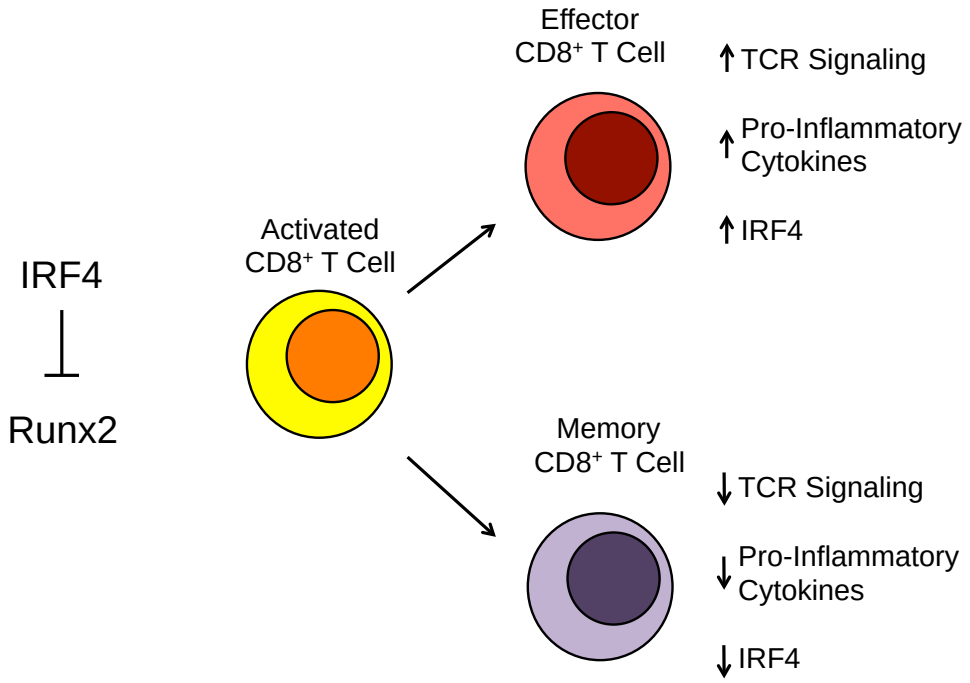

Figure 6.3 Model of IRF4 and Runx2-mediated terminal effector versus memory cell fate during acute viral infection

Work from Chapter V has shown that IRF4 is able to repress Runx2 expression. We hypothesize that inceased TCR signaling and pro-inflammatory cytokine signaling in activated $CD8^+$ T cells promotes increased expression levels and duration of IRF4. High levels of IRF4 lead to promotion of the terminal effector cell fate. Low TCR signaling and lower levels of pro-inflammatory cytokines lead to decreased levels of IRF4 and increased levels of Runx2. Increased levels of Runx2 promote Memory $CD8^+$ T Cell fate.

promoting terminal effector cell fate. Lower levels of TCR signaling, as well as a decrease in proinflammatory cytokines could promote memory cell fate through decreased levels of IRF4 and therefore increased levels of Runx2. Future work looking into the role of TCR signaling and pro-inflammatory cytokines in regulation of Runx2 *in vivo* will be required to really tease apart how these effector-promoting signals regulate Runx2, as well as molecular work teasing apart how IRF4 represses Runx2 expression in activated $CD8^+$ T cells.

Runx2 expression is not present in naïve $CD8^+$ T cells. We have two major hypotheses as to how this may be occurring. One hypothesis is Runx2 expression is not present in naïve $CD8^+$ T cells due to fact that the majority of the chromosomal DNA is inaccessible in naïve T cells (Kurachi et al., 2014). During $CD8^+$ T cell activation, the chromosomal DNA is opened up by several transcription factors including BATF and IRF4 (Kurachi et al., 2014). During this time, access to the *Runx2* gene may become accessible; however, IRF4 repression of Runx2 could inhibit Runx2 expression until IRF4 expression goes down. Another hypothesis is that the transcriptional regulators of Runx2 are not present in naïve T cells, and are expressed after T cell activation. These two hypotheses are not mutually exclusive, since Runx2 likely requires a transcriptional regulator to promote RNA polymerase binding to the *Runx2* gene. Further work determining which transcription factors are regulating Runx2 expression, and chromosomal accessibility of the *Runx2* gene in naïve versus

activated $CD8^+$ T cells will be required to determine how Runx2 is regulated in activated $CD8^+$ T cells on the molecular level.

Appendix I

Loss of Sox4 in the T cell compartment has no impact on CD8$^+$ T cell memory during LCMV-Armstrong infection

In Hu et al, Sox4 was identified as binding to the Runx2 promoter region, and was identified as a regulator of Runx2 expression (Hu et al. 2013). To test if Sox4 was regulating Runx2-mediated memory functions during LCMV-Armstrong infection, we infected *Sox4$^{fl/fl}$ CD4-cre$^+$* mice (hereby referred to as *Sox4$^{fl/fl}$* mice) with LCMV-Armstrong and looked for defects in MPCs during and after clearance of infection (Figure A.1). While we saw significant defects in proportions of KLRG1$^-$ pathogen-specific cells at day 7 post infection, no defect in the total cell number was seen (Figure A.1 A). A significant decrease in CD27, a surface marker associated with MPCs, was also observed in *Sox4$^{fl/fl}$* mice compared to WT controls (Figure A.1 B). At day 28 post infection, no difference in MPCs was observed between WT and *Sox4$^{fl/fl}$* mice (Figure A.1 C), indicating that any defects seen in MPCs early on in *Sox4$^{fl/fl}$* mice had no long term effect on the total number of the memory pool. While Sox4 may bind to the Runx2 promoter region in activated CD8$^+$ T cells, it seems loss of Sox4 does not mimic memory defects seen in Runx2 deficient mice. While this work was far from exhaustive, we chose to end this portion of the study to focus on elucidation of Runx2 in CD8$^+$ T cell memory.

Figure A.1. Loss of Sox4 in the T cell compartment has no impact on CD8$^+$ T cell memory during LCMV-Armstrong infection

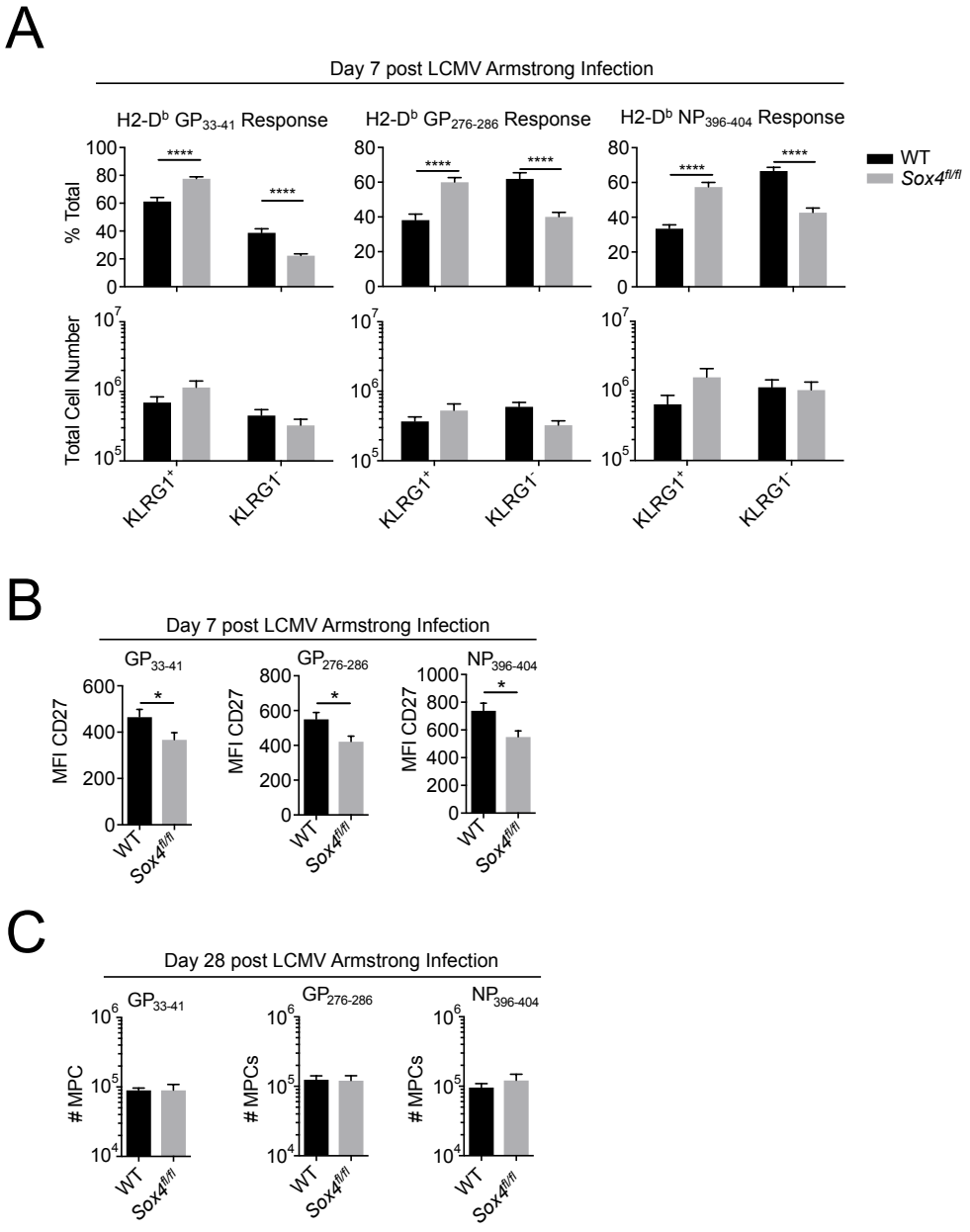

Figure A.1. Loss of Sox4 in the T cell compartment has no impact on $CD8^+$ T cell memory during LCMV-Armstrong infection

WT and *Sox4*$^{fl/fl}$ *CD4-cre*$^+$ mice were infected with $5*10^4$ PFU LCMV-Armstrong i.p. Spleens were harvested at day 7 and 28 post infection, and stained for pathogen-specifc $CD8^+$ T cells. **(A)** Percentage (top) and total number (bottom) of GP_{33-41} (left), $GP_{276-286}$ (middle), and $NP_{396-404}$ (right) specific $KLRG1^+$ and $KLRG1^-$ $CD8^+$ T cells. **(B)** MFI of CD27 in WT and *Sox4*$^{fl/fl}$ GP_{33-41} (left), $GP_{276-286}$ (middle), and $NP_{396-404}$ (right) specific cells at day 7 post infection. **(C)** Total number of GP_{33-41} (left), $GP_{276-286}$ (middle), and $NP_{396-404}$ (right) MPCs ($KLRG1^{lo}$ $CD127^{hi}$) at day 28 post infection. Data are representative of 2-3 experiments with 7-12 mice per group. Error bars indicate mean ± SEM.

Appendix II

Loss of IL-4 has no defect on $CD8^+$ T cell memory during LCMV-Armstrong infection

We performed a large *in vitro* cytokine panel to determine if any cytokines had an effect on Runx2 expression in activated $CD8^+$ T cells. IL-4 significantly and reproducibly downregulated Runx2 expression compared to no cytokine control (Figure A.2 A). From this we were interested to see if loss of IL-4 would have any effect on the memory population during LCMV-Armstrong infection (Figure A.2 B-D). To test this we infected WT and IL-4 KO mice with LCMV-Armstrong, and harvested spleens 90 days post infection. We looked for tetramer-specific cells, and found no defect in GP_{33}, GP_{276}, and NP_{396} specific responses in IL-4 KO mice compared to WT controls (Figure A.2 B-D). From these results, we determined that loss of IL-4 had no major impact on the total number of memory cells during LCMV-Armstrong infection. While this work was far from exhaustive, we chose to end this portion of the study to focus on elucidation of Runx2 in $CD8^+$ T cell memory.

Figure A.2. Loss of IL-4 has no defect on CD8$^+$ T cell memory during LCMV-Armstrong infection

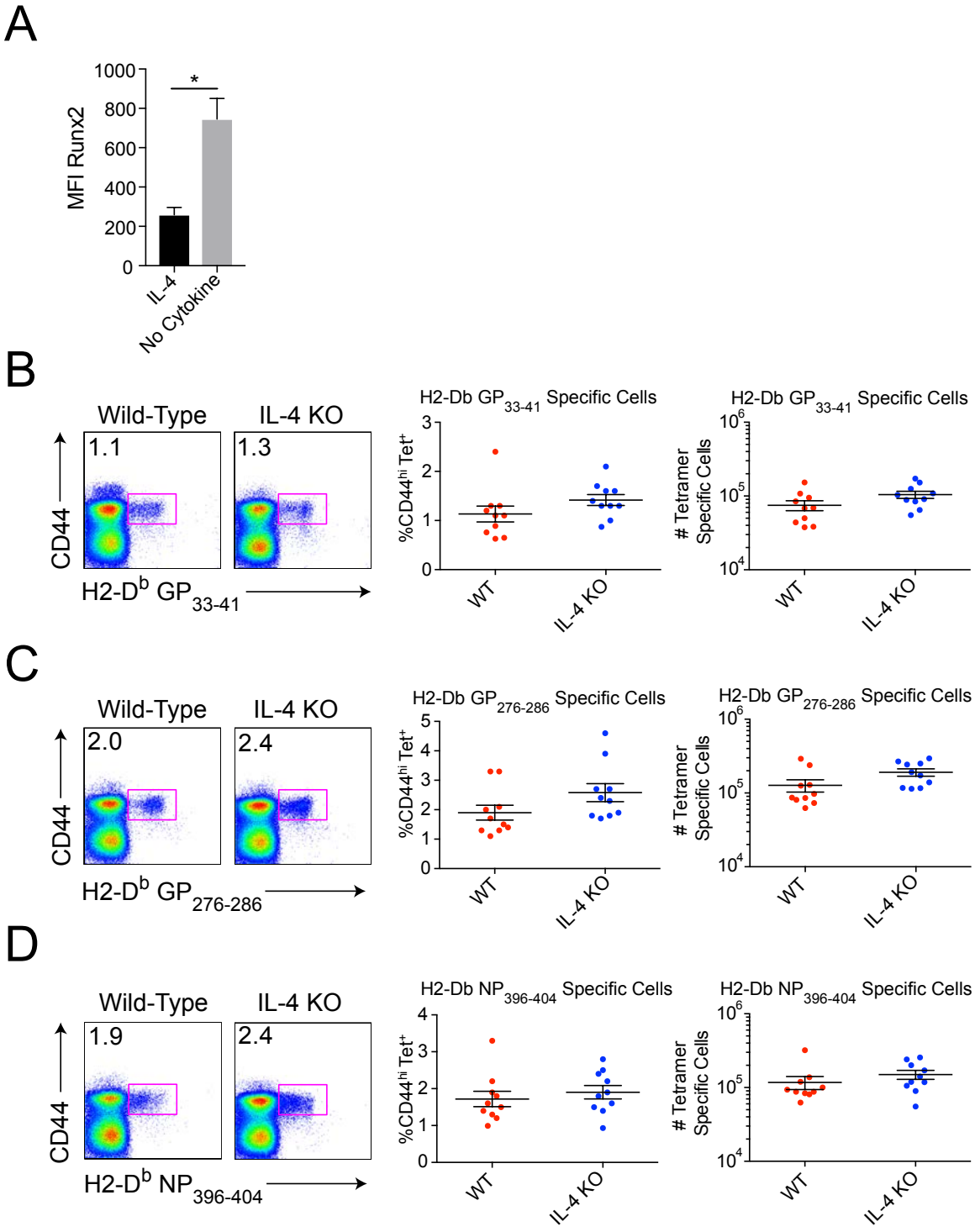

Figure A.2. Loss of IL-4 has no defect on $CD8^+$ T cell memory during LCMV-Armstrong infection

(A) P14 splenocytes were isolated from mice and incubated with GP_{33-41} peptide, IL-2, and with or without IL-4 for 4 days and stained for Runx2. **(B-D)** WT and IL-4 KO mice were infected with $5*10^4$ PFU LCMV-Armstrong i.p. Spleens were harvested at day 90 post infection, and stained for pathogen-specifc $CD8^+$ T cells. **(B)** The H2-D^b GP_{33-41} specific response. (left) Gating strategy for GP_{33-41} specific T cells. (center) Percentage of GP_{33-41} specific cells. (left) Total number of GP_{33-41} specific cells. **(C)** The H2-D^b $GP_{276-286}$ specific response. (left) Gating strategy for $GP_{276-286}$ specific T cells. (center) Percentage of $GP_{276-286}$ specific cells. (left) Total number of $GP_{276-286}$ specific cells. **(D)** The H2-D^b $NP_{396-404}$ specific response. (left) Gating strategy for $NP_{396-404}$ specific T cells. (center) Percentage of $NP_{396-404}$ specific cells. (left) Total number of $NP_{396-404}$ specific cells. Data are representative of two experiments with 10 mice per group. Error bars indicate mean ± SEM.

REFERENCES

Agarwal, P., Raghavan, A., Nandiwada, S. L., Curtsinger, J. M., Bohjanen, P. R., Mueller, D. L., & Mescher, M. F. (2009). Gene Regulation and Chromatin Remodeling by IL-12 and Type I IFN in Programming for CD8 T Cell Effector Function and Memory. *The Journal of Immunology*, *183*(3), 1695–1704. http://doi.org/10.4049/jimmunol.0900592

Ali, S. A., Dobson, J. R., Lian, J. B., Stein, J. L., van Wijnen, A. J., Zaidi, S. K., & Stein, G. S. (2012). A RUNX2-HDAC1 co-repressor complex regulates rRNA gene expression by modulating UBF acetylation. *Journal of Cell Science*, *125*(11), 2732–2739. http://doi.org/10.1242/jcs.100909

Altan-Bonnet, G., & Germain, R. N. (2005). Modeling T Cell Antigen Discrimination Based on Feedback Control of Digital ERK Responses. *PLoS Biology*, *3*(11), e356. http://doi.org/10.1371/journal.pbio.0030356

Aubert, R. D., Kamphorst, A. O., Sarkar, S., Vezys, V., Ha, S. J., Barber, D. L., Ye, L., Sharpe, A. H., Freeman, G. J., & Ahmed, R. (2011). Antigen-specific CD4 T-cell help rescues exhausted CD8 T cells during chronic viral infection. *Proceedings of the National Academy of Sciences*, *108*(52), 21182–21187. http://doi.org/10.1073/pnas.1118450109

Badovinac, V. P., Messingham, K. A. N., Jabbari, A., Haring, J. S., & Harty, J. T. (2005). Accelerated $CD8^+$ T-cell memory and prime-boost response after dendritic-cell vaccination. *Nature Medicine*, *11*(7), 748–756. https://doi.org/10.1038/nm1257

Badovinac, V. P., Porter, B. B., & Harty, J. T. (2002). Programmed contraction of $CD8^+$ T cells after infection. *Nature Immunology*, *3*(7), 619–626. https://doi.org/10.1038/ni804

Badovinac, V. P., Porter, B. B., & Harty, J. T. (2004). $CD8^+$ T cell contraction is controlled by early inflammation. *Nature Immunology*, *5*(8), 809–817. https://doi.org/10.1038/ni1098

Banerjee, A., Gordon, S. M., Intlekofer, A. M., Paley, M. A., Mooney, E. C., Lindsten, T., Wherry, E. J., & Reiner S. L. (2010). Cutting Edge: The Transcription Factor Eomesodermin Enables $CD8^+$ T Cells To Compete for the Memory Cell Niche. *The Journal of Immunology*, *185*(9), 4988–4992. http://doi.org/10.4049/jimmunol.1002042

Barber, D. L., Wherry, E. J., Masopust, D., Zhu, B., Allison, J. P., Sharpe, A. H., Freeman, G. J., & Ahmed, R. (2005). Restoring function in exhausted CD8 T cells during chronic viral infection. *Nature*, *439*(7077), 682–687. https://doi.org/10.1038/nature04444

Basler, M., Youhnovski, N., Van Den Broek, M., Przybylski, M., & Groettrup, M. (2004). Immunoproteasomes down-regulate presentation of a subdominant T cell epitope from lymphocytic choriomeningitis virus. *The Journal of Immunology*, *173*(6), 3925–3934. https://doi.org/10.4049/jimmunol.173.6.3925

Becker, T. C., Wherry, E. J., Boone, D., Murali-Krishna, K., Anita, R., Ma, A., &

Ahmed, R. (2002). Interleukin 15 Is Required for Proliferative Renewal of Virus-specific Memory CD8 T Cells. *Journal of Experimental Medicine*, *195*(12), 1541–1548. http://doi.org/10.1084/jem.20020369

Benson, M., Erickson, L., Gleeson, M., & Noelle, R. (2007). Affinity of antigen encounter and other early B-cell signals determine B-cell fate. *Current Opinion in Immunology*, *19*(3), 275–280. http://doi.org/10.1016/j.coi.2007.04.009

Berg, L. J., Finkelstein, L. D., Lucas, J. A., & Schwartzberg, P. L. (2005). Tec Family Kinases in T Lymphocyte Development and Function. *Annual Review of Immunology*, *23*(1), 549–600. http://doi.org/10.1146/annurev.immunol.22.012703.104743

Bergthaler, A., Flatz, L., Verschoor, A., Hegazy, A. N., Holdener, M., Fink, K., Eschli, B., Merkler, D., Sommerstein R., Horvath, E., Fernandez, M., Fitsche, A., Senn, B., Verbeek, J. S., Odermatt, B., Siegrist, C.-A., & Pinschewer, D. D. (2009). Impaired Antibody Response Causes Persistence of Prototypic T Cell–Contained Virus. *PLoS Biology*, *7*(4), e1000080. http://doi.org/10.1371/journal.pbio.1000080

Best, J. A., Blair, D. A., Knell, J., Yang, E., Mayya, V., Doedens, A., Dustin, M. L., Goldrath, A. W., & The Immunological Genome Project Consortium (2013). Transcriptional insights into the $CD8^+$ T cell response to infection and memory T cell formation. *Nature Immunology*, *14*(4), 404–412. http://doi.org/10.1038/ni.2536

Biswas, P. S., Gupta, S., Chang, E., Song, L., Stirzaker, R. A., Liao, J. K., Bhagat, G., & Pernis, A. B. (2010). Phosphorylation of IRF4 by ROCK2 regulates IL-17 and IL-21 production and the development of autoimmunity in mice. *Journal of Clinical Investigation*, *120*(9), 3280–3295. http://doi.org/10.1172/JCI42856DS1

Blackburn, S. D., Crawford, A., Shin, H., Polley, A., Freeman, G. J., & Wherry, E. J. (2010). Tissue-Specific Differences in PD-1 and PD-L1 Expression during Chronic Viral Infection: Implications for CD8 T-Cell Exhaustion. *Journal of Virology*, *84*(4), 2078–2089. http://doi.org/10.1128/JVI.01579-09

Blackburn, S. D., Shin, H., Freeman, G. J., & Wherry, E. J. (2008a). Selective expansion of a subset of exhausted CD8 T cells by alphaPD-L1 blockade. *Proceedings of the National Academy of Sciences*, *105*(39), 15016–15021. http://doi.org/10.1073/pnas.0801497105

Blackburn, S. D., Shin, H., Haining, W. N., Zou, T., Workman, C. J., Polley, A., Betts, M. R., Freeman, G. J., Vignali, D. A., & Wherry E. J. (2008b). Coregulation of $CD8^+$ T cell exhaustion by multiple inhibitory receptors during chronic viral infection. *Nature Immunology*, *10*(1), 29–37. https://doi.org/10.1038/ni.1679

Bollig, N., Brüstle, A., Kellner, K., Ackermann, W., Abass, E., Raifer, H., Camara, B., Brendel, C., Giel, G., Bothur, E., Huber, M., Paul, C., Elli, A., Kroczek, R. A., Nurieva, R., Dong, C., Jacob, R., Mak, T. W., & Lohoff, M. (2012). Transcription factor IRF4 determines germinal center formation through

follicular T-helper cell differentiation. *Proceedings of the National Academy of Sciences*, *109*(22), 8664–8669. http://doi.org/10.1073/pnas.1205834109
Brass, A. L., Kehrli, E., Eisenbeis, C. F., Storb, U., & Singh, H. (1996). Pip, a lymphoid-restricted IRF, contains a regulatory domain that is important for autoinhibition and ternary complex formation with the Ets factor PU.1. *Genes & Development*, *10*(18), 2335–2347. http://doi.org/10.1101/gad.10.18.2335
Brass, A. L., Zhu, A. Q., & Singh, H. (1999). Assembly requirements of PU.1-Pip (IRF-4) activator complexes: inhibiting function in vivo using fused dimers. *The EMBO Journal*, *18*(4), 977–991. http://doi.org/10.1093/emboj/18.4.977
Brooks, D. G., McGavern, D. B., & Oldstone, M. B. A. (2006a). Reprogramming of antiviral T cells prevents inactivation and restores T cell activity during persistent viral infection. *Journal of Clinical Investigation*, *116*(6), 1675–1685. http://doi.org/10.1172/JCI26856
Brooks, D. G., Trifilo, M. J., Edelmann, K. H., Teyton, L., McGavern, D. B., & Oldstone, M. B. A. (2006b). Interleukin-10 determines viral clearance or persistence in vivo. *Nature Medicine*, *12*(11), 1301–1309. https://doi.org/10.1038/nm1492
Brüstle, A., Heink, S., Huber, M., Rosenplänter, C., Stadelmann, C., Yu, P., Arpaia, E., Mak, T. W., Kamradt, T., & Lohoff, M. (2007). The development of inflammatory TH-17 cells requires interferon-regulatory factor 4. *Nature Immunology*, *8*(9), 958–966. https://doi.org/10.1038/ni1500
Burkett, P. R., Koka, R., Chien, M., Chai, S., Chan, F., Ma, A., & Boone, D. L. (2003). IL-15R alpha expression on CD8+ T cells is dispensable for T cell memory. *Proceedings of the National Academy of Sciences*, *100*(8), 4724–4729. http://doi.org/10.1073/pnas.0737048100
Cannarile, M. A., Lind, N. A., Rivera, R., Sheridan, A. D., Camfield, K. A., Wu, B. B., Cheung, K. P., Ding, Z., & Goldrath, A. W. (2006). Transcriptional regulator Id2 mediates CD8+ T cell immunity. *Nature Immunology*, *7*(12), 1317–1325. https://doi.org/10.1038/ni1403
Cao, W., Henry, M. D., Borrow, P., Yamada, H., Elder, J. H., Ravkov, E. V., Nichol, S. T., Compans, R. W., Campbell, K. P., & Oldstone M. B. A. (1998). Identification of alpha-dystroglycan as a receptor for lymphocytic choriomeningitis virus and Lassa fever virus. *Science*, *282*(5396), 2079–2081. http://doi.org/10.1126/science.282.5396.2079
Chang, J. T., Palanivel, V. R., Kinjyo, I., Schambach, F., Intlekofer, A. M., Banerjee, A., Longworth, S. A., Vinup, K. E., Mrass, P., Oliaro, J., Weninger, W., & Reiner, S. L. (2007). Asymmetric T lymphocyte division in the initiation of adaptive immune responses. *Science*, *315*(5819), 1687–1691. http://doi.org/10.1126/science.1139393
Chang, J. T., Wherry, E. J., & Goldrath, A. W. (2014). Molecular regulation of effector and memory T cell differentiation. *Nature Immunology Review*, *15*(12), 1104–1115. https://doi.org/10.1038/ni.3031
Chen, H., Ghori-Javed, F. Y., Rashid, H., Serra, R., Gutierrez, S. E., & Javed, A. (2011). Chondrocyte-Specific Regulatory Activity of Runx2 Is Essential for

Survival and Skeletal Development. *Cells Tissues Organs*, *194*(2-4), 161–165. http://doi.org/ 10.1159/000324743

Chen, J.-L., Morgan, A. J., Stewart-Jones, G., Shepherd, D., Bossi, G., Wooldridge, L., Hutchinson, S. L., Sewell, A. K., Griffiths, G. M., van der Merwe, A., Jones, E. Y., Galione, A., & Cerundolo, V. (2010). Ca^{2+} Release from the Endoplasmic Reticulum of NY-ESO-1–Specific T Cells Is Modulated by the Affinity of TCR and by the Use of the CD8 Coreceptor. *The Journal of Immunology*, *184*(4), 1829–1839. http://doi.org/10.4049/jimmunol.0902103

Choi, J. Y., Pratap, J., Javed, A., Zaidi, S. K., Xing, L., Balint, E., Dalamangas S., Boyce, B., van Wijnen, A. J., Lian, J. B., Stein, J. L., Jones, S. N., & Stein G. S. (2001). Subnuclear targeting of Runx/Cbfa/AML factors is essential for tissue-specific differentiation during embryonic development. *Proceedings of the National Academy of Sciences*, *98*(15), 8650–8655. http://doi.org/10.1073/pnas.151236498

Chopin, M., Preston, S. P., Lun, A. T. L., Tellier, J., Smyth, G. K., Pellegrini, M., Belz, G. T., Corcoran, L. M., Visvader, J. E., Wu, L., & Nutt, S. L. (2016). RUNX2 Mediates Plasmacytoid Dendritic Cell Egress from the Bone Marrow and Controls Viral Immunity. *Cell Reports*, *15*(4), 866–878. http://doi.org/10.1016/j.celrep.2016.03.066

Christo, S. N., Diener, K. R., Nordon, R. E., Brown, M. P., Griesser, H. J., Vasilev, K., Christo F. C., Hayball J. D. (2015). Scrutinizing calcium flux oscillations in T lymphocytes to deduce the strength of stimulus. *Scientific Reports*, *5*(1), 635. https://doi.org/10.1038/srep07760

Chung, Y., Chang, S. H., Martinez, G. J., Yang, X. O., Nurieva, R., Kang, H. S., Ma, L., Watowich, S. S., Jetten, A. M., Tian, Q., & Dong, C. (2009). Critical Regulation of Early Th17 Cell Differentiation by Interleukin-1 Signaling. *Immunity*, *30*(4), 576–587. http://doi.org/10.1016/j.immuni.2009.02.007

Cornberg, M., Kenney, L. L., Chen, A. T., Waggoner, S. N., Kim, S.-K., Dienes, H. P., Welsh, R. M., & Selin, L. K. (2013). Clonal exhaustion as a mechanism to protect against severe immunopathology and death from an overwhelming CD8 T cell response. *Frontiers in Immunology*, *4*, 475. http://doi.org/10.3389/fimmu.2013.00475

Cretney, E., Kallies, A., & Nutt, S. L. (2013). Differentiation and function of Foxp3(+) effector regulatory T cells. *Trends in Immunology*, *34*(2), 74–80. http://doi.org/10.1016/j.it.2012.11.002

Cretney, E., Xin, A., Shi, W., Minnich, M., Masson, F., Miasari, M., Belz, G. T., Smyth, G. K., Busslinger, M., Nutt, S. L., & Kallies, A. (2011). The transcription factors Blimp-1 and IRF4 jointly control the differentiation and function of effector regulatory T cells. *Nature Immunology*, *12*(4), 304–311. http://doi.org/10.1038/ni.2006

Cruz-Guilloty, F., Pipkin, M. E., Djuretic, I. M., Levanon, D., Lotem, J., Lichtenheld, M. G., Groner, Y., & Rao, A. (2009). Runx3 and T-box proteins cooperate to establish the transcriptional program of effector CTLs. *Journal of Experimental Medicine*, *206*(1), 51–59. http://doi.org/10.1084/jem.20081242

Cui, W., & Kaech, S. M. (2010). Generation of effector CD8$^+$ T cells and their conversion to memory T cells. *Immunological Reviews*, *236*, 151–166. https://doi.org/10.1111/j.1600-065X.2010.00926.x

Cui, W., Liu, Y., Weinstein, J. S., Craft, J., & Kaech, S. M. (2011). An Interleukin-21- Interleukin-10-STAT3 Pathway Is Critical for Functional Maturation of Memory CD8$^+$ T Cells. *Immunity*, *35*(5), 792–805. http://doi.org/10.1016/j.immuni.2011.09.017

D'Alonzo, R. C., Selvamurugan, N., Karsenty, G., & Partridge, N. C. (2001). Physical Interaction of the Activator Protein-1 Factors c-Fos and c-Jun with Cbfa1 for Collagenase-3 Promoter Activation. *Journal of Biological Chemistry*, *277*(1), 816–822. http://doi.org/10.1074/jbc.M107082200

Das, J., Ho, M., Zikherman, J., Govern, C., Yang, M., Weiss, A., Chakraborty, A. K., & Roose, J. P. (2009). Digital Signaling and Hysteresis Characterize Ras Activationin Lymphoid Cells. *Cell*, *136*(2), 337–351. http://doi.org/10.1016/j.cell.2008.11.051

Doering, T. A., Crawford, A., Angelosanto, J. M., Paley, M. A., Ziegler, C. G., & Wherry, E. J. (2012). Network Analysis Reveals Centrally Connected Genes and Pathways Involved in CD8$^+$ T Cell Exhaustion versus Memory. *Immunity*, *37*(6), 1130–1144. http://doi.org/10.1016/j.immuni.2012.08.021

Ducy, P., Starbuck, M., Priemel, M., Shen, J., Pinero, G., Geoffroy, V., Amling, M., & Karsentry, G. (1999). A Cbfa1-dependent genetic pathway controls bone formation beyond embryonic development. *Genes & Development*, *13*(8), 1025–1036.

Eisenbeis, C. F., Singh, H., & Storb, U. (1995). Pip, a novel IRF family member, is a lymphoid-specific, PU.1-dependent transcriptional activator. *Genes & Development*, *9*(11), 1377–1387.

Ejrnaes, M., Filippi, C. M., Martinic, M. M., Ling, E. M., Togher, L. M., Crotty, S., & Herrath, von, M. G. (2006). Resolution of a chronic viral infection after interleukin-10 receptor blockade. *Journal of Experimental Medicine*, *203*(11), 2461–2472. http://doi.org/10.1084/jem.20061462

Freeman, G. J., Wherry, E. J., Ahmed, R., & Sharpe, A. H. (2006). Reinvigorating exhausted HIV-specific T cells via PD-1–PD-1 ligand blockade. *Journal of Experimental Medicine*, *203*(10), 2223–2227. http://doi.org/10.1084/jem.20061800

Fu, X. Y., Kessler, D. S., Veals, S. A., Levy, D. E., & Darnell, J. E. (1990). ISGF3, the transcriptional activator induced by interferon alpha, consists of multiple interacting polypeptide chains. *Proceedings of the National Academy of Sciences*, *87*(21), 8555–8559. https://doi.org/10.1073/pnas.87.21.8555

Fuller, M. J., & Zajac, A. J. (2003). Ablation of CD8 and CD4 T Cell Responses by High Viral Loads. *The Journal of Immunology*, *170*(1), 477–486. http://doi.org/10.4049/jimmunol.170.1.477

Gaffen, S. L., Jain, R., Garg, A. V., & Cua, D. J. (2014). The IL-23–IL-17 immune axis: from mechanisms to therapeutic testing. *Nature Reviews Immunology*, *14*(9), 585–600. http://doi.org/10.1038/nri3707

Gallimore, A., Glithero, A., Godkin, A., Tissot, A. C., Plückthun, A., Elliott, T., Hengartner, H., & Zinkernagel, R. (1998). Induction and Exhaustion of Lymphocytic Choriomeningitis Virus–specific Cytotoxic T Lymphocytes Visualized Using Soluble Tetrameric Major Histocompatibility Complex Class I–Peptide Complexes. *Journal of Experimental Medicine*, *187*(9), 1383–1393. http://doi.org/10.1084/jem.187.9.1383

Ge, C., Yang, Q., Zhao, G., Yu, H., Kirkwood, K. L., & Franceschi, R. T. (2012). Interactions between extracellular signal-regulated kinase 1/2 and P38 Map kinase pathways in the control of RUNX2 phosphorylation and transcriptional activity. *Journal of Bone and Mineral Research*, *27*(3), 538–551. http://doi.org/10.1002/jbmr.561

Gerlach, C., van Heijst, J. W. J., Swart, E., Sie, D., Armstrong, N., Kerkhoven, R. M., Zehn, D., Bevan, M. J., Schlepers, K., & Schumacher, T. N. M. (2010). One naive T cell, multiple fates in $CD8^+$ T cell differentiation. *Journal of Experimental Medicine*, *207*(6), 1235–1246. http://doi.org/10.1084/jem.20091175

Godec, J., Cowley, G. S., Barnitz, A. R., Ozan, A., Root, D. E., Sharpe, A. H., & Haining, N. W. (2015). Inducible RNAi in vivo reveals that the transcription factor BATF is required to initiate but not maintain $CD8^+$ T-cell effector differentiation. *Proceedings of the National Academy of Sciences*, *112*(35), 512–517. http://doi.org/10.1073/pnas.1514097112

Goldrath, A. W., Sivakumar, P. V., Glaccum, M., Kennedy, M. K., Bevan, M. J., Benoist, C., Mathis, D., & Butz, E. A. (2002). Cytokine Requirements for Acute and Basal Homeostatic Proliferation of Naive and Memory $CD8^+$ T Cells. *Journal of Experimental Medicine*, *195*(12), 1515–1522. http://doi.org/10.1084/jem.20020033

Gomez-Rodriguez, J., Meylan, F. C. O., Handon, R., Hayes, E. T., Anderson, S. M., Kirby, M. R., Siegel, R. M., & Schwartzberg P. L. (2016). Itk is required for Th9 differentiation via TCR-mediated induction of IL-2 and IRF4. *Nature Communications*, *7*, 1–15. http://doi.org/10.1038/ncomms10857

Gronski, M. A., Boulter, J. M., Moskophidis, D., Nguyen, L. T., Holmberg, K., Elford, A. R., Deenick, E. K., Kim, H. O., Penninger, J. M., Odermatt, B., Gallimore, A., Grascoigne, N. R. J., & Ohashi P. S. (2004). TCR affinity and negative regulation limit autoimmunity. *Nature Medicine*, *10*(11), 1234–1239. https://doi.org/10.1038/nm1114

Grumont, R. J., & Gerondakis, S. (2000). Rel Induces Interferon Regulatory Factor 4 (IRF-4) Expression in Lymphocytes. *Journal of Experimental Medicine*, *191*(8), 1281–1292. http://doi.org/10.1084/jem.191.8.1281

Grusdat, M., McIlwain, D. R., Xu, H. C., Pozdeev, V. I., Knievel, J., Crome, S. Q., Robert-Tissot, C., Dress, R. J., Pandyra, A. A., Speiser, D. E., Lang, E., Maney, S. K., Elford, A. R., Hamilton, S. R., Scheu, S., Pfeffer, K., Bode, J., Mittrücker, H.-W., Lohoff, M., Huber, M., Häussinger, D., Ohashi, P. S., Mak, T. W., Lang, K. S., & Lang, P. A. (2014). IRF4 and BATF are critical for $CD8^+$ T-cell function following infection with LCMV. *Cell Death and Differentiation*,

21(7), 1050–1060. http://doi.org/10.1038/cdd.2014.19
Hanai, J., Chen, L. F., Kanno, T., Ohtani-Fujita, N., Kim, W. Y., Guo, W. H., Imamura, T., Ishidou, Y., Fukuchi, M., Shi, M. J., Stavnezer J., Kaabata, M., Miyazono, K & Ito, Y. (1999). Interaction and functional cooperation of PEBP2/CBF with Smads. Synergistic induction of the immunoglobulin germline Calpha promoter. *The Journal of Biological Chemistry*, *274*(44), 31577–31582. http://doi.org/10.1074/jbc.274.44.31577
Harada, H., Tagashira, S., Fujiwara, M., Ogawa, S., Katsumata, T., Yamaguchi, A., Komori, T., & Nakatsuka, M. (1999). Cbfa1 isoforms exert functional differences in osteoblast differentiation. *Journal of Biological Chemistry*, *274*(11), 6972–6978. http://doi.org/10.1074/jbc.274.11.6972
Harrington, K. S. (2002). Transcription factors RUNX1/AML1 and RUNX2/Cbfa1 dynamically associate with stationary subnuclear domains. *Journal of Cell Science*, *115*(21), 4167–4176. http://doi.org/10.1242/jcs.00095
Hassan, M. Q., Javed, A., Morasso, M. I., Karlin, J., Montecino, M., van Wijnen, A. J., Stein, G. S., Stein, J. L., & Lian J. B. (2004). Dlx3 Transcriptional Regulation of Osteoblast Differentiation: Temporal Recruitment of Msx2, Dlx3, and Dlx5 Homeodomain Proteins to Chromatin of the Osteocalcin Gene. *Molecular and Cellular Biology*, *24*(20), 9248–9261. http://doi.org/10.1128/MCB.24.20.9248-9261.2004
Hu, G., & Chen, J. (2013). A genome-wide regulatory network identifies key transcription factors for memory CD8. *Nature Communications*, *4*, 1–14. http://doi.org/10.1038/ncomms3830
Huang, G., Shigesada, K., Ito, K., Wee, H. J., Yokomizo, T., & Ito, Y. (2001). Dimerization with PEBP2beta protects RUNX1/AML1 from ubiquitin-proteasome-mediated degradation. *The EMBO Journal*, *20*(4), 723–733. http://doi.org/10.1093/emboj/20.4.723
Huber, M., & Lohoff, M. (2014). IRF4 at the crossroads of effector T-cell fate decision. *European Journal of Immunology*, *44*(7), 1886–1895. https://doi.org/10.1002/eji.201344279
Huber, M., Brüstle, A., Reinhard, K., Guralnik, A., Walter, G., Mahiny, A., von Löw, E., & Lohoff, M. (2008). IRF4 is essential for IL-21-mediated induction, amplification, and stabilization of the Th17 phenotype. *Proceedings of the National Academy of Sciences*, *105*(52), 20846–20851. http://doi.org/10.1073/pnas.0809077106
Huber, M., Heink, S., Pagenstecher, A., Reinhard, K., Ritter, J., Visekruna, A., Guralnik, A., Bollig, N., Jeltsch, K., Heinemann, C., Wittmann, E., Buch, T., da Costa, O. P., Brüstle, A., Brenner, D., Mak, T. W., Mittrücker, H.-W., Tackenberg, B., Kamradt, T., & Lohoff, M (2012). IL-17A secretion by $CD8^+$ T cells supports Th17-mediated autoimmune encephalomyelitis. *Journal of Clinical Investigation*, *123*(1), 247–260. http://doi.org/10.1172/JCI63681DS1
Huster, K. M., Busch, V., Schiemann, M., Linkemann, K., Kerksiek, K. M., Wagner, H., & Busch, D. H. (2004). Selective expression of IL-7 receptor on memory T cells identifies early CD40L-dependent generation of distinct $CD8^+$

memory T cell subsets. *Proceedings of the National Academy of Sciences*, *101*(15), 5610–5615. http://doi.org/10.1073/pnas.0308054101
Inman, C. K., Li, N., & Shore, P. (2005). Oct-1 Counteracts Autoinhibition of Runx2 DNA Binding To Form a Novel Runx2/Oct-1 Complex on the Promoter of the Mammary Gland-Specific Gene *β-casein*. *Molecular and Cellular Biology*, *25*(8), 3182–3193. http://doi.org/10.1128/MCB.25.8.3182-3193.2005
Intlekofer, A. M., Takemoto, N., Kao, C., Banerjee, A., Schambach, F., Northrop, J. K., Shen, H., Wherry, E. J., & Reiner, S. L. (2007). Requirement for T-bet in the aberrant differentiation of unhelped memory CD8 +T cells. *Journal of Experimental Medicine*, *204*(9), 2015–2021. http://doi.org/10.1084/jem.20070841
Intlekofer, A. M., Takemoto, N., Wherry, E. J., Longworth, S. A., Northrup, J. T., Palanivel, V. R., Mullen, A. C., Gasink, C. R., Kaech, S. M., Miller, J. D., Gapin, L., Ryan, K., Russ, A. P., Lindsten, T., Orange, J. S., Goldrath, A. W., Ahmed, R., & Reiner S. L. (2005). Effector and memory CD8+ T cell fate coupled by T-bet and eomesodermin. *Nature Immunology*, *6*(12), 1236–1244. https://doi.org/10.1038/ni1268
Jeannet, G., Boudousquié, C., Gardiol, N., Kang, J., Huelsken, J., & Held, W. (2010). Essential role of the Wnt pathway effector Tcf-1 for the establishment of functional CD8 T cell memory. *Proceedings of the National Academy of Sciences*, *107*(21), 9777–9782. http://doi.org/10.1073/pnas.0914127107
Ji, Y., Pos, Z., Rao, M., Klebanoff, C. A., Yu, Z., Sukumar, M., Reger, R. N., Palmer, D. L., Borman, Z. A., Muranski, P., Wang, E., Schrump D. S., Marincola, F. M., Restifo, N. P., & Gattinoni, L. (2011). Repression of the DNA-binding inhibitor Id3 by Blimp-1 limits the formation of memory $CD8^+$ T cells. *Nature Immunology*, *12*(12), 1230–1237. http://doi.org/10.1038/ni.2153
Johnson, K., Hashimshony, T., Sawai, C. M., Pongubala, J. M. R., Skok, J. A., Aifantis, I., & Singh, H. (2008). Regulation of Immunoglobulin Light-Chain Recombination by the Transcription Factor IRF-4 and the Attenuation of Interleukin-7 Signaling. *Immunity*, *28*(3), 335–345. http://doi.org/10.1016/j.immuni.2007.12.019
Joshi, N. S., & Kaech, S. M. (2008). Effector CD8 T Cell Development: A Balancing Act between Memory Cell Potential and Terminal Differentiation. *The Journal of Immunology*, *180*(3), 1309–1315. http://doi.org/10.4049/jimmunol.180.3.1309
Joshi, N. S., Cui, W., Chandele, A., Lee, H. K., Urso, D. R., Hagman, J., Gapin, L., & Kaech, S. M. (2007). Inflammation Directs Memory Precursor and Short-Lived Effector $CD8^+$ T Cell Fates via the Graded Expression of T-bet Transcription Factor. *Immunity*, *27*(2), 281–295. http://doi.org/10.1016/j.immuni.2007.07.010
Kaech, S. M., & Ahmed, R. (2001). Memory CD8+ T cell differentiation: initial antigen encounter triggers a developmental program in naïve cells. *Nature Immunology*, *2*(5), 415–422. http://doi.org/10.1038/87720
Kaech, S. M., & Cui, W. (2012). Transcriptional control of effector and memory

CD8$^+$ T cell differentiation. *Nature Reviews Immunology*, *12*(11), 749–761. http://doi.org/10.1038/nri3307
Kaech, S. M., & Wherry, E. J. (2007). Heterogeneity and Cell-Fate Decisions in Effector and Memory CD8+ T Cell Differentiation during Viral Infection. *Immunity*, *27*(3), 393–405. http://doi.org/10.1016/j.immuni.2007.08.007
Kaech, S. M., Tan, J. T., Wherry, E. J., Konieczny, B. T., Surh, C. D., & Ahmed, R. (2003). Selective expression of the interleukin 7 receptor identifies effector CD8 T cells that give rise to long-lived memory cells. *Nature Immunology*, *4*(12), 1191–1198. https://doi.org/10.1038/ni1009
Kallies, A., Xin, A., Belz, G. T., & Nutt, S. L. (2009). Blimp-1 Transcription Factor Is Required for the Differentiation of Effector CD8$^+$ T Cells and Memory Responses. *Immunity*, *31*(2), 283–295. http://doi.org/10.1016/j.immuni.2009.06.021
Kanno, T., Kanno, Y., Chen, L. F., Ogawa, E., Kim, W. Y., & Ito, Y. (1998). Intrinsic transcriptional activation-inhibition domains of the polyomavirus enhancer binding protein 2/core binding factor alpha subunit revealed in the presence of the beta subunit. *Molecular and Cellular Biology*, *18*(5), 2444–2454. http://doi.org/10.1128/MCB.18.5.2444
Kanno, T., Takahashi, T., Tsujisawa, T., Ariyoshi, W., & Nishihara, T. (2007). Mechanical stress-mediated Runx2 activation is dependent on Ras/ERK1/2 MAPK signaling in osteoblasts. *Journal of Cellular Biochemistry*, *101*(5), 1266–1277. http://doi.org/10.1002/jcb.21249
Kao, C., Oestreich, K. J., Paley, M. A., Crawford, A., Angelosanto, J. M., Ali, M.-A. A., Intlekofer, A. M., Boss, J. M., Reiner, S. L., Weinmann, A. S., & Wherry, E. J. (2011). Transcription factor T-bet represses expression of the inhibitory receptor PD-1 and sustains virus-specific CD8. *Nature Immunology*, *12*(7), 663–671. http://doi.org/10.1038/ni.2046
Kessler, D. S., Veals, S. A., Fu, X. Y., & Levy, D. E. (1990). Interferon-alpha regulates nuclear translocation and DNA-binding affinity of ISGF3, a multimeric transcriptional activator. *Genes & Development*, *4*(10), 1753–1765. http://doi.org/10.1101/gad.4.10.1753
Kilbey, A., Blyth, K., Wotton, S., Terry, A., Jenkins, A., Bell, M., Hanlon, L., Cameron, E. R., & Neil, J. C. (2007). Runx2 Disruption Promotes Immortalization and Confers Resistance to Oncogene-Induced Senescence in Primary Murine Fibroblasts. *Cancer Research*, *67*(23), 11263–11271. http://doi.org/10.1158/0008-5472.CAN-07-3016
Kingeter, L. M., Paul, S., Maynard, S. K., Cartwright, N. G., & Schaefer, B. C. (2010). Cutting Edge: TCR Ligation Triggers Digital Activation of NF-κB. *The Journal of Immunology*, *185*(8), 4520–4524. http://doi.org/10.4049/jimmunol.1001051
Kitoh, A., Ono, M., Naoe, Y., Ohkura, N., Yamaguchi, T., Yaguchi, H., Kitabayashi, I., Tsukada, T., Nomura, T., Miyachi, Y., Taniuchi, I., & Sakaguchi, S. (2009). Indispensable Role of the Runx1-Cbfb Transcription Complex for In Vivo-Suppressive Function of FoxP3$^+$ Regulatory T Cells.

Immunity, *31*(4), 609–620. http://doi.org/10.1016/j.immuni.2009.09.003
Klein, U., Casola, S., Cattoretti, G., Shen, Q., Lia, M., Mo, T., Ludwig, T., Rajewsky, K., & Dalla-Favera, R. (2006). Transcription factor IRF4 controls plasma cell differentiation and class-switch recombination. *Nature Immunology*, *7*(7), 773–782. https://doi.org/10.1038/ni1357
Knell, J., Best, J. A., Lind, N. A., Yang, E., D'Cruz, L. M., & Goldrath, A. W. (2013). Id2 Influences Differentiation of Killer Cell Lectin-like Receptor G1^{hi} Short-Lived CD8^{+} Effector T Cells. *The Journal of Immunology*, *190*(4), 1501–1509. http://doi.org/10.4049/jimmunol.1200750
Komori, T. (2018). Runx2, an inducer of osteoblast and chondrocyte di erentiation. *Histochemistry and Cell Biology*, *149*(4), 313–323. http://doi.org/10.1007/s00418-018-1640-6
Kotturi, M. F., Peters, B., Buendia-Laysa, F., Sidney, J., Oseroff, C., Botten, J., Grey, H., Buchmeier, M. J., & Sette, A. (2007). The CD8+ T-Cell Response to Lymphocytic Choriomeningitis Virus Involves the L Antigen: Uncovering New Tricks for an Old Virus. *Journal of Virology*, *81*(10), 4928–4940. http://doi.org/10.1128/JVI.02632-06
Kunz, S., Sevilla, N., McGavern, D. B., Campbell, K. P., & Oldstone, M. B. A. (2001). Molecular analysis of the interaction of LCMV with its cellular receptor α-dystroglycan. *The Journal of Cell Biology*, *155*(2), 301–310. http://doi.org/10.1083/jcb.200104103
Kurachi, M., Barnitz, R. A., Yosef, N., Odorizzi, P. M., DiIorio, M. A., Lemieux, M. E., Yates, K., Godec, J., Klatt, M. G., Regev, A., Wherry, E. J., & Haining, W. N. (2014). The transcription factor BATF operates as an essential differentiation checkpoint in early effector CD8+ T cells. *Nature Immunology*, *15*(4), 373–383. http://doi.org/ 10.1038/ni.2834
Kwon, H., Thierry-Mieg, D., Thierry-Mieg, J., Kim, H.-P., Oh, J., Tunyaplin, C., Carotta, S., Donovan, C. E., Goldman, M. L., Tailor, P., Ozato, K., Levy, D. E., Nutt, S. L., Calame, K., & Leonard, W. J. (2009). Analysis of Interleukin-21-Induced *Prdm1* Gene Regulation Reveals Functional Cooperationof STAT3 and IRF4 Transcription Factors. *Immunity*, *31*(6), 941–952. http://doi.org/10.1016/j.immuni.2009.10.008
Lazorchak, A. S., Schlissel, M. S., & Zhuang, Y. (2006). E2A and IRF-4/Pip Promote Chromatin Modification and Transcription of the Immunoglobulin κ Locus in Pre-B Cells. *Molecular and Cellular Biology*, *26*(3), 810–821. http://doi.org/10.1128/MCB.26.3.810-821.2006
Lee, K. S., Kim, H. J., Li, Q. L., Chi, X. Z., Ueta, C., Komori, T., Wozney, J. M., Kim, E.-G., Choi, J.-Y., Ryoo, H.-M., & Bae, S.-C. (2000). Runx2 is a common target of transforming growth factor beta1 and bone morphogenetic protein 2, and cooperation between Runx2 and Smad5 induces osteoblast-specific gene expression in the pluripotent mesenchymal precursor cell line C2C12. *Molecular and Cellular Biology*, *20*(23), 8783–8792. http://doi.org/10.1128/MCB.20.23.8783-8792.2000
Lee, P. P., Yee, C., Savage, P. A., Fong, L., Brockstedt, D., Weber, J. S.,

Johnson, D., Swetter, S., Thompson, J., Greenberg, P. D., Roederer, M., & Davis, M. M. (1999). Characterization of circulating T cells specific for tumor-associated antigens in melanoma patients. *Nature Medicine*, *5*(6), 677–685. http://doi.org/10.1038/9525

Levy, D. E., Kessler, D. S., Pine, R., Reich, N., & Darnell, J. E. (1988). Interferon-induced nuclear factors that bind a shared promoter element correlate with positive and negative transcriptional control. *Genes & Development*, *2*(4), 383–393. http://doi.org/10.1101/gad.2.4.383

Li, Y., Ge, C., Long, J. P., Begun, D. L., Rodriguez, J. A., Goldstein, S. A., & Franceschi, R. T. (2012). Biomechanical stimulation of osteoblast gene expression requires phosphorylation of the RUNX2 transcription factor. *Journal of Bone and Mineral Research*, *27*(6), 1263–1274. http://doi.org/10.1002/jbmr.1574

Lodolce, J. P., Boone, D. L., Chai, S., Swain, R. E., Dassopoulos, T., Trettin, S., & Ma, A. (1998). IL-15 receptor maintains lymphoid homeostasis by supporting lymphocyte homing and proliferation. *Immunity*, *9*(5), 669–676. https://doi.org/10.1016/S1074-7613(00)80664-0

Lohoff, M., Mittrücker, H.-W., Prechtl, S., Bischof, S., Sommer, F., Kock, S., Ferrick, D. A., Duncan, G. S., Gessner, A., & Mak, T. W. (2002). Dysregulated T helper cell differentiation in the absence of interferon regulatory factor 4. *Proceedings of the National Academy of Sciences*, *99*(18), 11808–11812. http://doi.org/10.1073/pnas.182425099

Lu, R. (2003). IRF-4,8 orchestrate the pre-B-to-B transition in lymphocyte development. *Genes & Development*, *17*(14), 1703–1708. http://doi.org/10.1101/gad.1104803

Ma, A., Koka, R., & Burkett, P. (2006a). Diverse Functions of IL-2, IL-15, and IL-7 in Lymphoid Homeostasis. *Annual Review of Immunology*, *24*(1), 657–679. http://doi.org/10.1146/annurev.immunol.24.021605.090727

Ma, S., Pathak, S., Trinh, L., & Lu, R. (2008). Interferon regulatory factors 4 and 8 induce the expression of Ikaros and Aiolos to down-regulate pre-B-cell receptor and promote cell-cycle withdrawal in pre-B-cell development. *Blood*, *111*(3), 1396–1403. http://doi.org/10.1182/blood-2007-08-110106

Ma, S., Turetsky, A., Trinh, L., & Lu, R. (2006b). IFN Regulatory Factor 4 and 8 Promote Ig Light Chain κ Locus Activation in Pre-B Cell Development. *The Journal of Immunology*, *177*(11), 7898–7904. http://doi.org/10.4049/jimmunol.177.11.7898

Man, K., Miasari, M., Shi, W., Xin, A., Henstridge, D. C., Preston, S., Pellegrini, M., Belz, G. T., Smyth, G. K., Febbraio, M. A., Nutt, S. L., & Kallies, A (2013). The transcription factor IRF4 is essential for TCR affinity–mediated metabolic programming and clonal expansion of T cells. *Nature Immunology*, *14*(11), 1155–1165. http://doi.org/10.1038/ni.2710

Marecki, S., Atchison, M. L., & Fenton, M. J. (1999). Differential expression and distinct functions of IFN regulatory factor 4 and IFN consensus sequence binding protein in macrophages. *Journal of Immunology*, *163*(5), 2713–2722.

Matloubian, M., Concepcion, R. J., & Ahmed, R. (1994). CD4+ T cells are required to sustain CD8+ cytotoxic T-cell responses during chronic viral infection. *Journal of Virology*, *68*(12), 8056–8063.

Matloubian, M., Kolhekar, S. R., Somasundaram, T., & Ahmed, R. (1993). Molecular determinants of macrophage tropism and viral persistence: importance of single amino acid changes in the polymerase and glycoprotein of lymphocytic choriomeningitis virus. *Journal of Virology*, *67*(12), 7340–7349.

Matsuyama, T., Grossman, A., Mittrücker, H.-W., Siderovski, D. P., Kiefer, F., Kawakami, T., Richardson C. D., Taniguchi, T., Yoshinaga, S. K., & Mak, T. W. (1995). Molecular cloning of LSIRF, a lymphoid-specific member of the interferon regulatory factor family that binds the interferon-stimulated response element (ISRE). *Nucleic Acids Research*, *23*(12), 2127–2136.

McLarren, K. W., Lo, R., Grbavec, D., Thirunavukkarasu, K., Karsenty, G., & Stifani, S. (2000). The mammalian basic helix loop helix protein HES-1 binds to and modulates the transactivating function of the runt-related factor Cbfa1. *The Journal of Biological Chemistry*, *275*(1), 530–538. http://doi.org/10.1074/jbc.275.1.530

Mempel, T. R., Henrickson, S. E., & Andrian, von, U. H. (2004). T-cell priming by dendritic cells in lymph nodes occurs in three distinct phases. *Nature*, *427*, 154–159. https://doi.org/10.1038/nature02238

Mercado, R., Vijh, S., Allen, S. E., Kerksiek, K., Pilip, I. M., & Pamer, E. G. (2000). Early Programming of T Cell Populations Responding to Bacterial Infection. *The Journal of Immunology*, *165*(12), 6833–6839. http://doi.org/10.4049/jimmunol.165.12.6833

Mercier, B. C., Cottalorda, A., Coupet, C. A., Marvel, J., & Bonnefoy-Berard, N. (2009). TLR2 Engagement on CD8 T Cells Enables Generation of Functional Memory Cells in Response to a Suboptimal TCR Signal. *The Journal of Immunology*, *182*(4), 1860–1867. http://doi.org/10.4049/jimmunol.0801167

Mittrücker, H.-W., Matsuyama, T., Grossman, A., Kündig, T. M., Potter, J., Shahinian, A., Wakeman, A., Patterson, B., Ohashi, P. S., & Mak, T. W. (1997). Requirement for the transcription factor LSIRF/IRF4 for mature B and T lymphocyte function. *Science*, *275*(5299), 540–543. http://doi.org/10.1126/science.275.5299.540

Moskophidis, D., Lechner, F., Pircher, H., & Zinkernagel, R. M. (1993). Virus persistence in acutely infected immunocompetent mice by exhaustion of antiviral cytotoxic effector T cells. *Nature*, *362*(6422), 758–761. http://doi.org/10.1038/362758a0

Mudter, J., Amoussina, L., Schenk, M., Yu, J., Brüstle, A., Weigmann, B., Atreya, R., Wirtz, S., Becker, C., Hoffman, A., Atreya, I., Biesterfeld, S., Galle, P. R., Lehr, H. A., Rose-John, S., Mueller, C., Lohoff, M., & Neurath, M. F. (2008). The transcription factor IFN regulatory factor–4 controls experimental colitis in mice via T cell–derived IL-6. *Journal of Clinical Investigation*. http://doi.org/10.1172/JCI33227DS1

Mudter, J., Yu, J., Zufferey, C., Brüstle, A., Wirtz, S., Weigmann, B., Hoffman, A., Schenk, M., Galle, P. R., Lehr, H. A., Lohoff, M., & Neurath, M. F. (2011). IRF4 regulates IL-17A promoter activity and controls RORγt-dependent Th17 colitis in vivo. *Inflammatory Bowel Diseases*, *17*(6), 1343–1358. http://doi.org/10.1002/ibd.21476

Mueller, S. N., & Ahmed, R. (2009). High antigen levels are the cause of T cell exhaustion during chronic viral infection. *Proceedings of the National Academy of Sciences*, *106*(21), 8623–8628. http://doi.org/10.1073/pnas.0809818106

Naoe, Y., Setoguchi, R., Akiyama, K., Muroi, S., Kuroda, M., Hatam, F., Littman, D. R., & Taniuchi, I. (2007). Repression of interleukin-4 in T helper type 1 cells by Runx/Cbfβ binding to the Il4 silencer. *Journal of Experimental Medicine*, *204*(8), 1749–1755. http://doi.org/10.1084/jem.20062456

Nayar, R., Enos, M., Prince, A., Shin, H., Hemmers, S., Jiang, J.-K., Klein, U., Thomas, C. J., & Berg, L. J. (2012). TCR signaling via Tec kinase ITK and interferon regulatory factor 4 (IRF4) regulates $CD8^+$ T-cell differentiation. *Proceedings of the National Academy of Sciences*. *109*(41) E2794-E2802 http://doi.org/10.1073/pnas.1205742109

Nayar, R., Schutten, E., Bautista, B., Daniels, K., Prince, A. L., Enos, M., Brehm, M. A., Swain, S. L., Welsh, R. M., & Berg, L. J. (2014). Graded Levels of IRF4 Regulate CD8+ T Cell Differentiation and Expansion, but Not Attrition, in Response to Acute Virus Infection. *The Journal of Immunology*, *192*(12), 5881–5893. http://doi.org/10.4049/jimmunol.1303187

Ning, Y. M., & Robins, D. M. (1999). AML3/CBFalpha1 is required for androgen-specific activation of the enhancer of the mouse sex-limited protein (Slp) gene. *Journal of Biological Chemistry*, *274*(43), 30624–30630. http://doi.org/10.1074/jbc.274.43.30624

Nishimura, R., Hata, K., Harris, S. E., Ikeda, F., & Yoneda, T. (2002). Core-binding factor alpha 1 (Cbfa1) induces osteoblastic differentiation of C2C12 cells without interactions with Smad1 and Smad5. *Bone*, *31*(2), 303–312. https://doi.org/10.1016/S8756-3282(02)00826-8

Ochiai, K., Maienschein-Cline, M., Simonetti, G., Chen, J., Rosenthal, R., Brink, R., Chong, A. S., Maienschein-Cline, M., Simonetti, G., Chen, J., Rosenthal, R., & Brink, R. (2013). Transcriptional Regulation of Germinal Center B and Plasma Cell Fates by Dynamical Control of IRF4. *Immunity*, *38*(5), 918–929. http://doi.org/10.1016/j.immuni.2013.04.009

Omilusik, K. D., Nadjsombati, M. S., Shaw, L. A., Yu, B., Milner, J. J., & Goldrath, A. W. (2010). Sustained Id2 regulation of E proteins is required for terminal differentiation of effector $CD8^+$ T cells. *Journal of Experimental Medicine*, *215*(2), 229–240. http://doi.org/10.1084/jem.20171584

Otto, F., Kanegane, H., & Mundlos, S. (2002). Mutations in the RUNX2 gene in patients with cleidocranial dysplasia. *Human Mutation*, *19*(3), 209–216. https://doi.org/10.1002/humu.10043

Paley, M. A., Kroy, D. C., Odorizzi, P. M., Johnnidis, J. B., Dolfi, D. V., Barnett, B.

E., Bikoff, E. K., Robertson, E. J., Lauer, G. M., Reiner, S. L., & Wherry, E. J. (2012). Progenitor and Terminal Subsets of CD8$^+$ T Cells Cooperate to Contain Chronic Viral Infection. *Science*, *338*(6111), 1220–1225. http://doi.org/10.1126/science.1229620

Pathak, S., Ma, S., Trinh, L., & Lu, R. (2008). A Role for Interferon Regulatory Factor 4 in Receptor Editing. *Molecular and Cellular Biology*, *28*(8), 2815–2824. http://doi.org/10.1128/MCB.01946-07

Peperzak, V., Veraar, E. A. M., Keller, A. M., Xiao, Y., & Borst, J. (2010). The Pim Kinase Pathway Contributes to Survival Signaling in Primed CD8$^+$ T Cells upon CD27 Costimulation. *The Journal of Immunology*, *185*(11), 6670–6678. http://doi.org/10.4049/jimmunol.1000159

Petrovas, C., Casazza, J. P., Brenchley, J. M., Price, D. A., Gostick, E., Adams, W. C., Precopio, M. L., Schacker, T., Roederer, M., Douek, D. C., & Koup, R. A. (2006). PD-1 is a regulator of virus-specific CD8$^+$ T cell survival in HIV infection. *Journal of Experimental Medicine*, *203*(10), 2281–2292. http://doi.org/10.1084/jem.20061496

Petrovas, C., Price, D. A., Mattapallil, J., Ambrozak, D. R., Geldmacher, C., Cecchinato, V., Vaccari, M., Tryniszewska, E., Gostick, E., Roederer, M., Douek, D. C., Morgan, S. H., Davis, S. J., Franchini, G., & Koup, R. A. (2007). SIV-specific CD8$^+$ T cells express high levels of PD1 and cytokines but have impaired proliferative capacity in acute and chronic SIVmac251 infection. *Blood*, *110*(3), 928–936. http://doi.org/10.1182/blood-2007-01-069112

Pircher, H., Bürki, K., Lang, R., Hengartner, H., & Zinkernagel, R. M. (1989). Tolerance induction in double specific T-cell receptor transgenic mice varies with antigen. *Nature*, *342*(6249), 559–561. http://doi.org/10.1038/342559a0

Pollizzi, K. N., Sun, I.-H., Patel, C. H., Lo, Y.-C., Oh, M.-H., Waickman, A. T., Tam, A. J., Blosser, R. L., Wen, J., Delgoffe, G. M., & Powell, J. D. (2016). Asymmetric inheritance of mTORC1 kinase activity during division dictates CD8+ T cell differentiation. *Nature Immunology*, *17*(6), 704–711. https://doi.org/10.1038/ni.3438

Popescu, I., Pipeling, M. R., Shah, P. D., Orens, J. B., & McDyer, J. F. (2014). T-bet:Eomes Balance, Effector Function, and Proliferation of Cytomegalovirus-Specific CD8$^+$ T Cells during Primary Infection Differentiates the Capacity for Durable Immune Control. *The Journal of Immunology*, *193*(11), 5709–5722. http://doi.org/10.4049/jimmunol.1401436

Pratap, J., Galindo, M., Zaidi, S. K., Vradii, D., Bhat, B. M., Robinson, J. A., Choi, J.-Y., Komori, T., Stein, J. L., Lian, J. B., Stein, G. S., & van Wijnen, A. J. (2003). Cell growth regulatory role of Runx2 during proliferative expansion of preosteoblasts. *Cancer Research*, *63*(17), 5357–5362.

Prlic, M., Hernandez-Hoyos, G., & Bevan, M. J. (2006). Duration of the initial TCR stimulus controls the magnitude but not functionality of the CD8 +T cell response. *Journal of Experimental Medicine*, *203*(9), 2135–2143. http://doi.org/10.1084/jem.20060928

Probst, H. C., Tschannen, K., Gallimore, A., Martinic, M., Basler, M., Dumrese, T., Jones E., & van den Broek, M. F. (2003). Immunodominance of an Antiviral Cytotoxic T Cell Response Is Shaped by the Kinetics of Viral Protein Expression. *The Journal of Immunology*, *171*(10), 5415–5422. http://doi.org/10.4049/jimmunol.171.10.5415

Qiao, M., Shapiro, P., Kumar, R., & Passaniti, A. (2004). Insulin-like Growth Factor-1 Regulates Endogenous RUNX2 Activity in Endothelial Cells through a Phosphatidylinositol 3-Kinase/ERK-dependent and Akt-independent Signaling Pathway. *Journal of Biological Chemistry*, *279*(41), 42709–42718. http://doi.org/10.1074/jbc.M404480200

Quigley, M., Martinez, J., Huang, X., & Yang, Y. (2009). A critical role for direct TLR2-MyD88 signaling in CD8 T-cell clonal expansion and memory formation following vaccinia viral infection. *Blood*, *113*(10), 2256–2264. http://doi.org/10.1182/blood-2008-03-148809

Raczkowski, F., Ritter, J., Heesch, K., Schumacher, V., Guralnik, A., Höcker, L., Raifer, H., Klein, M., Bopp, T., Harb, H., Kesper, D. A., Pfefferle, P. I., Grustdat, M., Lang, P. A., Mittrücker, H.-W., & Huber, M. (2013). The transcription factor Interferon Regulatory Factor 4 is required for the generation of protective effector $CD8^+$ T cells. *Proceedings of the National Academy of Sciences*, *110*(37), 15019–15024. http://doi.org/10.1073/pnas.1309378110

Rao, R. R., Li, Q., Odunsi, K., & Shrikant, P. A. (2010). The mTOR Kinase Determines Effector versus Memory $CD8^+$ T Cell Fat by Regulating the Expression of Transcription Factors T-bet and Eomesodermin. *Immunity*, *32*(1), 67–78. http://doi.org/10.1016/j.immuni.2009.10.010

Rengarajan, J., Mowen, K. A., McBride, K. D., Smith, E. D., Singh, H., & Glimcher, L. H. (2002). Interferon Regulatory Factor 4 (IRF4) Interacts with NFATc2 to Modulate Interleukin 4 Gene Expression. *Journal of Experimental Medicine*, *195*(8), 1003–1012. http://doi.org/10.1084/jem.20011128

Restifo, N. P., & Gattinoni, L. (2013). Lineage relationship of effector and memory T cells. *Current Opinion in Immunology*, *25*(5), 556–563. http://doi.org/10.1016/j.coi.2013.09.003

Richer, M. J., Nolz, J. C., & Harty, J. T. (2013). Pathogen-Specific Inflammatory Milieux Tune the Antigen Sensitivity of $CD8^+$ T Cells by Enhancing T Cell Receptor Signaling. *Immunity*, *38*(1), 140–152. http://doi.org/10.1016/j.immuni.2012.09.017

Rosenbauer, F., Waring, J. F., Foerster, J., Wietstruk, M., Philipp, D., & Horak, I. (1999). Interferon consensus sequence binding protein and interferon regulatory factor-4/Pip form a complex that represses the expression of the interferon-stimulated gene-15 in macrophages. *Blood*, *94*(12), 4274–4281.

Rubinstein, M. P., Lind, N. A., Purton, J. F., Filippou, P., Best, J. A., McGhee, P. A., Surh, C. D., & Goldrath, A. W. (2008). IL-7 and IL-15 differentially regulate $CD8^+$ T-cell subsets during contraction of the immune response. *Blood*, *112*(9), 3704–3712. http://doi.org/10.1182/blood-2008-06-160945

Rudra, D., Egawa, T., Chong, M. M. W., Treuting, P., Littman, D. R., & Rudensky, A. Y. (2009). Runx-CBF complexes control expression of the transcription factor Foxp3 in regulatory T cells. *Nature Immunology*, *10*(11), 1170–1177. http://doi.org/10.1038/ni.1795

Rutishauser, R. L., Martins, G. A., Kalachikov, S., Chandele, A., Parish, I. A., Meffre, E., Jacob, J., Calame, K., & Kaech, S. M. (2009). Transcriptional Repressor Blimp-1 Promotes $CD8^+$ T Cell Terminal Differentiation and Represses the Acquisition of Central Memory T Cell Properties. *Immunity*, *31*(2), 296–308. http://doi.org/10.1016/j.immuni.2009.05.014

Saito, M., Gao, J., Basso, K., Kitagawa, Y., Smith, P. M., Bhagat, G., Pernis, A., Pasqualucci, L., & Dalla-Favera, R. (2007). A Signaling Pathway Mediating Downregulation of BCL6 in Germinal Center B Cells Is Blocked by BCL6 Gene Alterations in B Cell Lymphoma. *Cancer Cell*, *12*(3), 280–292. http://doi.org/10.1016/j.ccr.2007.08.011

Sarkar, S., Kalia, V., Haining, W. N., Konieczny, B. T., Subramaniam, S., & Ahmed, R. (2008). Functional and genomic profiling of effector CD8 T cell subsets with distinct memory fates. *Journal of Experimental Medicine*, *205*(3), 625–640. http://doi.org/10.1084/jem.20071641

Sarkar, S., Teichgraber, V., Kalia, V., Polley, A., Masopust, D., Harrington, L. E., Ahmed, R., & Wherry, E. J. (2007). Strength of Stimulus and Clonal Competition Impact the Rate of Memory CD8 T Cell Differentiation. *The Journal of Immunology*, *179*(10), 6704–6714. http://doi.org/10.4049/jimmunol.179.10.6704

Sato, M., Morii, E., Komori, T., Kawahata, H., Sugimoto, M., Terai, K., Shimizu, H., Yasui, T., Ogihara, H., Yasui, N., Ochi, T., Kitamura, Y., Ito, Y., & Nomura, S. (1998). Transcriptional regulation of osteopontin gene in vivo by PEBP2αA/CBFA1 and ETS1 in the skeletal tissues. *Oncogene*, *17*(12), 1517–1525. http://doi.org/10.1038/sj.onc.1202064

Sawai, C. M., Sisirak, V., Ghosh, H. S., Hou, E. Z., Ceribelli, M., Staudt, L. M., & Reizis, B. (2013). Transcription factor Runx2 controls the development and migration of plasmacytoid dendritic cells. *Journal of Experimental Medicine*, *210*(11), 2151–2159. http://doi.org/10.1084/jem.20130443

Schlitzer, A., McGovern, N., Teo, P., Zelante, T., Atarashi, K., Low, D., Ho, A. W. S., See, P., Shin, A., Wasan, P. S., Hoeffel, G., Malleret, B., Heiseke, A., Chew, S., Jardine, L., Purvis, H. A., Hilens, C. M. U., Tam, J., Poidinger, M., Riccialdi-Castagnoli, P., Honda, K., Haniffa, M., & Ginhoux, F. (2013). IRF4 Transcription Factor-Dependent $CD11b^+$ Dendritic Cells in Human and Mouse Control Mucosal IL-17 Immune Responses. *Immunity*, *38*(5), 970–983. http://doi.org/10.1016/j.immuni.2013.04.011

Schluns, K. S., Kieper, W. C., Jameson, S. C., & Lefrancois, L. (2000). Interleukin-7 mediates the homeostasis of naïve and memory CD8 T cells in vivo. *Nature Immunology*, *1*(5), 426–432. http://doi.org/10.1038/80868

Schluns, K. S., Williams, K., Ma, A., Zheng, X. X., & Lefrancois, L. (2002). Cutting Edge: Requirement for IL-15 in the Generation of Primary and

Memory Antigen-Specific CD8 T Cells. *The Journal of Immunology*, *168*(10), 4827–4831. http://doi.org/10.4049/jimmunol.168.10.4827
Sciammas, R., & Davis, M. M. (2004). Modular Nature of Blimp-1 in the Regulation of Gene Expression during B Cell Maturation. *The Journal of Immunology*, *172*(9), 5427–5440. http://doi.org/10.4049/jimmunol.172.9.5427
Sciammas, R., Shaffer, A. L., Schatz, J. H., Zhao, H., Staudt, L. M., & Singh, H. (2006). Graded Expression of Interferon Regulatory Factor-4 Coordinates Isotype Switching with Plasma Cell Differentiation. *Immunity*, *25*(2), 225–236. http://doi.org/10.1016/j.immuni.2006.07.009
Sevilla, N., Kunz, S., Holz, A., Lewicki, H., Homann, D., Yamada, H., Campbell, K. P., de la Torre, J. C., & Oldstone, M. B. A. (2000). Immunosuppression and resultant viral persistence by specific viral targeting of dendritic cells. *The Journal of Experimental Medicine*, *192*(9), 1249–1260.
Shin, Haina, Blackburn, S. D., Blattman, J. N., & Wherry, E. J. (2007). Viral antigen and extensive division maintain virus-specific CD8 T cells during chronic infection. *Journal of Experimental Medicine*, *204*(4), 941–949. http://doi.org/10.1084/jem.20061937
Shin, Haina, Blackburn, S. D., Intlekofer, A. M., Kao, C., Angelosanto, J. M., Reiner, S. L., & Wherry, E. J. (2009). A Role for the Transcriptional Repressor Blimp-1 in $CD8^+$ T Cell Exhaustion during Chronic Viral Infection. *Immunity*, *31*(2), 309–320. http://doi.org/10.1016/j.immuni.2009.06.019
Shin, H. M., Kapoor, V. N., Guan, T., Kaech, S. M., Welsh, R. M., & Berg, L. J. (2013). Epigenetic Modifications Induced by Blimp-1 Regulate CD8+ T Cell Memory Progression during Acute Virus Infection. *Immunity*, *39*(4), 661–675. http://doi.org/10.1016/j.immuni.2013.08.032
Shin, Hyun Mu, Kapoor, V. N., Kim, G., Li, P., Kim, H.-R., Suresh, M., et al. (2017). Transient expression of ZBTB32 in anti-viral $CD8^+$ T cells limits the magnitude of the effector response and the generation of memory. *PLoS Pathogens*, *13*(8), e1006544. http://doi.org/10.1371/journal.ppat.1006544
Shirakabe, K., Terasawa, K., Miyama, K., Shibuya, H., & Nishida, E. (2001). Regulation of the activity of the transcription factor Runx2 by two homeobox proteins, Msx2 and Dlx5. *Genes to Cells*, *6*(10), 851–856. https://doi.org/10.1046/j.1365-2443.2001.00466.x
Shukla, V., & Lu, R. (2014). IRF4 and IRF8: governing the virtues of B lymphocytes. *Frontiers in Biology*, *9*(4), 269–282. http://doi.org/10.1007/s11515-014-1318-y
Slifka, M. K., & Whitton, J. L. (2000). Activated and Memory $CD8^+$ T Cells Can Be Distinguished by Their Cytokine Profiles and Phenotypic Markers. *The Journal of Immunology*, *164*(1), 208–216. http://doi.org/10.4049/jimmunol.164.1.208
Smelt, S. C., Borrow, P., Kunz, S., Cao, W., Tishon, A., Lewicki, H., Campbell, K. P., & Oldstone, M. B. A. (2001). Differences in Affinity of Binding of Lymphocytic Choriomeningitis Virus Strains to the Cellular Receptor α-Dystroglycan Correlate with Viral Tropism and Disease Kinetics. *Journal of*

Virology, *75*(1), 448–457. http://doi.org/10.1128/JVI.75.1.448-457.2001
Sowa, H., Kaji, H., Hendy, G. N., Canaff, L., Komori, T., Sugimoto, T., & Chihara, K. (2004). Menin Is Required for Bone Morphogenetic Protein 2- and Transforming Growth Factor β-regulated Osteoblastic Differentiation through Interaction with Smads and Runx2. *Journal of Biological Chemistry*, *279*(39), 40267–40275. http://doi.org/10.1074/jbc.M401312200
Staron, M. M., Gray, S. M., Marshall, H. D., Parish, I. A., Chen, J. H., Perry, C. J., Cui, G., Li, M. O., & Kaech, S. M. (2014). The Transcription Factor FoxO1 Sustains Expression of the Inhibitory Receptor PD-1 and Survival of Antiviral CD8(+) T Cells during Chronic Infection. *Immunity*, *41*(5), 802–814. http://doi.org/10.1016/j.immuni.2014.10.013
Staudt, V., Bothur, E., Klein, M., Lingnau, K., Reuter, S., Grebe, N., Gerlitzki, B., Hoffmann, M., Ulges, A., Taube, C., Dehzad, N., Becker, M., Stassen, M., Steinborn, A., Lohoff, M., Schild, H., Schmitt, E., & Bopp, T. (2010). Interferon-Regulatory Factor 4 Is Essential for the Developmental Program of T Helper 9 Cells. *Immunity*, *33*(2), 192–202. http://doi.org/10.1016/j.immuni.2010.07.014
Stemberger, C., Huster, K. M., Koffler, M., Anderl, F., Schiemann, M., Wagner, H., & Busch, D. H. (2007). A Single Naive $CD8^+$ T Cell Precursor Can Develop into Diverse Effector and Memory Subsets. *Immunity*, *27*(6), 985–997. http://doi.org/10.1016/j.immuni.2007.10.012
Sullivan, B. M., Emonet, S. F., Welch, M. J., Lee, A. M., Campbell, K. P., la Torre, de, J. C., & Oldstone, M. B. (2011). Point mutation in the glycoprotein of lymphocytic choriomeningitis virus is necessary for receptor binding, dendritic cell infection, and long-term persistence. *Proceedings of the National Academy of Sciences*, *108*(7), 2969–2974. http://doi.org/10.1073/pnas.1019304108
Sullivan, B. M., Juedes, A., Szabo, S. J., Herrath, von, M., & Glimcher, L. H. (2003). Antigen-driven effector CD8 T cell function regulated by T-bet. *Proceedings of the National Academy of Sciences*, *100*(26), 15818–15823. http://doi.org/10.1073/pnas.2636938100
Tahirov, T. H., Inoue-Bungo, T., Morii, H., Fujikawa, A., Sasaki, M., Kimura, K., Shiina, M., Sato, K., Kumasaka, T., & Ogata, K. (2001). Structural analyses of DNA recognition by the AML1/Runx-1 Runt domain and its allosteric control by CBFbeta. *Cell*, *104*(5), 755–767. https://doi.org/10.1016/S0092-8674(01)00271-9
Takemoto, N., Intlekofer, A. M., Northrup, J. T., Wherry, E. J., & Reiner, S. L. (2006). Cutting Edge: IL-12 Inversely Regulates T-bet and Eomesodermin Expression during Pathogen-Induced $CD8^+$ T Cell Differentiation. *The Journal of Immunology*, *177*(11), 7515–7519. http://doi.org/10.4049/jimmunol.177.11.7515
Tewari, K., Sacha, J., Gao, X., & Suresh, M. (2004). Effect of Chronic Viral Infection on Epitope Selection, Cytokine Production, and Surface Phenotype of CD8 T Cells and the Role of IFN-γ Receptor in Immune Regulation. *The*

Journal of Immunology, *172*(3), 1491–1500. http://doi.org/10.4049/jimmunol.172.3.1491

Thomsen, A. R., Johansen, J., Marker, O., & Christensen, J. P. (1996). Exhaustion of CTL memory and recrudescence of viremia in lymphocytic choriomeningitis virus-infected MHC class II-deficient mice and B cell-deficient mice. *The Journal of Immunology*, *157*(7), 3074–3080.

Tinoco, R., Alcalde, V., Yang, Y., Sauer, K., & Zuniga, E. I. (2009). Cell-Intrinsic Transforming Growth Factor-β Signaling Mediates Virus-Specific $CD8^+$ T Cell Deletion and Viral Persistence In Vivo. *Immunity*, *31*(1), 145–157. http://doi.org/10.1016/j.immuni.2009.06.015

Tominaga, N., Ohkusu-Tsukada, K., Udono, H., Abe, R., Matsuyama, T., & Yui, K. (2003). Development of Th1 and not Th2 immune responses in mice lacking IFN-regulatory factor-4. *International Immunology*, *15*(1), 1–10. https://doi.org/10.1093/intimm/dxg001

Vaillant, F., Blyth, K., Andrew, L., Neil, J. C., & Cameron, E. R. (2002). Enforced Expression of Runx2 Perturbs T Cell Development at a Stage Coincident with β -Selection. *The Journal of Immunology*, *169*(6), 2866–2874. http://doi.org/10.4049/jimmunol.169.6.2866

Vaillant, F., Blyth, K., Terry, A., Bell, M., Cameron, E. R., Neil, J., & Stewart, M. (1999). A full-length Cbfa1 gene product perturbs T-cell development and promotes lymphomagenesis in synergy with MYC. *Oncogene*, *18*, 7124–7134. https://doi.org/10.1038/sj.onc.1203202

van der Most, R. G., Murali-Krishna, K., Whitton, J. L., Oseroff, C., Alexander, J., Southwood, S., Sidney, J., Chesnut, R. W., Sette, R., & Ahmed, R. (1998). Identification of D^b- and K^b-Restricted Subdominant Cytotoxic T-Cell Responses in Lymphocytic Choriomeningitis Virus-Infected Mice. *Virology*, *240*(1), 158–167. http://doi.org/10.1006/viro.1997.8934

van Stipdonk, M. J., Lemmens, E. E., & Schoenberger, S. P. (2001). Naïve CTLs require a single brief period of antigenic stimulation for clonal expansion and differentiation. *Nature Immunology*, *2*(5), 423–429. http://doi.org/10.1038/87730

Verbist, K. C., Guy, C. S., Milasta, S., Liedmann, S., Kamiński, M. M., Wang, R., & Green, D. R. (2016). Metabolic maintenance of cell asymmetry following division in activated T lymphocytes. *Nature*, *532*(7599), 389–393. http://doi.org/10.1038/nature17442

Wang, D., Diao, H., Getzler, A. J., Rogal, W., Frederick, M. A., Milner, J., Yu, B., Crotty, S., Goldrath, A. W., & Pipkin, M. E. (2018). The Transcription Factor Runx3 Establishes Chromatin Accessibility of cis-Regulatory Landscapes that Drive Memory Cytotoxic T Lymphocyte Formation. *Immunity*, *48*(4), 659–674.e6. http://doi.org/10.1016/j.immuni.2018.03.028

Wee, H.-J., Huang, G., Shigesada, K., & Ito, Y. (2002). Serine phosphorylation of RUNX2 with novel potential functions as negative regulatory mechanisms. *EMBO Reports*, *3*(10), 967–974. http://doi.org/10.1093/embo-reports/kvf193

Welsh, R. M., & Seedhom, M. O. (2008). Lymphocytic Choriomeningitis Virus

(LCMV): Propagation, Quantitation, and Storage *Current Protocols in Microbiology*. *282*(15A.1.1–15A.1.11). https://doi.org/10.1002/9780471729259.mc15a01s8
Wherry, E. J. (2011). T cell exhaustion. *Nature Reviews Immunology*, *131*(6), 492–499. http://doi.org/10.1038/ni.2035
Wherry, E. J., & Ahmed, R. (2004). Memory CD8 T-Cell Differentiation during Viral Infection. *Journal of Virology*, *78*(11), 5535–5545. http://doi.org/10.1128/JVI.78.11.5535-5545.2004
Wherry, E. J., Barber, D. L., Kaech, S. M., Blattman, J. N., & Ahmed, R. (2004). Antigen-independent memory CD8 T cells do not develop during chronic viral infection. *Proceedings of the National Academy of Sciences*, *101*(45), 16004–16009. http://doi.org/10.1073/pnas.0407192101
Wherry, E. J., Blattman, J. N., Murali-Krishna, K., van der Most, R., & Ahmed, R. (2003). Viral Persistence Alters CD8 T-Cell Immunodominance and Tissue Distribution and Results in Distinct Stages of Functional Impairment. *Journal of Virology*, *77*(8), 4911–4927. http://doi.org/10.1128/JVI.77.8.4911-4927.2003
Wherry, E. J., Ha, S.-J., Kaech, S. M., Haining, W. N., Sarkar, S., Kalia, V., Subramaniam, S., Blattman, J. N., Barber, D. L., & Ahmed, R. (2007). Molecular Signature of $CD8^+$ T Cell Exhaustion during Chronic Viral Infection. *Immunity*, *27*(4), 670–684. http://doi.org/10.1016/j.immuni.2007.09.006
Williams, J. W., Tjota, M. Y., Clay, B. S., Vander Lugt, B., Bandukwala, H. S., Hrusch, C. L., Decker, D. C., Blaine, K. M., Fixsen, B. R., Singh, H., Sciammas, R., & Sperling, A. I. (2013). Transcription factor IRF4 drives dendritic cells to promote Th2 differentiation. *Nature Communications*, *4*, 1–12. http://doi.org/10.1038/ncomms3990
Williams, M. A., & Bevan, M. J. (2007). Effector and Memory CTL Differentiation. *Annual Review of Immunology*, *25*(1), 171–192. http://doi.org/10.1146/annurev.immunol.25.022106.141548
Workman, C. J., Cauley, L. S., Kim, I. J., Blackman, M. A., Woodland, D. L., & Vignali, D. A. A. (2004). Lymphocyte Activation Gene-3 (CD223) Regulates the Size of the Expanding T Cell Population Following Antigen Activation In Vivo. *The Journal of Immunology*, *172*(9), 5450–5455. http://doi.org/10.4049/jimmunol.172.9.5450
Wotton, D., Ghysdael, J., Wang, S., Speck, N. A., & Owen, M. J. (1994). Cooperative binding of Ets-1 and core binding factor to DNA. *Molecular and Cellular Biology*, *14*(1), 840–850. http://doi.org/10.1128/MCB.14.1.840
Xiao, G., Gopalakrishnan, R., Jiang, D., Reith, E., Benson, M. D., & Franceschi, R. T. (2002). Bone morphogenetic proteins, extracellular matrix, and mitogen-activated protein kinase signaling pathways are required for osteoblast-specific gene expression and differentiation in MC3T3-E1 cells. *Journal of Bone and Mineral Research*, *17*(1), 101–110. http://doi.org/10.1359/jbmr.2002.17.1.101
Xiao, Z., Casey, K. A., Jameson, S. C., Curtsinger, J. M., & Mescher, M. F.

(2009). Programming for CD8 T Cell Memory Development Requires IL-12 or Type I IFN. *The Journal of Immunology*, *182*(5), 2786–2794. http://doi.org/10.4049/jimmunol.0803484

Xin, A., Masson, F., Liao, Y., Preston, S., Guan, T., Gloury, R., Olshansky, M., Lin, J.-X., Li, P., Speed, T. P., Smyth, G. K., Ernst M., Leonard, W. J., Pellegrini, M., Kaech, S. M., Nutt, S. L., Shi, W., Belz, G. T., & Kallies, A. (2016). A molecular threshold for effector $CD8^+$ T cell differentiation controlled by transcription factors Blimp-1 and T-bet. *Nature Immunology*, *17*(4), 422–432. https://doi.org/10.1038/ni.3410

Yamagata, T., Nishida, J., Tanaka, S., Sakai, R., Mitani, K., Yoshida, M., Taniguchi, T., Yazaki, Y., & Hirai, H. (1996). A novel interferon regulatory factor family transcription factor, ICSAT/Pip/LSIRF, that negatively regulates the activity of interferon-regulated genes. *Molecular and Cellular Biology*, *16*(4), 1283–1294.

Yang, C. Y., Best, J. A., Knell, J., Yang, E., Sheridan, A. D., Jesionek, A. K., Li, H. S., Riviera, R. R., Camfield Lind, K., D'Cruz, L. M., Watowich, S. S., Murre, C., & Goldrath, A. W. (2011). The transcriptional regulators Id2 and Id3 control the formation of distinct memory CD8+ T cell subsets. *Nature Immunology*, *12*(12), 1221–1229. http://doi.org/10.1038/ni.2158

Yao, S., Buzo, B. F., Pham, D., Jiang, L., Taparowsky, E. J., Kaplan, M. H., & Sun, J. (2013). Interferon Regulatory Factor 4 Sustains CD8+ T Cell Expansion and Effector Differentiation. *Immunity*, *39*(5), 833–845. http://doi.org/10.1016/j.immuni.2013.10.007

Zaidi, S. K., Javed, A., Choi, J. Y., van Wijnen, A. J., Stein, J. L., Lian, J. B., & Stein, G. S. (2001). A specific targeting signal directs Runx2/Cbfa1 to subnuclear domains and contributes to transactivation of the osteocalcin gene. *Journal of Cell Science*, *114*, 3093–3102.

Zaidi, S. K., Pande, S., Pratap, J., Gaur, T., Grigoriu, S., Ali, S. A., Stein, J. L., Lian, J. B., van Wijnen, A. J., & Stein, G. S. (2007). Runx2 deficiency and defective subnuclear targeting bypass senescence to promote immortalization and tumorigenic potential. *Proceedings of the National Academy of Sciences*, *104*(50), 19861–19866. http://doi.org/10.1073/pnas.0709650104

Zajac, A. J., Blattman, J. N., Murali-Krishna, K., Sourdive, D. J. D., Suresh, M., Altman, J. D., & Ahmed, R. (1998). Viral Immune Evasion Due to Persistence of Activated T Cells Without Effector Function. *Journal of Experimental Medicine*, *188*(12), 2205–2213.

Zehn, D., Lee, S. Y., & Bevan, M. J. (2009). Complete but curtailed T-cell response to very low-affinity antigen. *Nature*, *457*(7235), 211–214. http://doi.org/10.1038/nature07657

Zeng, C., McNeil, S., Pockwinse, S., Nickerson, J., Shopland, L., Lawrence, J. B., Penman, S., Hiebert, S., Lian, J. B., van Wijnen, A. J., Stein, J. L., & Stein, G. S. (1998). Intranuclear targeting of AML/CBFalpha regulatory factors to nuclear matrix-associated transcriptional domains. *Proceedings of*

the National Academy of Sciences, *95*(4), 1585–1589. https://doi.org/10.1073/pnas.95.4.1585

Zeng, C., van Wijnen, A. J., Stein, J. L., Meyers, S., Sun, W., Shopland, L., Lawrence, J. B., Penman, S., Lian, J. B., Stein, G. S., & Hiebert, S. W. (1997). Identification of a nuclear matrix targeting signal in the leukemia and bone-related AML/CBF-alpha transcription factors. *Proceedings of the National Academy of Sciences*, *94*(13), 6746–6751. https://doi.org/10.1073/pnas.94.13.6746

Zheng, Y., Chaudhry, A., Kas, A., deRoos, P., Kim, J. M., Chu, T.-T., Corcoran L., Treuting, P., Klein, U., & Rudensky, A. Y. (2009). Regulatory T-cell suppressor program co-opts transcription factor IRF4 to control T_H2 responses. *Nature*, *458*(7236), 351–356. http://doi.org/10.1038/nature07674

Zhou, Xin, Ramachandran, S., Mann, M., & Popkin, D. (2012). Role of Lymphocytic Choriomeningitis Virus (LCMV) in Understanding Viral Immunology: Past, Present and Future. *Viruses*, *4*(11), 2650–2669. http://doi.org/10.3390/v4112650

Zhou, Xinyuan, Yu, S., Zhao, D.-M., Harty, J. T., Badovinac, V. P., & Xue, H.-H. (2010). Differentiation and Persistence of Memory $CD8^+$ T Cells Depend on T Cell Factor 1. *Immunity*, *33*(2), 229–240. http://doi.org/10.1016/j.immuni.2010.08.002

Zhu, Y., Ju, S., Chen, E., Dai, S., Li, C., Morel, P., Liu, L., Zhang, X., & Lu, B. (2010). T-bet and Eomesodermin Are Required for T Cell-Mediated Antitumor Immune Responses. *The Journal of Immunology*, *185*(6), 3174–3183. http://doi.org/10.4049/jimmunol.1000749

Ziros, P. G., Gil, A.-P. R., Georgakopoulos, T., Habeos, I., Kletsas, D., Basdra, E. K., & Papavassiliou, A. G. (2002). The Bone-specific Transcriptional Regulator Cbfa1 Is a Target of Mechanical Signals in Osteoblastic Cells. *Journal of Biological Chemistry*, *277*(26), 23934–23941. http://doi.org/10.1074/jbc.M109881200